

# **Identification of fire gases in early stages of fire in laboratory scaled and full scale fire experiments**

**by**

**Adam May**

A thesis submitted in partial fulfilment for the requirements of the degree of (PhD) at the University of Central Lancashire (in collaboration with – TYCO Fire Protection Products)

**January 2011**

# Student Declaration

## **Concurrent registration for two or more academic awards**

\*I declare that while registered as a candidate for the research degree, I have not been a registered candidate or enrolled student for another award of the University or other academic or professional institution

## **Material submitted for another award**

\*I declare that no material contained in the thesis has been used in any other submission for an academic award and is solely my own work

**Signature of Candidate** (Adam David Richard May )

---

**Type of Award**                      **PhD**

**School**                                      **Forensic and Investigative Sciences**

## **Abstract**

A series of reduced scale emulations of standard fires in a 2 m<sup>3</sup> enclosure have been developed for studies at laboratory scale enabling useful comparison and correlation with full scale EN54/7 and UL268 test fires. This makes study of standard test fire conditions and products substantially more accessible. The reduced scale test fire emulations have smoke obscuration characteristics matched to the fire standards and show acceptable matching of experimental CO levels

Sensor, fire detector, and analytical studies have been carried out on test fires in the 2 m<sup>3</sup> enclosure and in a full scale test room. Protocols were developed for capture of gas and vapours from fires on absorbent media and their subsequently desorption and analysis by GC/MS techniques. A data set of GC chromatograms has been generated for full and reduced scale test fires and for a number of non standard fire or false alarm related process including overheating of cooking oils and toasting bread. Analysis of mass spectrometry ion fragmentation spectra has been carried out and a wide range of products identified. Products occurring for a range of different fires include propene, benzene, and some polyaromatics.

The value of the scaled test fire emulations has been demonstrated by monitoring response of a range of sensors, detectors and instruments including electrochemical gas sensor, experimental and conventional light scattering smoke detectors, and ion mobility measurement equipment (FAIMS).

The study has provided information on fire characteristics and products to inform future research and development on fire detection technologies.

# Table of Contents

ORGANISATION OF STUDY AND THESIS.....	18
<b>CHAPTER 1 BACKGROUND AND OVERVIEW .....</b>	<b>20</b>
1.0 HISTORY AND IMPACT OF FIRE DETECTORS AND DETECTION .....	20
1.1 FIRE PROCESSES AND PROPERTIES.....	21
1.1.1 Types of combustion in fires (flaming, smouldering, stoichiometry).....	21
1.1.2 Development of Fires.....	23
1.1.3 Flames and free radical chemistry.....	25
1.2 FIRE PRODUCTS (AIRBORNE MATERIALS).....	27
1.2.1 Particulate (Smoke).....	27
1.2.2 Gases and Vapours.....	27
1.3 HEAT RELEASE AND PRODUCT TRANSPORT .....	31
1.4 EARLIER STUDIES ON FIRE DEVELOPMENT AND PRODUCTS RELEVANT TO DETECTION ...	33
1.5 FIRE DETECTION TECHNOLOGY AND TESTING .....	34
1.5.1 Ionization Smoke detectors.....	37
1.5.2 Optical Smoke detection devices.....	38
1.5.3 Temperature sensors.....	40
1.5.4 Carbon monoxide gas sensors .....	41
1.6.5 Multi criteria Fire Detectors .....	42
1.5.6 Use of fire detectors in this study .....	43
1.6 FALSE ALARMS AND DETECTION RELIABILITY .....	44
1.6.1 Cooking fumes.....	47
1.7 DETECTOR VALIDATION, STANDARD TEST FIRES.....	49
1.7.1 Standard Test Fires.....	53
1.7.2 Standard fire test rooms.....	59
1.8 REDUCED SCALE TESTING AND MODELLING.....	61
1.8.1 FE/DE (Fire Emulation/Detector Evaluation) device.....	62
1.8.2 Cone Calorimeter.....	63
1.8.3 The NBS smoke box.....	64
1.9 METHODS OF ANALYSIS.....	65
1.9.1 Particulate sizes.....	65
1.9.2 Gas/Vapour Measurements.....	66
1.9.3 Gas sample collection by absorbent media.....	67
1.9.4 Gas chromatography.....	69
1.9.5 Infra-Red Spectroscopy (NDIR, FTIR).....	73
1.9.6 Ion Mobility Spectrometry – IMS and FAIMS.....	74
<b>CHAPTER 2 EXPERIMENTAL METHODS .....</b>	<b>76</b>
2.0 FIRE ENCLOSURES .....	76
2.0.1 NBS Smoke Chamber.....	76
2.0.2 Fire source samples for NBS chamber.....	77
2.0.3 Data monitoring in NBS smoke chamber.....	77
2.0.4 Collection and analysis of air samples from NBS chamber.....	78
2.0.5 GC Analysis Conditions for PU4500 at Bolton.....	79
2.1 TYCO SMOKE TUNNEL.....	80
2.1.1 Smoke Tunnel data monitoring.....	80
2.1.2 Equipment and Calibration Procedures at TYCO Sunbury.....	81
2.2 UCLAN FIRE CHAMBER.....	82
2.2.1 UCLan enclosure Sensor, Detector, and Sampling locations.....	84
2.2.2 UCLan Enclosure - Airflow.....	86
2.2.3 UCLan Enclosure Hot plate.....	86
2.2.4 UCLan Enclosure Spark generation ignition source.....	86
2.3 DETECTORS EMPLOYED .....	86
2.3.1 Calibration of Optical Scatter devices.....	90
2.3.2 Electrochemical sensor response calibration.....	91

2.3.3	CO sensors in 801PC devices.....	92
2.3.4	Electrochemical sensor for hydrogen 7HYT.....	94
2.3.5	Electrochemical sensor for oxidisable gases (Ethylene oxide sensor) 7ETO.....	95
2.3.6	Electrochemical Oxygen Sensor Citicel 2FO.....	97
2.3.7	Fire Detector Temperature sensor Calibration.....	97
2.3.8	UCLan Enclosure NDIR for CO and CO <sub>2</sub> .....	98
2.3.9	UCLan Enclosure Humidity sensors.....	100
2.3.10	UCLan Enclosure Optical Density measurements.....	101
2.4	GAS COLLECTION, CHROMATOGRAPHY, AND ANALYSIS - GC/MS SYSTEM.....	103
2.4.1	Collection of Fire Gases on Absorbent Media.....	103
2.4.2	Gas chromatography - Injection.....	106
2.4.2.1	GC Thermal Trap Injection.....	106
2.4.2.2	GC Direct Injection.....	108
2.4.3	5890 Series II GC-MS.....	109
2.4.4	Mass spectrometry: VG Trio 2000 conditions.....	111
2.4.5	Measurements relating quantities of collected material to GC/MS data.....	112
2.4.6	Absorption tube Validation Schedules.....	113
2.4.7	Column loading measurements appropriate for Tenax samples.....	115
2.4.8	Column loading measurements appropriate for Carboxen samples.....	117
2.4.9	Other GC/MS system Validation Checks.....	119
2.5	FULL-SCALE FIRE TEST ROOM (BRE) – DETECTOR/SENSOR DEPLOYMENT.....	119
2.6	STANDARD FIRE TESTS.....	123
2.6.1	Standard EN 54/7 Fire Tests in full scale test room (BRE).....	124
2.6.2	Additional fire tests in BRE full scale tests.....	124
<b>CHAPTER 3 SCALING OF FIRES – ISSUES AND MEASUREMENTS.....</b>		<b>125</b>
3.1	PRACTICAL AND THEORETICAL BASIS FOR SCALING TEST FIRES.....	125
3.1.1	SELECTION OF TEST FIRE AND DETECTOR SITES IN UCLAN ENCLOSURE.....	131
3.2	SCALING REQUIREMENTS OF SPECIFIC FIRES (FUEL GEOMETRY).....	135
3.2.1	Scaled wood cribs (UL268 fire B emulation).....	136
3.2.2	Scaled smouldering wood (BS EN54/7 TF2 emulation).....	137
3.2.3	Scaled smouldering cotton fire (BS EN54/7 TF3 emulation).....	138
3.2.4	Scaled flaming liquid fires (EN54/7 TF5 and UL268 fire C emulations).....	139
3.2.5	Scaled Polyurethane foam fire (BS EN54/7 TF4 emulation).....	140
3.2.6	Scaled flaming paper fire (UL268 fire A emulation).....	140
3.3	TESTS AT SCALES APPROPRIATE TO 2 M <sup>3</sup> UCLAN ENCLOSURE.....	140
3.3.1	Standard Test Fire Emulations for 2 m <sup>3</sup> UCLan Enclosure.....	141
3.3.2	Smouldering wood (BS EN54/7 TF2 scaled emulation).....	141
3.3.3	Burning wood (UL268 fire B scaled emulation).....	142
3.3.4	Smouldering cotton (BS EN54/7 TF3 scaled emulation).....	143
3.3.5	Burning polyurethane (BS EN54/7 TF4 scaled emulation).....	144
3.3.6	Burning pool fire: Heptane: Toluene 97:3 (BS EN54/7 TF5 scaled fire).....	145
3.3.7	Flaming liquid fire II: Toluene:Heptane (75:25) (UL268 fire C emulation).....	146
3.3.8	Smouldering paper (UL268 fire A emulation).....	146
3.4	NON STANDARD FIRE AND NUISANCE SOURCE TESTS IN UCLAN ENCLOSURE.....	148
3.4.1	Burning pool fire III: Methanol.....	148
3.4.2	Electrical fire scenario 1: Overheated plastic coated wire.....	148
3.4.3	Electrical fire scenario 2: Overheated printed circuit boards.....	149
3.4.4	Nuisance false fire alarm scenario 1: Toasting Bread.....	149
3.4.5	Nuisance false fire alarm scenario 2: Overheating cooking oils.....	150
3.4.6	Nuisance false fire alarm scenario 3: Cigarette smoke.....	151
3.8	PRACTICAL AND CALCULATED SCALING OF STANDARD FIRE TESTS.....	152
<b>CHAPTER 4 DATA PRESENTATION.....</b>		<b>154</b>
4.0	CHAPTER OVERVIEW.....	154
4.0.1	Obscuration data.....	156
4.0.2	Oxidizable gases.....	157

4.0.3 Major Combustion Related Gases (CO <sub>2</sub> and O <sub>2</sub> ) .....	158
4.1 SENSOR DATA SUMMARY FOR EMULATIONS OF STANDARD TEST FIRES .....	159
4.1.1 Scaled Smouldering wood (BS EN 54/7 TF2 Emulations) .....	160
4.1.2 Smouldering cotton (BS EN 54/7 TF3 Emulations).....	161
4.1.3 Burning Polyurethane Foam (BS EN 54/7 TF4 Emulations).....	162
4.1.4 Burning pool fire - Heptane (BS EN 54/7 TF5 Emulations).....	163
4.1.5 Burning pool fire - Heptane (UL268 fire C Emulation) .....	164
4.1.6 Burning Paper (UL268 fire A Emulation) .....	165
4.1.7 Flaming wood (UL268 fire C Emulation) .....	166
4.2 STANDARD FIRE TESTS AT BRE AND UCLAN EMULATIONS: -SENSOR DATA PLOTS .....	167
4.2.1 Smouldering Wood BS EN54/7 TF2 (BRE full scale and Emulations) .....	167
4.2.2 Smouldering Cotton BS EN54/7 TF3 (BRE full scale and Emulations).....	168
4.2.3 Polyurethane foam burn BS EN54/7 TF4 (BRE full scale and Emulations) .....	168
4.2.4 Flaming Heptane BS EN54/7 TF5 (BRE full scale and Emulations) .....	169
4.3 SENSOR DATA SUMMARY FOR NON-STANDARD TESTS IN UCLAN 2 M <sup>3</sup> ENCLOSURE.....	170
4.3.1 Overheating Printed Circuit Boards (PCB) in UCLan Enclosure .....	170
4.3.2 Burning Mixed Polyurethane Foams in UCLan Enclosure .....	172
4.3.3 Overheating Polymer Coated Wire in UCLan Enclosure.....	173
4.3.4 Overheating Cooking Oils in UCLan Enclosure .....	174
4.3.5 Cigarette Smoking in UCLan Enclosure .....	175
4.3.6 Bread Toasting and Re-Toasting in UCLan Enclosure.....	176
4.4 SUMMARY OF PARAMETERS FOR REDUCED SCALE FIRES .....	177
4.4.1 CHANGE IN TEMPERATURES.....	179
4.5 GC-MS DATA (GC CHROMATOGRAMS) .....	180
4.6 GC CHROMATOGRAMS FOR UCLAN. EMULATIONS OF STANDARD FIRES .....	182
4.6.1 Scaled Smouldering wood (EN 54/7 TF2 Emulations) .....	182
4.6.2 Smouldering cotton (EN 54/7 TF3 Emulations).....	183
4.6.3 Burning Polyurethane Foam (BS EN 54/7 TF4 Emulations).....	184
4.6.4 Burning pool fire - Heptane (BS EN 54/7 TF5 Emulations).....	185
4.6.5 Burning pool fire - Heptane (UL268 fire C Emulation).....	186
4.6.6 Burning Paper (UL268 fire A Emulation) .....	187
4.6.7 Flaming wood (UL268 fire B Emulation).....	188
4.7 GC CHROMATOGRAMS FOR EN54/7 FIRES CONDUCTED AT BRE.....	189
4.8 GC FOR NON-STANDARD TESTS IN UCLAN. ENCLOSURE.....	191
4.8.1 Burning Mixed Polyurethane Foams in UCLan Enclosure .....	191
4.8.2 Overheating PCBs in UCLan Enclosure.....	191
4.8.3 Overheating Polymer Coated Wire in UCLan Enclosure.....	192
4.8.4 Overheating Cooking Oils in UCLan Enclosure .....	192
4.8.5 Bread Toasting and Re-Toasting in UCLan Enclosure.....	193
<b>CHAPTER 5 INTERPRETATION OF GC-MS RESULTS.....</b>	<b>195</b>
5.1 MS SPECTRA ANALYSIS PROCESSES.....	195
5.1.1 Unlabeled and unknown peaks.....	197
5.1.2 Library matching acquired spectra .....	198
5.1.3 Mass analysis .....	199
5.1.4 Fragmentation analysis .....	201
5.1.5 Isotope analysis.....	202
5.2 ANALYSIS OF GC/MS FROM TEST FIRES .....	203
5.3 EXAMPLES OF CARBOXEN AND PORO PLOT Q CHROMATOGRAMS .....	204
5.3.1 BS EN 54-7 Standard fires – products captured on Carboxen .....	205
5.3.2 UL268 Scaled fires – products captured on Carboxen.....	209
5.3.3 Full scale BS EN 54 Fire tests– products captured on Carboxen.....	212
5.3.4 Non-Standard fires with polymer fuels– products captured on Carboxen .....	216
5.3.5 Non-Standard Fires –cooking oils -products on Carboxen.....	219
5.3.6 Toasting Bread.....	222
5.3.7 Methanol Flaming Liquid Fire.....	227

5.3.8 Non standard smouldering paper.....	228
5.3.9 Cigarettes .....	229
5.4 EXAMPLE CHROMATOGRAPHS FROM TENAX SAMPLES.....	229
5.4.1 Scaled EN 54 fires at UCLan – products captured on Tenax.....	230
5.4.2 Scaled fires based on UL268 standard fires – products captured on Tenax.....	234
5.4.3 Other fires.....	237
5.5 SUMMARY OF PRODUCT IDENTIFICATION FOR BS EN 54/7 TEST FIRES .....	238
<b>CHAPTER 6 DISTINGUISHING FIRES WITH ADDITIONAL FIRE</b>	
<b>CHARACTERISTICS.....</b>	<b>241</b>
6.1 DISTINGUISHING FIRES BY SCATTER.....	241
6.3.1 UCLan Smouldering wood (TF2).....	251
6.3.2 UCLan Smouldering cotton (TF3).....	252
6.3.3 UCLan Flaming polyurethane (TF4) .....	253
6.3.4 UCLan Flaming pool fire – Heptane (TF5).....	254
6.3.5 Sunbury smoke tunnel tests.....	255
6.3.6 BRE FULL SCALE SMOULDERING WOOD (TF2) .....	256
6.3.7 BRE Smouldering cotton (TF3).....	257
6.3.8 BRE Flaming polyurethane (TF4).....	258
6.3.9 BRE Flaming Pool fire – Heptane(TF5).....	259
6.4 SMOKE PARTICLE SIZE ANALYSIS BY CASCADE IMPACTOR .....	261
6.5 FAIMS MEASUREMENTS (HIGH FIELD ASYMMETRIC ION MOBILITY SPECTROMETRY) .....	265
6.5.1 Principles and Background.....	265
6.3.2 Experimental Work with FAIMS equipment .....	267
6.4.1 Smouldering wood (TF2).....	270
6.4.2 Smoldering cotton (TF3) .....	271
6.4.3 Flaming polyurethane (TF4) .....	272
6.4.4 Flaming Pool fire (TF5).....	273
<b>CHAPTER 7 DISCUSSION AND CONCLUSION .....</b>	<b>274</b>
7.1 REVIEW OF WORK AND RESULTS .....	274
7.1.1 Development of Reduced Scale Test Fires .....	274
7.1.2 Sensor Measurements .....	275
7.1.3 GC/MS study.....	277
7.1.4 Optical Scatter and Particle Size Measurements.....	280
7.1.5 FAIMS measurements.....	280
7.2 SUMMARY, APPLICATIONS AND FUTURE DEVELOPMENTS .....	281

## TABLE OF TABLES

Table 1 : Gas concentrations reported in the literature from cellulose pyrolysis study at 500°C [31].....	29
Table 2 : In the pyrolysis study [31] only 2 gases were observed in high concentrations at temperatures above 800°C.....	30
Table 3 Smoke points of typical oils and fats .....	49
Table 4 List of current standards and test fuels .....	54
Table 5 Conditions for Pye Unicam PU4500 for initial GC work at Bolton.....	79
Table 6 Summary of MX 801 Detectors and Variants .....	89
Table 7 Cross sensitivity table taken from Honeywell data sheets. ....	93
Table 8 Cross sensitivity of the 7HYT cell as derived from CiTi technology product data sheet. ....	95
Table 9 Cross sensitivity of 7EtO cell derived from manufacturers data sheet .....	96
Table 10 Output for randomly selected obscuration device measurements .....	102
Table 11 Program settings for the TDCT injection system .....	107
Table 12 Sample desorption parameters on the CDS5200 pyroprobe system .....	109
Table 13 Temperature program used on the 5890 Series II gas chromatogram to examine the desorbed samples from Tenax absorbent resin traps. ....	110
Table 14 The temperature program used to examine volatile samples collect on Carboxen traps. ....	111

Table 15	Examples of validation A injection for Tenax and Carboxen tubes.....	114
Table 16	Examples of validation B injection results for Tenax and Carboxen tubes .....	114
Table 17	The amount of each analyte introduced in each injection based upon published concentrations of analyte in grob (II) standard. ....	115
Table 18	Summary of MX 801 Detectors and Variants .....	123
Table 19	Detector ceiling arc temperatures for tests in BS EN54/7 room at BRE.....	128
Table 20	Calculated values of fire power requirements and ratio factors for 0.2, 2, and 10°C temperature rises at detector positions in EN54/7 and UL268 rooms, and UCLan enclosure. ....	129
Table 21	Published Heat Release Rates for Standard Test Fires.....	130
Table 22	Fuel Quantities for Standard Test Fires and UCLan Emulations .....	153
Table 23	Properties from the scaled fires based on the BS-EN 54-7 standard fired carried out in the UCLan enclosure. ....	177
Table 24	Properties from the scaled fires based on the scaled UL268 standard fires carried out in the UCLan scaled fire enclosure.....	177
Table 25	Properties from the scaled fires based on the scaled non-standard polymer based fires carried out in the UCLan enclosure .....	178
Table 26	Properties from the scaled fires based on the scaled non-standard sources based on cooking fuels used as false alarm scenarios.....	178
Table 27	Properties from the scaled fires based on the scaled non-standard sources based on the progression of toasting used as false alarm scenarios. ....	179
Table 28	Elemental analysis based on the exact masses of the elements involved in the potential structure 78 m/Z ion .....	200
Table 29	Calculated number of saturations + ring structures.....	200
Table 30	The Mass ions corresponding to peaks A-M from the chromatogram for smouldering wood fire (TF2 Emulation). ....	205
Table 31	The peaks IDs in the table represents the mass ions corresponding to the peaks A-O from Figure 132 .....	206
Table 32	The peak ID corresponds to the peaks in the chromatogram shown in Figure 133, relating to the scaled flaming polyurethane fire (TF4).....	207
Table 33	The peak ID corresponds to the peaks in the chromatogram shown in Figure 134, relating to the scaled flaming pool fire (TF5).....	208
Table 34	The peak ID correspond to the peaks in the chromatogram shown in Figure 135, relating to the scaled representation of the smouldering paper fire based on the UL268 standard fire (Fire A) .....	209
Table 35	The peak ID correspond to the peaks in the chromatogram shown in Figure 136, relating to the scaled representation of the flaming wood fire described in the UL268 standard (Fire B) .....	210
Table 36	The peak ID corresponds to the peaks in the chromatogram shown in Figure 137, relating to the scaled representation of the flaming pool heptane fire of the UL268 standard fire (Fire C) .....	211
Table 37	Identified components from the spectra shown in figure 138 taken from the full scale BRE smouldering wood fire (TF2) .....	212
Table 38	Identified components from the spectra shown in Figure 139 taken from the full scale BRE smouldering cotton fire based on the BS EN 54 standard fire (TF3).....	213
Table 39	Identified components from the spectra shown in Figure 140 taken from the full scale BRE flaming polyurethane based on the standard BS EN 54 fire (TF4). ....	214
Table 40	The identified components from the spectra shown in Figure 141. ....	215
Table 41	The table represents the data from the peaks identified in the spectra shown in Figure 142. ....	216
Table 42	This table shows the mass ion data collected from analysis of the spectra shown in Figure 143. ....	217
Table 43	Table of the mass ions and potential identifications from the flaming mixed polyurethane fires. These peaks correspond to the peaks shown in the Figure 144.....	218
Table 44	These ions represent the peaks from the chromatogram traces identified in Figure 145. ....	219
Table 45	These ions represent the peaks from the chromatogram traces identified in Figure 146 .....	220
Table 46	These ions represent the peaks from the chromatogram traces identified in Figure 147.....	221
Table 47	These ions represent the peaks from the chromatogram traces identified in Figure 149.....	223
Table 48	These ions represent the peaks from the chromatogram traces identified in Figure 150.....	224
Table 49	These ions represent the peaks from the chromatogram traces identified in Figure 151.....	225
Table 50	These ions represent the peaks from the chromatogram traces identified in Figure 152.....	226
Table 51	These ions represent the peaks from the chromatogram traces identified in Figure 153.....	227
Table 52	These ions represent the peaks from the chromatogram traces identified in Figure 154.....	228
Table 53	These ions represent the peaks from the chromatogram traces identified in Figure 155.....	230
Table 54	These ions represent the peaks from the chromatogram traces identified in Figure 156.....	231
Table 55	These ions represent the peaks from the chromatogram traces identified in Figure 157.....	232
Table 56	These ions represent the peaks from the chromatogram traces identified in Figure 158.....	233

Table 57 These ions represent the peaks from the chromatogram traces identified in Figure 159.....	234
Table 58 These ions represent the peaks from the chromatogram traces identified in Figure 160.....	235
Table 59 These ions represent the peaks from the chromatogram traces identified in Figure 161.....	236
Table 60 These ions represent the peaks from the chromatogram traces identified in Figure 162.....	237
Table 61 Common gasses observed in the scaled standard fires in the UCLan enclosure with the library match values presented.....	239
Table 62 List of devices used in the standard fire tests indicating the wavelengths of the associated components used in the detectors.....	243
Table 63 Normalization factors for each of the TYCO devices used in Figures 165 and 166.....	248
Table 64 Cut of Point $D_p$ and Geometric Mean Diameter GMD for the New Star Cascade Impactor with 2L./minute air flow rate.....	263
Table 65 Approximate response ratio of total oxidisable gas and CO sensors both calibrated with CO and with signals expressed as CO ppm or CO ppm equivalent.....	276
Table 66 Ranges for CO concentration from measurements in UCLan reduced and BRE full scale EN54/7 test fires TF2,TF3, TF4, and TF5.....	277
Table 67 Common gases observed in the scaled standard fires in the UCLan enclosure with the library match values presented (F,R>750 considered good match).....	279

## TABLE OF EQUATIONS

Equation 1 Stoichiometric oxidation of hydrocarbon.....	22
Equation 2 Chain Reaction Stages.....	26
Equation 3 Thermal energy balance.....	31
Equation 4 Drysdale equation for ceiling mounted temperature detectors.....	32
Equation 5 Overall Oxidation Reaction for CO in Electrochemical Cell.....	41
Equation 6 Expression for absorbance index ( $m$ ).....	51
Equation 7 Expression for fractional transmission.....	51
Equation 8 Optical density calculation of smoke density.....	51
Equation 9 Expression to convert %Obsc/m from $m$ .....	52
Equation 10 Expression to convert obscuration per meter (%Obsc/m) from optical density per meter $OD_m$ .....	52
Equation 11 Expression to convert obscuration per meter (%Obsc/m) from optical density per foot ( $OD_f$ ).....	52
Equation 12 Expression converting %Obsc/m from fractional transmission $T_s$ .....	52
Equation 13 Expression for the calculation of the dimensionless parameter $y$ .....	52
Equation 14 Expression connecting the $y$ parameter to the concentration of particulates ( $Z$ ) and the average particle diameter ( $d$ ) in a specific chamber.....	53
Equation 15 Rate theory equation ( $K_c$ is the equilibration constant for the interaction of the analytes in gas chromatography. $C_s$ is the concentrations of the analyte in the stationary phase and $C_m$ is the concentration of the analyte in the mobile phase).....	70
Equation 16 Beer Law governing optical absorption.....	73
Equation 17 Calculation of the oxygen gas concentration using the 2FO oxygen cell.....	97
Equation 18 Calculation of the transmission fraction of light through smoke.....	102
Equation 19 Calculation of the obscuration per meter ( $\%Obsc.m^{-1}$ ) for any path length ( $d$ ) from transmission measurements.....	102
Equation 20 Calculation of the obscuration per meter $\%Obsc.m^{-1}$ for the UCLan device.....	102
Equation 21 Temperature rise from ceilings when $r > 0.18 \times H$ .....	126
Equation 22 Temperature rise from ceilings when $r < 0.18 \times H$ .....	126
Equation 23 Minimum fire intensity $r > 0.18 \times H$ .....	127
Equation 24 Minimum fire intensity $r < 0.18 \times H$ .....	127
Equation 25 Ion intensity in GC plots.....	180
Equation 26 Number of saturations.....	200
Equation 27 re-arrangement of equation 26.....	200
Equation 28 Device signal from raw output and clean air (pedestal) value.....	244
Equation 29 Excel calculation normalised signal values.....	247
Equation 30 Device Response ratio calculation.....	247

## TABLE OF FIGURES

Figure 1 Triangle of combustion .....	23
Figure 2 Overview of typical processes occurring in the early stages of polymer combustion. ....	24
Figure 3 Polyaromatics formation in combustion identified by laser induced fluorescence.....	30
Figure 4 Cut a way of a typical detector.....	39
Figure 5 Optical Scatter Detector layout .....	39
Figure 6 Diagrammatic representation of electrochemical CO sensor.....	42
Figure 7 10 year survey of the causes of false alarms in the UK looking at the source of the call outs which were discovered as false alarms. (Source UK GOV figures) .....	46
Figure 8 BS EN54/7 TF2 Obscuration limits .....	55
Figure 9 BS EN54/7 TF3 Obscuration limits .....	56
Figure 10 BS EN54/7 TF4 Obscuration limits .....	56
Figure 11 BS EN54/7 TF5 Obscuration limits .....	57
Figure 12 UL268 fire A Obscuration limits .....	58
Figure 13 UL268 fire B Obscuration limits.....	58
Figure 14 UL268 fire C Obscuration limits .....	59
Figure 15 Diagram of a standard fire test room taken from BS EN 54-7 (2001)[1]. ....	60
Figure 16 Diagram of the standard room taken from the description in UL-268 [3]. ....	61
Figure 17 Schematic diagram of the FE/DE equipment described by Grosshandler .....	63
Figure 18 Cascade Impactor Principle.....	66
Figure 19 Sorption Tube operation.....	68
Figure 20 Schematic diagram of GC-MS system.....	71
Figure 21 Schematic of electron ionization mass spectrometry source.....	72
Figure 22 Diagram showing the path of created ions through quadrapole GC-MS .....	72
Figure 23 NDIR system for measurement on gas.....	74
Figure 24 Example image of an FTT supplied smoke chamber.....	76
Figure 25 TYCO Smoke Tunnel photograph .....	80
Figure 26 TYCO smoke tunnel dimensions .....	80
Figure 27 Design of UCLan. in-house fire test enclosure .....	83
Figure 28 Schematic of the device layout on the roof the UCLan fire enclosure. ....	84
Figure 29 Standard detector calibration run using joss sticks in TYCO smoke tunnel.....	90
Figure 30 Extended CO range 801PC calibration. ....	94
Figure 31 The figures show the response of the 7HYT sensor (V) to the increasing levels of hydrogen...95	
Figure 32 CO test of 7ETO sensor linked to MX device .....	96
Figure 33 Example 801PC temperature channel calibration .....	98
Figure 34 The figure shows the validation checks used for the NDIR device in the 2m3 UCLAN fire chamber . ....	99
Figure 35 Example of three-point calibration curve used for the analysis of humidity data Conversion of RH % to ppm. ....	101
Figure 36 Diagrammatic representation of fire product sampling set up for fire enclosures.....	104
Figure 37 Schematic for the TDCT injection system .....	107
Figure 38a Direct injection system Ready Position.....	110
Figure 39 Schematic of transfer of sample injected onto cotton wad in sample chamber to sorption tube. .....	113
Figure 40 Gas chromatogram from grob (II) standard onto Tenax sample tube. ....	116
Figure 41 Plot of moles of the measured analytes contained in injected volume of the test mixture. ....	117
Figure 42 Plot of moles of the measured analyte injected into the vapour trap and absorbed on Carboxen versus the GC/MS peak areas for each species. ....	118
Figure 43 Diagram of the BRE Watford BS EN 54-7compliant fire test room showing actual room dimensions, fire source position, and detector locations. ....	120
Figure 44 Equipment lay out in room over BRE test rooms for tests in May 2010.....	122
Figure 45 Test position grid on UCLan enclosure base .....	132
Figure 46 Example optical scatter responses from 7 TYCO fire detection devices to joss stick wad smoke for source location. ....	133
Figure 47 A graphical representation of the effectiveness of smoke generation/ transfer to detectors from each source site.....	133
Figure 48 Effect of floor to ceiling temperature differences on joss stick wad tests in UCLan enclosure	135
Figure 49 Example wooden crib schematic.....	137
Figure 50 Orientation of cotton wick samples in a self-burning chimney orientation (a) and a flat open orientation .....	138

Figure 51 Schematic diagram showing the location and size of the wood blocks used in the scaled smouldering wood experiments.....	141
Figure 52 Schematic diagram of the construction of wood cribs used in the scaled burning wood experiments.....	142
Figure 53 schematic diagrams of the cotton samples used in the scaled smouldering cotton fire experiments.....	143
Figure 54 Schematic diagram of the arrangement of samples burnt in the scaled burning polyurethane fires. The diagram also shows the location of the fire retardant polyurethane used in the mixed fuel sample tests.....	144
Figure 55 Schematic diagram of the polyurethane sample placement in the scaled fire enclosure test box.....	145
Figure 56 schematic diagrams of the scaled burning paper fire apparatus. n.....	147
Figure 57 Schematic of the smoking machine used in the scaled fire enclosure. ....	151
Figure 58 Measurements of CO by electrochemical (6th Sense Cell) and NDIR systems. ....	158
Figure 59 Obscuration versus time for 6 replications of TF2 (wood pyrolysis).....	160
Figure 60 CO and oxidizable gas (by 7EtO) concentrations versus time for 6 replications of TF2 (wood pyrolysis) e.....	160
Figure 61 Changes in CO <sub>2</sub> and O <sub>2</sub> concentrations versus time for 6 replications of TF2 (wood pyrolysis) Emulations in UCLan 2 m <sup>3</sup> Enclosure.....	160
Figure 62 Obscuration versus time for 6 replications of TF3 (cotton smoulder) Emulations in UCLan 2 m <sup>3</sup> Enclosure.....	161
Figure 63 CO and oxidizable gas (by 7EtO) concentrations versus time for 6 replications of TF3 (cotton smoulder) Emulations in UCLan 2 m <sup>3</sup> Enclosure.....	161
Figure 64 Changes in CO <sub>2</sub> and O <sub>2</sub> concentrations versus time for 6 replications of TF3 (cotton smoulder) Emulations in UCLan 2 m <sup>3</sup> Enclosure.....	161
Figure 65 Obscuration versus time for 6 replications of TF4 (Polyurethane foam burn) Emulations in UCLan 2 m <sup>3</sup> Enclosure.....	162
Figure 66 CO and oxidizable gas (by 7EtO) concentrations versus time for 6 replications of TF4 (Polyurethane foam burn) Emulations in UCLan 2 m <sup>3</sup> Enclosure.....	162
Figure 67 Changes in CO <sub>2</sub> and O <sub>2</sub> concentrations versus time for 6 replications of TF4 (Polyurethane foam burn) Emulations in UCLan 2 m <sup>3</sup> Enclosure.....	162
Figure 68 Obscuration versus time for 6 replications of TF5 (Flaming Heptane) Emulations in UCLan 2 m <sup>3</sup> Enclosure.....	163
Figure 69 CO and oxidizable gas (by 7EtO) concentrations versus time for 6 replications of TF5 (Flaming Heptane) Emulations in UCLan 2 m <sup>3</sup> Enclosure.....	163
Figure 70 Changes in CO <sub>2</sub> and O <sub>2</sub> concentrations versus time for 6 replications of TF5 (Flaming Heptane) Emulations in UCLan 2 m <sup>3</sup> Enclosure.....	163
Figure 71 Obscuration versus time for 6 replications of UL fire C (Flaming Heptane) Emulations in UCLan 2 m <sup>3</sup> Enclosure.....	164
Figure 72 CO and oxidizable gas (by 7EtO) concentrations versus time for 6 replications of UL fire C (Flaming Heptane) Emulations in UCLan 2 m <sup>3</sup> Enclosure.....	164
Figure 73 Changes in CO <sub>2</sub> and O <sub>2</sub> concentrations versus time for 6 replications of UL fire C (Flaming Heptane) Emulations in UCLan 2 m <sup>3</sup> Enclosure.....	164
Figure 74 Obscuration versus time for 6 replications of UL fire A (Burning Paper) Emulations in UCLan 2 m <sup>3</sup> Enclosure.....	165
Figure 75 CO and oxidizable gas (by 7EtO) concentrations versus time for 6 replications of UL fire A (Burning Paper) Emulations in UCLan 2 m <sup>3</sup> Enclosure.....	165
Figure 76 Changes in CO <sub>2</sub> and O <sub>2</sub> concentrations versus time for 6 replications of UL fire A (Burning Paper) Emulations in UCLan 2 m <sup>3</sup> Enclosure.....	165
Figure 77 Obscuration versus time for 6 replications of UL fire B (Flaming Wood) Emulations in UCLan 2 m <sup>3</sup> Enclosure.....	166
Figure 78 CO and oxidizable gas (by 7EtO) concentrations versus time for 6 replications of UL fire B (Flaming Wood) Emulations in UCLan 2 m <sup>3</sup> Enclosure.....	166
Figure 79 Changes in CO <sub>2</sub> and O <sub>2</sub> concentrations versus time for 6 replications of UL fire B (Flaming Wood) Emulations in UCLan 2 m <sup>3</sup> Enclosure.....	166
Figure 80 Obscuration versus time for standard TF2 (wood pyrolysis) at BRE (2 runs) and Emulations in UCLan 2 m <sup>3</sup> Enclosure.....	167
Figure 81 Carbon Monoxide (CO) versus time for standard TF2 (wood pyrolysis) at BRE (2 runs) and Emulations in UCLan 2 m <sup>3</sup> Enclosure.....	167
Figure 82 Obscuration versus time for standard TF3 (smouldering cotton) at BRE (2 runs) and Emulations in UCLan 2 m <sup>3</sup> Enclosure.....	168

Figure 83 Carbon Monoxide (CO) versus time for standard TF3 (smouldering cotton) at BRE and Emulations in UCLan 2 m <sup>3</sup> enclosure .....	168
Figure 84 Obscuration versus time for standard TF4 (Polyurethane foam burn) at BRE and Emulations in UCLan 2 m <sup>3</sup> Enclosure (Polyurethane foam burn) at BRE .....	169
Figure 85 Carbon Monoxide (CO) versus time for standard TF4 (Polyurethane foam burn) at BRE and Emulations in UCLan 2 m <sup>3</sup> enclosure .....	169
Figure 86 Obscuration versus time for standard TF5 (flaming heptane) at BRE and Emulations in UCLan 2 m <sup>3</sup> enclosure .....	170
Figure 87 Carbon Monoxide (CO) versus time for standard TF5 (flaming heptane) at BRE and Emulations in UCLan 2 m <sup>3</sup> enclosure .....	170
Figure 88 Obscuration versus time for 6 replications for Overheated PCBs in UCLan 2 m <sup>3</sup> Enclosure ..	171
Figure 89 CO and oxidizable gas (by 7EtO) concentrations versus time for 6 replications for Overheated PCBs in UCLan 2 m <sup>3</sup> enclosure .....	171
Figure 90 Obscuration versus time for 6 replications of mixed Polyurethane foam burns in UCLan 2 m <sup>3</sup> Enclosure .....	172
Figure 91 CO and oxidizable gas (by 7EtO) concentrations versus time for 6 replications of mixed Polyurethane foam fires in UCLan 2 m <sup>3</sup> enclosure .....	172
Figure 92 Changes in CO <sub>2</sub> and O <sub>2</sub> concentrations versus time for 6 replications of mixed Polyurethane foam burns in UCLan 2 m <sup>3</sup> enclosure .....	172
Figure 93 Obscuration versus time for 6 replications for Overheated Polymer Coated Wire in UCLan 2 m <sup>3</sup> enclosure .....	173
Figure 94 CO and oxidizable gas (by 7EtO) concentrations versus time for 6 replications for Overheated Polymer Coated Wire in UCLan 2 m <sup>3</sup> enclosure .....	173
Figure 95 Obscuration versus time for Overheating of a range of Cooking Oils (3 replications each) in UCLan 2 m <sup>3</sup> enclosure .....	174
Figure 96 CO and oxidizable gas (by 7EtO) concentrations versus time for Overheating of a range of Cooking Oils (3 replications each) in UCLan 2 m <sup>3</sup> enclosure .....	174
Figure 97 Obscuration versus time for 6 replications of Cigarette Smoking Tests in UCLan 2 m <sup>3</sup> enclosure .....	175
Figure 98 CO and oxidizable gas (by 7EtO) concentrations versus time for 6 replications of cigarette Smoking Tests in UCLan 2 m <sup>3</sup> enclosure .....	175
Figure 99 Changes in CO <sub>2</sub> and O <sub>2</sub> concentrations versus time for 6 replications of cigarette smoking tests in UCLan 2 m <sup>3</sup> enclosure .....	175
Figure 100 Obscuration versus time for 3 replications for toasted and re-toasted bread in UCLan 2 m <sup>3</sup> enclosure .....	176
Figure 101 CO and oxidizable gas (by 7EtO) concentrations versus time for 3 replications for toasted and re-toasted bread in UCLan 2 m <sup>3</sup> enclosure .....	176
Figure 102 Example changes in temperature for a range of fuels examined in the UCLan scaled enclosure. ....	179
Figure 103 GC/MS Chromatograms for material from carboxen tubes used for 6 replications of TF2 (wood pyrolysis) Emulations in UCLan 2 m <sup>3</sup> enclosure .....	182
Figure 104 GC/MS Chromatograms for material from tenax tubes used for 6 replications of TF2 (wood pyrolysis) Emulations in UCLan 2 m <sup>3</sup> enclosure .....	182
Figure 105 GC/MS Chromatograms for material from carboxen tubes used for 6 replications of TF3 (cotton smoulder) Emulations in UCLan 2 m <sup>3</sup> enclosure .....	183
Figure 106 GC/MS Chromatograms for material from tenax tubes used for 6 replications of TF3 (cotton smoulder) Emulations in UCLan 2 m <sup>3</sup> enclosure .....	183
Figure 107 GC/MS Chromatograms for material from carboxen tubes used for 6 replications of TF4 (Polyurethane foam burn) Emulations in UCLan 2 m <sup>3</sup> enclosure .....	184
Figure 108 GC/MS Chromatograms for material from tenax tubes used for 6 replications of TF4 (Polyurethane foam burn) Emulations in UCLan 2 m <sup>3</sup> enclosure .....	184
Figure 109 GC/MS Chromatograms for material from carboxen tubes used for 6 replications of TF5 (Flaming Heptane) Emulations in UCLan 2 m <sup>3</sup> enclosure .....	185
Figure 110 GC/MS Chromatograms for material from tenax tubes used for 6 replications of TF5 (Flaming Heptane) Emulations in UCLan 2 m <sup>3</sup> enclosure .....	185
Figure 111 GC/MS Chromatograms for material from carboxen tubes used for 6 replications of UL fire C (Flaming Heptane) Emulations in UCLan 2 m <sup>3</sup> enclosure .....	186
Figure 112 GC/MS Chromatograms for material from tenax tubes used for 6 replications of UL fire C (Flaming Heptane) Emulations in UCLan 2 m <sup>3</sup> enclosure .....	186
Figure 113 GC/MS Chromatograms for material from carboxen tubes used for 6 replications of UL fire A (Burning Paper) Emulations in UCLan 2 m <sup>3</sup> enclosure. Also shows results for green paper of type that may be found in washroom litterbin .....	187

Figure 114 GC/MS Chromatograms for material from tenax tubes used for 6 replications of UL fire A (Burning Paper) Emulations in UCLan 2 m <sup>3</sup> enclosure .....	187
Figure 115 GC/MS Chromatograms for material from carboxen tubes used for 6 replications of UL fire B (Flaming Wood) Emulations in UCLan 2 m <sup>3</sup> enclosure .....	188
Figure 116 GC/MS Chromatograms for material from tenax tubes used for 6 replications of UL fire B (Flaming Wood) Emulations in UCLan 2 m <sup>3</sup> enclosure.....	188
Figure 118 GC/MS Chromatograms for material from carboxen tube used EN54/7 TF3 (smouldering cotton) fire at BRE.....	189
Figure 117 GC/MS Chromatograms for material from carboxen tube used EN54/7 TF2 (smouldering wood) fire at BRE.....	191
Figure 119 GC/MS Chromatograms for material from carboxen tube used EN54/7 TF4 (Polyurethane foam burn) fire at BRE .....	190
Figure 120 GC/MS Chromatograms for material from carboxen tube used EN54/7 TF5 (Flaming Heptane) fire at BRE .....	192
Figure 121 GC/MS for material from carboxen tubes used for 3 replications of mixed polyurethane foam burns and a TF4 Emulation in UCLan 2 m <sup>3</sup> enclosure.....	191
Figure 122 GC/MS Chromatograms for material from carboxen tubes used for 6 replications for Overheated PCBs in UCLan 2 m <sup>3</sup> enclosure.....	191
Figure 123 GC/MS Chromatograms for material from carboxen tubes used for 6 replications for overheated PVC coated wire in UCLan 2 m <sup>3</sup> enclosure.....	192
Figure 124 GC/MS chromatograms for material from carboxen tubes used for overheating cooking oil tests in UCLan 2 m <sup>3</sup> Enclosure.....	192
Figure 125 GC/MS chromatograms from carboxen tubes used for 1 <sup>st</sup> 2 <sup>nd</sup> , and 3 <sup>rd</sup> Toasting operations replicated with 3 bread slices in UCLan 2 m <sup>3</sup> Enclosure .....	193
Figure 126 GC/MS chromatograms from carboxen tubes used for 2 <sup>nd</sup> Toasting operation in UCLan 2 m <sup>3</sup> Enclosure, with drying applied to absorbent media for slices 4, 5, and 6 .....	194
Figure 127 GC/MS chromatograms for tenax tubes used for 6 replications of 2 <sup>nd</sup> Toasting of bread slices in UCLan 2 m <sup>3</sup> Enclosure.....	194
Figure 128 Example chromatogram .....	197
Figure 129 Fragmentation pattern for benzene.....	202
Figure 130 Example of chromatogram taken from flaming polyurethane fire peak.....	203
Figure 131 Representative chromatogram for Carboxen captured sample from smouldering wood TF2 .....	205
Figure 132 Representative chromatogram for Carboxen captured sample from smouldering cottonwood TF3 emulation in UCLan enclosure.....	206
Figure 133 Representative chromatogram for Carboxen captured sample from polyurethane foam burn TF4 emulation in UCLan enclosure.....	207
Figure 134 Representative chromatogram for Carboxen captured sample from flaming heptane TF5 emulation in UCLan enclosure.....	208
Figure 135 Representative chromatogram for Carboxen captured sample from paper fire UL268 fire A emulation in UCLan enclosure.....	209
Figure 136 Representative chromatogram for Carboxen captured sample from flaming wood UL268 fire B emulation in UCLan enclosure.....	210
Figure 137 Representative chromatogram for Carboxen captured sample from flaming heptane UL268 fire C emulation in UCLan enclosure.....	211
Figure 138 Chromatogram for Carboxen captured sample from smouldering wood TF2 fire at BRE.....	212
Figure 139 Chromatogram for Carboxen captured sample from smouldering cotton TF3 fire at BRE.....	213
Figure 140 Chromatogram for Carboxen captured sample from polyurethane foam burn TF4 fire at BRE .....	214
Figure 141 Chromatogram for Carboxen captured sample from flaming heptane TF5 fire at BRE .....	215
Figure 142 Representative chromatogram for Carboxen captured sample from PCB heated on hotplate in UCLan enclosure. ....	216
Figure 143 Representative chromatogram for Carboxen captured sample from PVC covered wire heated on hotplate in UCLan enclosure.....	217
Figure 144 Representative chromatogram for Carboxen captured sample from a flaming polyurethane foam fire in UCLan enclosure.....	218
Figure 145 Representative chromatogram for Carboxen captured sample from overheated vegetable oil in UCLan enclosure.....	219
Figure 146 Representative chromatogram for Carboxen captured sample from overheated olive oil in UCLan enclosure.....	220
Figure 147 Representative chromatogram for Carboxen captured sample from overheated cooking fat in UCLan enclosure.....	221

Figure 148 Images of toast representing 0-3 toasting experiments .....	222
Figure 149 Representative chromatogram for Carboxen captured sample from first toasting of bread slice in UCLan enclosure. ....	223
Figure 150 Is a representative chromatogram for Carboxen captured sample from second toasting of bread slice in UCLan enclosure. ....	224
Figure 151 Is a representative chromatogram for Carboxen captured sample from third toasting of bread slice in UCLan enclosure.....	225
Figure 152 Is a representative chromatogram for Carboxen captured sample from second toasting of bread slice in UCLan enclosure.....	226
Figure 153 The figure represents those components captured and eluted from Carboxen sample tubes.....	227
Figure 154 Representative chromatogram for Carboxen captured sample from green paper (wash room hand towel type). ....	228
Figure 155 Representative chromatogram for Tenax captured sample from smouldering wood TF2 emulation in UCLan enclosure. ....	230
Figure 156 Representative chromatogram for Tenax captured sample from smouldering cotton TF3 emulation in UCLan enclosure. ....	231
Figure 157 Representative chromatogram for Tenax captured sample from polyurethane foam burn TF4 emulation in UCLan enclosure. ....	232
Figure 158 Representative chromatogram for Tenax captured sample from flaming heptane TF5 emulation in UCLan enclosure. ....	233
Figure 159 Representative chromatogram for Tenax captured sample from burning paper UL268 fire A emulation in UCLan enclosure. ....	234
Figure 160 Representative chromatogram for Tenax captured sample from flaming wood UL268 fire B emulation in UCLan enclosure. ....	235
Figure 161 Representative chromatogram for Tenax captured sample from flaming heptane UL268 fire C emulation in UCLan enclosure. ....	236
Figure 162 Representative chromatogram for Tenax captured sample from 2 <sup>nd</sup> Toasting of bread in UCLan enclosure. ....	237
Figure 163 Example chromatogram for Tenax captured sample from cigarette carried out in UCLan enclosure.....	238
Figure 164 Example plots of the mass spectra acquired from experimental results compared to the GC-MS spectra from standard library taken from NIST web book .....	240
Figure 165 Response of different types of detectors described in table 62 to 5 joss sticks and 0.2m/s airflow in TYCO smoke tunnel. ....	245
Figure 166 Composites of calibration runs carried out in the Sunbury smoke tunnel .....	246
Figure 167 Composite of calibration runs. The “normalised” signal was plotted versus signal from TYCO device.....	249
Figure 168 Multiple calibration values from blue, UV LEDs fire detection devices .....	250
Figure 169 Multiple TF2 in UCLan enclosure “normalised” signal V. std. signal (add. 17).....	251
Figure 170 TF2 emissions collected during scaled UCLan experiments .....	251
Figure 171 Multiple TF3 UCLan emulations “normalised” signal versus signal from standard TYCO device(add. 17) .....	252
Figure 172 TF3 emissions collected during scaled UCLan experiments .....	252
Figure 173 Multiple TF4 UCLan emulations “normalised” signal versus signal from standard TYCO device (add. 17) .....	253
Figure 174 Multiple TF4 emissions collected during scaled UCLan experiments .....	253
Figure 175 Multiple TF5 UCLan emulations “normalised” signal versus signal from standard TYCO device (add. 17) .....	254
Figure 176 Multiple TF5 emissions collected during scaled UCLan experiments .....	254
Figure 177 Pyrolysing Wood (TF2 emulation in smoke tunnel).....	255
Figure 178 Full scale smouldering wood TF2 experiment carried out at BRE.....	256
Figure 179 An example smouldering wood fire (TF2) data collected during BRE experiment .....	256
Figure 180 Full scale smouldering cotton TF3 experiment carried out at BRE.....	257
Figure 181 An example smouldering cotton fire (TF3) data collected during BRE experiment .....	257
Figure 182 Full scale smouldering cotton TF4 experiment carried out at BRE “normalised” signal versus signal from standard TYCO device(add. 17).....	258
Figure 183 The recorded data collected during BRE a single experiment flaming polyurethane (TF4) fire .The Blue & UV LED detector outputs are converted into a ratio of “normalised” output: TYCO Standard device (add. 17) signals Vs. (bit-ped) from standard TYCO device( add. 17).....	258
Figure 184(a) Full scale smouldering cotton TF5 experiment carried out at BRE “normalised” signal versus signal from standard TYCO device(add. 17), (b) Ratio of normalised UCLan output data:output from standard TYCO device( add. 17) Vs. standard TYCO device (bit-ped) output ( add. 17).....	259

Figure 185 The recorded data collected during BRE a single experiment flaming heptane pool fire (TF5) . Blue & UV LED detector outputs are converted into a ratio of “normalised” output: TYCO standard device (add. 17) signals Vs. (bit-ped) from standard TYCO device( add. 17).....	260
Figure 186 Diagram shows how the stages of the cascade impactor are constructed. ....	262
Figure 187 Particulate mass concentrations versus size For BS EN54/7 fire emulations. ....	264
Figure 188 Particulate mass concentrations versus size For UL268 fire emulations and bread toasting. ....	264
Figure 189 Particulate number concentrations versus size For BS EN54/7 fire emulations.....	265
Figure 190 Principle of FAIMS Operation (a) effect of field on mobility, (b) application of pulsed asymmetric field to selectively deflect ions to filter electrodes. ....	266
Figure 191 Representation of FAIMS Filter Operation.....	267
Figure 192 Representation of Display of FAIMS Spectra with Ion current shown on 3d graph or as false colour scale(b) . ....	267
Figure 193 FAIMS Instrument operating to collect spectra for gases in TYCO smoke tunnel. ....	268
Figure 194 Example clear air plot from capillary file prior to the collection of smoke from standard fire . The blue background display is the positive ion trace and the red background image on the right represents the negative ions produced after the gas is passed through the ionization source. ....	269
Figure 195 The figure represents the FAIMS response (a) to clear air, (b) to material in smoke during a pyrolysing wood fire in the Sunbury smoke tunnel, and (c) to a full scale TF2 fire in the BRE test room. ....	270
Figure 196 The figure represents the FAIMS response (a) to clear air, (b) to material in smoke during a smouldering cotton wick fire in the Sunbury smoke tunnel, and (c) to a full scale TF3 fire in the BRE test room. ....	271
Figure 197 The figure represents the FAIMS response (a) to clear air, (b) to material in smoke during a polyurethane foam burn in the Sunbury smoke tunnel, and (c) to a full scale TF4 fire in the BRE test room. ....	272
Figure 198 Results from regulated inlet to a FAIMS device in clean air (a) and smoke from a flaming polyurethane fire in the Sunbury smoke tunnel (b). Figure C is the FAIMS response from a full scale TF4 test at BRE. ....	273

## ACKNOWLEDGEMENTS

I would like to thank the ESPRC for supplying the funding for this project in collaboration with TYCO. I would also like to thank the staff of University of Central Lancashire (UCLan) for their and time with the project. In particular I would like to thank Professor T R Hull, Micheal Ward, Stephen Harris and John Milnes.

I would also like to thank Dr John Shaw of TYCO Fire Protection Products for his infinite patience and help in getting this thesis complete and also his and his familys kind hospitality on my visits to TYCO in Sunbury.

Finally I would like to take the opportunity to thank my wife for her patience and understanding. I know we have been over a lot in the last three years and I know you have always been there for me. I would also like to thank her for reminding me that anything is possible if you really want it. I love you sweetheart.

## ABBREVIATIONS

UL – Underwriters Laboratories  
BS - British Standard  
IR – Infer Red  
CO – Carbon Monoxide  
CO<sub>2</sub> – Carbon Dioxide  
HCN – Hydrogen Cyanide  
C- Carbon  
H- Hydrogen  
O – Oxygen  
S – Sulphur  
Cl – Chloride  
Q<sub>a</sub> - Heat release  
T – Temperature  
T<sub>s</sub> – Fractional Transmission  
FAIMS – high Field Asymmetric Ion Mobility Spectrometry  
MEMS – Micro Electro Mechanical Systems  
ppm – Parts per million (gas concentration)  
PPM – Parts Per Million Accuracy in Mass Spectrometry  
UCLan – University of Central Lancashire  
m – Absorbance index  
dB – Decibels  
OD – Optical density  
P - Radiated power  
%Obsc/m –% Obscuration per meter

## INTRODUCTION

This study is directed at characterising airborne emissions of fires (e.g gas, aerosol, identities, concentrations, time evolution) at the early stages, relevant to detection. A primary target is characterisation of standard test fires used for detector approvals (BS EN 54-7:2001 [1] and UL 217 [2], [3]) but interest extends to scenarios beyond test standards including electrical pyrolysis events, and identified false alarm stimuli (e.g. tobacco smokes, cooking fumes). While products from well developed fires have been well documented, relatively little research has been directed at identifying products other than smoke and CO from early stage fires or the standard test fires. This is an impediment to rational innovation in fire detection.

When conceived it was envisaged that the project would be primarily directed at characterising fire gases. However aerosol (smoke) generation is an important aspect of nuisance fires and a major factor in their detection, and many possible fire gases may be involved in exchange with smoke particles. The study therefore includes some measurements related to smoke detection and characterisation.

Modern fire detection systems are commonly based on measurements of one or more of heat, smoke, or CO emissions often with fuzzy logic algorithms. Current fire detection systems are in fact quite effective in providing alarms for most real fire scenarios. However even with combinations of these measurements avoidance of false alarms can require alarm thresholds to be set higher than may be desirable. This arises from the range and variability of real fires, and of false alarm stimuli such as dust, mists, steam, engine or cooking fumes, and heat from controlled source. In principle this situation could be improved if more fire specific target measurements could be identified. This study is aimed at determining whether any such targets exist and can be identified, and in particular at investigating gas and vapour emissions from early stage fires as potential targets.

## **Organisation of Study and Thesis**

The investigation involves a number of stages covered in chapters of this thesis.

**Chapter 1** addresses the background and existing knowledge base on fire, fire development, fire chemistry and products, and fire detection. This background review includes reference to fire product types (smoke particles, gasses/vapours), and false alarm stimuli as their effects on the fire detection industry and detection products. The operation of conventional detectors is covered along with the means for detector validation (test fires).

**Chapter 2** presents fire product measurement means and specific sensing and detectors and systems used in this study, with particular emphasis on application of GC/MS to gas/vapour analysis. Other detectors and analytical systems are introduced with some detail on their use in the study. The test environments used are described including the full scale standard fire test room along with introduction of issues involved in emulating at reduced scale a series of standard detector validation test fires, and some false alarm stimuli. Operating protocols for the sensing and analytical systems are provided.

**Chapter 3** deals with the detail of generating reduced scale emulations of test fires in a 2 m<sup>3</sup> chamber including description of fuels, and equipment for containment, and means of ignition.

**Chapter 4** presents a subset of the test results for the series of reduced scale test fires and some non-standard fires and false alarm stimuli and with results of a short study with full scale test fires. The parameters covered in chapter 4 include measurements of optical obscuration by smoke (conventionally used to define validity of test fires), measurements of some gases by electrochemical or IR systems ( CO, oxidisable gases, CO<sub>2</sub>, O<sub>2</sub> ), and GC elution time plots from the GC/MS system. Results for multiple tests of each type are presented.

**Chapter 5** covers analysis of the GC/MS results including identification of mass fragments for peaks from elution plots for examples tests, and where appropriate indication of the molecular species present.

**Chapter 6** covers results from application of some supplementary analysis systems to scaled or full sized tests. These include:

- Optical scatter measurements from conventional and experimental detectors over near infrared and visible blue wavebands for smoke in reduced and full scale tests.
- Particle size analysis using impactor measurements for smoke in reduced scale tests.
- FAIMS measurements for vapours from full scale fire tests and reduced scale emulations in a smoke tunnel.

**Chapter 7** includes summary and some further analysis of the results and presentation of conclusions.

## **CHAPTER 1 BACKGROUND AND OVERVIEW**

### **1.0 History and impact of fire detectors and detection**

Unwanted fires are dangerous and destructive events that are costly in terms of both lives and property. Since the mid 1970s there has been an increase in the use of automated fire detection systems [4]. Automated fire detection systems, smoke detectors in particular, have been credited as the single most influential technological advance in reducing the number of fire deaths [5]. From a commercial standing they represent a cheap and effective way to prevent loss of property and materials by early detection of fire especially in unmanned remote facilities.

Industrialists looking to protect their property facing spiralling financial losses first used fire detectors. Before automated fire detection systems, companies relied on roaming fire watchmen. As population centres increased the areas which these watchmen would patrol would grow larger and larger. Early watchman had to detect and personally raise a response from typically volunteer/part time fire fighters in the event of fire. The introduction of the telegraph made communication easier, but it was not until 1863 Alexander Ross developed the first automated fire detector. This was incorporated a self-restoring bi-metallic heat detector marketed as the "Watkins Thermostat". The Underwriters Bureau of New England endorsed this [6]. The Underwriters Bureau like the equivalent Fire Officers Committee (FOC) in the UK was established in the 1800s. Both organizations were comprised of mainly representatives of most of the major fire insurers in the UK and USA. The main purpose of both organizations was to set insurance tariffs for various classes of trade. The FOC began publishing codes of practice and these codes quickly became established the world over as best practice for fire safety. Organizations complying with these codes would receive a reduction in insurance costs. When the FOC and Underwriters Laboratories (UL) began approving fire detection systems, the purpose for the FOC never really changed from the initial conception. As result the published codes focused more on the loss of property and materials rather than the loss of life. This began to change in the UK when the British Standards Institution (BSI) issued their codes of practice in 1951 CP 327.404/402/501 where protection of life became a priority, and where the specialist nature of fire detection systems was finally fully recognized. [7]

## 1.1 Fire Processes and Properties

Fire, is understood as sustained oxidative process operating on a fuel with emission of heat conveniently and is described with reference to the fire triangle (Figure 1) which presents the components (fuel, oxygen, and heat) required for starting and sustaining fire.

At early stages of fire, heat may be supplied as an ignition source such as overheating electrical circuit, spark, or existing flame (match). Fires may be flaming where gaseous fuel components react

though they may originate from vaporisation, pyrolysis or partial oxidation of solid or liquid fuels.

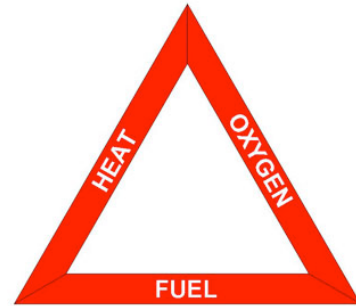


Figure 1 Triangle of combustion

Smouldering fires involve reaction directly in the body of usually porous solid fuels. For the purposes of this thesis the interest is fire, combustion and flame processes related primarily to unwanted or nuisance fires rather to controlled combustion in heating equipment and engines, and interest is most particularly in the early stages where fires may not have yet reached a self sustaining condition. Thus pyrolysis which may lead to fire but is essentially primary break down of fuel by heat is included.

Fire processes generate products which include heat and materials generated by the action of heat and the oxidative reactions on the fuel which include full and partial oxidation products, particulates and condensates (smoke). These products may form the basis for fire detection. A key aspect determining which fire products are formed is the type of combustion.

### 1.1.1 Types of combustion in fires (flaming, smouldering, stoichiometry)

Self-sustaining fires may be divided into smouldering and flaming modes though fires may switch between these modes.

In flaming combustion gaseous fuel (or at least fuel dispersed in the air) undergoes rapid oxidation generating sufficient heat to sustain reaction and generally to produce radiation making the flame visible [8]. This occurs with a gaseous fuel or in gaseous fuel produced above the surface of a solid or liquid fuel by pyrolysis or evaporation of that fuel.[9]

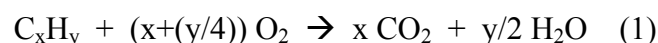
Smouldering combustion occurs at surfaces on or within a porous fuel body. Smouldering combustion can propagate in porous materials if they are amenable to transport of gases (fuel and oxygen). Porous bodies may be relatively insulating reducing heat loss from the fire site allowing slow but self-sustaining growth of the fire. Gas borne pyrolysis products from a smouldering fire may eventually become involved in generation of a flaming fire.

Pyrolysis process on a solid fuel maintained by an external heat source may proceed in a way similar to a smoulder fire. They may terminate if the heat source is removed or develop to smouldering or flaming fires.

Another difference in these forms of combustion is the temperatures involved. In flaming combustion the temperature of the flame can be as high as 1000°C or more whereas sustained smouldering combustion generally occurs at around 600°C.

In statistics published by the NFPA(National Fire Protection Agency) [10] they predicted that 55% of deaths associated with fires occur due to smouldering fires because these involve oxygen supply limited combustion with generally incomplete fuel oxidation and produce a great deal of toxic carbon monoxide. In addition they are very difficult to detect at an early stage as smoke aerosol generation is limited and may be filtered out by the fuel body or surrounding material. Further the restricted thermal output from smouldering fires can limit formation of buoyant plumes in the surrounding air and consequently not facilitate transport of fire products to detectors[11]

Combustion products from fires depend on the reaction stoichiometry i.e. whether sufficient oxidant is available in hot reaction zones to complete reaction to fully oxidised products (CO<sub>2</sub> and H<sub>2</sub>O for simple hydrocarbons and cellulose) as indicated for a stoichiometric oxidation in equation 1 below;



Equation 1 Stoichiometric oxidation of hydrocarbon

In complete combustion where there is sufficient oxygen present C and H from the fuels can be oxidized entirely. Entrainment of air may introduce other products into the plume and at sufficiently high temperatures nitrogen from the air may also be involved in formation of NO<sub>x</sub> species as minor products.

Oxygen may be abundant but local concentrations within fires influence the products generated. Controlled mixing, achieved in efficient burners or incineration equipment, may not occur in nuisance fires. Although complete combustion may occur in some flaming fires, both smouldering and flaming fires can lead to incomplete combustion. The degree of combustion will affect the range of products, which may be observed. When oxygen deficient conditions occur within the fire a wide range of products can potentially occur but generation of significant amounts of carbon monoxide CO is generally observed [12] and CO to CO<sub>2</sub> yield ratios are to some extent characteristic of fire stoichiometry and fuel and types [13][14]

### **1.1.2 Development of Fires**

Development of flaming fires may be divided into a series of stages. Where fuel and oxidant (air) are present, ignition generally involves some energetic input eg, a flame or glowing ember, heating (e.g. electrical, frictional) or spark. Ignition in some fires in porous fuel bodies e.g coal dust, organic liquid contaminated rags, can arise spontaneously due to initially slow exothermic reactions accelerating as heat build up in thermally insulating conditions.[15]

Ignition processes have been examined in the literature and a homogeneous system of ignition related to the collision theory of molecules developed by Semenov [16]. Heterogeneous ignition theory was proposed by Frank-Kamenetskii [17] and essentially requires an outside body to be involved in ignition, e.g. a match or other heat source. Certainly for uncontrolled nuisance fires the ignition events or inputs are unplanned and undesired and may be too small or obscured to provide useful detection targets in themselves.

Following ignition there are various stages of fire development. For solid fuels such as wood or polymer, development of a flaming fire involves a series of distinct but

overlapping stages. These include preheating distillation or gasification, and char formation. The fire progresses by a feedback process where heat from the existing reaction passes by radiation, conduction or convection to the fuel bed generating mobile reactive products, which feed and maintain the fire. If insufficient heat transfer occurs to the fuel, or suitable fuel becomes unavailable then the fire dies out. The type of fuel and the environment will dictate how the fire develops. Figure 2 shows the components in the development of a flaming fire on a solid fuel such as wood or polymer. In some cases char formation may not occur where a polymer undergoes simple thermal depolymerisation to inflammable vapours and then the situation is akin to that for a flammable liquid fire where evaporation of the liquid provides gaseous fuel for the flame.

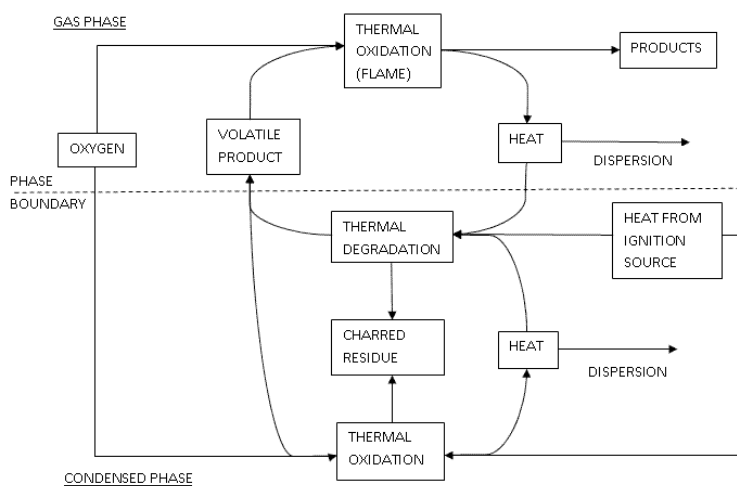


Figure 2 Overview of typical processes occurring in the early stages of polymer combustion.

In the preheating stage, which may be driven by some external heat source or existing fire, vapours and water are driven off from the fuel by a distillation/thermolysis process, and at this stage typically include quite large molecular products forming smokes and generating the odour commonly associated with the burning fuel. The preheating stage is a point where a great deal of energy is lost through the evaporation of moisture and vapours and in some cases conduction through the fuel. This is a major energetic hurdle for combustion. The preheating stage may proceed until the fuel is heated to a point referred to as the flash point. At the flash point the vapours above the fuel have reached sufficient concentrations and temperature to react rapidly with oxygen in the air generating a flame, which will be maintained if sufficient fuel vapours continue to be supplied.

Gasification occurs when there is sufficient heat to start decomposing larger molecules thermally. The resultant products are typically smaller and more volatile. Gasification typically involves the making and breaking of covalent bonds and this involve either consumption or generation of energy (endothermic and exothermic reactions). Where oxidation reactions occur as part of the gasification this will normally result in heat release (exothermic).

An important stage for many fuels is the formation of char [18], a carbon structural form that protects the surface of the fuels, helps retain heat and provides a catalytic surface at which gasification/ oxidation reactions can proceed at an accelerated rate. The formation of the char may precede the production of some of the more flammable products and provides an interface in which oxidant may reach and react with the fuel molecules.

In the development of combustion reactions involving oxidant and the fuel leading to a fire, the oxidant is typically oxygen but other oxidants may support combustion e.g. fluorine, nitrates etc. For the mass of nuisance fires oxygen is the oxidant due to its abundance in the atmosphere and the relative ease of formation of dioxygen based free radicals, which can be involved in development of free radical reactions prevalent in flaming combustion.

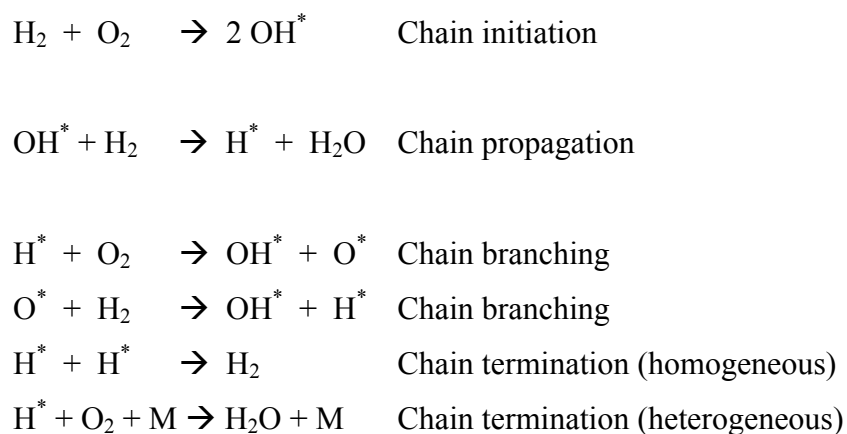
### **1.1.3 Flames and free radical chemistry**

A flame is a region where gaseous fuel reacts rapidly with oxidant gas (oxygen). Flame form and luminosity depends on the flow and mixing of reactants. Hot oxygenated flames are characterised by molecular radiation while incandescence of particulates generally generated in oxygen deficient regions yields broadband, often yellow, emissions. The prevailing theory regarding development of gas phase combustion and flames is the free radical chain reaction theory. This is explained in detail in a number of academic texts [19,20]. Free radicals having unpaired electrons represent higher energy states are much more reactive than stable molecules. The higher energy means reactions will proceed via lower energy pathways than are available for combinations of more stable molecules. When free radicals react with an electronically stable molecule then the process generally generates one or in some cases more than one new free radicals. These types of reactions are referred to as propagation, branching or initiation

reactions. When two free radicals react to produce an electronically stable product this is referred to as a termination reaction. Free radical propagation may also be terminated by interaction of radicals with solid surfaces including smoke.

When reactions form products with release of energy (exothermic reactions) this energy may be fed back into the system to drive additional reactions. A key feature of a fire is whether it is self sustaining and depends on the combination of continuing availability of fuel and oxidant, energy release and relative rates of free radical chain initiation, propagation and branching reactions, and of chain termination reactions.

Lilly [21] gives an overview of the combustion and ignition processes important reactions for the ignition of hydrogen in air. The corresponding processes for a hydrogen flame are illustrated in equation 2:



Equation 2 Chain Reaction Stages

For hydrocarbons and other carbon containing fuels, including products of solid fuel pyrolysis, the processes are similar but more complex involving a wide range of free radical species [22].

Carbon containing free radicals, especially in oxygen depleted conditions can be involved in polymerisation processes generating larger molecules and smoke,[23] and peroxy radicals (R- or H-OO\* not indicated above) have been reported to be involved [24],[25].

## **1.2 Fire Products (airborne materials)**

Fire products is a term used to describe the material produced by oxidative combustion of a fuel. These include vapours, particulates, smoke, decomposition products, gases and water.

### **1.2.1 Particulate (Smoke)**

Particulates are formed during incomplete combustion of organic fuels. The type of smoke depends both on fuel type and the type of fire. Non flaming conditions as in smouldering or fuel pyrolysis generates vapours which include higher molecular weight species which if they escape the combustion zone cool and condense into fine droplets forming a mist or usually pale or grey smoke, with particle sizes of the order of  $\sim 1 \mu\text{m}$ .

Particulates from flaming fires are generally solid material resulting from pyrolysis and incomplete combustion with relatively high carbon content though usually lacking a clear graphitic structure. Polyaromatics and polyacetylene particles are believed to be precursors that agglomerate to form small particles, which may be  $0.1 \mu\text{m}$  or less the smoke appears black [26].

Both white and black smokes may absorb some of the lower molecular weight volatile materials and this accumulation of other components is potentially a mechanism for the loss of many of the combustion gases available for detection. Benzene and the other PAH components observed in early gases are thought to be lost through absorption onto these particles.

Measurements to quantify smoke generation other than particle collection methods include smoke opacity measurements, and effects on conductivity of ionised air. Both smoke obscuration and ion mobility effects form the basis mechanisms used to characterise fires and define acceptance criteria for standard fires.

### **1.2.2 Gases and Vapours**

Full combustion of simple organic fuels leads predominantly to formation of  $\text{CO}_2$  and  $\text{H}_2\text{O}$ . In investigations aimed at understanding the properties of materials, which may burn, measurement of these species, and particularly of  $\text{CO}_2$  are required. However both

CO<sub>2</sub> and H<sub>2</sub>O are present at substantial levels in normal air and those levels, in confined spaces at least, vary for reasons quite unconnected to the incidence of nuisance fires.

Oxygen limitation to the combustion is almost invariably present in part of any nuisance fire and so products of incomplete combustion are to be expected. Carbon monoxide CO has been identified in a wide range of nuisance fire scenarios although there are some cases where early generation can be quite low (overheating electrical circuits causing pyrolysis of polymers in PCBs and some other components). Jackson and Robins studied the generation of CO [12]. CO is considered the primary precursor to CO<sub>2</sub> formation by a free radical reaction with OH\* and any fire region where supply of OH\* is depleted is likely to lead to survival and release of CO. Background concentrations of CO are usually 1ppm or less, although tobacco smoking and vehicle emission can increase this, though rarely beyond 10 ppm. Levels of CO of 30 ppm or more are considered in the fire detection industry as good indicators of fires. Given the toxicity of CO, where exposure can result in death quite rapidly, detection of levels above ~200 ppm even if not related to nuisance fires, can be considered of real value.

It has been suggested that hydrogen might be a significant fire product and useful detection target. Hydrogen is present in the environment with ambient levels in the 1-5ppm levels. Some free radical termination processes could at least conceivable lead to hydrogen generation but evidence for hydrogen as a combustion gas away from the fuel bed is mixed. The group involved in the study by Jackson and Robbins had high sensitivity selective hydrogen sensors available (Pd gate FET devices) and reported significant levels in some fires, but they concluded that levels were not sufficiently high or common across fire types to form a useful detection target. Pfister [27] and Amamoto [28] carried out further tests in wooden houses where they determined that hydrogen was present at up to 20ppm levels. This work indicated hydrogen response in large building fires seemed to be faster than for CO and CO<sub>2</sub>. However in small laboratory tests it was found the response varied, being largest in under ventilated conditions and as the temperatures increase.

Other gases have been identified as fire products, especially where they relate to toxicity. Some such as HCN with elements present other than C, H, and O have been significantly studied in relation to occupant survival. HCN can be formed from incomplete combustion of nitrogen containing polymers such as polyurethanes. Given

that fuels containing significant non C,H,O content such as S, Cl constitute only a subset of available nuisance fire fuels, their utility as detection targets is limited. It is detection of a fire that is needed rather than fuel or fire classification, and any useful detection target must be general enough to be generated irrespective of the presence of non C,H,O fuels.

The range of volatile compounds which potentially could be generated by the combustion, pyrolysis, and evaporation of hydrocarbons, cellulosics, and other C,H,O containing fuels is very wide. The gases produced from fires have been studied in some detail driven by the desire to investigate the toxicity of smoke [29]. Some of the gases have key roles in the early combustion process and others lead to the formation of other fire products including soot and fire vapours. Some studies have used IR techniques to identify products but while this has worked under conditions where products are formed at high concentrations e.g. some cone calorimeter experiments for material characterisation, at low concentrations to be expected early in fire growth the data reported tends to be limited to recognition of presence of C-H, or C-C bonds without identifying particular species. [30]

A group of candidate target gases is provided by a GC/MS study of cellulose pyrolysis in air and nitrogen at temperatures from 400°C to 800°C reported by Sakuma [31].

Those recorded as appearing at >3mg/g cellulose at 500°C in air are reported in table 1.

Candidate target gases in Cellulose (500°C)	Observed conc.(mg/g)
Acetaldehyde	15.7
Acrolein	20.8
3-Buten-2-one	3.7
Furan	4.6
2-Furaldehyde	3.4
Furan-2-5-dialdehyde	5.5
2-Buten-4-olide	3.6
Acetic Acid	4.8
5-hydroxymethyl-2-furaldehyde	7.8
1,4:3,6-Dianhydro $\alpha$ -D-glucopyranose	5.7

Table 1 : Gas concentrations reported in the literature from cellulose pyrolysis study at 500°C [31].

At 800°C those components were largely absent but aromatic hydrocarbons became significant (table 2).

Candidate target gases in Cellulose (800°C)	Observed conc.(mg/g)
Benzene	14.6
Toluene	4.9

Table 2 : In the pyrolysis study [31] only 2 gases were observed in high concentrations at temperatures above 800°C, which is consistent with other observations .

It is not clear that the data presented by Sakuma is a full inventory and the absence of some smaller molecules may reflect an artefact of the analytical system. Many of the identified products have high molecular weights and will have low volatility and as such are likely to be unavailable for gas sensing due to condensation or absorption on smoke.

There is a mass of literature identifying generation of polyaromatics in smokes and even within flames of simple hydrocarbons. Much of this literature motivated by health concerns concentrates on tobacco smoke but the products are clearly more widespread. Many measurements of combustion-generated polyaromatics involve fluorescence detection. Some laser induced fluorescence (LIF) measurements have been applied in free air, flames, and exhausts from combustion sources. Figures 3a and 3b below are from a web site maintained by Zizak [32].

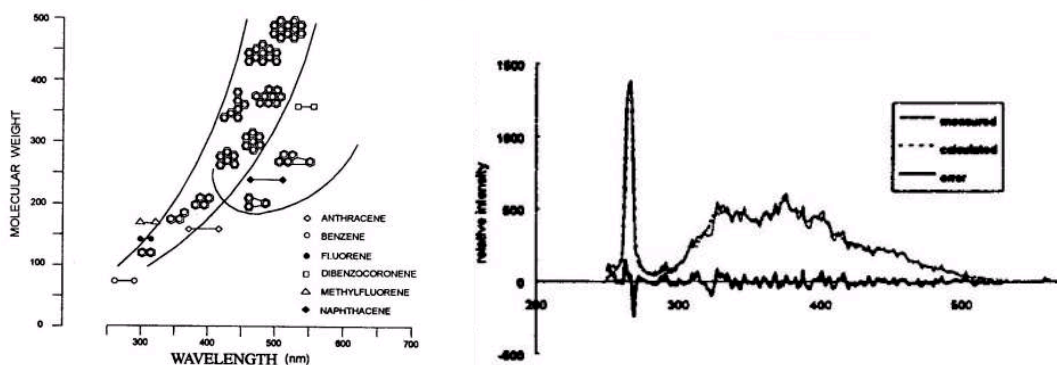


Figure 3 Polyaromatics formation in combustion identified by laser induced fluorescence. Figure 3a fluorescence shift PAH size, and 3b LIF measurements on Fiat exhaust

While the mass of measurements on smoke have first involved liquid extraction of the polyaromatics. Pinnick [33] has reported direct measurements of fluorescence on tobacco smoke ascribed to polyaromatics.

Acrolein (2-propenal) and has an unpleasant “burnt” odour and has been identified as a product from burning fossil fuels and cigarettes [34] It has been identified as one of the possible fire components that can be detected with MEMS electronic nose arrays such as the Karlsruhe micronose Kamina [35]

A study [36] of wood stove emissions, perhaps more relevant to flaming and relatively well ventilated conditions indicated formaldehyde, acetaldehyde, and acetone as most significant products, though acrolein, propanal, crotonaldehyde, and 2-butanone were indicated as of significance and reported to be present from cited work.

Characteristic products relating to biomass burning were investigated by Simoneit [37] but concentrated on larger molecular weight species and in particular levoglucosan, for which low volatility is an impediment to sensing in the gas phase.

### 1.3 Heat Release and Product transport

Heat is generated by the exothermic oxidation reaction in a fire. Its release from fires is evidenced in two major aspects of fire. Heat is released as radiant energy. This may be broadband from surfaces including fuel and non-gaseous products (smoke, embers), and as specific bands e.g. from hot CO<sub>2</sub> at ~4.3μm. This and some other wavebands are used in specialised flame fire radiation detectors. Heat is also released by conduction through air and particularly non-gaseous phases, including fuel beds, and particularly by convection in fire plumes. Energy transferred to product particulates and gases produces a fire plume, the extent of which depends on buoyancy forces arising from density of hot gases being lower than that of the surrounding air.

One of the definitions of a fire compared to non-fire event is based on thermal balance. The thermal balance is an assessment of the energy requirement to volatilize more reactants from the bulk fuel and the energy lost to the environment compared to the energy produced in the system (equation 3).

$$E < E_{\text{reaction}} - (E_{\text{Vol}} + E_{\text{rad}} + E_{\text{conv}}) \quad (3)$$

Equation 3 Thermal energy balance

$E_{\text{reaction}}$  is the thermal energy available in the system from the reactions in the combustion zone.  $E$  is the energy required to sustain combustion,  $E_{\text{Vol}}$  is the energy required to volatilize the fire products,  $E_{\text{rad}}$  and  $E_{\text{conv}}$  are energy losses from radiative and convection heat sources.

If reactions produce more energy than is lost, then the fire develops and is self-sustaining if not then self-extinction can occur.

As fires develop and produces heat at an increasing rate, which is transferred into the plumes, the plume is accelerated upwards away from the fuel bed. Plume transport has been the subject of much research and fire model development, including use of computational fluid dynamics (CFD) codes. It is common practice to locate fire detectors on the ceiling protected areas. This is based on the simple principle that heat rises, or in more depth, on the assumption that when fires develop they produce more heat energy and this is transmitted into the plumes that is then accelerated upwards away from the fuel bed. Relationships have proposed for plumes linking rate of heat output from a fire to variation of temperature with height. Some of this material is summarised by Drysdale [38] Simplifying assumptions may be made and applicability of these expressions to weak plumes near onset of fire and especially for obscures smouldering sources, nevertheless such expression can provide some guidance relevant to scaling of fire tests. Temperature with a plume falls as the plume rises due partly to entrainment of adjacent air and formulae reproduced by Drysdale for ceiling mounted temperature sensors indicate a relationship of the form (equation 4).

$$Q_a = c. \Delta T.H^{2.5} \quad (4)$$

Equation 4 Drysdale equation for ceiling mounted temperature detectors

Where  $Q_a$  is heat output rate required for alarm,  $\Delta T$  is a temperature rise at a detector, and  $H$  is the height from the fire source. This impacts on time for detection. If detection for a room 2 m high requires ~ 100 watt source, a 4m high room requires ~ 600 watt source.

## 1.4 Earlier Studies on Fire development and products relevant to Detection

Prior work [39] [40] [41] and the existing literature relating to fire detection [42] provides a significant amount of information on physical characteristics of smoke and a little on gases, especially carbon monoxide [43] but little useful for identifying organic vapours which may be potential detection targets. Much more information has been available for well-established fires and controlled combustion situations <sup>44</sup>but its *relevance to the early* stages of fire important for successful detection is not established. A project aim is to reveal information on chemical species evolution from incipient/early stages fires. Such information may determine whether it is practical to differentiate between various fire types and false alarm events e.g. cooking toast. In addition to deployment of smoke detectors and a limited range of gas sensor systems the work is intended to help identify other species present, particularly by application of GC/MS to collected sample.

The issue of fire source identification and more commonly false alarms has cost and safety impacts on fire detection, on detector manufacture and installation companies, their customers, and not least on the fire service, the resources of which are significantly impacted by the rate of response to invalid alarms. Intelligent selection and deployment of sensors has been impeded by poor information on relevant fire product characteristics.

The progress of developed fires and the products generated have been widely studied as they are of importance to building and occupant survival. Whilst ignition in controlled conditions as in gaseous fuel streams and in engines is well researched and understood, the issues for very early stage nuisance fires relevant to detection is less well covered. Toxicity studies of fire products and smoke related to survival and escape has driven a great deal of research on specific fire gases. However much of this is limited to concentrations having physiological effects [45]. There also has been some interest in gases evolving in the early stages of fire, but only for specific gases [46]. Some of these gases including CO, HCN are used as indicators of fire gas toxicity while CO/CO<sub>2</sub> ratio [47] provide an indication of fire type/oxygen depletion. Limitations in the range of products identified have arisen from use of sensors of low or limited specificity and only very limited use of spectroscopic methods capable of identifying species at low concentrations. Further components present at the early stages of fire development may

be consumed in secondary combustion reactions or absorbed onto surfaces or into aerosols (smoke) [48][49].

For example small organic molecules such as acetone may be generated as initial products in hydrocarbon oxidation or fuel pyrolysis but then may be fully oxidised to CO<sub>2</sub> and H<sub>2</sub>O or may be precursors in further reactions forming larger molecules, which may include polyaromatics (PAH), which can then react or condense into soot particles.

A study of fire gases from reduced scale fires which included GC/MS analysis was carried out under a European programme and some results published by Persau [50]. The programme was principally directed at gas sensing of fires using conducting polymer based sensors and contains only selective information on the range of molecular species found. FTIR measurements did indicate presence of acetic acid, ethanol, formaldehyde, ethane, and toluene. A series of more complex molecules were indicated as markers for some specific fires/combustion sources.

There have been many studies on fire products from relatively well controlled sources including diffusion flames on gaseous fuels. Smith [51] proposed a model that was intended to reliably predict major gas yields with time. Their model, based on the turbulence in a diffusion flame, predicted that the gas evolution of the major species (CO<sub>2</sub>, O<sub>2</sub>, CO) vary dependent on both the heat release rate and turbulent mixing component of plumes.

## **1.5 Fire Detection Technology and Testing**

The range of fire products allows different methods to be considered for fire detection. Primarily fires have been detected by heat, presence of smoke, presence of gas, and radiative emissions. Whatever the form of detection, all detectors must be able to access some fire output and detect a signal indicative of a fire. There have been a range of good reviews on the subject including the 30 year review published by the Boston deputy fire chief Joseph Fleming. [52]

Fires detection relies on measurement of some emission from the fire source. This may use radiation from the fire/flame, or the temperature or constituents (smoke, gases) of the surrounding air body or fire plume. Flame detection by means of radiation from hot

gases (especially CO<sub>2</sub> at ~4.3 μm) is a specialised area relevant to the protection of specific installations (oil processing and storage plant) and not covered in this study.

For detectors responding to material fire products (smoke, gases) there is a requirement that these products transfer to a detection site. This is overwhelmingly a matter of air movement or convection. Diffusion although aiding local transport is ineffective alone in providing timely response over more than cm distances. The main mechanism of transport in fire plumes is convection. In air the movement of particulates by diffusion is extremely limited. Local diffusion may occur within the plume, and in the case of some gasses, this can mean specific components may transfer locally from the plume (especially for small mobile gases such as CO or CO<sub>2</sub>).

Flaming fires are often detected earlier because the fire products are rapidly transmitted to the detector, as the fuel typically has a greater rate of energy output capable of powering a buoyant plume. Smouldering fires are more difficult to detect because a plume may not develop or is slow moving because of the low rate of energy input.

The location of typical fire detectors, according to common practice is to place detectors on the roof of the protected area. This is based on the simple principle that heat rises due to effects on air density.

Detectors for protection of most commercial and residential properties rely on detection of one or more of temperature, smoke, and gases, particularly CO. Heat (temperature) sensors, most usually based on thermistors in modern products are more widely deployed, have high reliability and low susceptibility to generation of erroneous signals (false alarms) but generally require that a fire source becomes relatively well developed before it can be detected. They are useful in specific sites where temperatures are normally closely controlled e.g. for computer server rooms where detection of very small changes in temperature is adequate, with one such system having been developed by Ericson (monitoring temperature in controlled environments [53]). Temperature detectors are not considered the best choice in the domestic or general work environments unless other detectors (smoke, gases) are prone to generate false alarms e.g. in kitchens.

Some locations require installation of specific types of detectors. These include optical obscuration detectors for smoke where long path lengths are available, as in atria, and aspirated systems where air sampling flows are piped to very sensitive detectors (usually for smoke particulates). However the overwhelmingly most important and widespread industrial and residential fire detection systems are the point detectors, usually ceiling mounted. Predominantly these employ smoke detection technologies, though the use of CO sensing for fire detection is becoming more widespread. It is becoming commonplace for point detectors to combine at least two (smoke and temperature) sensors, and often three, (smoke, CO, and temperature) sensors and to use combinations of signals, and rates of change, to recognise fire conditions and generate alarms.

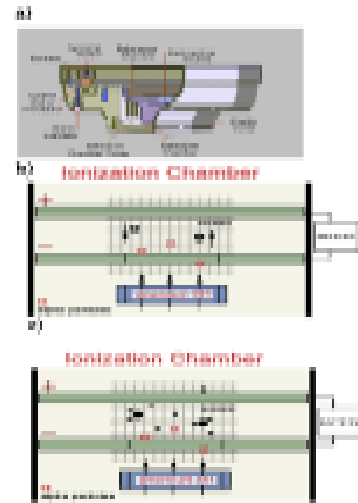
The smoke sensors used in point detectors are normally “ionization” detectors, or optical detectors as described below. Although detection using gases other than CO has been proposed for some specialised environments, the mass of point detectors using detection of fire gases rely on CO detection technology.

### 1.5.1 Ionization Smoke detectors

Figure 4 represents an ionization device, and the ionization chamber function as described by Litton [54].

Figure 4 (a) cut a way of a typical detector. 4 (b) ionization chamber in the clear state. In this state the ionization source ionizes the gases in the air generating a current between the two plates unit.

4(c) particulates (smoke) from a fire absorb/ take up charge from ionized gases. The lower mobility of the relatively massive (as compared to molecular) particles results in less current flowing which triggers an alarm.



Ionization detectors presently are the cheapest type of smoke detector. Each has a small (~ 0.2 mg) radioactive source emitting alpha particles (Americium 241). The detector comprises a chamber where the alpha particles cause ionization of the air furnished with electrodes passing a current through that air. The detection chamber has openings allowing ingress of air, and smoke in the case of fire. Smoke particles pick up ions/charge from the air and being very much more massive than the original ions this decreases the current through the air. It is this decrease in current, which stimulates an alarm. In practice there are usually two ionisation chambers where smoke cannot enter the second reference chamber and the electronic sensing of the decrease in current in one in response to smoke ingress is sensed as a differential effect on the electrode potentials.

Ionization devices are known to respond rapidly to fast developing flaming fires that give off dark grey and black smokes [55]. They are sensitive to particle numbers and respond well to very small particles (< 1  $\mu\text{m}$  ). Commercial devices achieve adequately high sensitivity at the cost of low dynamic range and are susceptible to false alarms. There are also environmental concerns about the disposal of the Americium. In itself it is not a major pollutant but it is radioactive with a half-life of 470 years. In conjunction with other detectors and controlling algorithms ionization devices have a role in

commercial devices [56], but their susceptibility to false alarms and issues with deployment of radioactive sources mean that they are becoming less favoured in commercial establishments at least.

The high incidence of fires attended where such devices have been disconnected show these devices are prone to false alarms and it is argued that ionization smoke detectors do not provide a sufficient level of survivability in domestic environment as they respond slowly to smouldering fires. In 2006 a court in Indianapolis prosecuted First Alert and BRK awarding a family \$2.8 million damages because the ionization smoke alarm did not give the advertised levels of protection [57].

### **1.5.2 Optical Smoke detection devices**

When light is incident on a particle it can either be absorbed, reflected, refracted and diffracted. If the light incident on the smoke particle is of a sufficiently larger wavelength than the size of the particles then all modes of reflection can be observed. When the wavelength is of a similar size to the smoke particles then the different mechanisms of reflection cannot be differentiated and so is referred to as scatter.

Measurements of smoke density may be made either by measurements of obscuration (attenuation of a light beam passing through the smoke) or by measurement of light scattering by smoke. The obscuration measurement range appropriate to fire detection requires significant path lengths ( $\sim 1$  m) and the method is not well suited to compact point detectors (available light path of a few cm). It has niche applications in real detection scenarios but is routinely deployed as a standard method for validating test fires as indicated in a section below. Although light scattering can contribute to attenuation of light beams, the physics of light absorption and scattering are different and while correlations may be established for particular smoke sources no rigorous mathematical conversion exists.

Light scattering by smoke is well suited to compact point detectors. While measurements of light scattering by particulates are an established way of characterising such materials with a developed theoretical base (Rayleigh and Mie scattering), these theories and corresponding mathematics are probably of limited utility at the concentrations relevant to smoke detection where a significant measurement volume is

employed, multiple scattering for is probable, and particle sizes and shapes are uncontrolled. Nevertheless optical scatter based point type smoke detectors are firmly established as reliable devices for fire detection [58]. Below is a diagrammatic representation of an optical scatter type point detector (figure 5).

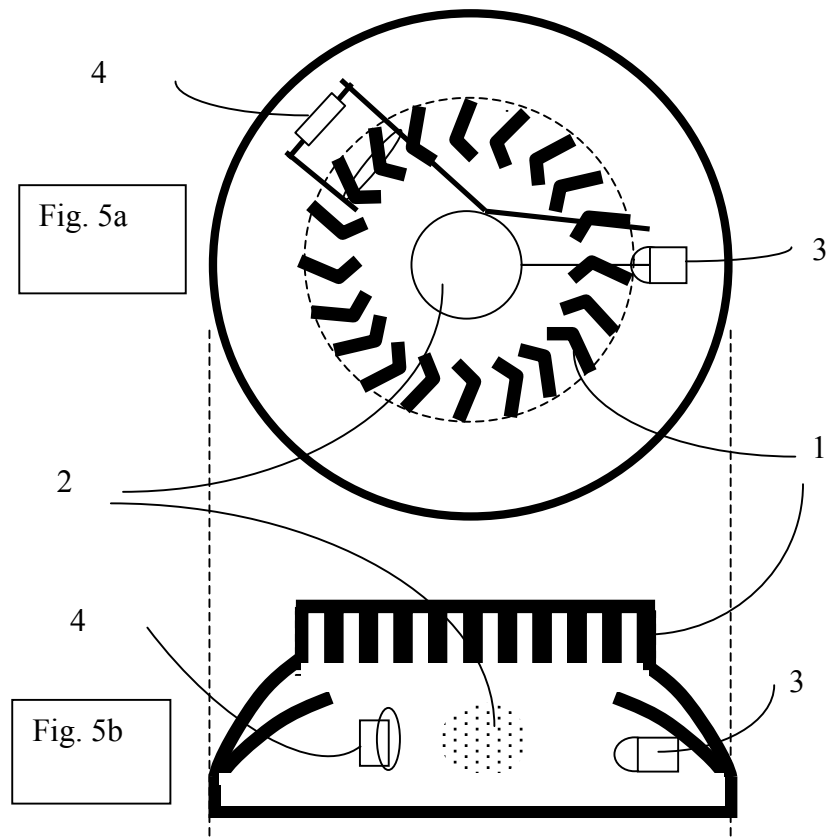


Figure 5 Optical Scatter Detector layout – 5a) Plan view, 5b) side view.

The chamber has vents 1 allowing air to pass to the interior and a detection volume 2 defined by intersecting regions illuminated by LED 3 and the field of view of photosensor 4

Light from LED 1 passes though detection volume and in the absence of smoke most is absorbed or scattered by the chamber walls with little falling on the photosensor positioned off of the beam line. When smoke enters the detection region, part of the light from the LED is scattered towards the photosensor with resultant increase in sensor signal. Conventionally the LED is operated in a short pulsed mode (<1ms every ~5 seconds). Until recently LEDs emitting in the near IR (~850 nm) were used but there are some moves towards (additionally) using blue LEDs (~465 nm) as it has been suggested on the basis of some experimental work and Mie scattering theory that this may give size discrimination capability [59].

Design of the housing around the detection region is crucial to enable smoke ingress without allowing interference from external lights. Sometimes marketed as “toast proof” [60] optical scatter devices are most sensitive to pale or grey smokes, which are typically smokes produced by pyrolysis or from smouldering e.g. from smouldering sources like fabrics. A feature of the optical scatter devices is that Mie theory suggests different smokes respond differently depending on the size, shape, and refractive index of the smoke particulates.

### **1.5.3 Temperature sensors**

Point heat detectors monitor the changes in the ambient temperature via at least one thermistor or other temperature sensor. Paired detectors in and out of ambient airflow may be used to counter issues with slow changes in ambient temperatures triggering false alarms. Alarm criteria for temperature sensor based fire detectors fall into two categories. Fixed-point detectors can be triggered if the temperature rises above a preset value. Common temperature thresholds range from 47-58°C. Rise of heat (RoH) detectors respond to a rapid rise in temperature above baseline. The rate of increase typically needed by a RoH alarm is typically between 6.7-8.3°C min<sup>-1</sup>. Common environmental effects that are associated with false alarms do not influence temperature sensors; dust, insects etc. They can respond to nuisance sources such as opening ovens, heat ducts or steam.

The use of heat detectors as a primary mechanism to detect fires is not favoured in residential properties and hotels. Temperature sensors used in these situations will typically invoke an alarm response to a fire, but the size and type of a fire required to produce a temperature change sufficient to invoke an alarm is often substantial and may not be sufficiently early to ensure survival of occupants. Temperature sensors are widely deployed where smoke sensors are prone to false alarms or where their exposed components are subject to damage by the environment (marine use). They are routinely included with smoke detectors as back up or use in combined sensor alarm algorithms.

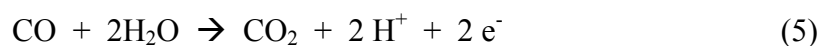
### 1.5.4 Carbon monoxide gas sensors

The first commercial CO fire detector was released in 1999 by ADT. Electrochemical sensors typically sense CO concentration by an oxidation process.

CO sensors can react promptly to slow developing smouldering fires involving carbon rich fuels. Although in fires the main mechanism of transport of fire products is convection, because CO is a highly mobile gas it is thought it is able to diffuse quickly to point detectors. This means CO can move ahead of the plume and provide rapid fire detection. This is particularly useful in slow developing or low energy fires.

The use of CO gas sensors in fire detectors is governed by BS ISO 7240-8:2007 [61]. CO sensors however are not the most rapid to respond rapidly to flaming fires. They have some susceptibility to false alarms from environmental factors involving release of oxidisable vapours, though for moderately short term emission events this issue is effectively dealt with by including of activated carbon filters as in the Honeywell 6<sup>th</sup> Sense electrochemical CO sensors widely employed in fire detection systems. Processes which actually generate CO such as cigarette smoking and operation of combustion equipment or engines in poorly ventilated spaces can give rise false alarms as can emissions of other small easily oxidised hydrocarbons (acetylene, ethane).

Electrochemical CO sensors of the type widely used in fire detection operate by monitoring the current corresponding to the oxidation of CO molecules that diffuse to the sensing electrode. The cells are run in amperometric mode and the current is proportional to the diffusion-limited rate of CO molecule arrival at the electrode. CO is consumed by the reaction, which may be written as (equation 5):



Equation 5 Overall Oxidation Reaction for CO in Electrochemical Cell

Each CO molecule oxidised to CO<sub>2</sub> provides two electrons to the external circuit. Water and hydrogen ions are in the cell electrolyte. Figure 6 is a diagrammatic representation of a two electrode (sensing and counter) electrochemical CO sensor employing platinum electrodes and a sulphuric acid electrolyte. The sensing Pt electrodes consist of

Platinum black adjacent to a gas permeable PTFE membrane not wetted by the acid electrolyte.

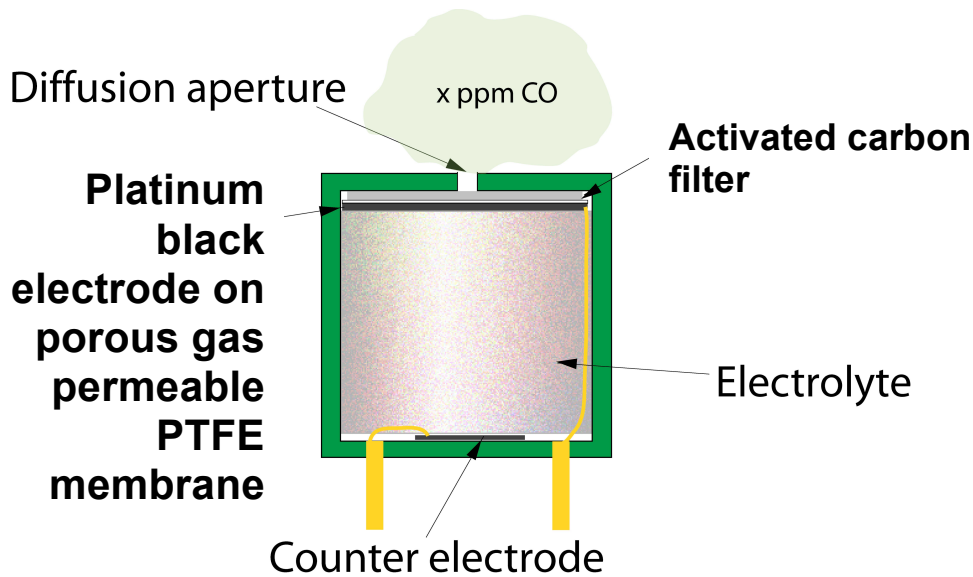


Figure 6 Diagrammatic representation of electrochemical CO sensor.

CO diffusion to the electrode is limited by the small orifice at the top of the cell and filter structures and the dimensions of these components effectively set the sensitivity,  $\sim 45$  nA/ppm CO for the Honeywell 6<sup>th</sup> Sense devices.

### 1.6.5 Multi criteria Fire Detectors

These newer types of detection system look to offer the best possible combination of increased sensitivity to actual fires while reducing the incidence of false alarms. They take in data from more than one source (e.g. carbon monoxide, optical scatter, temperature) and applying these inputs in suitable algorithms can generate more discriminatory alarms. A variety of simple and complex algorithms have been applied by commercial detector system producers and this has included some use of fuzzy logic.

Recently Cleary [62] performed a study, investigating the potential improvements observed in response time and the response to false alarms using dual ionization/photo detectors compared to individual ionization and photo detectors. The dual detectors used an OR logic algorithm where the alarm would be triggered if either the photo optic or the ionization detector reached their alarm thresholds. The devices were tested in two different settings using simulations of real fires rather than full or reduced scale

standard tests. The study also reported on a small study carried out by the NRCC in 2003 [63] using off the shelf dual detectors.

The finding of the study was not conclusive. In some instances improvements in time to alarm were observed, but often the standard error encountered in measuring the time to alarm was comparable to of the actual measurement. The size of this error may be related to the relatively small sample size but often the fires being detected comprised of a mixture of fuels and combustion processes (e.g. smouldering and flaming combustion). In some of the tests there was also some uncertainty as to the sensitivity of the component types of the combined detector.

The present study while including use of some multifunction detectors is set up to access individual sensor responses and is not aimed directly at validating multi-criteria operation or algorithms used for this purpose.

### **1.5.6 Use of fire detectors in this study.**

The study is primarily directed at applying analytical techniques, especially GC/MS, to characterise fire products. However to aid future possible correlation of the results with practical existing detector devices it was deemed appropriate to include a series of standard commercial detectors as produced by TYCO and operate these with a system designed to emulate operation of a fire panel and output the data to Excel readable files. The detectors have been used to investigate and validate the behaviour of the scaled fire emulations but are also used as tools to investigate the behaviour of standard and non standard fires.

The outputs from the sensors incorporated in the detectors are provided as 8 bit digital outputs and the standard detector types used were TYCO MX system 801 series detectors as below:

801PH – Optical scatter (850nm), and temperature (thermistor) outputs.

801PC – Optical scatter (850 nm), temperature (thermistor), and CO outputs.

801I – Ionisation smoke detectors.

Additionally some experimental detectors were used which were constructed using modified 801 series units and providing outputs to the same panel simulation and data storage based equipment. These units included device with different LEDs and photosensors to allow scatter measurements at different wavelength, including blue LED emissions (465 nm). Some devices incorporated both blue and standard NIR (850 nm) and blue (465 nm) in the same detector addressing the same detector volume. Additional single Led devices were used to supply scatter information on a longer NIR wavelength (1070 nm), and a near UV wavelength (370 nm).

A further 801 series unit was converted to give %RH output and another as a 3 channel A to D unit allowing some analogue signals to be converted and stored on the same log files as the data from the standard 801 series devices.

The dynamic range within the 8 bit output for the CO detectors in 801PC devices covered the range from 0 to a maximum of ~120 ppm CO. One unit was converted so that the CO output dynamic range was extended up to ~400 ppm.

Before supply for use in equipment at UCLan (Preston), 801 series were checked and calibrated at the TYCO laboratory in Sunbury. CO calibration was carried out using calibrated CO in air supplied by BOC or Air Liquide and where appropriate a gas blender unit (Signal Model 821). Temperature sensor operation was checked in a heat tunnel at a relatively slow (n°C/min.) temperature rise. Operation of optical scatter devices was checked using a smoke tunnel and joss sticks as smoke sources.

## **1.6 False Alarms and Detection Reliability.**

Fire detection systems are not infallible. As recently as 1986 one researcher, Cooper [64] stated fire detection systems simply did not work, and the belief that fire detectors were unreliable and only useful as a supplement to a watchman system to compensate for failings in building design was common only 20 years ago. Improvements in standardized testing and codes of practice regarding both the installation and manufacture along with changes in government legislation have improved performance and perception and seen widespread deployment of alarm systems, but nevertheless incidence of false alarms remains high.

According to 2006 UK fire statistics [65] of all fire emergency calls responded to, 65% or 283,800 were false alarms, which could be directly attributable to automated fire detection systems. In greater Manchester alone in 2007 of the 13,500 emergency calls initiated by automated fire detection systems only 60 required the deployment of equipment [66]. The Chief of Greater Manchester fire services stated his force spent 97,000 man-hours responding to false alarms in 2007. This has a cost .The example in greater Manchester in 2007 cost the taxpayer more than £2,000,000, and there were additional losses due to by disruption to business. More importantly it costs finite resources, while units are responding to false alarms they cannot also be attending real fires where lives are at risk.

Importantly false alarms reduce confidence in fire alarms and can lead to users becoming complacent, ignoring fire alarms or simply turning alarms off. Assuming alarms to be false alarms is dangerous; and in some cases it can be catastrophic. Edwards [67] highlights the issues of complacency around false alarms at Faslane and Coulport, two of the UKs Naval facilities that host the nuclear warheads for the UK trident deterrent.

Most fire authorities and local councils give advice to reduce false alarms [68]. Such steps include regular maintenance of alarms, proper sighting of alarms away from sources of dust and steam, not allowing smoking near detectors etc. Advice also includes not leaving cooking oil unattended, though that is as much about avoiding real fires. While cooking oils and fumes can produce false alarms [69], equally unattended cooking oil can very quickly become a real fire.

A false alarm is defined by the Colins dictionary as:

Noun *a needless alarm given in error or with intent to deceive, or an occasion on which danger is perceived but fails to materialize.*

There a number of scenarios that may result in a false alarm. These include ;

1. Pollutants in the air setting off smoke detectors;
2. Extremely high temperatures (from equipment or weather effects) setting off heat detectors;
3. Vandalism or malicious acts;
4. Errors in using the system;
5. The equipment being faulty or poorly maintained;
6. Fire detectors or red 'break glass' boxes being in the wrong place; and
7. The fire-detection system not being appropriate for the building or how it is used;
8. Inappropriate activities in protected areas such as cooking, toasting outside kitchens.

Figure 7 shows that despite technical improvements, a rising proportion of the false alarms are ascribed to apparatus malfunction. Greater system complexity may play a role in the increase in false alarms from automated fire detection systems (more things to go wrong). Nevertheless there are issues relating to how the detectors detect fires.

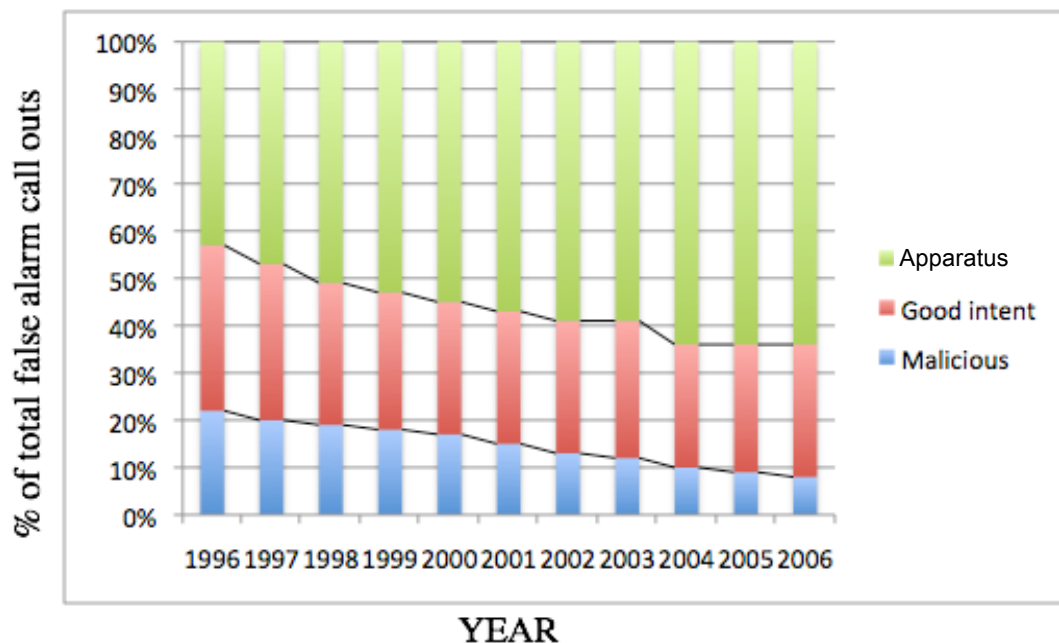


Figure 7 10 year survey of the causes of false alarms in the UK looking at the source of the call outs which were discovered as false alarms. (Source UK GOV figures)

Some of the most common sources of false alarms are cooking fumes, smoking, dust, burning toast [70], steam and other aerosols. The positioning of detectors, and

selection of detector types can eliminate some of these sources, but can also increase true detection times and reduce protection. Some sources of false alarms e.g cigarette smoking, may reduce as society changes and different practices become more or less accepted. However eliminating specific sources does not overcome the issue that the detectors employ what can be relatively non-specific sensors [71].

Standards that have been established for validation of fire detectors try to eliminate factors limiting detector response. (e.g. EMC interference effects, protection from some larger objects entering detection volumes), but there is no general agreement on defining tests against false alarm stimuli. There has been some research and generation of literature, especially in relation to fumes generated by cooking [72] but generally work has gone no further than that.

Part of the problem is being able to replicate false alarm stimuli under laboratory conditions. For example steam is a potential false alarm signal. Hoteliers often complain that steam from showers in particular invoke a large number of false alarms. However steam induced false alarms have often proven difficult to reproduce in the laboratory but recent work has led researchers to believe the type and persistence of steam droplets is dependant on local environmental condition, ventilation, and availability of condensing surfaces. [73]

So this highlights an issue in the proposed work. In presenting data on some scale simulation of false alarm stimuli as well as real or potential fires, the results were largely limited to measurements using sensors conventionally applied in detection and give a little insight as to means that would enable discrimination between true and false alarm conditions

### **1.6.1 Cooking fumes**

Cooking related incidents are amongst the most significant false alarms leading to fire services call outs. Xie [74] performed a study, using FE/DE (section 1.8.1) to investigate responses of common detector types to cooking fumes establishing that ionization detectors were most prone to false alarms though optical scatter devices can not reasonably be described as immune to cooking based stimuli. Cooking produces smoke

particulates, vapours and gases which depend on the food being cooked and mode of cooking, or over cooking. and the method of cooking.

Gas burners, and to a lesser degree electrical hobs, have associated with formation of NO<sub>x</sub> gases which from a background of 0.2- 0.5ppm can rise with a 4 ring kitchen gas burner to 1-3ppm [75] .

Example cooking processes identified as causing false alarm issues are toasting, and heating of cooking oils and fats. Cigarette smoking is a further known false alarm cause.

### **1.6.1.1 Toasting**

Toasting bread can produce a number of products, both vapour and particulates. Overheating especially of crumbs on toaster elements can lead to more extreme effects and triggering of alarms particularly for ionization detectors.

Toasting involves dehydration, caramelization, maillard browning reactions and eventually oxidation. Bread is mostly made up of carbohydrates (starches and some cellulose), simple sugars and proteins. Caramalisation involves the direct thermal decomposition of sugars above 120°C and may contribute to the formation of polyaromatic hydrocarbons along with simple combustion products that are formed by the stepwise oxidative thermal decomposition of the sugars.

### **1.6.1.2 Cooking oil**

All cooking oils are triglycerides where glycerol is attached three long hydrocarbon chains (fatty acids). As the temperature increases the oil is subject to oxidation and polymerisation reactions and likelihood of ignition and progression to a real fire increases. Oil chemistry affects the progress of reactions and the temperature at which smoke generation occurs (smoke point) as indicated in table 3 below

Type of Fat/Oil	Typical Saturated fat content	Typical Monosaturated fat content	Typical polyunsaturated fat content	Smoking point
Butter	66%	30%	4%	150
Lard	41%	47%	2%	138-201
Coconut Oil	92%	6%	2%	177
Corn Oil	13%	25%	62%	236
Olive Oil	14%	73%	11%	190
(Extra Virgin)				
Olive Oil (refined)	14%	73%	11%	225
Sesame Oil	14%	43%	43%	232
Sunflower Oil	11%	20%	69%	246

Table 3 Smoke points of typical oils and fats [76]

### 1.6.1.3 Cigarettes

Because of the health concerns cigarette smoke is probably the most widely researched of all the environmental smoke with estimates of the numbers of identifiable compounds greater than 2000. Amid other aromatic species, presence of Benzo{a}pyrene was identified by Copper and Lindsey [77]

## 1.7 Detector Validation, Standard Test fires

Series of standard fire tests have been developed for functional validation of detectors. While these fires are not grossly unrepresentative of real fire scenarios they are constrained by a need to be carried out rapidly and reproducibly. This probably means they may not adequately cover conditions corresponding to slow growth smouldering fires.

All the standard tests have specific requirements with respect to fuel types, quantities, test room dimensions and conditions. Further individual test validity has to be confirmed by measurements of smoke with instruments of defined type and location. Most generally the specified test equipment employs optical obscuration, with characteristics of light source, photosensor, and separation provided in the standards. These provisions differ between standard bodies e.g. UL268 require a specific incandescent light source while the EN54/7 standard specifies a near infra-red source (LED). Specialised ionization based smoke detectors (MICs) may also be specified.

These function broadly in the same way as commercial point type ionization smoke detectors but have induced air flow and narrowly defined geometric constraints. They have a wider effective dynamic range than commercial ionization detector devices.

Although MICs are deployed at many standard test houses and one is in use for operation in a smoke tunnel at the TYCO R&D laboratory in Sunbury, their relative expense and operational requirements meant that one was not available for deployment at UCLan.

Smoke measurement by optical obscuration requires a light path from source to photosensor. Photosensor output when there is clear air and no obstruction in the light path corresponds to 100% transmission (0% obscuration), while complete obstruction of the light path corresponds to 0% transmission (100% obscuration). The devices specified are expected to give a linear output between transmission and photosensor output and that is assumed correct i.e. 2 point calibration is deemed adequate. The UL268 standard specifies an incandescent bulb and a selenium photoresistor sensor. These are archaic devices, and the selenium devices difficult to source. No doubt this system will be replaced at some point and no attempt was made to emulate it in this study at UCLan. The wavelength of the light used in BS EN 54-7 has the following requirements;

1. At least 50% of the radiated power shall be within a wavelength range from 800nm to 950nm.
2. Not more than 1% shall be in the wavelength range below 800nm.
3. Not more than 10% shall be in the wavelength range above 1050nm.

The requirements are met readily available LED sources and well matched Silicon photodiode detectors which are essentially similar to those used in most commercial optical scatter smoke detectors.

The standards differ in the way the photosensor output is processed to yield a parameter taken as the measure of density of fire aerosols in the detector light path. BS EN54/7 uses units dB/m and UL 268 % Obscuration per foot. The Beer Lambert Law is assumed to apply for light passing through smoke and mathematically these parameters are interconvertible. However, where differently specified light sources and sensors are

used, as for the EN and UL standards) the values even for identical smokes will not necessarily correspond exactly.

The BS-EN standard characterizes the optical properties using an absorbance index of the smoke aerosol measured in the path length of the detector.

The absorbance index is designated  $m$  is measured in  $\text{dB m}^{-1}$ , and defined by the expression:

$$m = (10 \cdot \log(P_o/P_s))/d \quad (6)$$

Equation 6 Expression for absorbance index ( $m$ )  $d$  is the optical path length in meters (m),  $P_o$  is the radiated power received without smoke aerosol,  $P_s$  is the radiated power received with smoke aerosol

The ratio  $P_o/P_s$  is  $1/T_s$  where  $T_s$  is the fractional transmission which is calculated from the photosensor output by the expression:

$$T_s = (v_s - v_b)/(v_c - v_b) \quad (7)$$

Equation 7 Expression for fractional transmission  $v_c$  is photosensor output for clear air,  $v_b$  is photosensor output with light path blocked, and  $v_s$  is photosensor output with smoke between source and photosensor

UL standards describe the optical properties of the aerosol in terms of the optical density per unit length, defined by the expression:

$$OD = (\log(P_o/P_s))/d \quad (8)$$

Equation 8 Optical density calculation of smoke density. OD is optical density per unit length,  $d$  is the optical path length,  $P_o$  is the radiated power received without smoke aerosol,  $P_s$  is the radiated power with smoke aerosol.

Common usage for the UL standard in particular allows expression of smoke density in a more immediately understandable units, % obscuration per unit length (usually per foot in the usage in USA, but per metre is commonly used). In this study smoke densities will normally be expressed as % obscuration/metre and conversion to this unit of values expressed as the absorbance index  $m$  in  $\text{dB/m}$  and optical density per unit length OD (as in the standards) is by the expressions below.

Converting %Obsc/ m (% Oobscuration per meter) from  $m$  dB/m

$$\%Obsc/m = 100.(1-10^{(-m/10)}) \quad (9)$$

Equation 9 Expression to convert %Obsc/m from  $m$

Converting %Obsc/m from optical density per metre ( $OD_m$ )

$$\%Obsc/m = 100.(1-10^{(-OD_m/100)}) \quad (10)$$

Equation 10 Expression to convert obscuration per meter (%Obsc/m) from optical density per meter  $OD_m$

Converting Optical density per foot ( $OD_f$ ) to %Obsc/m

$$\%Obsc/m = 100.(1-10^{(-0.3048.OD_f/100)}) \quad (11)$$

Equation 11 Expression to convert obscuration per meter (%Obsc/m) from optical density per foot ( $OD_f$ )

For experimental work where fractional transmission  $T_s$  is obtained from beam sensor measurements with path length  $d$  metres using equation 9 above, conversion from obscuration (%Obsc/m) to transmission is by the expression 12;

$$Obs. \% / m = 100.(1-10^{(d-1. \log T_s)}) \quad (12)$$

Equation 12 Expression converting %Obsc/m from fractional transmission  $T_s$

For the ionization type (MIC) smoke sensors, a dimensionless parameter  $y$  is used to quantify the fire aerosols. This parameter  $y$  is calculated from the MIC ion current values using the expression:

$$y = (I_o/I) - (I/I_o) \quad (13)$$

Equation 13 Expression for the calculation of the dimensionless parameter  $y$  where  $I_o$  is the chamber current with clear air and  $I$  with smoke aerosol

Normal ionization type fire detectors may be calibrated against a MIC but normally have a lower dynamic range. In forced airflow there is fairly good correspondence with MIC output, but this may not remain true where smoke entry to the detectors is not aided by such flow. Parameter  $y$  relates the concentration of the particles ( $Z$ ) and the

average particle diameter (**d**) and a chamber constant ( $\square$ ) appropriate for the MIC used as indicated in expression below reproduced from BS EN 54-7:2001.

$$Z \cdot d = \eta \cdot y \quad (14)$$

Equation 14 Expression connecting the  $y$  parameter to the concentration of particulates ( $Z$ ) and the average particle diameter ( $d$ ) in a specific chamber.

In addition to  $y$  and  $m$ , temperature and air flow are monitored throughout standard fire tests as these have an impact on the flow of smoke in the test rooms and need to be within set bounds for a valid test. The temperature output and the stability of the air are monitored as they. The temperature should be between 18-28°C and the temperature difference between the top and bottom of the room must be no more than 2°C.

### **1.7.1 Standard Test Fires**

Standard methods have been established to ensure that each fire detection system on the market will respond in a predictable way in an actual fire. The two standards of greatest international significance are BS EN 54-7 and UL268. There are others such as AS1603[78] and AS3786 9 [79] from Australia and standards that relate specifically to the construction and installation of fire detectors BS5839 [80].

In the past there were standards for the testing of ionization and optical devices (Underwriters Laboratory UL 167), (Underwriters Laboratories UL 168). The problem with using many standards is it becomes increasingly complicated for the end user and allowed product manufacturers to pick and choose which standards to test their devices against.

There have been a number of reviews based on the standard fires. Grosshandler [81] carried out a detailed study of measurements and candidate signatures for early fire detection in 1995 but methods applied did not include GC based gas characterisation techniques.

The standards incorporate or define a number of test fires which use a number of different fuels burning in different conditions to assess the response of the detectors as indicated in table 4 below.

<b>Standard</b>	<b>Test identification</b>	<b>Fuel</b>	<b>Type of combustion</b>
<b>UL 268</b>	Test A	Paper	Smouldering
	Test B	Wood	Flaming
	Test C	Heptane/toluene	Flaming
<b>BS EN 54</b>	TF2	Wood	Smouldering
	TF3	Cotton	Smouldering
	TF4	Polyurethane	Flaming
	TF5	Heptane/toluene	Flaming

Table 4 List of current standards and test fuels

The environments for test fires are defined (test rooms – below), as are the fuel quantities and their arrangement, and means of ignition. Test fire outputs are primarily defined in terms of smoke production as measured by optical absorption and MIC ionization sensor response.

The tests and choice of fuels employed in standards varied somewhat as the standards were developed and some other “standard fires” have gone out of regular use e.g. TF8 smouldering fabric. Some of the changes have come from the desire to amalgamate similar standards into a simpler uniform testing regime. Standards do exist for other markets although there have been moves to achieve conformity between standards.

The choice of the fuels has in some cases come under in for some criticism as not being representative of fires encountered in real scenarios. While such claims can be justified, test fires need to be fairly simple to set up, of relatively short duration, and show good reproducibility. The smouldering test fires are rather artificial as the development of true smouldering fires within porous beds can take hours to develop and exhibit low reproducibility. None of the standard fires used to validate fire detection systems use multi fuel systems, and do not represent fires that flash over, though conditions for such should not occur before detection by standard well sited detectors.

The present standards incorporate or define a number of test fires indicated in Table 2 above which use a number of different fuels burning in different conditions to assess the response of detectors. Short descriptions of BS EN54/7 fires T2,T3,T4 and T5, and UL268 fires A,B, and C derived from those standards are provided below. Test fire

outputs are primarily defined in terms of smoke production as measured by optical absorption and MIC ionization sensor response.

Quantities in the descriptions below have been converted to metric units and optical densities to obscuration %/m where the standards used other units.

**BS EN54/7 Test TF2 – Wood smouldering (more correctly pyrolysing)**

Fuel – 10 dried beech wood sticks (5% moisture content) each 75x25x20 mm arranged on hotplate as in Figure 8 a. Hotplate is 220 mm diameter 2 kW hot plate with concentric grooves (2mm deep, 5 mm wide) controlled to heat from ambient to 600°C in 11 minutes.

End of test  $m = 2 \text{ dBm}^{-1} = 36.9 \text{ \% obs./m}$ . Validity bounds as shown in Figure 8 b

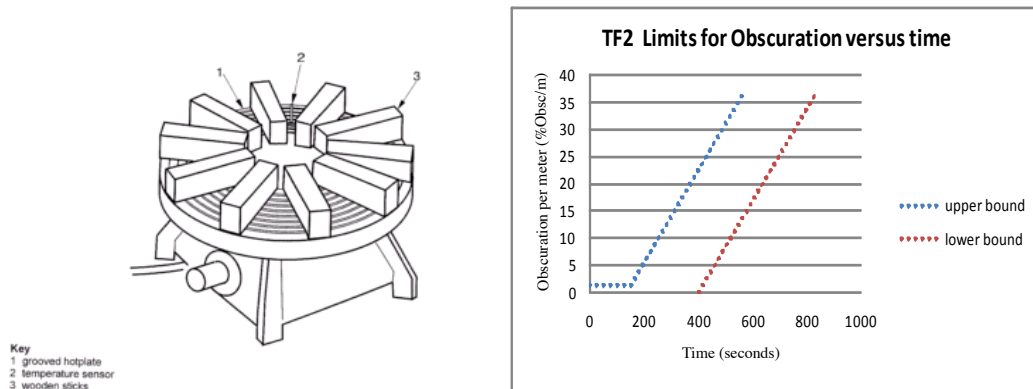


Figure 8 (a) TF2 hot plate and wood, and (b) BS EN54/7 TF2 Obscuration limits

**BS EN54/7 Test TF3 – Cotton wick smouldering**

Fuel – 90 pieces of braided cotton wick each 80 cm long and weighing 3 g. The wicks are fastened to a 10 cm50 diameter ring and suspended 1m over a non combustible plate as indicated in Figure 8 a

Ignition – lower end of each wick ignited by a flame so that the wicks continue to glow.

Any flaming wick is blown out. Test starts when all wicks are glowing.

End of test  $m = 2 \text{ dBm}^{-1} = 36.9 \text{ \% obs./m}$ . Validity bounds as shown in Figure 9 b

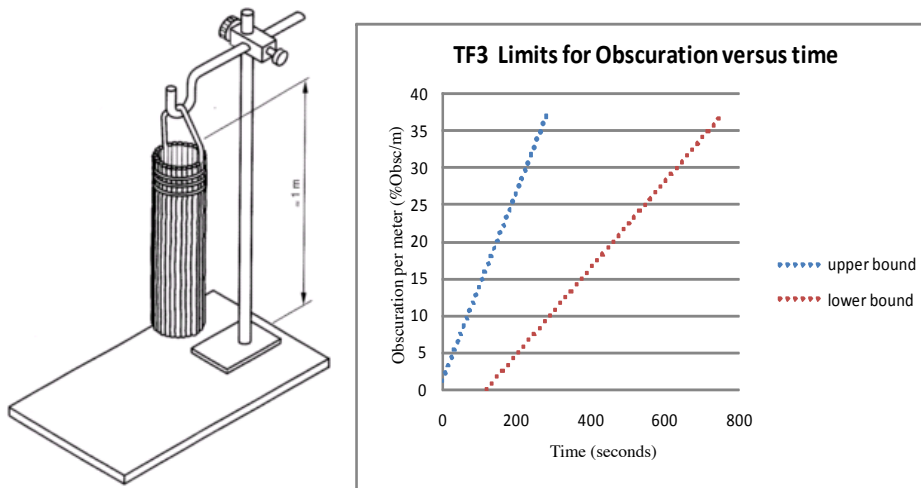


Figure 9(a) TF3 Wick arrangement, and (b) BS EN54/7 TF3 Obscuration limits

**BS EN54/7 Test TF4 – Flaming polyurethane foam**

Fuel – soft polyurethane foam,  $0.02 \text{ g cm}^{-3}$ . 3 mats  $50 \times 50 \times 2 \text{ cm}$  placed on top of each other on an aluminium foil base with edges folded to form a tray.

Ignition – ignite with flame at corner of lower mat. A small quantity of methanol may be used as an aid.

End of test  $m = 1.73 \text{ dBm}^{-1} = 32.9 \text{ \% obs./m}$ . Validity bounds as shown in Figure 10.

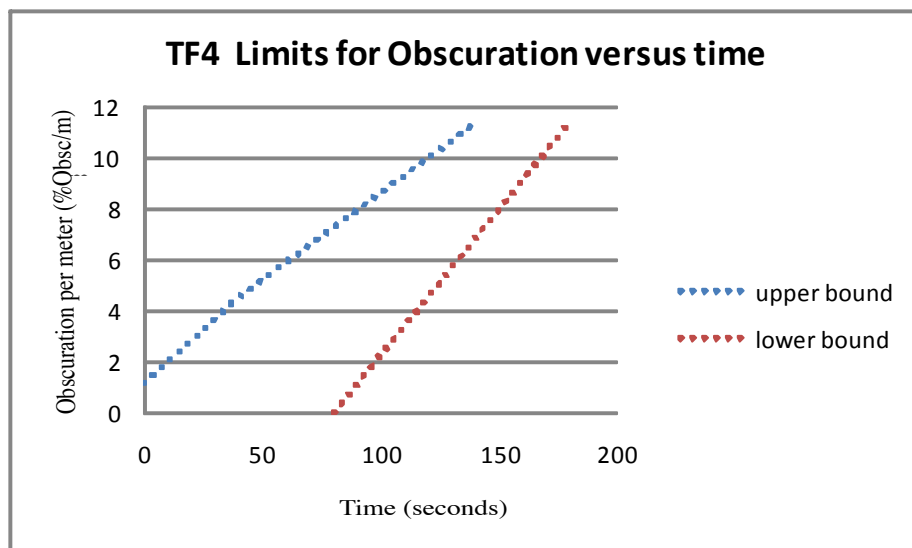


Figure 10 BS EN54/7 TF4 Obscuration limits

**BS EN54/7 Test TF5 – Flaming liquid (heptanes)**

Fuel – 650 g of n- heptanes mixed with 3% toluene by volume in a square steel tray  $330 \times 330 \times 50 \text{ mm}$ .

Ignition – by flame or spark

End of test  $m = 1.24 \text{ dBm}^{-1} = 24.8 \text{ \% obs./m}$ . Validity bounds as shown in Figure 11.

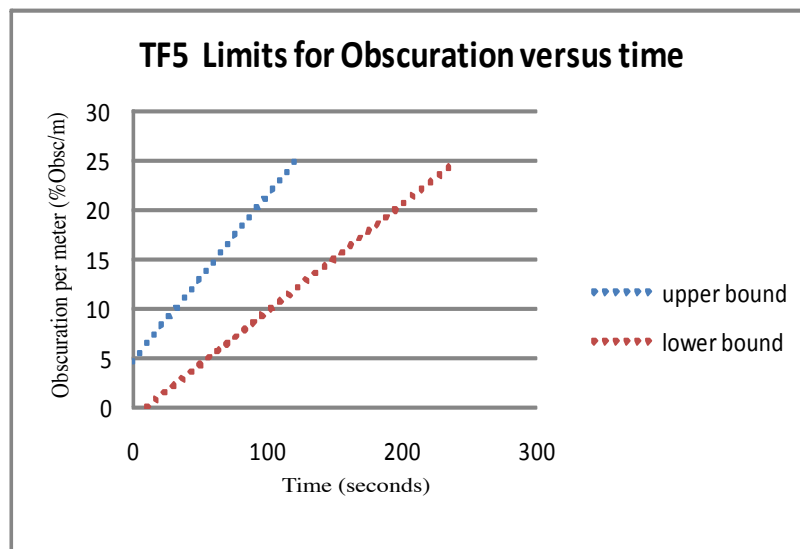


Figure 11 BS EN54/7 TF5 Obscuration limits

Unlike the BS EN54/7 standards, the UL268 definitions of the fires do not generally incorporate useful graphical representations of bounds for obscuration versus time. Plots deriving from the descriptions are included below but are only interpretations of the descriptions provided. The obscuration values for the UL268 and EN54/7 test are based on differently defined measurement systems. A direct comparison does not appear to exist in the open literature. As the UL268 system employs an incandescent source extending into the visible region, it will probably yield higher obscuration values for most smokes than the EN54/7 system operating in the near IR.

**UL 268 Test A – Paper smouldering (may go to flame)**

Fuel - 42.6 g of shredded newsprint (6-10 mm by 25.4 to 102 mm) tamped into thin steel open ended cylinder (102 mm diameter, 305 mm height) to fill lower 2/3, and with a hole 25 mm diameter through the centre of the packed paper. Cylinder base supported 900 from floor.

Ignition – spark probes at base

Profile- Test duration 4 minutes. Flame breakthrough 1-3 minutes. First smoke peak (smoulder) at 1-3 minutes 64-78% obs./m . Maintain obscuration for 20-30 sec at > 12.5 % obs./m. Second peak (flame) not to exceed 37 % obs./m.

Validity bound interpretation is shown in Figure 13.

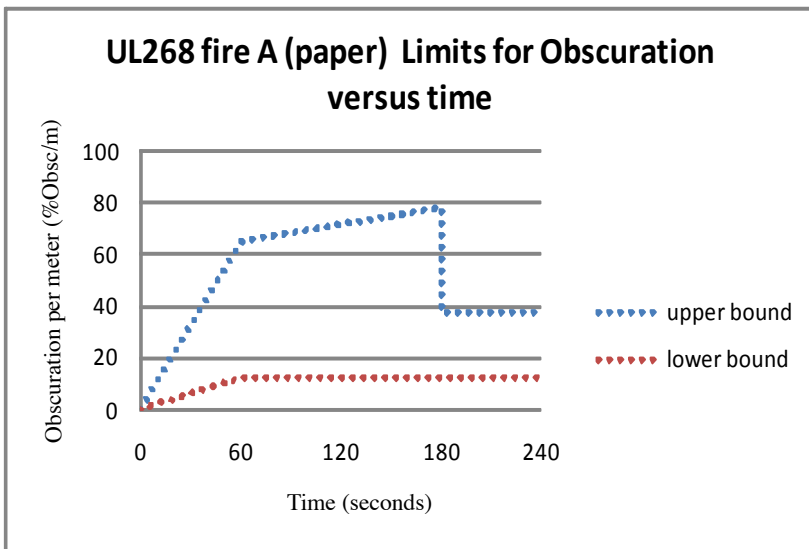


Figure 12 UL268 fire A Obscuration limits

**UL 268 Test B – Wood flaming**

Fuel – 3 layers fixed at right angles of 6 pieces of dried Douglas fir wood (19.1x19.1x152 mm), overall dimensions 152x152x64 mm). Supported on ring 900 mm from floor.

Ignite – by flames from 4 ml denatured alcohol in small dish 89 mm below wood. Spark probe to ignite alcohol.

Profile – Test duration 4 minutes. Smoke arrival at ceiling detectors 80-120 sec, >12.5 % obs./m for at least 60 seconds, and not exceeding 46 % obs./m. Flame breakthrough 150-190 seconds. Validity bound interpretation is shown in Figure 13.

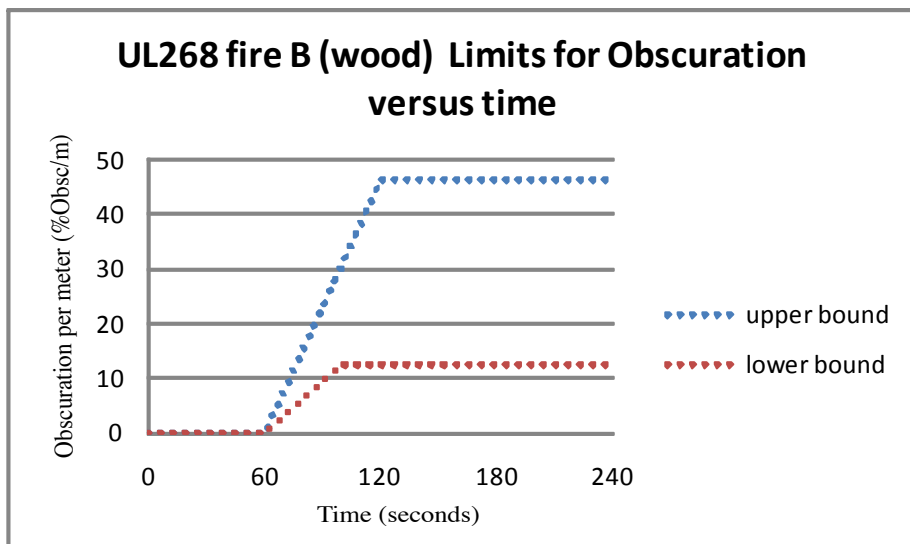


Figure 13 UL268 fire B Obscuration limits

## UL 268 Test C – Flammable liquid fire

Fuel – 75% heptane, 25% toluene mix in a 158 mm diameter, 32 mm deep steel pan supported 900 mm from floor. Fuel quantity to be sufficient to generate a smoke obscuration peak between 19.5 and 35.7 % obs./m within a 40 to 240 seconds period from ignition. (Fuel volume not stated in standard but believed to be ~40 ml [82]).  
Ignition - by spark igniter in vapour over pan.

Profile – Test duration 4 minutes. Obscuration of 19.5 and 35.7 % obs./m within a 40 to 240 seconds period from ignition, not exceeding 36.7 % obs./m.

Validity bound interpretation is shown in Figure 14.

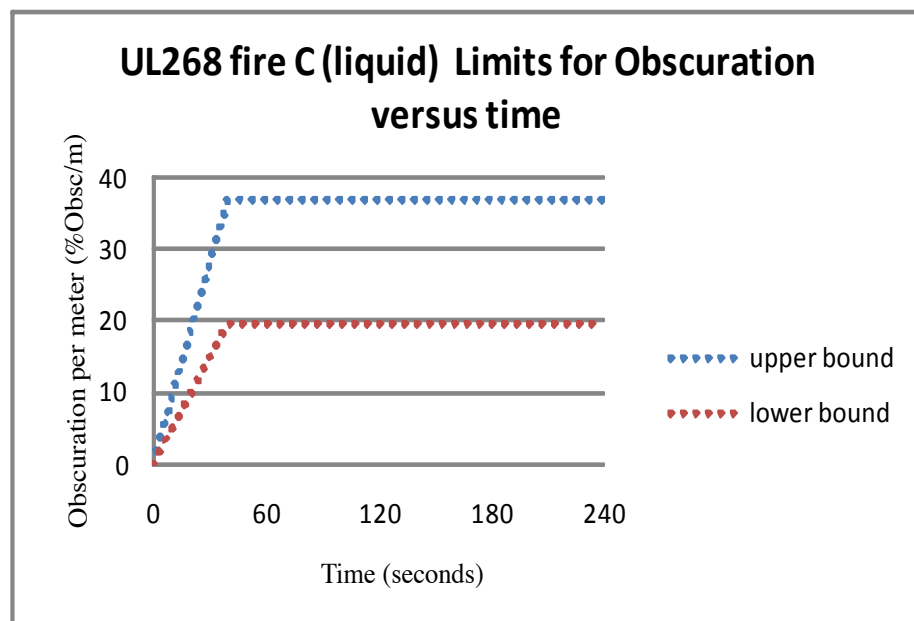
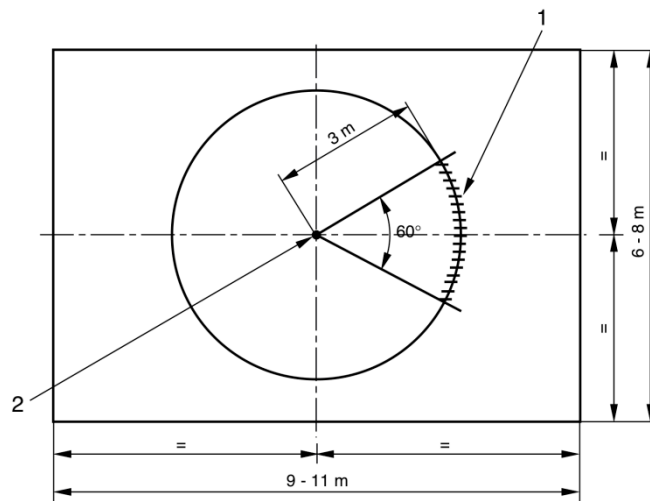


Figure 14 UL268 fire C Obscuration limits

In addition to fuels, the test fire definitions cover the test environments and detector positioning and those details for test fires are defined below under test rooms

### 1.7.2 Standard fire test rooms

Standard test rooms are of sufficiently large scale to allow the development of fires to a condition, which is comparable to unwanted fires in the work place. The rooms are provided with ventilation means but there is minimal airflow during tests. The detectors are located at a distance from the fire to represent a transmission distance comparable to that found in common room fires. Figures 15 and 16 represent the room dimensions of standard rooms in the BS EN 54-7 standard and UL 217/268 standard.



**Key**  
 1 specimens and measuring instruments  
 2 position of test fire

Figure 15 Diagram of a standard fire test room taken from BS EN 54-7 (2001)[1].

The above diagram shows the location of the fire sources (1) and the location of detector placement. Detectors are placed at equidistant points along the arc of the 60° cone 3m away from the fire source

The dimensions illustrated on the diagram are the typical length and width of the standard rooms. The height of the standard room is 4 m.

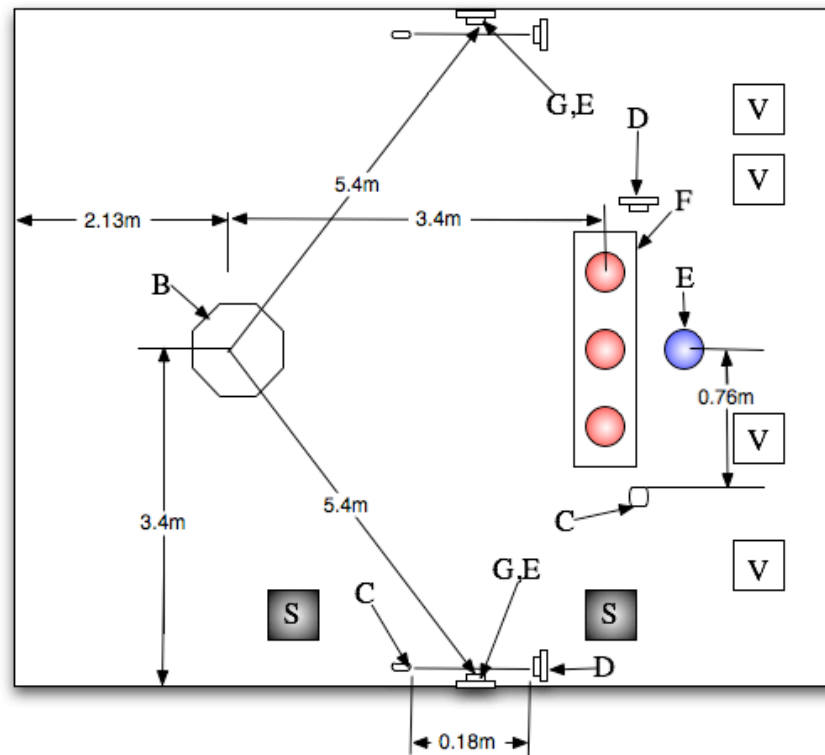


Figure 16 Diagram of the standard room taken from the description in UL-268 [3].

The room dimensions (not illustrated) are: 11 x 6.7 x 3.0 m (length x width x height). The test fire is located 2.13m from the rear wall and 3.4m from the side walls. The fuel is elevated 0.9 m from the floor for test B and C and 0.2 m from the floor in test A. C is a light assembly, D is a photocell used for optical density measurements. E is a MIC, F and G are the test panels for locating the fire detectors. S is the air supply and V are ventilation points used to clear the room after the test.

## 1.8 Reduced scale testing and modelling

This work does include some measurements employing full-scale test rooms but these are not readily accessible and use at test houses involves considerable costs (~£1000/day at BRE) [83]. This study predominantly involves measurements at conveniently reduced scales requiring development of suitable reduced scale versions of fire tests.

As indicated earlier transport in fire plumes depends on source size (power) and chamber dimensions (distance to ceiling and detectors). It was not the purpose of the

present study to significantly investigate scaling issues but to generate convenient scale fires having smoke output characteristics (obscuration versus time) similar to those specified for standard test fires. Reduced scaling inevitably affects fire source size and character as greater surface to volume ratios tend to proportionately greater heat loss rates, sometimes affecting stability and form of fire, and presumably products [84]. Further reduction in source to sensor distances can potentially affect transport times and progress of secondary processes such as aggregation of products into smoke particles, and mixing with surrounding air. Setting up reduced scale systems for fire characterisation has a long history, some aspects of which are covered below.

There has always been a problem in predicting the fire aerosol composition from small-scaled tests. The drive behind scale modelling has been driven by an interest in measuring the toxic components expected in a fire aerosol [85]. The most significant of which is carbon monoxide. In a study Barbrauskas [86] examined a series of bench scale tests looking at the production of carbon monoxide. He concluded that the predicted values of CO from most reduced scale tests significantly over estimated its concentration when translated to larger scale tests. However Barbrasuka study was concerned with developed fires. They stated that the small bench scale fires were most comparable to early stage fires of larger scale fires, because the amount of fuel compared was similar.

### **1.8.1 FE/DE (Fire Emulation/Detector Evaluation) device**

The concept of the FE/DE (Fire Emulation/Detector Evaluation – figure 17) device was first proposed by Grosshandler [87] and work soon started at NIST to develop the apparatus. The FE/DE is commonly seen as a loop or open pipe typically between 0.3-0.6 X 0.3-0.6 m cross sectional area with an internal volume around 2 m<sup>3</sup>. The FE/DE is described in detail [88] and has been used in many investigations into early smoke determination. The FE/DE works by passing air through the tunnel at variable speeds over a test section containing detectors and other relevant measuring equipment. Into the air stream smoke from a fuel source can be added. The humidity and temperature of the air can be controlled through the addition of water vapour, through a water jet, and electronic heaters. In addition other conditions in a fire can be emulated by adding particulate dust and other gases depending on the model used. The Honeycomb in the

FE/DE is used to ensure a flat or controlled flow of the smoke over the test section. This allows a flat flow of smoke over the detectors.

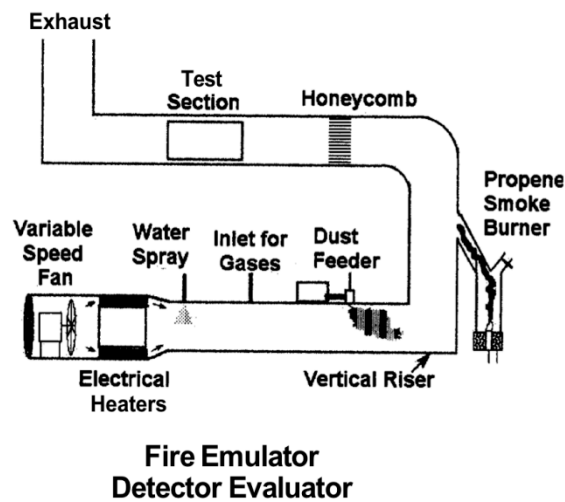


Figure 17 Schematic diagram of the FE/DE equipment described by Grosshandler

While the output from the FE/DE has shown to be able to emulate many fire conditions in terms of detector response, the artificially ventilation/airflow can certainly affect how fuels burn. It was felt that it would be better to keep to a simpler firebox structure for the present study with fuel ventilation and product distribution controlled by buoyancy driven convective processes as for the standard fires. Some measurements in this study were performed using a recirculating smoke tunnel (chapter 2), which in character may resemble some aspects of the FE/DE unit though without most sophisticated analytical kit. It was observed that shielding fuel from the direct airflow was in some cases required to produce smoke levels comparable to those seen for fires without forced ventilation.

### 1.8.2 Cone Calorimeter.

There are a number of other experimental methods that try to characterise fire in terms, gaseous products ( $\text{CO}$ ,  $\text{CO}_2$ ,  $\text{H}_2\text{O}$ ), smoke particulates and other components. Many of the small scale investigations into fires have been carried out on the cone type devices where a radiant source is used to pyrolyse and in some cases ignite the fuel. While these studies can cover early stages of pyrolysis which may correspond to how some nuisance fires start, the geometry and air flow arrangements are rather specific. While much is

learnt about flammability characteristics and toxic gas generation, cone experiments are not easily related to many early stage fires and the standard fire tests.

### **1.8.3 The NBS smoke box**

The NBS smoke box is a device that has been utilized as a method of generation of smoke in studies of for a range of fuels. The NBS smoke box, which can enclose a cone heater, comprises a sealed stainless steel box with provision for fire product monitoring e.g. obscuration meter. The box has an internal volume of approximately  $0.5\text{m}^3$

Gases are kept under a moderate positive pressure and use of heated chamber walls is intended to prevent loss of gases and particulates by deposition on the surfaces. While this system ensures maintenance of mixture of the gases formed so that they may be collected, the confined geometry and heating again do not emulate conditions in the standard fire tests or many real nuisance fires where air entrainment is significant.

### **1.8.4 Computer models**

Computerized modelling has been widely applied to the fire situation, most particularly characterising the mass transport aspects. However they are mainly applicable to relatively well developed fire situations where the boundary conditions can be well defined. Theory has been developed relating energy output and fuel to combustion. However most of this theory relates to fully developed fires and therefore may not apply to early stage fires, and small real fires may deviate considerably from characteristics indicated by computational modelling theory [89]. While it is certainly to be expected that computational models can be applied to the modelling of plume transport and its effects on detector performance, that is dependant on the reliability with which source characteristics can be defined. Olenick and Capenter [90] provided a good review of all the available programs. The major issue with application of computer modelling to fires near their inception is difficulty in specifying the progress of processes involved in ignition and variability in early stage growth. While there may be possibilities to improve scaling experiments based on application of computational methods this route was not followed in the present study.

## **1.9 Methods of Analysis**

There are numerous standard methods for the analysis of contaminants and fire aerosols in the literature. Some are included in this study. However those generally applied in the past have not generally been capable of specifically identifying compounds present in vapours or aerosols at the concentrations present in the early stages of combustion.

Fire products become dispersed in the air and in many cases application of analytical methods requires some sample collection and concentration of the material. Factors affecting sampling and validity of subsequent analysis include solubility, volatility, reactivity of analytes and the sensitivity of the proposed analytical method.

### **1.9.1 Particulate sizes**

There have been a number of studies examining the properties of smoke. Particulates in smoke are important in detection by light absorption and scattering, and mobility effects in air ionization based detectors.

Different types of smoke produce different types and sizes of particulates and this is expected to be a cause of known differences in sensitivity of conventional detector types to different fires.

Work carried out by Weinert et al [91] showed that the particle sizes varied with the type of fuel and the type of combustion. It also demonstrated that the properties identified for smokes are affected by the different measurement techniques applied. Weinert measured the sizes of particulates from different types of fires using an optical particulate counter (OPC - an active cavity laser scattering cell and focused jet of particles) and a cascade impactor to determine the particle's number size distribution. The cascade impactor principle is illustrated in Figure 18 below.

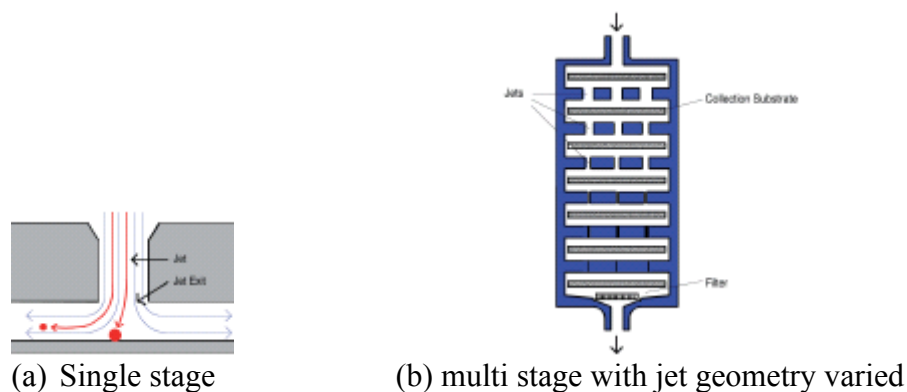


Figure 18 Cascade Impactor Principle (a) single stage, (b) series

The cascade impactor comprises of a series of size exclusion filters, which separate particulates on the basis of the aerodynamic diameter whereby the higher momentum of more massive particles allows them to cross the air stream at a bend while less massive particles are carried onwards.

### 1.9.2 Gas/Vapour Measurements

Gas sampling can be performed on a continuous or batch basis. Continuous sampling includes direct exposure of sensor systems to the sample environment or to aspirated gas flows. Typically direct sensing systems can include complex systems like FTIR systems and FAIMS devices to simple NDIR and electrochemical and other gas sensors. As long as sensor sensitivity is adequate to cover the concentration range without significant sample processing, continuous sampling is preferable and may approach real time monitoring of target species. Sensor response times and measurement chamber volumes, as in much FTIR or NDIR kit, can introduce systematic response delays. However examination of mixtures or low concentrations may yield signals which can be weak and/or complex so that resolution into individual species is not possible. Under these circumstances, batch sampling to concentrate is indicated, and allows application of chromatographic separation processes.

Technique suitability depends on the stability of the target analyte, analysis technique, and storage requirements (whether sample can be immediately transferred to an analysis system or needs to be retained for later measurements). For vapours in smoke arising from relatively hot sources but mixing with cool entrained air, vapours are expected to be subject to condensation, and agglomeration/ absorption onto smoke particles or

losses onto surfaces. Application of instrumental methods requiring well controlled inputs, such as GC/MS, tends to favour batch type processing where most conveniently a series of collected samples are presented for analysis. Some difficult to absorb gases (e.g. CO, H<sub>2</sub>) or reactive / unstable gases (NO<sub>x</sub>) are best dealt with by direct sensor measurements or grab bag sampling. However for the range of hydrocarbons and partially oxidised hydrocarbons fire products expected from earlier work is appropriate for collection on absorbent media for later desorption and analysis.

### **1.9.3 Gas sample collection by absorbent media**

Although previous work on early stage fires has shown significant elevations (>10 ppm) of CO concentration generally observed [5] and CO<sub>2</sub> and H<sub>2</sub>O generation, if not concentration change, must in most cases be substantial, other products may be present in the environment in very low concentrations. These concentrations are often lower than the limits of detection of analysis devices such as GC-MS so sample pre-concentration is necessary. There are three main methods of pre-concentration: absorption into liquid/ extractant phase, cryogenic collection, and absorption onto a solid sorbent from which material may thermally desorb. Cryogenic methods have the disadvantage that considerable amounts of water are condensed with the sample. Adsorptive methods, such as the use of absorbent liquids or solid liquid phase extraction, where samples must be desorbed from the collection medium with a solvent, liquid or gas present different problems of contamination. Thermal adsorbent trapping, where a sample is collected on a collection matrix (e.g. absorbent resins) at a specific temperature and then desorbed at a different temperature is attractive for fire gas analysis as the actual degree of sample handling is quite small.

Figure 19 illustrates operation of sorbent tubes. Species from gas pumped through the sorbent material packing are captured on the packing. The tube can be stored at low temperature retaining the absorbed material. When a clean gas flow (eluent) is passed through the tube and the temperature raised the trapped gases are released. If the temperature rise is moderate then some resolution of the products may be achieved at this stage. At higher temperatures all products come off with little separation.

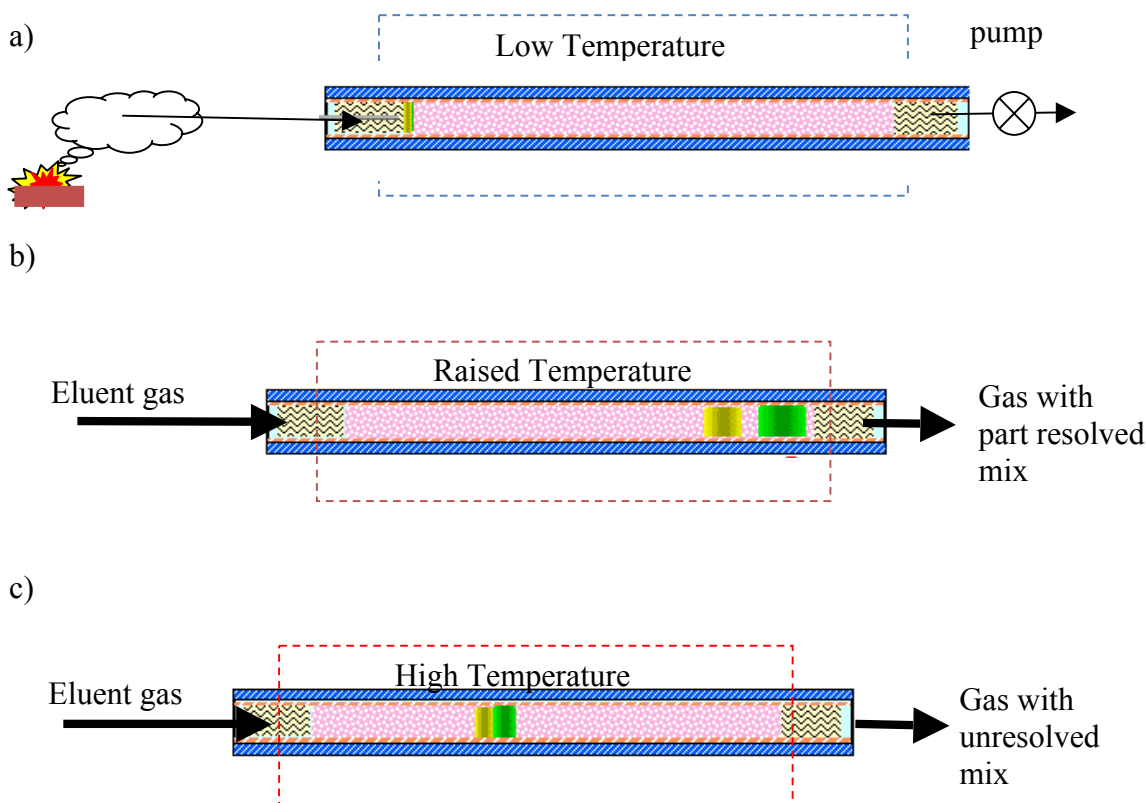


Figure 19 Sorption Tube operation – a) vapour capture, b) desorption with some resolution, c) desorption of concentrated sample without resolution.

Choice of sorbent affects the range/ type of gases, which are absorbed, and readily the sample can be recovered for analysis. These can be described as the adsorption and desorption parameters and are different for every kind of resin used. Guidance data is available for a number of commercially available sorbents indicating species which maybe absorbed and desorbed and suitable sorption tube loadings, gas flows, and temperatures.

There are many of commercially available resins and with composites and multiple resin columns the number of products can be listed in the hundreds. They can be broadly grouped as molecular sieves, graphitized carbon black and porous organic polymers. Several publications have looked at the advantages and disadvantages of different types of resins and absorbents. Tenax is a very popular absorbent and is recognised as the material of choice in standard methods for environmental gas analysis [92][93]. It is a porous hydrophobic polymer based upon the 2,6 diphenylene oxide. It

has been specifically developed for the sampling of volatiles and semi volatile components from air and other matrices. It has low water affinity and is useful in a wide range of environments where moisture can be an issue especially with graphitised resins.

Because Tenax has a limited range of compounds for which it shows useful absorbent properties it is common to co-package or layer with other material [94] to extend the range of analytes that can be trapped. Common materials used to complement Tenax are molecular sieves such as Carboxen 1000. This gives a wide potential of collectable volatile materials from C1-C15.

An issue with using carbosieve resins like carbotrap 1000 is that they collect water [95] which can interfere with analysis in a number of ways. It can decrease the safe sampling volume[96], and lead to interactions on the resin. For some sorbants moisture is bound only lightly and is removable by a purge of dry gas. Resins such as Tenax and Chromosorb 103 have very low affinity for water (typically < 5mg.g).

#### **1.9.4 Gas chromatography**

Gas chromatography comprises of two complementary techniques that may be used to identify components based on their masses and volatilities. It has been long established as a technique for the separation of volatiles in the gaseous phase, which do not thermally decompose and for a long time was the gold standard in analytical techniques. Broadly it consists of injecting a short pulse of analyte mixture within an eluent stream down a column containing or coated with an absorbent medium, the stationary phase. Differences in binding between different species and the stationary phase result in different transit times through the column and hence separation.

The phenomenon of band dispersion in chromatography columns is understood in terms of the rate theory. Transfer of an analyte between the mobile and the stationary phase tends to a local equilibrium concentration ratio between the phases as indicated by equation 15.

$$K_c = C_s/C_m \quad (15)$$

Equation 15 Rate theory equation ( $K_c$  is the equilibration constant for the interaction of the analytes in gas chromatography.  $C_s$  is the concentrations of the analyte in the stationary phase and  $C_m$  is the concentration of the analyte in the mobile phase).

Flow of the mobile phase disturbs this equilibrium and the analyte progresses down the column with the rate of movement being greater for species which bind less strongly to the stationary phase (lower  $K_c$ ) and hence for gas chromatography exhibit higher vapour pressures in the column.

Measurement of the separation requires a means of determining how long each analyte species takes to transfer through the column. This is achieved by having a detector responsive to presence of any of those species at the end of the column. Elution or retention time for a particular species is the period between the sample injection and detection of that species at the end of the column. With many detectors (gas conductivity, flame ionisation) there is little or no information on species identification and further means such as using samples consisting of or spiked with known species may be required to aid species identification. Connecting an inlet to a mass spectrometer (MS) to the GC column end and feeding a portion of the flow to the MS provides both a general species detection means (total ion current) and a means of identifying components from the resulting mass/charge ratio spectrum of ion fragments.

#### **1.9.4.1 GC-MS instrumentation**

Once the samples elute in GC/MS they then enter into the mass spectrometer. There is a great deal of literature covering the background of mass spectrometry [97]. The components of the GC/MS are shown in Figure 20.

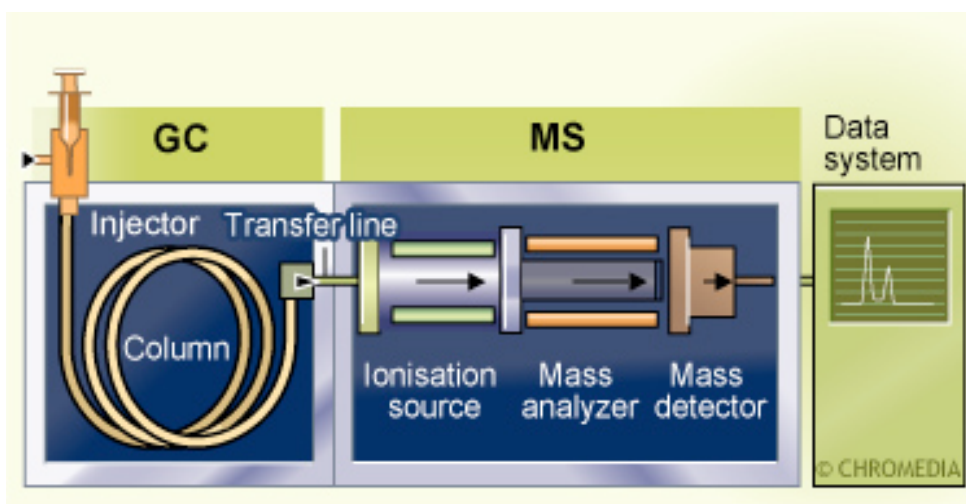


Figure 20 Schematic diagram of GC-MS system taken from [98]

The ionization source is within an evacuated chamber and the most popular form employs electron ionization of gaseous molecules as represented in Figure 21. Here the molecules are impacted by accelerated electrons, which transfer the energy from the electrons to the molecular particles. This energy transfer is more than sufficient to ionize the molecules. The excessive energy is absorbed exciting the ions to higher energy levels and initially there is little secondary ionization. As these energy levels return to normal there is a release of energy that can be of the order of chemical bonds resulting in fragmentation. This generates a series of daughter ion mixtures. Included in these mixtures are the parent ion, and both positive and negative ions. Negative ions are collected in an anode trap and an electrical field accelerates the positive ions into the analyser. These fragmentation patterns are dependent on the original structure of the molecule and can be used to identify analytes. There is much literature on the identification of molecules from their fragmentation patterns and some reference to that and the principles involved will be made within the body of this thesis.[99]

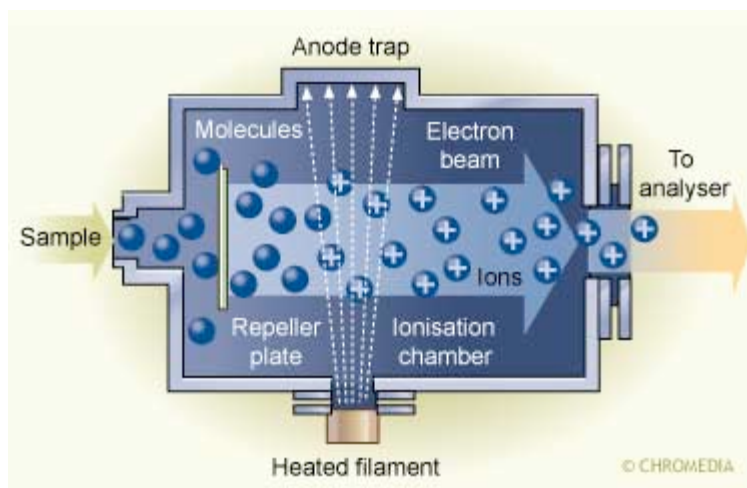


Figure 21 Schematic of electron ionization mass spectrometry source

When the ions enter the analyser part of the instrumentation they are focused by a series of magnets. In a quadrupole instrument there are four rods that are equidistant and held in a square orientation. The internal radius of the rods equals the smallest radius of curvature of the hyperbolic path taken by ions (Figure 22). Those ions that do not follow this path are absorbed and do not reach the detector. By sweeping the frequencies, specific ions of particular mass to charge ratios ( $m/Z$ ) can be allowed to pass. Alternatively the instrument can be held at a particular frequency to deliver a high sensitivity analysis of particular masses.

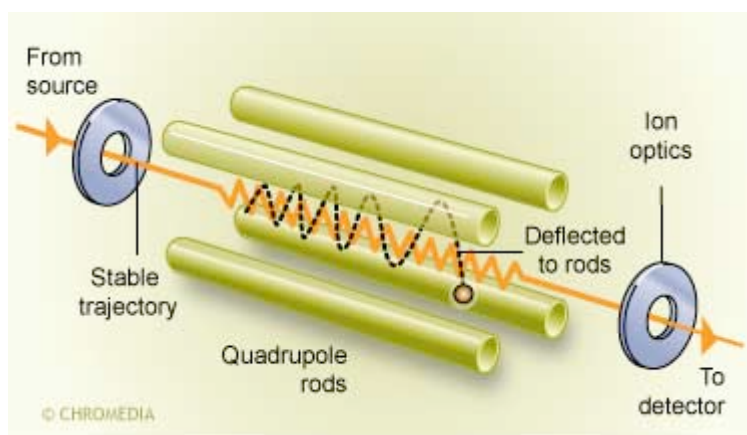


Figure 22 Diagram showing the path of created ions through quadrupole GC-MS

The detector is typically a photomultiplier cell which possesses a phosphor surface. When an ion impacts on this surface the energy is translated into light and this optical emission is detected and the signal is recorded on a data logger.

### 1.9.5 Infra-Red Spectroscopy (NDIR, FTIR)

Infra-Red (IR) spectroscopy relies on measurements from absorption of radiation (mainly in 2.5–25  $\mu\text{m}$  range) corresponding to primarily vibrational energies associated with chemical bonds. IR absorption generally follows the Beer Lambert Law (equation 16) and so concentration can be linearly related to absorbance.

$$\ln(I_0/I) = -\alpha C L \quad (16)$$

Equation 16 Beer Law governing optical absorption

Where  $I_0$  is intensity in the absence of the absorbing species, and  $I$  intensity with it present,  $\alpha$  is absorption coefficient,  $C$  concentration of the species, and  $L$  path length.

The absorption pattern may provide a “finger print” identifying molecular species but as peaks may be relatively broad, this can be compromised if concentrations are low or samples contain mixtures. This can be the case for fire products. Selection rules do not allow IR absorption for totally symmetric bonds and so the main components of air ( $\text{N}_2$ ,  $\text{O}_2$ ) do not interfere with IR monitoring. IR measurements have been used widely where relatively high concentrations can be achieved; For example, characterising products from fire testing of materials in cone calorimeters. However their utility at levels appropriate for early stage fire detection is limited. A number of studies have been undertaken but while the data may be relied on to measure concentrations of  $\text{CO}_2$ ,  $\text{CO}$  (possibly less reliably),  $\text{H}_2\text{O}$ , and in some cases  $\text{HCN}$ , under the dilute conditions relevant to fire detection it may show the presence, but generally not identity, of molecules having C-H and C-C bonds.

There are a range of IR based measurement techniques which can be applied to gases including dispersive methods (grating based scanned wavelength or more modern FTIR (Fourier transform IR)) where a range of wavelengths are covered and non dispersive methods NDIR where filters provide wavelength selection (figure 24).

Whichever method is used the quality of information gathered depends on the absorption coefficients, path lengths and concentrations being able to yield sufficient absorption levels and on ensuring that any absorption peak overlaps can be dealt with. After some initial consideration of the options and in view of the known limitations, it was decided that IR measurements on gases within the present study would not employ

FTIR, but be limited to determination of CO<sub>2</sub> and CO concentrations using NDIR equipment of the sort represented in simplified form in Figure 23 below. Real units may employ reflectors to increase path length, reference paths, and chopped or modulated sources.

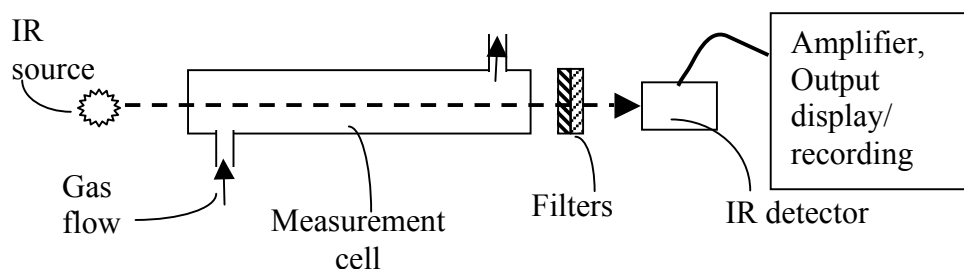


Figure 23 NDIR system for measurement on gas

### 1.9.6 Ion Mobility Spectrometry – IMS and FAIMS

Ions formed in air by interaction of gas molecules with an ionization source have a mobility characteristics dependent on the ion size and structure, including whether or to what extent they bind to other molecules, especially H<sub>2</sub>O. In principle the process is similar to that used in an ionization smoke detector, but much more sophisticated equipment is required to enable one to distinguish between molecules rather than just between molecules and relatively massive smoke particles. Measurements based on this mobility can yield spectral information and it can under some circumstances be possible to infer some species identity or broader characteristics. Although Ion mobility spectrometry (IMS [100] and its variant FAIMS [101]) yields information relating to the mobility of ions, this is complicated by the presence of air. It is not possible to directly determine molecular structure from ion mobility spectra as is possible to do using mass spectrometry carried out under vacuum conditions.

IMS is a relatively simple separation technique and comprises of an ionization source [102], a drift tube and ion detector plate. The sample gas is passed through the ionization source and pulsed via a signal clipper into the drift tube where they enter a flow of supporting gas. A field is applied along the length of the drift tube and ions of different mobility have different tube transit times. Conceptually conventional IMS may be likened to time of flight mass spectrometry, however the way the ions are formed,

environment, and mechanism of drift differ hence ion mobility spectra are quite different.

High field asymmetric ion mobility spectroscopy (FAIMS) is gaining popularity as an analytical tool. As for conventional ion mobility spectrometry (IMS) the method is applicable at normal atmospheric pressures. It differs in field strengths and the modes in which they are applied and this results in rather different spectral separations and crucially scope for device miniaturisation. FAIMS was first developed in Russia with further development in Canada, the USA, and UK. This has resulted in improvements in device geometry and some development of microengineered units. FAIMS may be applied either for direct measurements on an environment via a filtered input or as a detector attached to a GC column.

There have been some studies on fire gases relevant to detection using ion mobility techniques but the material available in the open literature is rather sparse. This may reflect secrecy issues related to real or potential use of IMS and FAIMS in detection of warfare agents. A FAIMS unit produced by Owlstone in Cambridge UK based on a microengineered silicon electronic filter structure was made available for measurements at a late stage in the present study.

## CHAPTER 2 EXPERIMENTAL METHODS

### 2.0 Fire enclosures

A target of the work was to characterise gas emissions for early stage fires under conditions where those products could be transported to detectors in real room size environments. In particular to characterise those products for examples of the standard fire tests used for validation of detectors. Practical and cost considerations required that measurement methods be developed on reduced scale fires and enclosures. The testing in this study was carried out predominantly in a laboratory scale custom-built 2 m<sup>3</sup> box and a full scale BS EN54/7 standard fire testing room (at BRE Watford). Some early testing was carried out in a NBS smoke chamber (Standard Smoke Density Chamber ISO 5659), and further work and some sensor calibration in a smoke tunnel at TYCO Sunbury.

#### 2.0.1 NBS Smoke Chamber



Figure 24 Example image of an FTT supplied smoke chamber. Image is taken from the FTT web catalogue

The initial work in laboratory scale chamber investigations was carried out in a commercially available FTT (Fire Testing Technologies) NBS smoke chamber installed at Bolton University (figure 24). This unit contains the ISO 5659 cone radiant heater for the burning of samples. The internal dimensions of the FTT NBS smoke box experimental chamber are 914 x 914 x 610 mm, a volume of 0.51m<sup>3</sup>

## **2.0.2 Fire source samples for NBS chamber**

The samples used in the NBS smoke chamber consisted of dried untreated 3 ply plywood cut into 75 x 75 x 5mm squares. The samples were wrapped in foil on 3 sides and placed in a sample holder leaving an area of 65 x 65 mm exposed to a radiant flux in a cone heater delivering fluxes of 11, 25 and 50kW using a heat source calibrated on a daily basis. The sample mass was monitored before and after analysis.

This equipment was suitable for preliminary work only as the chamber size and normal mode of operation were unsuitable for emulation of any of the standard fires. The preliminary tests in the NBS enclosure involving wood pyrolysis could not be considered a reasonable emulation of EN54/7 TF2 but did allow some exploratory work sensor and fire detector operation and on sample collection, use of absorbent media, and GC kit operation.

The NBS smoke box has a range of fixtures suited more to setting up small fires for toxicity testing. The inbuilt cone heater could not be operated at less than 11 kW dimensions and as a result there was far too much energy in the system and the production of smoke was far too quick. The heated walls and the recirculation of the combusted air through the cone resulted in strong forced convection and lack of cool air for entrainment into smoke. While it would be possible to turn off some functions, the small size of the enclosure was regarded as introducing excessive scaling issues and so construction of a larger chamber was planned. This was progressed after the study moved from Bolton University to UCLan. (Preston).

## **2.0.3 Data monitoring in NBS smoke chamber**

Data was monitored in real time using inbuilt monitoring devices. These included optical obscuration and mass loss. In addition TYCO fire detectors were used to monitor carbon monoxide concentration (CO), temperature, and smoke density by optical scattering (all by standard 801PC detectors) and smoke density by effects on conduction in ionised air (801I detector).

In-built data handling for the NBS equipment was supported by the FTT supplied software. The TYCO detector operation and data handling was performed in real time usually with 5 second polling interval by a TYCO MX panel simulator box with

associated software and PC. The TYCO propriety software used (TMenu) operates in DOS and generates log files of the 8bit outputs from the detectors, which can then be processed in Excel.

The system was transferred to UCLan and with some additional detectors used there and in fire tests at BRE.

#### **2.0.4 Collection and analysis of air samples from NBS chamber**

Samples were collected using Tedlar bags with an Airbus ABD 0031 gas sampling system. In this system gas is drawn from the fire chamber by a differential pressure system involving enclosure of a deflated Tedlar bag within a box that can be evacuated by a vacuum pump. As the box is evacuated air is drawn into and inflates the Tedlar bag. Gas lines to the smoke chamber were attached to both 6 and 12 litre Tedlar bags and gases collected during fire tests. Filling of Tedlar bags from the smoke box took 60-90 seconds.

Tedlar bag contents were subsequently slowly pumped out through absorbent resin (AR) tubes to absorb the fire product vapours. The absorbent resins used included activated carbon (75mg), Tenax (100mg) and chomosorb III (75mg) and Carboxen 1000 (75mg). For GC analysis the sample tubes were desorbed using a Chromopack thermal desorption cold trap (TDCT) injection system linked to a Pye Unicam PU4500 gas chromatogram (GC) using flame ionization detection (FID) as a detection device.

While there was initially some continuation of sample collection using Tedlar bags at UCLan., sample storage issues with this method requiring simultaneous operation of fire tests and GC/MS equipment favoured a change to a more convenient system of direct collection of fire gases onto absorbent media filled tubes. The original work with samples from the NBS enclosure indicated that Tenax was the absorbant of choice as poor results were obtained with Carboxen 1000. However that was based on the GC column in use with the Pye Unicam PU4500 at that time, and later work at UCLan involved identification of a column characteristics more suited for use with Carboxen material.

### 2.0.5 GC Analysis Conditions for PU4500 at Bolton.

GC operation is described in more detail for a GC/MS system at UCLan later in this chapter (section 2.2). Conditions used for the PU4500 for the preliminary work carried out at Bolton University are given in table 5.

The column used for the analysis was an Alltech Heliflex AT column (length 30 m, internal diameter 0.32 mm, and coating thickness 1  $\mu\text{m}$ ). The Alltech Heliflex AT column is a 100% dimethylpoysiloxane coated capillary column used as a general-purpose analytical column. The stable range of the column is -60 to 350°C, and as it has a non-polar coating analytes are eluted in accordance to boiling temperatures.

Parameter	Set Point
Injector Temp	50°C
Detector Temp	120°C
Initial column temperature	40°C
Initial hold time	15min
Gradient	4°C/min
Final Temperature	120°C
Final hold time	5 minutes

Table 5 Conditions for Pye Unicam PU4500 for initial GC work at Bolton with a Heliflex GC column as used for fire gases collected on Tenax sorption tubes

The carrier gas used on the PU4500 system was high purity helium with a flow rate of 1ml min<sup>-1</sup>. Samples were analysed using a flame ionization detector (FID).

## 2.1 TYCO Smoke Tunnel

A smoke tunnel with air recirculation at the TYCO laboratory in Sunbury was employed in this study for smoke detector calibration and some further tests. Figure 25 is a labelled photograph of the tunnel. The chamber dimensions and airflow direction are shown diagrammatically in Figure 26. Although airflow could be varied it was set at 0.2 m/s for all tests in this study.

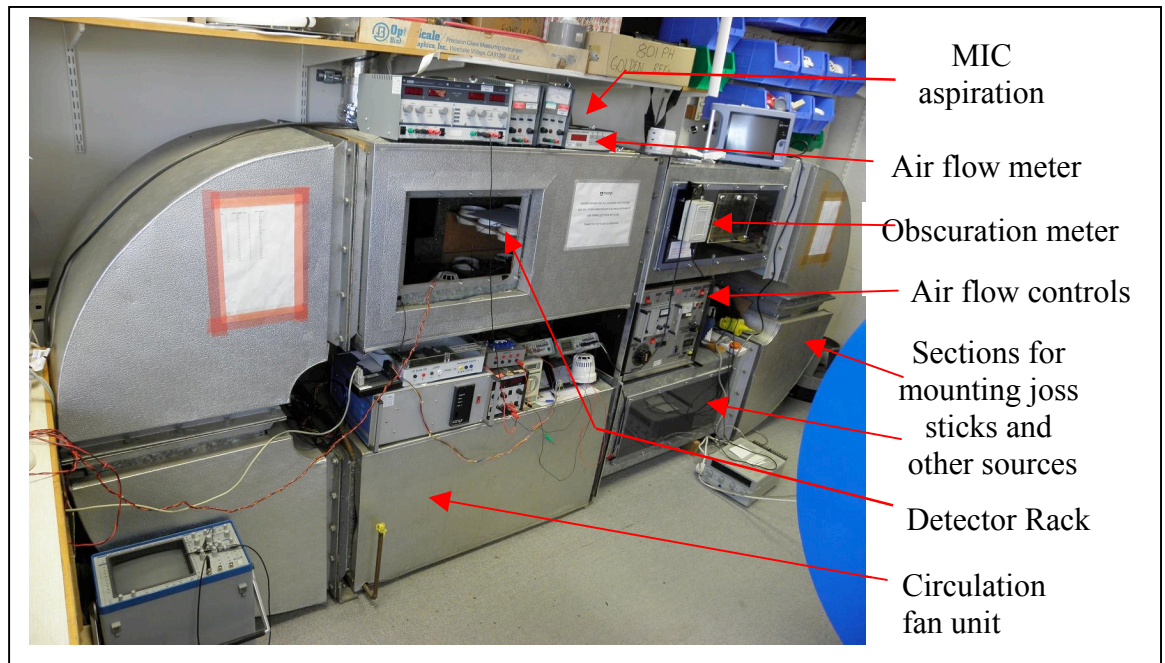


Figure 25 TYCO Smoke Tunnel photograph

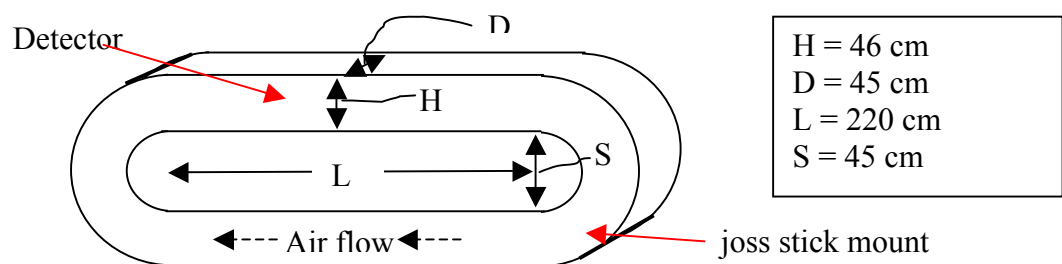


Figure 26 TYCO smoke tunnel dimensions

### 2.1.1 Smoke Tunnel data monitoring

The smoke tunnel was fitted with detector bases for TYCO detectors which could be coupled to a MX panel simulator box and computer (PC not shown in figure 26) allowing output from 801 series detectors (8 bit digital with polling interval normally

set to 5 seconds) to be collected and stored as data files which were subsequently processed in Excel. The smoke tunnel was also equipped with MIC ionization detector (not visible in photograph) and an optical absorption meter with design characteristics close to the BS EN54/7 specification. Unlike the designs used in standard test fire rooms, the tunnel absorption meter has light source and photo-detector on the same side of the tunnel and a retro-reflector on the opposite side of the tunnel so path length is twice tunnel width. Output from these units was converted to via a PICO Technology Ltd ADC-16 to allow recording as data files on a PC.

Within this study the smoke tunnel at TYCO Sunbury was primarily used for smoke response calibration/ validation work on standard MX series commercial smoke detectors (types 801PC, 801PH, and 801I) and experimental variants based on those designs.

The smoke tunnel was also used for tests using the Owlstone FAIMS equipment following its transport to Sunbury from UCLan. (Preston) for the May 2010 standard fire tests at BRE. Details covering the FAIMS equipment, test procedures, and results are provided in chapter 6.

### **2.1.2 Equipment and Calibration Procedures at TYCO Sunbury**

TYCO supplied standard and non-standard smoke detectors and some sensor devices and ancillary equipment for use in the study. This equipment was primarily utilised at UCLan. In the fire test room at BRE but visits to the TYCO Fire Protection Products R&D facility at Sunbury were used to carry out checks and calibration runs on devices along with TYCO staff using facilities at that site including a re-circulating smoke tunnel, a small heat tunnel, and a CO sensor calibration system. The CO calibration system used certified (< than 1% error) bottled CO in artificial air with a gas blender (Signal Model 821 Gas divider) mixing with cleaned air (from Signal AS80 Air Purifier) to give selectable concentrations at 10% intervals relative to the CO/air bottle.

## 2.2 UCLan fire Chamber

Although a target of the work was to characterise fire gas emissions on full-scale standard fires, availability and cost of standard test room facilities required that method development and a body of measurements be carried out at a more convenient smaller scale. Dimensions of a 2 m<sup>3</sup> box structure (1 m<sup>2</sup> base, 2 m. height) were selected as practically convenient. A series of experiments were conducted to determine behaviour of the smoke in the box and to identify suitable scaled fire sources to emulate behaviour of standard full-scale fire tests. All the fire test experiments at UCLAN were carried out in the in-house constructed enclosure illustrated in Figure 27, which was constructed from a frame of welded angle iron with extension legs added (500mm) along with coasters to make the entire enclosure mobile. Sheets of standard 10mm plasterboard were slotted into the four sides of the frame (1000 x 2000 mm) and held in place by the base (1000 x 1000mm) before being sealed in place.

The diagram of the smoke chamber roof displays the location of the optical bench meter (path length 691mm), and the location of the TYCO fire detection units. The sensors are positioned on a 60° arc at the front of the smoke chamber. The smoke chamber floor diagram shows the fire source location 200 mm from the back of the smoke chamber. The roof was constructed to allow access to the sensor locations and allow easy cleaning. The roof was constructed of two layers of plasterboard to aid disassembly and cleaning and for convenience in attaching sensors, fire detectors, and gas aspiration lines.

To clear the experimental chamber between experiments an extraction point was cut centrally into the rear wall 1500mm from the base of the chamber. A 35W centrifugal shower fan kit was connected (ex Screwfix). The extraction rate of the fan was 110m<sup>3</sup> per hour (1.8m<sup>3</sup> per minute). The chamber is designed to not be entirely airtight so changes in pressure can be accommodated.

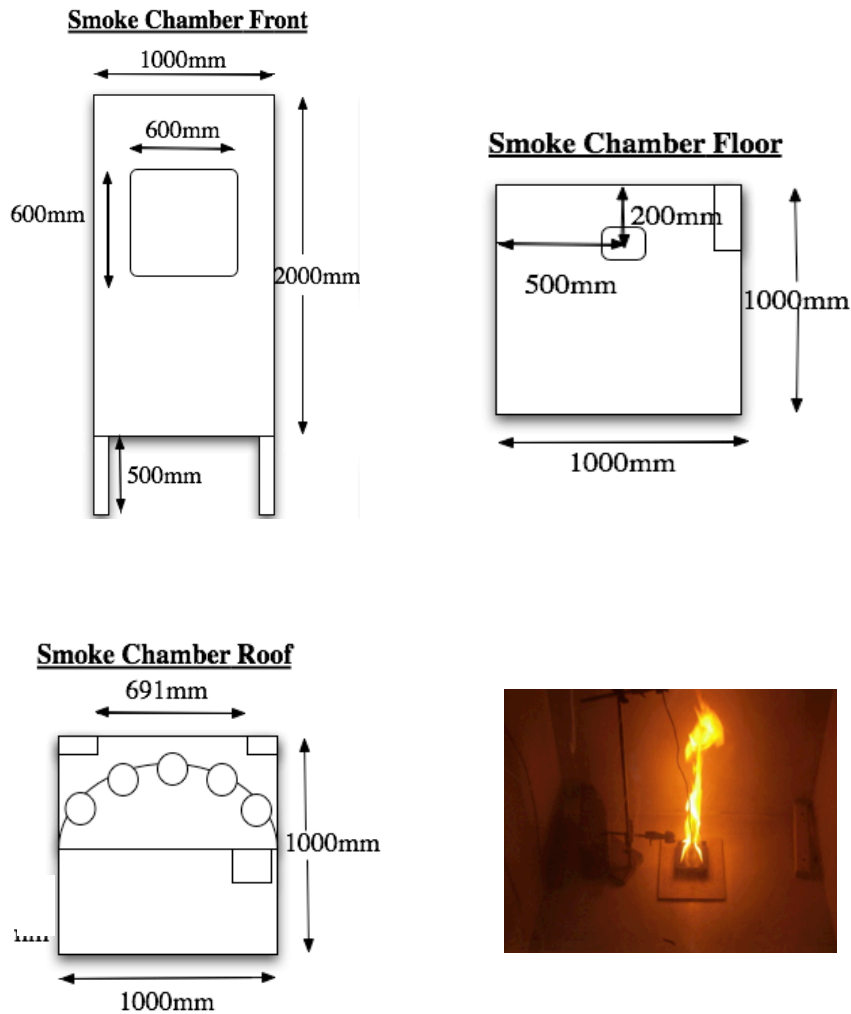


Figure 27 Design of UCLan. in-house fire test enclosure

A 600 x 600mm inspection opening was cut into the front wall of the smoke chamber with the bottom of the opening located 800mm above the chamber floor. A dense foam rubber door seal was put in place surrounding the opening on the outside of the enclosure. A removable door/ inspection hatch comprising a 10mm thick clear polycarbonate sheet was held in place over the opening by two beams. The beams were designed to be located on threaded bolts fixed to the chamber walls so that tightening wing nuts on the bolts forced the beams to push the polycarbonate sheet onto the foam rubber producing a stable air tight seal over the opening.

All walls were internally treated with a PVA type plasterboard sealant, and then painted with low VOC heat resistant paint, and layers of commercial white matt paint. In between tests the chamber is cleaned out using dry micro fibre cloths. When smoke

deposits built up to the point they could not be removed using this method an additional layer of paint was added. This was only done between series of experiments to reduce variance factors

### 2.2.1 UCLan enclosure Sensor, Detector, and Sampling locations

Positions for detectors, sensors, and sampling at the roof of the UCLan 2 m<sup>3</sup> enclosure were as indicated in Figure 28. The TYCO devices 39,211, 17, 209 and 100 were positioned in equally spaced locations on the roof of the enclosure at least 150 mm away from any adjacent devices or the side/rear walls of the enclosure. The devices 3 & 9 were located on the sidewalls of the enclosure 200mm from the roof and 300mm from the rear wall of the enclosure. Device 5 was located outside the box and was used as a control reference. The remaining devices were TYCO experimental devices and positioned on the rear wall 200mm from the roof and at equally spaced points along the wall. Adjacent devices were located at least 150mm apart and 150mm from the sidewalls.

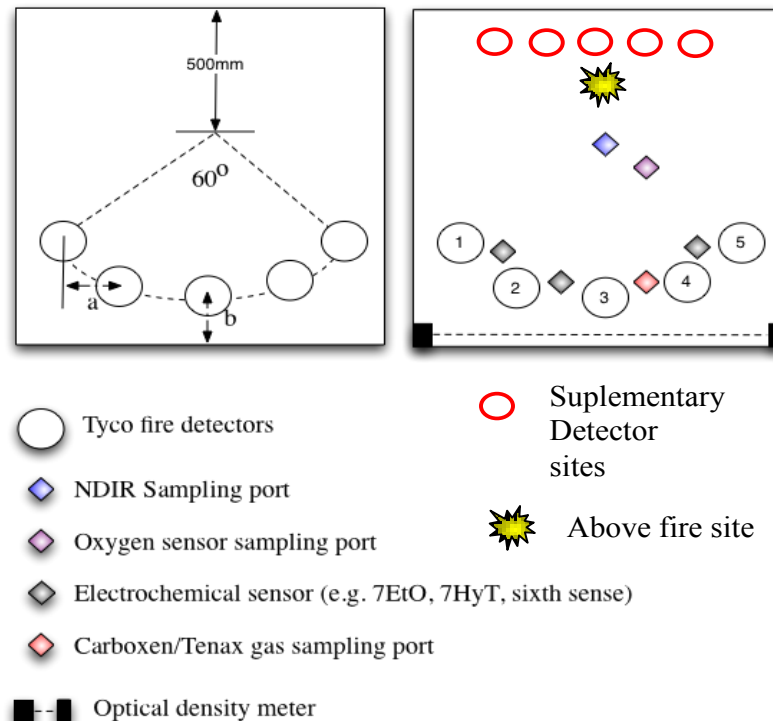


Figure 28 Schematic of the device layout on the roof the UCLan fire enclosure. Spacing:- a= 150 mm, minimum detector base to wall b = 200mm

The key in Figure 28 shows the locations of the other measuring devices. The NDIR sample line was centrally located in the ceiling and sampled gases at  $21 \text{ min}^{-1}$  through a 6mm OD flexible Teflon tube (0.25mm WT). The electrochemical sensors were positioned equal distances (150mm) from the NDIR sampling point and along the  $60^\circ$  sampling arc. The 7EtO cell passive sampled the gases where as the 7HYT sensor has a small computer-cooling fan attached to aid aspiration. Finally 4 equivalent sampling ports were cut close to the TYCO devices to allow for the collection of fire gases onto the sorbent resins. These also used 6mm OD Teflon sampling tubes sampling at a rate of  $70\text{-}120 \text{ ml min}^{-1}$ . Assessments were made using joss sticks to ensure the proximity of the sampling ports did not adversely affect the gas flow to the detectors.

The fire detectors used were based on TYCO's MX 800 series BS EN 54 compliant fire detectors as indicated in table 6. The output from the detectors monitored with MX data recording system consisting of a panel emulator, associated software and PC. Many of these devices and the panel simulator were used both at UCLan and for full-scale standard test fires performed at BRE, Watford.

Detectors are arranged on a common power and communication loop connected to the MX panel emulator. Over 100 detectors may be connected to the communication loop. Generally the loop used with the enclosure comprised of 7 standard detectors with 5 detectors arranged on the ceiling of the UCLan fire enclosure as indicated in Figure 28. Additional detectors could be located on bases located on the interior sidewalls of the enclosure 200mm from the roof and directly adjacent to detectors at the end of the roof arrangement.

In addition to the standard detectors for many of the tests 5 non-standard fire detectors were connected to the loop and located at supplementary detector bases near of the front of the fire enclosure 300mm from the roof with 150 mm between detector bases.

Following each test the smoke was evacuated and the fire debris was weighed. The sampling system was cleaned and replaced where appropriated and the walls of the fire enclosure were cleaned between tests and prior to new tests the temperatures were allowed to equilibrate.

### **2.2.2 UCLan Enclosure - Airflow**

The Airflow in the fire enclosure was monitored using a calibrated hot wire anemometer between fire tests. Flow was checked at locations 200mm from the floor, at mid height, 200mm from the roof, at centre and near walls (up to 18 locations) New tests were carried out when all measurements showed airflows less than  $0.1 \text{ m s}^{-1}$ . Data was recorded throughout each of the fire tests (not presented) with the average and maximum values noted. The values were not presented as the airflow was primarily a pretest check and during the tests the airflow was never greater than  $0.2 \text{ ms}^{-1}$ .

### **2.2.3 UCLan Enclosure Hot plate**

BS EN54/7 test fire TF2 involves heating wood on a hot plate. Similar arrangement was required for use in the UCLan enclosure for reduced scale emulations of TF2 and for some other tests (heating electrical PCB, PVC insulated wire, and cooking oil). The hot plate used in the final versions of the scaled fire tests was a commercially available single (1100kW) hot plate, the surface of which (diameter = 75mm) was formed with 2mm grooves. The heating rate as measured using a thermocouple in contact with the hot plate was  $11^{\circ}\text{C}$  per minute.

### **2.2.4 UCLan Enclosure Spark generation ignition source**

A spark generator source was constructed with step up transformer, control circuitry and shielding. Two prepared copper electrodes across which a spark could travel provided the ignition source. The copper electrodes are placed close to a fuel source within the scaled fire enclosure and allowed remote ignition of test fires. It was primarily used in rapid onset fires including heptane pool fires (TF5 type fire and UL268 fire), methanol fires, smouldering and flaming paper fires and flaming polyurethane foam fires.

## **2.3 Detectors employed**

Optical scatter and ionization type smoke detectors provided for use in this study were either standard MX series units or variants produced by modification of MX series detectors. TYCO MX series detectors are configured to convert output from incorporated sensors to a 8 bit digital form. The digital output is transferred via a two

wire common power and signal loop, which can carry multiple devices (up to 200 standard unit). Response is collected in Excel readable log files. The log files record time and sensor bit outputs and each device on a loop is identified by an address (0 to 255) and unique serial number. The standard detectors are types 801PC, 801PH, and 801I:

- 801PC: Commercial device with sensors for three detection channels (optical scatter, carbon monoxide, and temperature). The optical scatter uses an IR wavelength (~850 nm) LED
- 801PH: Commercial device with two detection channels (optical scatter and temperature). The optical scatter channel uses an~850 nm LED as for 801PC but with higher (~x 3) sensitivity setting. No unmodified versions of this device type were in regular use for this study.
- 801I: Ionization type smoke detectors supplied with normal high sensitivity commercial product setting. These units operate by measuring ion current in air ionized by Am<sup>241</sup>. Smoke particles bind to ions and being relatively massive compared with the gaseous species are less mobile reducing the ion current. These units operate on the same principle as the MIC devices included in fire test standards but without aspirated airflow and with narrower dynamic range covered within the bit output limits. A device modified to give a wider dynamic range was employed in the later BRE tests.

Non standard optical scatter detectors were generally based on 801PC or 801PH devices incorporating one or more LEDs covering wavelengths other than or addition to the 850 nm (near IR) of standard devices. The standard 801PC and PH devices employ silicon photodiodes provided with optical wavelength filtering built into the packaging. All the non standard devices, including those with blue or UV LEDs, also employed silicon photodiodes but of types selected to pass relevant wavelengths. These devices were constructed to allow monitoring of scattering at different wavelengths as this may be expected to depend on particle size and type. In general the theory of Mie scattering suggests smaller particles should increase scattering at shorter wavelengths. Fire smokes may consist of a broad range of sizes so the effects were not necessarily expected to be predictable. These special devices were supplied from TYCO Sunbury and included devices with LEDs operating at ~465 nm (blue), 850 nm (near IR – standard), 1070 nm (near IR – longer than standard), and 370 nm (UV).

Two of the special devices produced by TYCO and employed in this study use light sources which are combined blue (465 nm) and near IR (~850 nm) emitters so that the same optical test volume is addressed by both wavelengths. One device (address 32, type BIR) has blue and IR led chips together in the same optical pack, while the other (address 12, type Phosphor) has a blue (465 nm) LED loaded with a phosphor which emits near IR (predominantly ~850 nm) when excited by blue light. These units use time based filtering to separate out photodiode signals arising from the blue and IR emissions and scattering.

Detectors linking to the MX801 logging system used in this study are summarised in table 6 below.

MX Address	Serial Number	Model/ type	Further Information
3	12019CBCE	801PC	Standard type – NIR scatter, temperature, CO
6	12019CC56	801PC	Standard type– NIR scatter, temperature, CO
9	92019CC09	801PC	Standard type– NIR scatter, temperature, CO
102	120049EA8	801PC	Standard type– NIR scatter, temperature, CO
117	12019CC2E	801PC	Standard type– NIR scatter, temperature, CO
39	12019CC11	801PC	Standard type. – NIR scatter, temperature, CO Generally wall mounted in UCLan enclosure.
17	1200C0C9C	801PC modified	With extended CO range (> 400 ppm). Standard NIR scatter, temperature
1	120049F36	801PC modified	With unfiltered CO cell, Zellweger, Part No. 2119B1003. Standard NIR scatter, temperature
209	92019301A	801I	Standard Ionization type
210	8006FBE8	801I modified	Ionization type with ~6x extended dynamic range.
211	820044C2D	801I	Standard Ionization type
32	20382815	BIR	special dual LED IR and blue
12	20382805	Phosphor	blue LED and IR phosphor device
170	9200002A4	801PH blue LED	blue LED in 801PH detector type package
38	12019CC13	801PC UV LED	UV LED (370nm) in 801PC detector type package
47	12019CBFF	801PC longer NIR LED	IR LED (1070nm) in 801PC detector type package
100	920000266	801PH modified	Humidity sensor replacing optical in 801PH, provided with min-fan.
135	8000060	801PC modified	801PC converted to give bit outputs from 3 analogue inputs to MX log. Chan. av0 and av1 used for 7ETO and 7HYT cells.

Table 6 Summary of MX 801 Detectors and Variants

### 2.3.1 Calibration of Optical Scatter devices.

Unlike optical obscuration where span can be unequivocally set by measurements in clear air (0% obscuration) and completely blocked (100% obscuration), optical scatter device sensitivity is dependant on device geometry, LED and photodiode choice and amplification settings, and finally the nature of the smoke. There are really no absolute scattering standards which may be employed for optical scatter fire detectors. Function and stability checks on devices can however be carried out by recording detector response to reproducible aerosols under reproducible air flow conditions. This is achieved at TYCO Sunbury using fan driven smoke tunnels with aerosol or smoke from a generator or reproducible combustion source. Devices for this study were “calibrated” using smoke from 5 smouldering joss sticks (taken from a large stock held for this purpose) and an air flow of 0.2 m./sec. using the in-house smoke tunnel described above. Calibration runs were performed before devices were supplied to UCLan. At about mid point and the end of the study. For most calibration runs reproducibility of the test was checked by including a “gold standard” reference optical scatter detector held at TYCO Sunbury for checking other reference devices used in setting levels for factory production testing. In some runs measurements of optical absorption and MIC output were also collected. Results from a typical run carried out under the standard conditions are presented in Figure 29 below showing response with time as smoke levels increase for a standard 801PC detector, a “gold standard” detector held for quality control purposes at TYCO Sunbury, and Obscuration %/m calculated from the tunnel obscuration meter output.

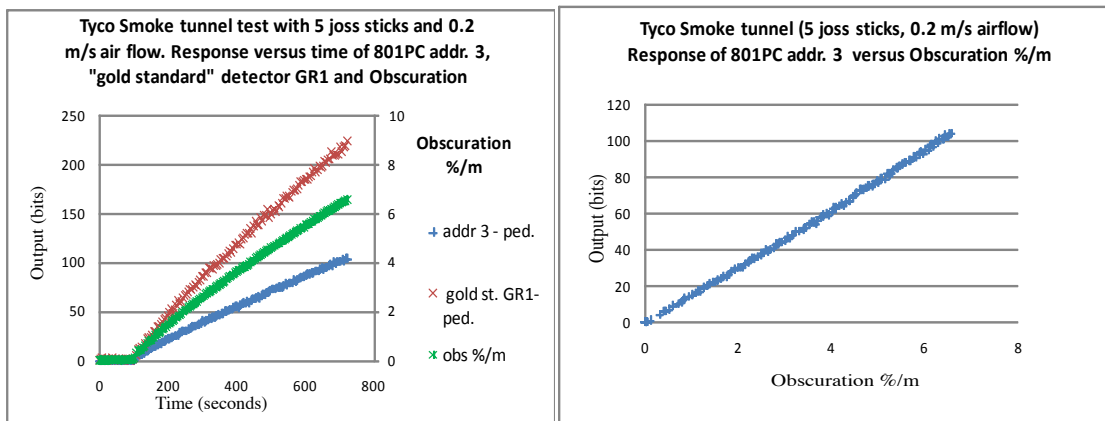


Figure 29 Standard detector calibration run using joss sticks in TYCO smoke tunnel.

The image on the left is the responses versus time as smoke increases. The image on the right is the 801PC (address 3) optical scatter channel output change versus obscuration.

Response versus obscuration is shown above as bit output minus the pedestal value (bits output for clean air).

At UCLan additional validation/ stability testing was carried out at monthly intervals using 5 smouldering joss sticks (same batch as used at TYCO Sunbury) in the UCLan Reduced scale enclosure described below but with a large office fan operated in the enclosure to provide good mixing and smoke transport. Device outputs were checked against previous measurements and response of a secondary standard detector used at UCLan only in these stability test runs.

### **2.3.2 Electrochemical sensor response calibration**

The majority of electrochemical gas sensors used in the study were supplied and initially calibrated at TYCO Sunbury and then periodically recalibrated at both Sunbury and more frequently at UCLan Preston. Honeywell 6<sup>th</sup> Sense CO sensors (originally developed and marketed by Zellweger before acquisition by Honeywell) are incorporated in 801PC detectors supplied for the project and these were calibrated in the detectors i.e. corresponding detector outputs calibrated. One further 6<sup>th</sup> Sense CO sensor was provided for operation outside of a detector operated with a potentiostat and calibrated as described for the 7ETO electrochemical cell below.

One 801PC detector (addr. 1) used in a limited number of tests did incorporate a 3 electrode Zellweger CO (H) sensor cell, Part No. 2119B1003, which is geometrically very similar to the 6<sup>th</sup> Sense CO sensors and believed to contain similar electrode materials but no activated carbon filter. Operated in 3 electrode mode this unit has a sensitivity of ~100 nA/ppm CO. When operated in an 801PC detector in 2 electrode mode (reference electrode not connected) as for the standard 6<sup>th</sup> Sense cells, the CO response is approximately halved leading to CO channel detector sensitivity very similar to the standard 801PC units.

Two further detectors purchased by TYCO from City Technology were supplied for use in the study. These were a hydrogen sensor 7HYT, and an ethylene oxide sensor 7ETO and performance was checked at TYCO Sunbury before supply to UCLan. Using potentiostat circuits based on designs provided on the City Technology website or a Sycopel Scientific Ltd Ministat 251 Precision Potentiostat.

Both are 3 electrode designs with sensing, counter and reference electrodes. The 7HYT device is operated with sensing and reference electrodes held at the same potential (zero bias). The 7ETO device is operated with sensing electrode held 300 mV positive with respect to the reference electrode.

The 7ETO device was purchased on the basis that the City Technology data sheet indicates that although it is produced as an ethylene oxide sensor, it shows a wide cross sensitivity to other oxidisable gases. Testing of the 7ETO device at it is expected to show non selective response to a wide range of oxidisable gases.

### **2.3.3 CO sensors in 801PC devices**

The study included measurements of CO from test fires and other sources using electrochemical gas sensors. Primarily this was carried out using 801PC fire detectors incorporating electrochemical CO sensors (Honeywell 6<sup>th</sup> Sense). These are 2 electrode devices with a working (sensing) electrode and a counter/ reference electrode as described in chapter 1.

The Honeywell 6<sup>th</sup> Sense CO detectors are engineered to show very little response to most potential interferants such as organic vapours at least partly because they incorporate activated carbon filters to prevent such species reaching the sensing electrode. It has a nominal range of 0-500ppm and technical information on performance and operations is available from the City Technologies (Honeywell) data sheet [103]. Cross sensitivity data from the sensor manufacturer is included below as table 7. Checks carried out at TYCO Sunbury also showed that response by these sensors to hydrogen is not only relatively low but also transient so that for slow growing fires at least (smouldering types) even if hydrogen is present it may not affect CO readings significantly.

Gas	Concentration used (ppm)	Reading (ppm CO)	Gas	Concentration used (ppm)	Reading (ppm CO)
CO	50	50	CH <sub>2</sub> CH <sub>2</sub>	100	85
H <sub>2</sub> S	10	38	CO <sub>2</sub>	5000	0
SO <sub>2</sub>	2	1	NH <sub>3</sub>	50	0
NO <sub>2</sub>	3	-1	CH <sub>4</sub>	5000	0
Cl <sub>2</sub>	2	<2	CH <sub>3</sub> CH <sub>2</sub> OH	40	12
H <sub>2</sub>	100	10			

Table 7 Cross sensitivity table taken from Honeywell data sheets.

The 801PC detectors incorporate circuitry which acts as a potentiostat maintaining zero potential between the electrodes and converts the current which passes as CO is oxidised at the working electrode to a bit output. Standard construction 801PC devices have an output of 2 to 2.5 bits/ppm CO giving a dynamic range of ~100 ppm. Units generally have a pedestal (zero CO) value of ~22-30 bits and a maximum output of 255 bits. One device (address 17) was converted to lower sensitivity to give a dynamic range of ~500 ppm CO and much of the data presented is derived from that device.

The detectors were checked and calibrated at TYCO Sunbury before supply to UCLan and ~mid way and at the end of the study using certified (< than 1% error) bottled CO in artificial air supplied by Air Liquide (original bottle 411 ppm, later bottle 416 ppm) and a gas blender (Signal Model 821 Gas divider – recalibrated annually by manufacturer) mixing with cleaned air (from Signal AS80 Air Purifier which passes pumped air over heated Pt to remove any oxidisable material) to give selectable concentrations at 10% intervals relative to the CO/air bottle. Some further checks were carried out directly with certified 36.5 ppm (< than 1% error) CO in artificial air supplied by BOC which gave results consistent with the gas supplied by the blender. Little change in sensitivity was found over the period of the study.

Figure 30 shows test results for the extended CO range 801PC device.

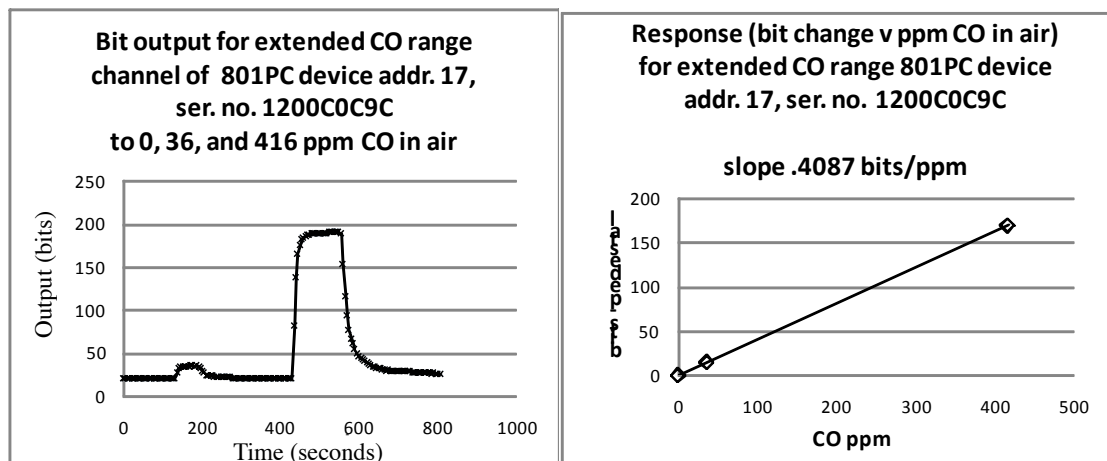


Figure 30 Extended CO range 801PC calibration. (Left) Is a measurement versus time (Right) Is the response versus CO concentration in air

The CO response for 801PC smoke detectors, and for the NDIR CO measurement system was checked at approximately weekly intervals at UCLan using controlled volume feed from bottled gas (CO/CO<sub>2</sub> mix from BOC 6000ppm/4%) into the 2 m<sup>3</sup> enclosure with fan assisted mixing.

### 2.3.4 Electrochemical sensor for hydrogen 7HYT

The City Technologies hydrogen sensor (7HYT) was used both with and without fan aspiration of air to the sensor to monitor hydrogen concentrations during experiments both at UCLan and at BRE. It has a nominal range of 0-1000ppm with a resolution of 2ppm under normal operating conditions. The 7HYT sensor has known but limited cross sensitivity to a range of gases including carbon monoxide as indicated in the table below reproduced from the device data sheet. Initial measurements at TYCO Sunbury confirmed response to hydrogen (generated electrochemically in a ~20 litre Perspex enclosure) was as given in the data sheet ~30 nA/ppm and the TYCO CO calibration confirmed that cross sensitivity to CO was low (<5% of hydrogen response) as indicated cross sensitivity information taken from the device data sheet reproduced as table 8 below.

Gas	Concentration used (ppm)	Reading (ppm H <sub>2</sub> equivalent)	Gas	Concentration used (ppm)	Reading (ppm H <sub>2</sub> equivalent)
CO	300	0<X<60	CH <sub>2</sub> CH <sub>2</sub>	100	80
H <sub>2</sub> S	15	<3	NO <sub>2</sub>	5	0
SO <sub>2</sub>	5	0	HCN	10	3
Cl <sub>2</sub>	1	0	HCl	5	0
NO	35	10			

Table 8 Cross sensitivity of the 7HYT cell as derived from CiTi technology product data sheet. Values correspond to the unmodified cell without the zorflex filters

To reduce the cross sensitivity vapours in smoke the 7HYT was placed behind a filter of Zorflex activated carbon cloth (Calgon) when used for fire tests. Once transferred to UCLan, the 7HYT hydrogen sensors were calibrated on a monthly basis using a 2-point (0 and 500 ppm) measurement based on high purity bottled hydrogen injected into a chamber containing a mixing fan. Output from the potentiostat across a 5000 Ω measuring resistor remained close to 75 mV, in line with data sheet response of 30 nA/ppm.

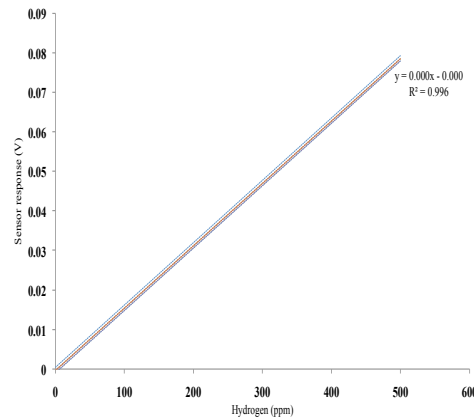


Figure 31 The figures show the response of the 7HYT sensor (V) to the increasing levels of hydrogen

### 2.3.5 Electrochemical sensor for oxidisable gases (Ethylene oxide sensor) 7ETO

The 7ETO device was purchased on the basis that the City Technology data sheet indicates that although it is produced as an ethylene oxide sensor, it shows a wide cross sensitivity to other oxidisable gases as indicated in table 9 derived from the cell data sheet.

Gas	Concentration used (ppm)	Reading (ppm Et <sub>2</sub> O equivalent)	Gas	Concentration used (ppm)	Reading (ppm Et <sub>2</sub> O equivalent)
CO	200	80	CH <sub>3</sub> CH <sub>2</sub> OH	100	55
C <sub>7</sub> H <sub>8</sub>	100	20	CH <sub>3</sub> COCH <sub>2</sub> CH <sub>3</sub>	100	10

Table 9 Cross sensitivity of 7EtO cell derived from manufacturers data sheet

The unit was calibrated both at TYCO Sunbury and at UCLan. Using CO and responses in fire tests are expressed as “equivalent CO ppm” and should be the sum of signal arising from CO and that from other oxidisable gases such as simple and partially oxidised hydrocarbons. Tests carried out did not include measurements of relative sensitivities to organic species and CO but the data sheet information indicates that will be very dependant on structure. It is likely that sensitivity will be particularly high to small easily oxidised molecules such aldehydes and unsaturated hydrocarbons.

Unit calibration at TYCO employed the equipment described earlier and as used for CO testing of 801PC detectors. Figure 32 shows response to CO of the 7ETO cell coupled via potentiostat and buffer to one channel of a modified MX detector (address 135, 801PC modified to provide 3 A to D channels).

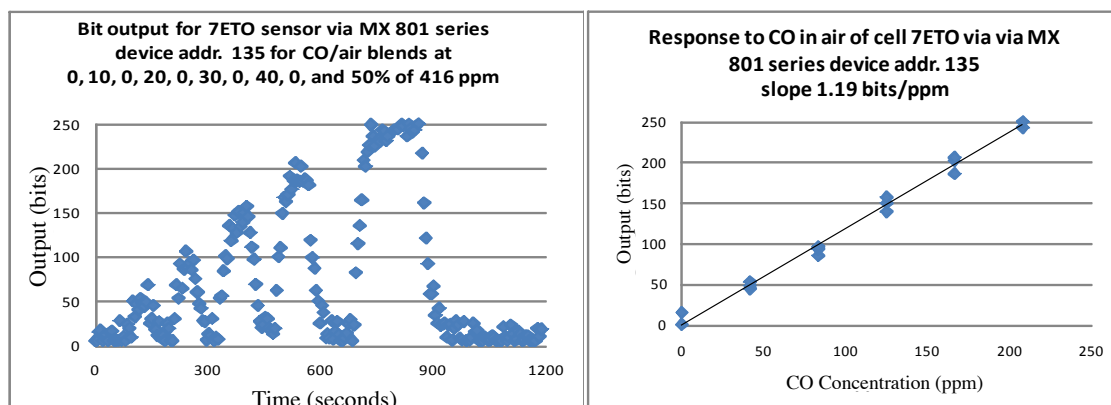


Figure 32 CO test of 7ETO sensor linked to MX device (left) Measurements versus time (right) Response versus ppm CO in air

This unit was used at UCLan and at BRE. The sensor output was calibrated against known CO concentrations from CO/CO<sub>2</sub> calibration gases (BOC 6000ppm/4%) in the scaled fire enclosure) on a weekly basis and monitored for variation. All results from the 7EtO device are reported as ppm equivalence of CO concentration.

### 2.3.6 Electrochemical Oxygen Sensor Citicel 2FO

Oxygen concentrations within the UCLan 2 m<sup>3</sup> enclosure was measured using a 2FO selective oxygen sensor produced by CiTiceL which was used and calibrated at UCLan only. This device has a current output related to oxygen content of gas by

Equation 17 below. When new the device gave ~0.4 mA in normal air and this declined only slowly during the period studied.

$$S = K.\ln(1/(1-C)) \quad (17)$$

Equation 17 Calculation of the oxygen gas concentration using the 2FO oxygen cell.

Where S is signal, C is oxygen concentration expressed as a fraction i.e. 0.209 for air, and K a proportionality constant determined by calibration.

Output was monitored by a DVM across a load resistor (50 Ohm) resistor (giving ~20 mV in air). During tests the values were recorded manually as variations were small and changes were not rapid.

The 2FO electrochemical cell has a bulk flow cap to reduce interference from sudden fluctuations of pressure, and an operational range of 0-25% O<sub>2</sub>. To check for changes in sensitivity the unit was calibrated on a monthly basis using high purity nitrogen (BOC) and air as 0 and 20.9% oxygen.

### 2.3.7 Fire Detector Temperature sensor Calibration

801PC and 801PH devices and some of the variants used for this study incorporate thermistor devices for temperature measurements and provide output in bit form. The temperature response of each device was calibrated before supply to UCLan in flowing air in a heat tunnel at TYCO Sunbury and in house method, recording bit output response during a 3 °C/minute temperature ramp. Figure 33 shows a plot produced from an example record. Temperature sensitivity for these devices is very stable.

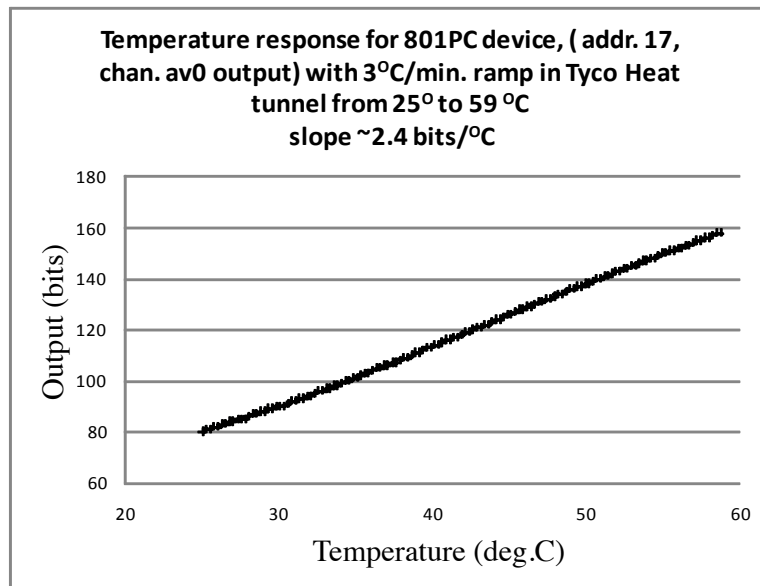


Figure 33 Example 801PC temperature channel calibration

At UCLan, validation of detector temperature sensor response was carried out on a continuing basis by referring the devices temperature response to that of a K type thermocouple itself checked periodically with ice (0°C) and steam above boiling water (100°C).

### 2.3.8 UCLan Enclosure NDIR for CO and CO<sub>2</sub>

A general introduction to the application of the IR techniques and particularly NDIR was provided in chapter 1. A dual fixed wavelength NDIR device (Unicam 22PU NDIR) was used with the UCLan 2 m<sup>3</sup> enclosure to monitor the carbon monoxide and carbon dioxide concentrations in the fire gases. Gas input to the NDIR system was from a fixed sampling point in the roof of the fire enclosure. As the NDIR system uses an aspirated sampling pump care was taken to ensure sampling did not interfere with the smoke transport to sensor/ detector locations.

The NDIR device sampled at a rate of 2 l min<sup>-1</sup> with a sampling time of 15 seconds. The sample path length was 10 mm. High purity nitrogen gas was used to provide a reference zero value and this was checked on a daily basis using the inbuilt instrument validation system. The span was checked on a daily basis using a maximum value was supplied by calibration CO/CO<sub>2</sub> gas.

An additional validation in the UCLan enclosure was carried out each week. This involved measuring the response of the CO and CO<sub>2</sub> channels to 10 litres of CO/CO<sub>2</sub> (6000ppm/4% in air) calibration gas fed into the enclosure at a rate of 1.7 litre min<sup>-1</sup> (for 353 seconds). A fan was used to ensure the calibration gas was adequately mixed in the 2 m<sup>3</sup> enclosure to give 30 ppm CO, 0.02% CO<sub>2</sub>. After gas injection and mixing the instrumental readings for the CO/CO<sub>2</sub> levels were monitored until the levels reached a plateau.

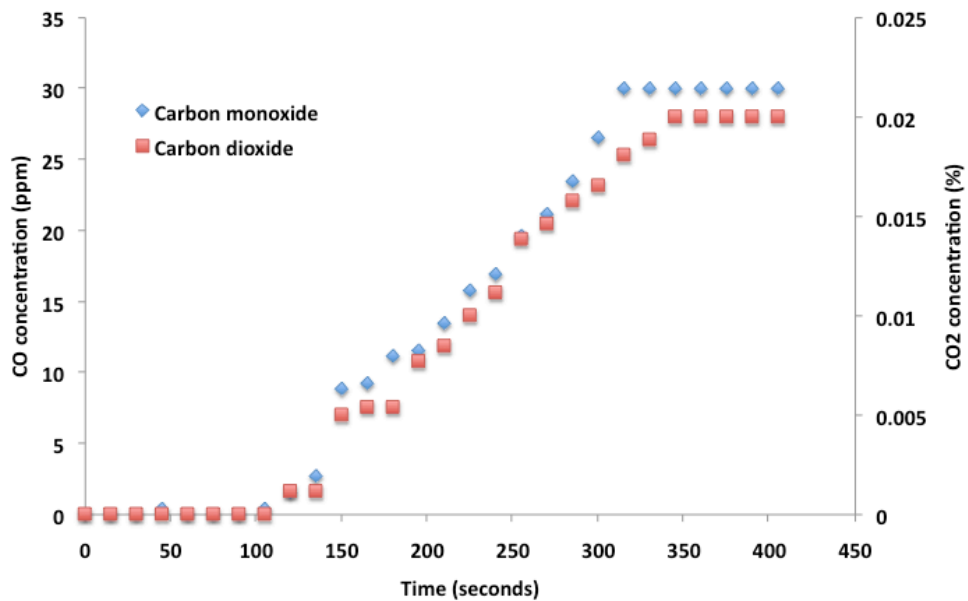


Figure 34 The figure shows the validation checks used for the NDIR device in the 2m<sup>3</sup> UCLAN fire chamber , The values are averages of regular checks (n=13)

### 2.3.8.1 UCLan Enclosure Calculation of CO/CO<sub>2</sub> yield by NDIR

The NDIR gives us a convenient method for defining yield and ratios of CO and CO<sub>2</sub> formed in fires. The Ratio is expected to vary depending on fire type and the degree of fire development and may also be informative with respect to nuisance sources.

If at a given time CO concentration = a ppm, and increase in CO<sub>2</sub> concentration = b ppm.

Then CO/CO<sub>2</sub> ratio = a/b (assuming volume ratios used for ppm definition equate to molar ratios, which should apply well for these gases in air at atmospheric pressure.

Using ppm values averaged over the test duration to calculate CO/ CO<sub>2</sub> may provide a value generally characteristic of fire type. Calculations based on a series point of time ppm values and yielding the corresponding ratios may be taken as indicative of fire condition development.

One may attempt to calculate yields of CO and CO<sub>2</sub> from combustion based on weights of fuel before and after fires but the validity of that depends on the degree of gas mixing in the enclosure, a feature not controlled in these fire test emulation experiments. Values are not therefore presented.

### **2.3.9 UCLan Enclosure Humidity sensors**

Humidity sensor : The moisture changes in the enclosure were monitored using a humidity sensor device (HONEYWELL HUMIDITY SENSOR, 2.54MM, SIP , HIH-4000-001, Farnell stock code 1187547) which was coupled into a modified TYCO 801PH fire sensor (addr. 100, ser.no920000266) where the photo-sensor input is replaced by humidity sensor input. This allowed humidity sensor output to be monitored and logged in bit form simultaneously to the same files produced for the TYCO smoke detectors. A miniature fan (25x25x10mm, NMB, 1004KL-01W-B40-B00, Farnell stock code 1545794) was mounted into the detector cover to produce a significant airflow over the sensor, as response was otherwise excessively slow.

A three point validation of the humidity sensor range was performed using conditions corresponding to 0% RH, 41% RH and 100% RH (dry bottled air, and air bubbled through fine frit in salt solution and pure water). Using these values a response chart (figure 35) was constructed from which humidity readings could be calculated.

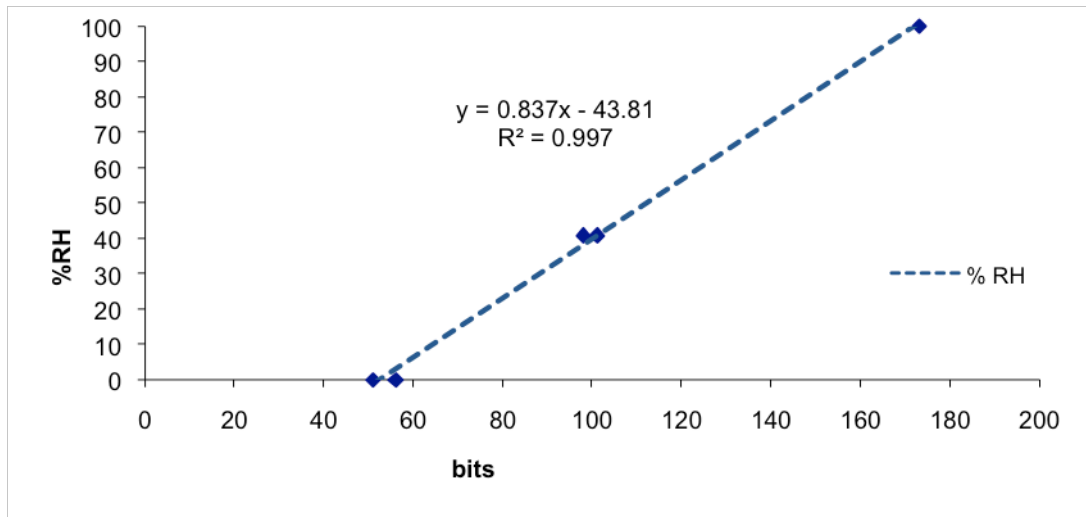


Figure 35 Example of three-point calibration curve used for the analysis of humidity data Conversion of RH % to ppm values based on temperature and literature tables.

### 2.3.10 UCLan Enclosure Optical Density measurements

The BRE test room is equipped with an Obscuration measurement system as required by BS EN54/7. Such commercially produced equipment was not available for the UCLan measurements so an in house built obscuration detector was constructed for incorporation into the enclosure using an 890 nm IR LED ( $10^\circ$  viewing angle) and a receptor separated by a 0.691m path length. The LED and photosensor were chosen to meet the specification of a light source from the BS-EN 54 standard – as below

The wavelength of the light was selected so it has the following specifications;

4. At least 50% of the radiated power shall be within a wavelength range from 800nm to 950nm.
5. Not more than 1% shall be in the wavelength range below 800nm.
6. Not more than 10% shall be in the wavelength range above 1050nm.

Prior to each test the obscuration device range was checked by measuring the output in free air and completely obscured by a non trans-missive sheet.

The analogue output from the unit was linked via a buffer amplifier to a TYCO 801PC detector (address 135) converted to provide A to D function so that it could be simultaneously logged onto the same data files containing the output of TYCO smoke detectors. The bit output for the system is linearly related to photosensor output and covers the full range between 0 and 100% transmission. The bit output is converted to Obscuration ( $\%Obsc.m^{-1}$ ) using the path length 0.69 m using the expressions below;

Output fully obscured = a bits (typically 4 bits)  
 Output for clear air = b bits (typically 155 bits)  
 Output for a smoke level = c bits

$$\text{Transmission Fraction through smoke} = T_s = (c-a)/(b-a) \quad (18)$$

Equation 18 Calculation of the transmission fraction of light through smoke.

For a path length m.

$$\text{Obscuration as \%Obsc.m}^{-1} = 100 \times (1-T_s^{1/d}) \quad (19)$$

Equation 19 Calculation of the obscuration per meter (%Obsc.m<sup>-1</sup>) for any path length (d) from transmission measurements.

So for UCLan obscuration unit path length = 0.691 m

$$\text{Obscuration as \%Obsc.m}^{-1} = 100 \times (1-T_s^{1.447}) \quad (20)$$

Equation 20 Calculation of the obscuration per meter %Obsc.m<sup>-1</sup> for the UCLan device

System stability, particularly under low smoke obscuration conditions. Table 8 below is a random selection of bit output values collected at the instrument calibration stage carried out before test fire emulations in the UCLan enclosure.

Sample	100%	0%
1	154	4
2	156	4
3	154	4
4	161	4
5	158	4
6	164	4
7	152	4
8	154	4
9	151	4
10	160	4

Table 10 Output for randomly selected obscuration device measurements

A significant issue was signal to noise which was particularly significant at low obscuration levels. While the output when obscured (low light) is stable, it is clear that there is significant variation under clear air conditions amounting to up to ~13 bits (from column 2 of Table 8) corresponding to an obscuration range of ~12 %/m. Taking

multiple measurements reduces the “noise” and clear air bit values tend to cluster around 155 bits. Some variation in performance was observed related to stability of the optical obscuration detector arising from the use of a battery to power the unit but this element was largely dealt with by the 2-point calibration being carried out before each test. Smoothing during actual smoke measurements when smoke levels are changing is more complex and inevitably introduces some effects on time response for obscuration measurements. The data was smoothed using a post processing Savitsjy-Golay filter. The Savizky-Golay[104] smoothing filter is essentially a local polynomial regression fit that works in similar way to moving averages, but retains the features of distribution such as the minima and maxima that can be sometimes otherwise lost using other smoothing techniques.

To check the response of the optical device is linear over the entire range of the light span two filters (Neutral density filters supplied by Omega Optical) were used to measure the optical response at specific obscuration. These were listed as 0.3 and 0.8 obscuration filters. Measurements using the UCLan obscuration device resulted in optical transmission decreasing by  $68 \pm 4\%$  and  $20 \pm 3\%$  respectively.

## **2.4 Gas collection, chromatography, and analysis - GC/MS system**

Collection of gases/vapours using absorbent media and application of GC and GC/MS to measuring and identifying such products was introduced in general terms in chapter 1. Section in this chapter deal with the actual sample collection processes employed at UCLan and at fire tests at BRE Watford, and the procedures for GC/MS measurements on those samples at UCLan.

### **2.4.1 Collection of Fire Gases on Absorbent Media**

Samples of fire gases were collected onto absorbent media in sample tubes for subsequent GC/MS analysis. Unless otherwise stated, the sampling point was located in the centre of the fire enclosure roof. Figure 36 shows a schematic of the sampling arrangement.

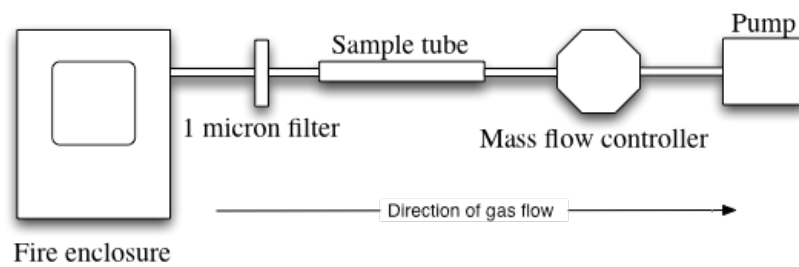


Figure 36 Diagrammatic representation of fire product sampling set up for fire enclosures. The 1-micron filter is to remove particulates.

Connections were made with 6mm Teflon coated plastic tubing. To prevent the build up of adsorbed vapours from fires in the sampling arrangement the tubing was replaced or cleaned on a daily basis during testing or on changes of fire type. Tubing was cleaned by flushing with clean water and methanol and then blown dry.

Filters used were Whattmans 0.1 micron filters (polydisc TF 0.1 $\mu$ m), inspected between fire tests and replaced if filter was being substantially darkened or every 50 tests (sooner in the case of contamination). The filter was also changed whenever the fuel type was changed.

The sample tubes used were 110 mm long with a diameter of 6mm OD and 4mm ID. Tenax sample tubes were packed with 135mg of 60:80 mesh Tenax TA, and Carboxen sample tubes were packed with 500mg of 60:80 mesh Carboxen 1000.

The sampling rates for these different materials were:

- For Tenax sample tubes                      70 ml min<sup>-1</sup>
- For Carboxen sample tubes                120 ml min<sup>-1</sup>

Flows were set with a mass flow controller and mains powered pump unit capable of providing smoothed flow rates up to 2000 ml min<sup>-1</sup>.

Resins were conditioned prior to use in accordance to the manufacturers guidance [105]. Between sample collections the absorbent containing sample tubes were cleaned/conditioned using a shorter conditioning process (15minute in helium flow at 320-350°C for Tenax and 280°C for Carboxen).

Equipment, components, and methods can introduce sampling variation which may need to be controlled or monitored by the operator. Although each sample tube provided by a commercial source has been tested for conformity in the amount and packaging of the material, variations within the sets of sample tubes used may confer variability to the data set through slight changes in the way the absorbent surface is made available to the analytes or packing differences affecting flow resistance and so changes in pressure and/or flow during collection or desorption. To allow systematic effects of this type to be identified a system of sample tube tracking was used. Each of the sample tubes supplied from Sigma Aldrich is supplied with an identifying serial number and other sample tubes were etched with a glass-engraving pen and given in house identification numbers. Each sample tube was labelled and catalogued so the response could be monitored historically. This allowed sample tube use to be tracked between experiments and linked to individual tests and GC/MS runs.

On a 3 month cycle each sample tube is checked using a standard injection. The standard injection was part of a validation check. For Carboxen samples 1ul of 2 Propanol was injected directly onto a clean 500mg Carboxen sample resin trap that was then desorbed under normal test conditions. In the case of Tenax samples 1ul of n-heptane (ex sigma GC purity standard) onto a Tenax sample tube. It was noted that for a given test type, greater GC reproducibility was seen when the same sample tube was used as compared to when samples were collected on different tubes. Each tube can be used for 50 samples before either being replaced or cleaned out and repacked with a new absorbent material charge.

The tubes were checked for background/carryover between samples repeating the analysis program with the cleaned/conditioned tube in place of a sample tube and the background levels assessed. If carryover was observed then the tube was subjected to an additional cleaning procedure and if persistent contamination is observed then the sample tube is replaced.

Collected samples were analysed within 24 hours of collection where possible. Samples that needed to be stored were kept in sealed storage tubes at 4°C for up to 3 months.

## **2.4.2 Gas chromatography - Injection**

GC analysis requires injection of a small volume of sample into a carrier gas stream (eluent) which carries it onto the column for separation by partition between the fluid and stationary phases which affects the column transit time (retention time) for a chemical species. Separation quality depends on the injection process and a number of variants exist. Injection via a cooled trap and direct injection were both examined.

Samples on the Trio 2000 system were injected onto the 5890 GC using a CDS pyroprobe thermal desorption system. There are two modes in which the pyroprobe can operate. Either into a trapping mode where sample is concentrated onto a trap and then desorbed from that trap onto the GC column, or it can be operated in a direct mode where the sample is directly desorbed onto the GC column without a trapping stage.

### **2.4.2.1 GC Thermal Trap Injection**

The TDCT (thermal desorption cold trap) system uses an oven to heat the sorption tube loaded with sample to induce material to be desorbed into non reactive carrier gas flow (Helium). The duration of the heating of the sample is described as desorption time. A section of capillary between the sample sorption tube and the beginning of the GC column is cooled with liquid nitrogen cooled nitrogen gas to condense and concentrate the sample gases into a small injection slug. Following the desorption period the capillary is rapidly heated with an induction heater and the vaporised sample flushed onto the column. Once on the column the sample is eluted in accordance with the conditions and chromatographic conditions of the GC.

The TDCT thermal trap injection system is illustrated in Figure 38 below.

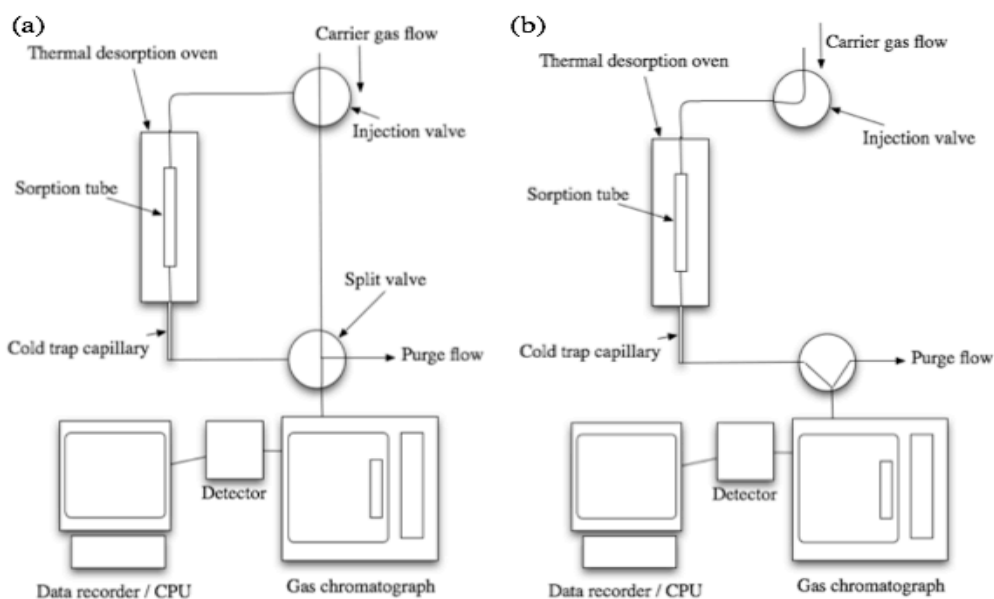


Figure 37 Schematic for the TDCT injection system. The diagram shows the system in load (a) and injects modes (b)

37a shows an arrangement where the sorption tube is loaded into the heater while carrier gas alone passes into the GC. 37b corresponds to injection conditions where sample first collected at the cold capillary is then injected into the flow onto the GC column when the cooled capillary is heated.

The carrier gas flow rate used for the sample through the TDCT was  $6\text{ ml min}^{-1}$ , which was put though a split injection system (not shown in figure) to reduce the on column flow to  $1\text{ ml min}^{-1}$ . Setting used are shown in Table 11 below:

Pre cool time	Trap cooling temperature	Desorption time	Desorption temperature	Injection time
5 min	-100°C	10 min	280°C	3 minutes

Table 11 Program settings for the TDCT injection system

## 2.4.2.2 GC Direct Injection

In direct mode the sample is directly desorbed onto the GC column without a trapping stage. This is represented diagrammatically in Figures 38 a, b, and c below.

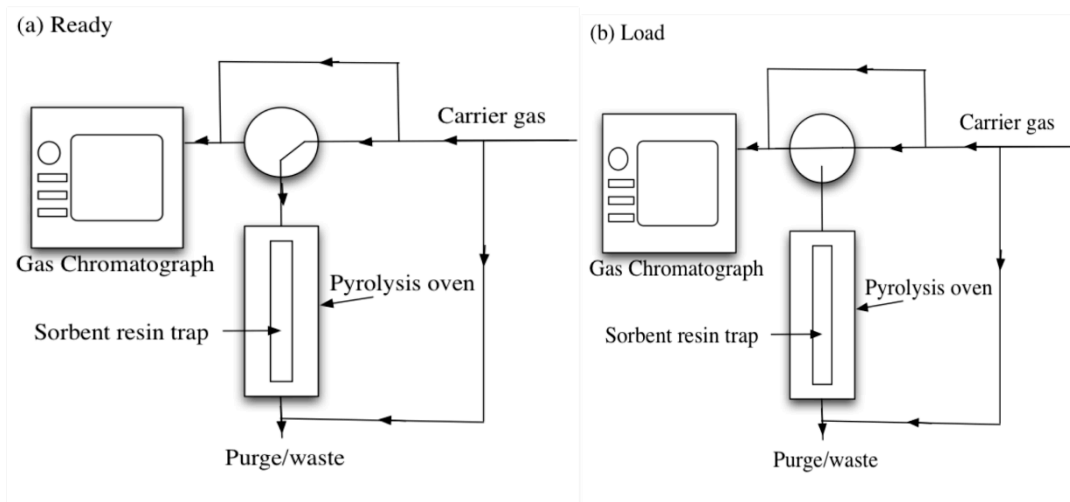


**Figure 38a Direct injection system Ready Position**

Direct injection for pyroprobe CDS5200 injection system.

The system in ready position purges the trap at the rest temperature and the split from the injection system flows to waste.

**Figure 38 b Load Position**

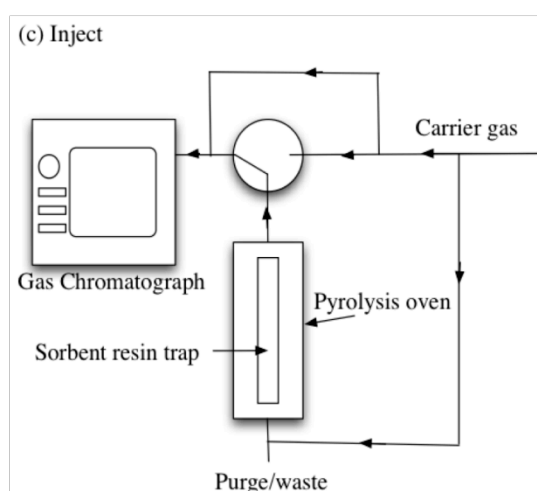
**Direct injection for pyroprobe CDS5200 injection system**

The load position redirects the flow away from the trap and the sample is heated at a controlled rate to the desorption temperature. Carrier gas

**Figure 38 c Inject Position**

Direct injection for pyroprobe CDS5200 injection system

In inject mode the carrier gas direction is reversed and flows through the heated trap and injects the desorbed sample onto the gas chromatographic column. After the injection the system returns to a ready state



After trials to establish the best method and with some modification of the injection system it was decided that a direct injection protocol would be adopted for samples collected onto absorbent traps from the fire enclosure. The conditions selected are as shown in Table 12

	Rest temperature	Desorption temperature	Desorption time (min)	Injection time (min)
Carboxen trap	40°C	250°C	4.00	0.5
Tenax trap	40°C	320°C	4.00	0.5

Table 12 Sample desorption parameters on the CDS5200 pyroprobe system

### 2.4.3 5890 Series II GC-MS

A series of experiments were used to optimise the GC conditions on the 5890 system. A smaller bore column meant lower flow rates could be used and the detection method for this GC system was a trio mass spectrometer. The 5890 series II can be programmed in a more advanced way to allow multi stage elutions.

During the course of the tests it was found that using the same column for samples collected on Carboxen and on Tenax did not provide satisfactory performance and so the procedures were modified to employ a different column with each.

#### 2.4.3.1 GC Column 1 - for samples on Tenax

Column 1 used for samples absorbed on Tenax was a Varian WCOT fused silica (length 50 m, I.D. 0.25mm) CP SIL 5 CB low bleed/MS column. The CP SIL is 100% dimethylpolysiloxane stationary phase and separates components almost 100% based on the boiling temperatures of the analytes . The carrier gas was high purity helium set to a flow rate of 0.72ml/minute. The column conditions chosen are given in Table 13.

Parameter	Set Point
Injector Temp	180°C
Initial column temperature	40°C
Initial hold time	5min
Gradient A	
Gradient ramp	5°C/min
Final temperature	90°C/min
Hold time	0 min
Gradient B	
Gradient ramp	10°C/min
Final temperature	190°C/min
Hold time	0 min
Gradient C	
Gradient ramp	20°C/min
Final temperature	290°C/min
Hold time	10 minutes
Final run time	40 minutes
Cooling time	5 minutes

**Table 13 Temperature program used on the 5890 Series II gas chromatogram to examine the desorbed samples from Tenax absorbent resin traps.**

#### **2.4.3.2 GC Column 2 – for samples on Carboxen**

The second column used was a CP-PoraPLOT Q GC column supplied by Varian. The CP-Portaplot column (length 30m, I.D. 0.32 µm) uses a stationary phase bound to an open porous polymer, which allows for the analysis of a large range of volatile components. The carrier gas flow rate is set to 1ml/min and the column conditions used are outlined in Table 14.

Parameter	Set Point
Injector Temp	50°C
Detector Temp	120°C
Initial column temperature	40°C
Initial hold time	15min
Gradient	4°C/min
Final Temperature	120°C
<i>Final hold time</i>	<i>5 minutes</i>

Table 14 The temperature program used to examine volatile samples collect on Carboxen traps. The Carboxen samples are eluted at lower temperatures than used for Tenax samples.

#### **2.4.4 Mass spectrometry: VG Trio 2000 conditions.**

The MS detector used for the experiments on samples produced at UCLan and BRE was a VG Trio 2000. The source temperature was set to 180°C. The data acquisition is in continuous centroid scan mode and scanning. A full scan took 0.1 second with a scan time of 0.3 seconds. There was no solvent deal built into the method.

The mass range analysed is between 25-250m/Z. The instrument is run in the positive electron ionization (EI+ve) mode with electron ionization energy of 70eV.

The Trio was serviced annually and calibrated as part of that process. On a daily basis the tuning gas checked using reference material as the standard.

Compound identification analysis using the mass fragment spectra corresponding to GC peaks was carried out using Wiley/NIST compound library visualised using mass lynx software, in part taking the automated best match candidates, and in part by visual examination informed by the NIST library. Compound identification is covered along with presented experimental data in chapter 5..

## **2.4.5 Measurements relating quantities of collected material to GC/MS data**

It was desirable to gather not only information on the identity/ molecular size of materials collected on the absorption tubes, but also some value that could indicate quantities so that concentrations in the smoke could be estimated. The amount of material is important in determining if individual components are worth studying as potential targets for fire detection. In order to relate GC/MS data to quantities of material generated in tests and aspirated to absorbent tubes it was necessary to check the reproducibility of the absorption, desorption and GC operation.

Use of an internal standard to validate the amount of material on the column was considered as allowing calculation of the approximate the amounts of material present in the smoke. Early experiments were hampered by the large degree of variability of the samples, both in terms of the types and amounts of specific analytes captured. It was felt that arranging a marker dosing protocol for the UCLan enclosure or the aspiration line to absorbent tubes was not straightforward and that using an internal standard was not a reliable method. Alternative arrangements were made to check on absorbent tube loading and resultant GC/MS spectra.

A series of experiments were carried out involving dosing measured amounts of known compounds onto absorption tubes and then carrying out GC/MS analyses to validate absorption tube performance and further to determine relationships between analyte loading on tubes and resultant GC/MS elution peaks.

The absorption tube validation schedule involved tests (using 1  $\mu$ l injections of n-hexane for Tenax tubes and 2-propanol for Carboxen tubes ) to determine run to run reproducibility for individual tubes (validation stage A) and check for any changes arising from ageing or use (validation stage B).

Further tests with a wider range of volatile compounds and a range of dosing levels were carried out to provide a more general guide to the relationships between absorbent tube loading and GC/MS peak areas.

Transfer of measured amounts of analyte to the absorbent tubes was carried out by injection with a micro-syringe through a sealable opening in a sample chamber onto a cotton pad within a system allowing air to be drawn through the pad and then pass through the absorbent tube.

A form of the system for transferring materials via the cotton pad is represented diagrammatically in figure 39 below with provision in some tests for air recirculation through the pump: With the sample loop was set up as indicated in figure 39, an injection of 1.0  $\mu\text{l}$  of the sample liquid was onto the cotton bed and the pump started with the air flow set to 78ml/min. Flow was continued for 15 minutes and the sample tube out and subsequently subjected to the relevant standard desorption and GC/MS protocols.

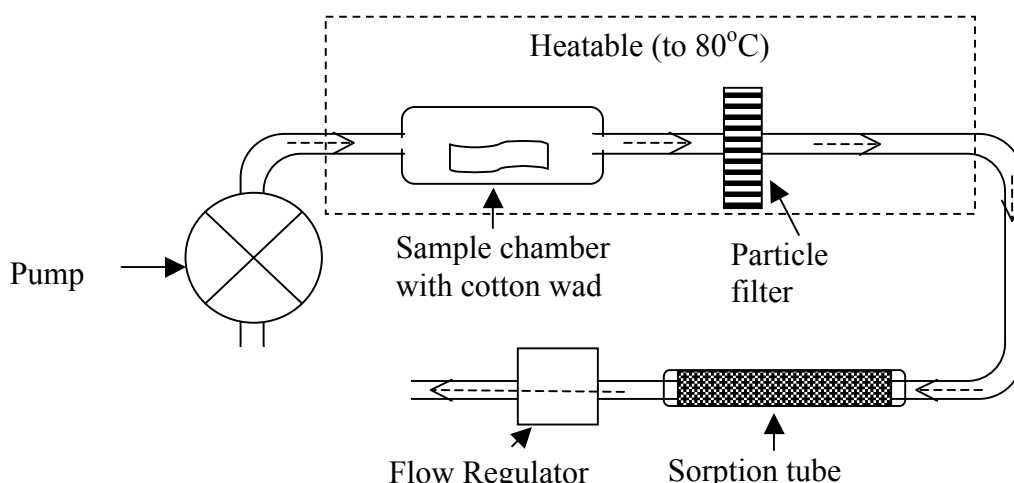


Figure 39 Schematic of transfer of sample injected onto cotton wad in sample chamber to sorption tube.

Total volume  $\sim 74$  ml (pump, chamber, tubing, absorbent tube).

#### 2.4.6 Absorption tube Validation Schedules

Validation schedule A was a process to check operation of a new or newly filled absorbent tube. Validation schedule B was to check on stability of performance. For Tenax tubes the injected dose was 1  $\mu\text{l}$  of n-hexane and for Carboxen it was 1  $\mu\text{l}$  of 2-propanol.

Validation A involved use of 6 repeat injections to establish the typical response for the selected tube. Acceptable performance validating an absorbent filled tube for fire test measurements was taken as GC/MS peak area for each of the 6 tests being within 95% of the sample mean. Table 15 shows results for representative successful validation A tests for a Tenax tube and a Carboxen tube.

Tenax (n-hexane) validation A			Carboxen (2-propanol) validation A		
	Peak area	% Mean		Peak Area	% Mean
1	3491724	102	1	4767991	97
2	3290942	96	2	4840402	98
3	3590918	105	3	5134174	104
4	3388567	99	4	5097223	103
5	3395367	99	5	4738220	96
6	3329091	97	6	4990550	101
Mean	3414435		Mean	4928093	

**Table 15 Examples of validation A injection for Tenax and Carboxen tubes**

Validation B applied to each sorbent tube after the validation A standard had been met was a validity check on stability of the response which was carried out on a monthly basis (or more often if required). The validation B check for a tube involved three injections and the responses were checked against the standard established by validation A for that tube. To be compliant the GC/MS peak area for each validation B injection was required to differ by no more than 5% from the mean for the two injections and by no more than 10% of the mean value from validation A (tube standard).

Table 16 shows results for representative successful validation B tests for a Tenax tube and a Carboxen tube.

Tenax (n-hexane) Sample B				Carboxen (2-Propanol) Sample B			
	Peak Area	%Mean (B)	%Mean (A)		Peak Area	%Mean (B)	% Mean (A)
1	3530271	101	104	1	5011692	102	102
2	3525049	100	103	2	4597446	100	93
3	3498071	99	102	3	4783199	98	97
Mean	3525049			Mean	4897446		

**Table 16 Examples of validation B injection results for Tenax and Carboxen tubes**

Where validation B results for a tube were significantly different from the validation A value ( $\pm 10\%$ ) or the validation B results showed significant variance (mean  $\pm 5\%$ ) then additional injections were run to a maximum of 6. If deviation from standard was confirmed the tube was taken out of use. If not suffering any obvious physical damage the tube was usually cleaned and refilled before submitting once more to the validation A protocol.

Difficulties with reproducibly dispensing the small sample volume (1  $\mu\text{l}$ ) injection may be responsible for introduction of a significant amount of variation seen in measurement repetitions.

#### 2.4.7 Column loading measurements appropriate for Tenax samples

The types of material captured onto Tenax represent the larger less volatile range of compounds. The commercially available grob II standard from Sigma Aldrich contains species which may be taken as representative of this range though not necessarily matched to any fire products. The materials could be injected direct to the Tenax tube and then desorbed to the GC column. A series of three increasing amounts of material were applied to the sorption tube (2,5, 7 $\mu\text{l}$ ) providing the loadings indicated in table 17 below:

Analyte	Concentration in standard ( $\mu\text{g}/\text{mL}$ )	Mass of analyte injected onto column( $\mu\text{g}$ )		
		2 $\mu\text{L}$	5 $\mu\text{L}$	7 $\mu\text{L}$
n-decane	280	0.56	1.4	1.96
2,6-dimethylaniline	320	0.64	1.6	2.24
2,6-dimethylphenol	320	0.64	1.6	2.24
methyl decanoate	420	0.84	2.1	2.94
methyl dodecanoate	420	0.84	2.1	2.94
methyl undecanoate	420	0.84	2.1	2.94
Nonanal	400	0.8	2	2.8
1-octanol	360	0.72	1.8	2.52
n-undecane	280	0.84	2.1	2.94

**Table 17 The amount of each analyte introduced in each injection based upon published concentrations of analyte in grob (II) standard.**

An example GC plot corresponding to a 2  $\mu\text{l}$  injection of grob (II) standard is shown below as figure 40.

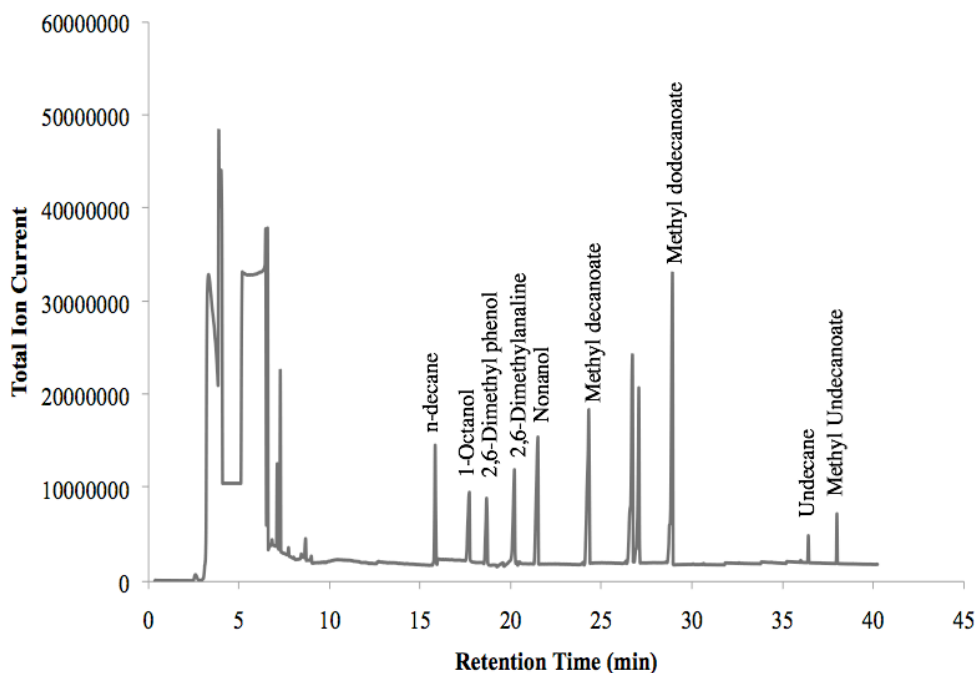


Figure 40 Gas chromatogram from 2µl injection of grob (II) standard onto Tenax sample tube, which was thermally desorbed as described. Vertical units are arbitrary units representing the current from the PM tube .

GC/MS ion current output values result from a series of instrument settings and is based on multiplier response and amplification factors. The scale is essentially arbitrary but for a well-maintained unit should be relatively stable for a give operational mode. Peak areas calculated from such plots are in units of the current scale (arbitrary units and the time scale (minutes)).

Injected moles data derived from Table 15 (masses/ molecular weights) plotted against peak area values derived from GC/MS plots for the 2, 5, and 7 µl injections yields Figure 41 below.

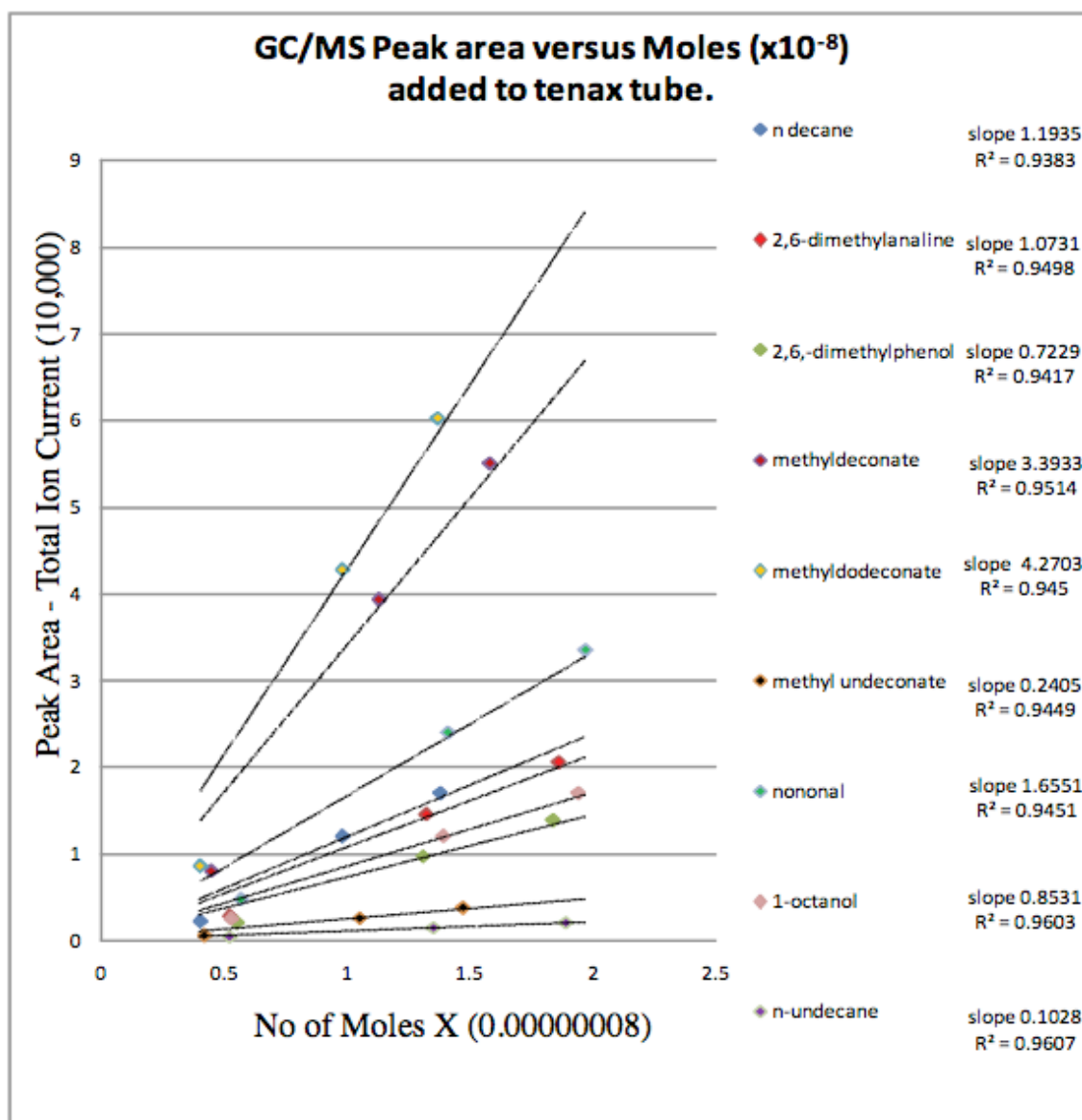


Figure 41 Plot of moles of the measured analytes contained in injected volume of the test mixture (Grob II standard) against peak area for each species.

#### 2.4.8 Column loading measurements appropriate for Carboxen samples

A series of experiments was carried out to determine a relationship between the GC/MS peak areas of analytes captured in a Carboxen sorption tube and the tube loading. Single injections of known amounts of specific analytes were placed into the sample vapour trap (Figure 39) on a solid support (cotton wad). The sample chamber was held at 80°C for 15 minutes while the air was circulated using a flow controlled pump at 100 ml per minute to equilibrate. At each loading the 500mg Carboxen resin tube was tested as described above for normal fire test samples.

Injected mole values for each species calculated from the injected volumes, liquid densities and molecular weights are plotted against peak area values derived from GC/MS plots for the 5, 10,15, and 20  $\mu\text{l}$  injections yields figure 42 below.

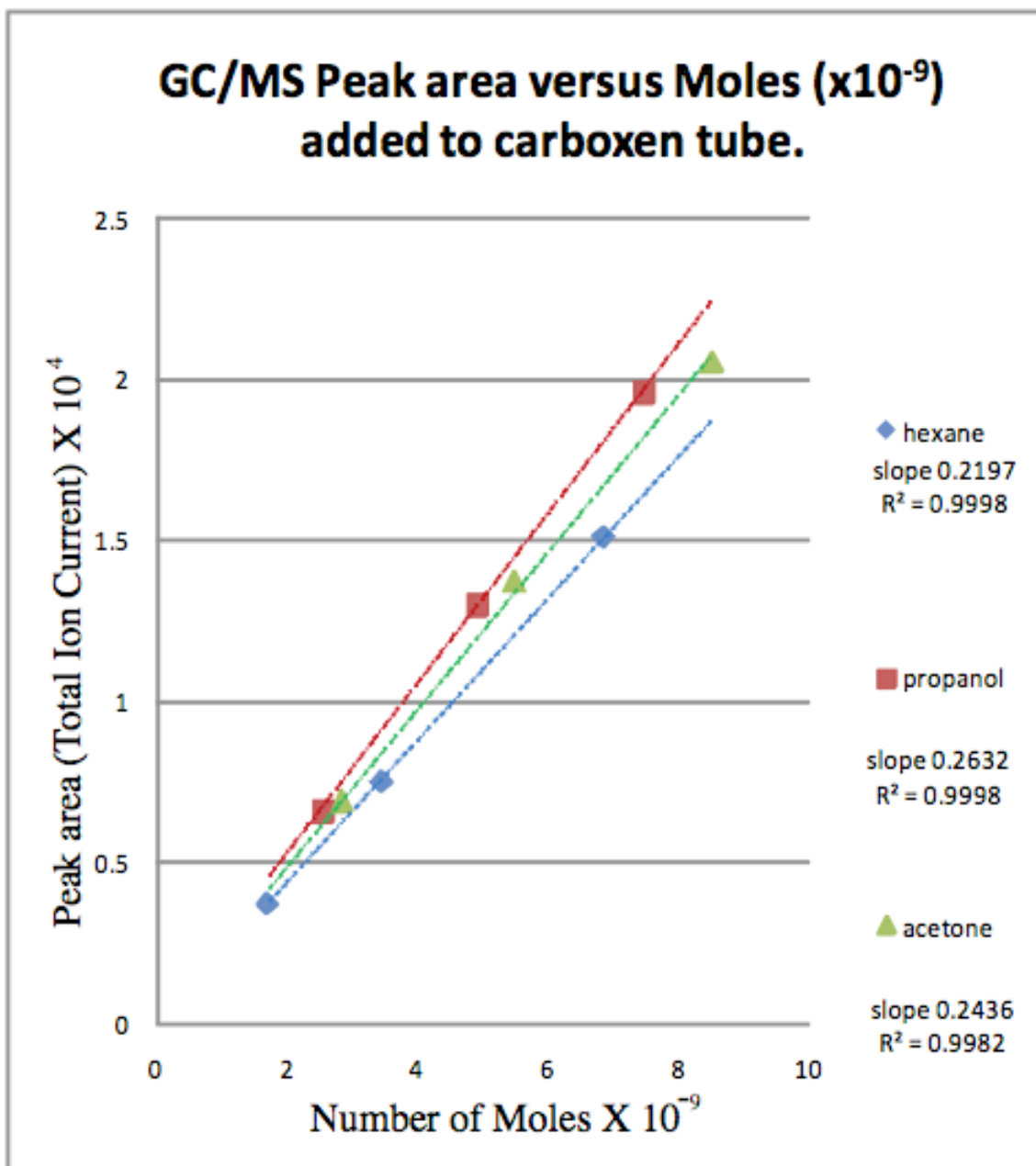


Figure 42 Plot of moles of the measured analyte injected into the vapour trap and absorbed on Carboxen versus the GC/MS peak areas for each species. Peak area is an arbitrary value used from an integral of the total ion current.

It is necessary to assume that loss of material from the injected volumes (5, 10,15, and 20  $\mu\text{l}$ ) is not gross, or at least consistent with that occurring in fire gas captures experiments. Weighing the cotton support before and after each injection checks the assumption that the entire sample is vaporised. It is also assumed that 15 minutes is sufficient time to achieve equilibration and transfer. The volume of the vapour trap including the connections is 74ml.

Each of the points in the plot shown as Figure 42 is an averaged value based on 5 repeat injections. The error in these injections is measured (RSD <6%). These compounds were selected to be representative of the types of gases seen in the analysis as a small hydrocarbon, alcohol and aldehyde. Time and availability of appropriate standard material mean there were only a few analytes being studied. This was to establish a general indication of scale rather than a reliable calibration allowing the GC/MS data to be converted to concentrations of gases in the air pumped through the absorbent tubes.

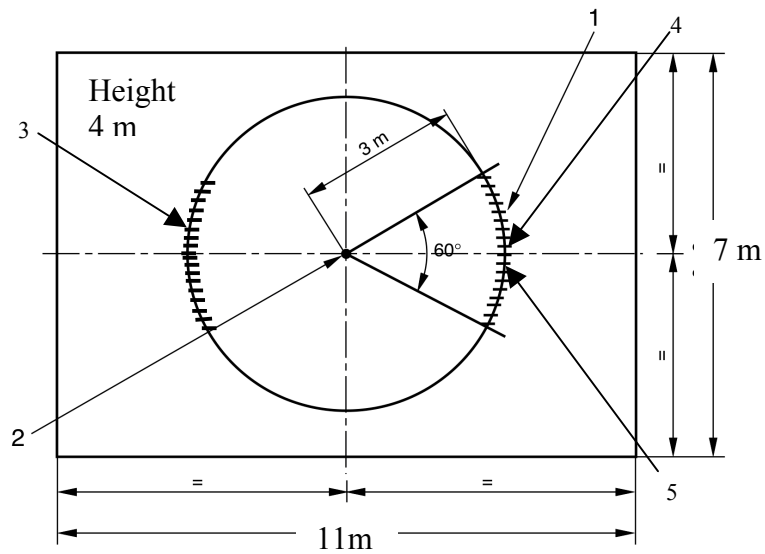
Figures 41 and 42 indicate a linear relationship with loading and the GC peak area.

#### **2.4.9 Other GC/MS system Validation Checks**

The trio 2000 system was serviced at least once a year, and the mass ranges calibrated against a standard. On a daily basis the mass tuning was checked using an internal standard Heptacosafuorotributylamine m/Z 69,212,507, 649 and compared to standard values .

#### **2.5 Full-scale fire test room (BRE) – Detector/Sensor Deployment**

Standard test rooms are designed to allow validation testing of fire detectors with standard test fires. They are of sufficiently large scale to allow the development of fires to a condition comparable to unwanted fires in the workplace. The rooms are ventilated between fires but during tests there is minimal induced airflow in the room to avoid complications with gas and smoke transport issues. The Building Research Establishment Ltd, Watford,( BRE) has a test room used in this study shown as Figure 43 below with location of addition detector sites used in some tests and locations of the BRE MIC inlet and BRE Optical Obscuration unit.



**Key**  
 1 specimens and measuring instruments  
 2 position of test fire

- 1/ Primary Detector Arc on ceiling    2/ Fire source (floor centre)  
 3/ Supplementary Detector Arc        4/ MIC inlet  
 5/ Obscuration unit (suspended below ceiling)

Figure 43 Diagram of the BRE Watford BS EN 54-7 compliant fire test room showing actual room dimensions, fire source position, and detector locations.

The standard room is 4 m high and dimensions illustrated are those for the BRE Watford test room and within the ranges specified by BS EN54/7.

16 equivalent sampling/detector location ports are located on the ceiling at equidistant points along a 60-degree arc on a 3m radius circle centred above the fire site. The centre section of the primary arc is used as the location for the BRE obscuration meter and aspiration point for the BRE MIC unit. For normal commercial detector validation fire testing purposes only that arc is used but the second arc is considered adequate for supplementary tests. Sample ports are grouped into banks of 4 across the outer 20 degrees of each arc. A range of standard and non-standard TYCO fire detectors and electrochemical H<sub>2</sub> and oxidisable gas sensors (City technology 7HYT and 7ETO types) were located at sampling points along the arcs. The detectors were fitted to standard ceiling mount bases and the electrochemical cells suspended about 10 cm below the ceiling. Pumped sampling lines for collection of gases/vapours on sorption tubes for subsequent GC/MS analysis were fed into sampling port locations, taking care that inlets were far enough from detectors to avoid causing smoke transport issues. For the

second BRE tests a further inlet line through one port in the secondary arc was provided for input to an Owlstone FAIMS unit incorporating its own pump. Aspiration tubes for BRE MIC, for sorption tubes for GC/MS, and for FAIMS equipment were positioned so as not to significantly interfere with room conditions or airflow adjacent to other detectors or sensors.

Samples for GC/MS were captured on Tenax and Carboxen absorption tubes using flow controlled pumps as for the reduced scale test in the UCLan 2 m<sup>3</sup> enclosure and described earlier. Samples were collected over the complete duration of the test (from before ignition to end of test based on BS EN54/7 specification).

In the later BRE tests additional sampling of smoke particulates onto a glass fibre filter was carried out with a pumped system located ~ 1m from fire sources. This smoke aspiration was not started until each fire test was complete and continued during the room air clearing stage. These smoke particulate samples were collected for fluorescence measurements directly on the smoke material. Measurements on samples of this type carried out at UCLan and at the University of Central London indicated that background fluorescence from the filters was too high to allow useful analysis. Some further work on collection of smoke particulates by impingement on low fluorescence microscope slides was started but is not reported within this thesis.

The TYCO devices used were a selection of 801PC (3 measurement channel devices – smoke by 850 nm photo scattering, CO, and temperature), and 801I (1 measurement channel device - smoke by effect on ion current through air ionised by Am<sup>241</sup> source), and other experimental units as described in earlier. The TYCO detector operation and data handling was performed with a TYCO MX panel simulator box with associated software and PC.

Smoke density was monitored by BRE equipment defined in BS EN54/7, consisting of an optical obscuration meter and pumped ionisation type detector (MIC). Outputs from the BRE units were recorded for all tests at 1-second intervals and data files provided by BRE staff. Humidity and temperatures in the room are monitored prior to and throughout the testing. After each test smoke is evacuated using built in air conditioning ventilation systems. These are also used to ensure the room temperature is even in the

test room to reduce stratification effects, particularly exclusion of fire products from the roof area which may occur if a layer of warmer air exists there before the fire starts. I

All the full-scale tests referred to in this project were carried out using the BRE test room in February 2009 and in May 2010. All BRE measurements were compliant with BS EN 54/7:2001. Measurements with TYCO detectors and non standard measurements performed at the BRE tests (e.g. hydrogen, and oxidisable gas sensing by electrochemical sensors and sampling for GC/MS etc.) were performed in accordance with methods developed at reduced scale with sampling as described above.

The BRE fire test room is constructed with a second room above it providing access to the detector or sensor mounting ports and facility for setting up instrumentation. Figure 44 below represents a plan of that room showing detector and sensor locations for the tests at BRE in May 2010. The tests carried out in February 2009 involved less detectors, which were predominantly sited at the ports adjacent to the BRE instruments (Obscuration unit and MIC).

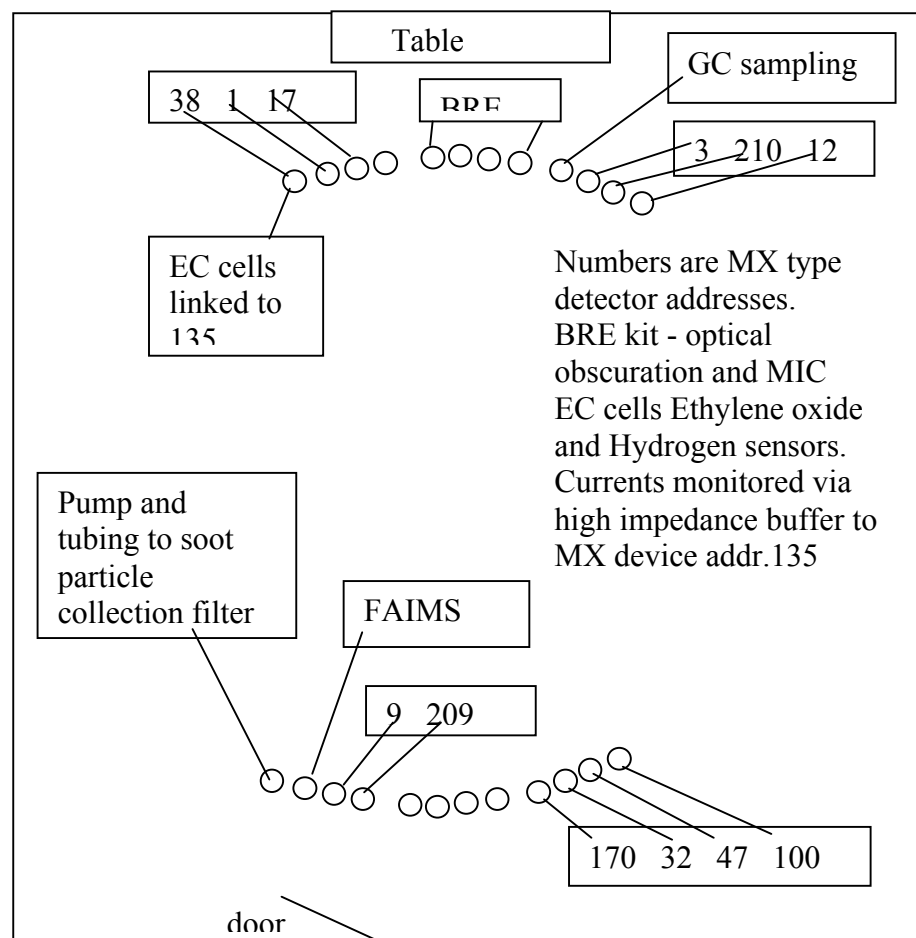


Figure 44 Equipment lay out in room over BRE test rooms for tests in May 2010

The detector and sensor devices deployed in this BRE test are selected from the same group used with the UCLan enclosure, but additional equipment deployed includes the BRE MIC and Optical Obscuration meter, and a FAIMS instrument supplied by UCLan. The UCLan NDIR system for CO and CO<sub>2</sub> measurement, and the obscuration unit, which is built into the UCLan enclosure, were not deployed at BRE.

The detectors linked to the TYCO MX series panel simulator are listed below as table 18.

MX Address	Serial Number	Model/ type	Further Information
3	12019CBCE	801PC	Standard type – NIR scatter, temperature, CO
9	92019CC09	801PC	Standard type– NIR scatter, temperature, CO
17	1200C0C9C	801PC	With extended CO range (> 400 ppm).
1	120049F36	801PC modified	Standard NIR scatter, temperature
209	92019301A	801I	With unfiltered CO cell, Zellweger, Part No. 2119B1003. Standard NIR scatter, temperature
210	8006FBE8	801I modified	Standard Ionization type
32	20382815	BIR	Ionization type with ~6x extended dynamic range.
12	20382805	Phosphor	special dual LED IR and blue
170	9200002A4	801PH	blue LED and IR phosphor device
38	12019CC13	801PC UV LED	blue LED in 801PH detector type package
47	12019CBFF	801PC longer NIR LED	UV LED (370nm) in 801PC detector type package
100	920000266	801PH modified	IR LED (1070nm) in 801PC detector type package
135	8000060	801PC modified	Humidity sensor replacing optical in 801PH, provided with min-fan.
			801PC converted to give bit outputs from 3 analogue inputs to MX log. Chan. av0 and av1 used for 7ETO and 7HYT cells.

Table 18 Summary of MX 801 Detectors and Variants

## 2.6 Standard Fire Tests

The most commonly applied standard test fires defined under EN54/7 and UL 268 were described in chapter 1. The EN54/7 fires were the basis of most of the measurements in the full scale test room at BRE. Both EN54/7 and UL268 test fires were used as the basis for emulations at reduced scale at UCLan.

### **2.6.1 Standard EN 54/7 Fire Tests in full scale test room (BRE)**

The standard test fires carried out at both visits to the test room at BRE Watford were EN54/7 test fires TF2 (wood pyrolysis), TF3 (smouldering cotton wick), TF4 (flaming polyurethane foam) and TF5 (flaming heptane pool). Quantities, ignition procedures, and smoke density acceptance criteria were as defined in EN54/7 and described in chapter 1.

### **2.6.2 Additional fire tests in BRE full scale tests**

Additional fires not included in usual EN54/7 set but defined by other standards were performed in the earlier BRE test (flaming Decalin, and Smouldering Cotton towel (sometime TF8)). No results are presented because the fires were not repeated in later full scale fire tests but commented on here to represent the other fires that were carried out.

#### **2.6.2.1. Decalin pool fire. (first BRE test only)**

Decalin, a heavy hydrocarbon  $C_{10}H_{18}$  (Decahydronaphthalene), is used as an industrial solvent for resins and fuel additive. Samples in full scale tests were prepared by measuring out 170g of decalin into a 120 x 120 x 20 mm steel dish with 5g of ethyl alcohol used as an ignition promoter. Decalin burns with a very heavy black smoke and orange flame.

## CHAPTER 3 SCALING OF FIRES – ISSUES AND MEASUREMENTS

### 3.1 Practical and theoretical basis for scaling test fires

A major target of this study is to characterise the products from the standard fires used for detector validation. Ideally this would be done on full scale test fires in the appropriate fire rooms. However these facilities are large and access is expensive (~£1000/ day in 2008) and this limits their availability. Although some measurements and sample collection was always envisaged as part of the study, it was never expected that this could represent a large part of the work. In order to develop the measurement and sensing methodologies and gather a substantial body of data it was considered necessary to arrange for tests at a more convenient reduced scale. A significant issue then arises concerning how to scale the test components and what the target criteria for reduced scale tests should be. The early measurements carried out at Bolton University using the NBS smoke box indicated that using a chamber of that size ( $0.5 \text{ m}^3$ ) would introduce real difficulties in generation reduced scale emulations of the standard fires. It was therefore decided that a fairly substantial fire enclosure was needed, although still somewhat constrained by available laboratory space. Dimensions for a test enclosure 2 m high on a 1 m square base were selected as practically convenient and as allowing a height for plume rise not too grossly less than the 3 and 4 m heights used for the UL and EN54/7 test rooms. While lateral dimensions may not be insignificant, consideration of the literature on fire plumes suggested that height was more important.[106]

Scaling of fires has long been a goal of fire researchers for a variety of reasons. The variety of sizes and locations unwanted fires means studying them in situ is both dangerous and prohibitively expensive. Fires can be extremely complex involving differential conservation equations involving mass, momentum, and energy, and definition of appropriate boundary conditions [107] and this makes computerized scaled models approximate at best. The trade offs often encountered in scaling work are illustrated by the compressive review of the theoretical factors provided by [108] which more than 28 dimensionless factors were identified to address the scaling problem.

Simpler approaches were taken by [109] and [110] but the applicability of much of the work to early stage fires and detection is not well established.

Expressions relating to fire product transport were considered when developing reduced scale tests but the purpose of this study was not to progress modelling of fires and fire scaling. The scaling work was directed at establishing practical reduced scale fires for the UCLan 2 m<sup>3</sup> enclosure that would be useful emulations of the full scale tests for analysis and for sensor and detector testing.

Fire detectors in real applications are generally mounted on ceiling locations on the basis that warm fire products rise and crucially because ceilings provide convenient sites where detectors are less likely to suffer physical interference, abuse or accidental damage. Fire site to detector distances will most generally be several metres as for the standard fire tests. Transfer of fire products (heat smoke, gases) to detectors remote from the fire source must be brought about primarily by convective processes and in the absence of externally forced convection that depends on the buoyancy forces resulting from gas density reducing with rising temperatures near the fire site. There has been much study of the fluid mechanics of fire plumes though little has been directed towards the detection issue. Based on a study of moderate to large fires Alpert [111] generated the equations 21 and 22 below for the temperature rise at ceilings above a fire and at radii about that point.

$$T_{\max} - T_o = 5.38 \times (Q_c / r)^{2/3} / H \quad (21)$$

Equation 21 Temperature rise from ceilings when  $r > 0.18 \times H$

Where  $T_{\max}$  is maximum gas temperature near a ceiling of height  $H$  metres for a fire of intensity  $Q_c$  M.Watts at a distance  $r$  metres from the point above the fire where  $r > 0.18 \times H$ , and where  $T_o$  is the initial ambient temperature.

For  $r < 0.18 \times H$  the Alpert indicated an alternative expression

$$T_{\max} - T_o = 16.9 \times Q_c^{2/3} / H^{5/3} \quad (22)$$

Equation 22 Temperature rise from ceilings when  $r < 0.18 \times H$

Drysdale [112] reproduces the above expressions and rearranges them to apply to the issue of fire size required to activate a ceiling mounted temperature sensor based fire detector producing equations 23 and 24 below.

For  $r > 0.18 \times H$ , the minimum fire intensity  $Q_{\min}$  require to activate an alarm responding at temperature  $T_L$  is:

$$Q_{\min} = r \times (H \times (T_L - T_o)/5.38)^{3/2} \quad (23)$$

Equation 23 Minimum fire intensity  $r > 0.18 \times H$ . Where  $Q_{\min}$  is the minimum fire intensity  $r$  is the fire radii,  $(T_L - T_o)$  is the temperature change from origin to detector,  $H$  is the room height .

and for  $r < 0.18 \times H$  the expression becomes:

$$Q_{\min} = ((T_L - T_o)/16.9)^{3/2} \times H^{5/2} \quad (24)$$

Equation 24 Minimum fire intensity  $r < 0.18 \times H$

While the expressions are developed only for heat measurement detectors their application where other detectors are used is reasonable given that the same convective processes carry heat, smoke and gases from fire source to ceiling. The temperature rises for the standard test fires are not specified but temperatures at the detection points in fire test rooms are routinely measured and Table 19 below provides some example results derived from data files supplied by BRE staff for test fires carried out for TYCO in the fire test room at BRE Watford.

Test	Description	Limit dB/m	Min.T °C	Max.T °C	T°C at dB/m limit	T°C at dB/m =0.5	T°C at dB/m =1	T°C at MIC y=1	T°C alarm range
TF2	Pyrolyse wood	2	19.6	20.1	20.0	19.9	19.8	19.9	0.3 - 0.4
TF3	Smoulder cotton	2	19.6	20.2	20.1	19.8	19.8	19.8	0.2 – 0.4
TF4	Flaming PU foam	1.73	20.4	41.1	41.0	25.2	31.0	22.0	2 – 20
TF5	Flaming Heptanes	1.24	19.5	88.2	77.8	40.1	67.0	29.5	9 - 20
TF1* ~UL B	Flaming wood	2*	20.5	70.6	22.5	20.6	21.3	31.4	0.1 - 2

Table 19 Detector ceiling arc temperatures for tests in BS EN54/7 room at BRE  
\*flaming wood fire according to rarely used EN54 definition similar to UL 268 fire B.

This provide some target temperature rises which might be applied in 23 and 24 along with room and reduced scale enclosure dimensions to calculate heat output rates corresponding to alarm conditions in the room and enclosure. The ratio of these heat output rates may be indicative of the fire source scaling that should be applied. On the basis of the values shown in / above it was considered worth calculating fire outputs rates test room and reduced scaled fire enclosure dimensions for temperature rises of 0.2, 2, and 10°C. Results for the dimensions for BS EN54/7 and UL268 rooms and the UCLan enclosure are provided in Table 20 below.

Chamber	H m.	r m.	T <sub>d</sub> °C	T <sub>o</sub> °C	Eq.3 MW	Eq.4 MW	EN/box ratio factor	UL/box ratio factor
EN54/7 room	4	3	20.2	20	0.172			
UL268 room	3	5.3	20.2	20	0.197			
UCLan Box a	2	0.2	20.2	20		0.007	24	27
UCLan Box b	2	0.6	20.2	20	0.12		14	16
EN54/7 room	4	3	22	20	5.440			
UL268 room	3	5.3	22	20	6.242			
UCLan Box a	2	0.2	22	20		0.230	24	27
UCLan Box b	2	0.6	22	20	0.385		14	16
EN54/7 room	4	3	30	20	60.82			
UL268 room	3	5.3	30	20	69.79			
UCLan Box a	2	0.2	30	20		2.575	24	27
UCLan Box b	2	0.6	30	20	4.301		14	16

Table 20 Calculated values of fire power requirements and ratio factors for 0.2, 2, and 10°C temperature rises at detector positions in EN54/7 and UL268 rooms, and UCLan enclosure.

For the UCLan enclosure distances (r) across the chamber roof of 0.2 and 0.6 metres were used. Only equation 18 is used for the fire test rooms but equations 23 and 24 are applied as appropriate for r values for the UCLan enclosure.

Conveniently as indicated in Table 20 above the calculated ratios for heat output rates for rooms and enclosures do not depend on the value entered for temperature rise. This simply arises from the temperature difference entering both expressions 23 and 24 in the same form. Whether this insensitivity to temperature difference holds true for real fires of interest is uncertain. Although Drysdale applies the expressions derived from the work by Alpert to fire detection, the expressions are based on work with fires and dimensions generally larger than the standard test fires. Thus extrapolation to smaller fires and fires where heat output rates are not fixed may not be justified. Certainly heat output rates of the type shown in Table 21 below as published by Grosshandler [113] for standard test fires does not appear to be consistent with corresponding calculated values shown in Table 20.

Test fire	Consumption rate (g/second)	Average heat release rate
TF2 – Smouldering wood	0.11	5.6kW
TF3 – Smouldering cotton	0.19	2.3kW
TF4 – Burning Polyurethane	1.2	3.2kW
TF5 – Burning heptane	3.1	30kW
UL A – Newsprint	0.18	3.2kW
UL B – Dry fir wood	2.5	52kW

Table 21 Published Heat Release Rates for Standard Test Fires

Nevertheless the scaling ratios indicated in Table 20 where the ratio factors suggest that sources in the UCLan enclosure should have power outputs ~10 to 30 times lower than those used in standard fire test rooms provided a starting point for consideration of reduced scale source generation. This was certainly likely to be better than simply taking the room to enclosure volume ratios ( $> 100$ ) as a starting point. Heat output ratios must be related to the size of fire source but whether that is better indicative of fuel volume or fuel area is not immediately clear and likely to depend on fire type.

In addition to the amount of fuel required for reduced scale tests there is the issue of the geometrical arrangement of the fuel, provisions to control excessive heat loss by conduction or radiation from small fuel bodies and means of ignition. These issues were not considered to be theoretically tractable within the scope of this study. Therefore the procedure adopted was simply to try out what seemed appropriately scaled sources and modify in the light of their performance i.e. whether the fires could be ignited, continue to develop without self extinguishing, and generated an appropriate amount of smoke.

This last point relates to the method chosen to determine whether the scaled fires were to be considered reasonable emulations of the full-scale tests. As the qualification criteria for standard test fires are, or may reasonably be converted to, obscuration versus time plots as presented in chapter 1, it was decided that the reduced scale emulations of those fires should meet the same obscuration versus time characteristics. This does dictate that source sizes are sufficient to maintain the combustion process over the test period i.e. scaling should reduce rate of combustion not just total product yields.

An optical obscuration measurement unit was available at the start of the study at Bolton University but unfortunately it proved impossible to arrange transfer of the equipment to UCLan. An obscuration unit was constructed in house at UCLan but did not become available until some considerable time after test work on the UCLan enclosure had started. Therefore initial test fire scaling studies at UCLan employed TYCO optical scatter detectors (801PC type) using calibrations against obscuration with joss stick smoke carried out in the TYCO Sunbury smoke tunnel. This was known not to be satisfactory as the relationship between obscuration and scattering changes with smoke type. However it allowed scaled test fire development to proceed to generate preliminary fire designs and protocols. Once the UCLan obscuration unit became available these preliminary scaled test fires were re-evaluated and where appropriate modified to provide the requisite absorption versus time characteristics.

### **3.1.1 Selection of test fire and detector sites in UCLan enclosure**

For standard test fire rooms the distances to walls are relatively large and so effects of walls on fire development and fire product transfer should be small. The walls of the UCLan enclosure are necessarily closer to the fire sources position and to the detector positions. The detector positions within the UCLan enclosure were selected at the design stage and a preliminary fire source location also designated. It was desirable to establish whether there were systematic differences between sensitivity for different detector positions and what effect fire source position might have.

A series of experiment were carried out to evaluate effects on smoke transport. In particular these experiments examined the effect of the side and corner effect on smoke movement. The floor of the enclosure was marked up as 10 by 10 grid of 10 cm squares as indicated in

Figure 45 below. Each intersection of lines on the grid, other than with the walls, defines one of 81 test positions identifiable by a number-letter combination. Groups of 5 standard 7cm length joss sticks (as used for calibration work in the TYCO Sunbury smoke tunnel) were loosely bound with wire to constructed joss stick wads to use as smouldering smoke sources. Each experiment consisted of placing a smouldering wad onto one of the test positions. Each wad was burnt for 1200 seconds and responses recorded for the optical scatter channels of seven 801PC detectors located in 7 locations of the standard loop as described in chapter 2 section 2.1.5 and following.



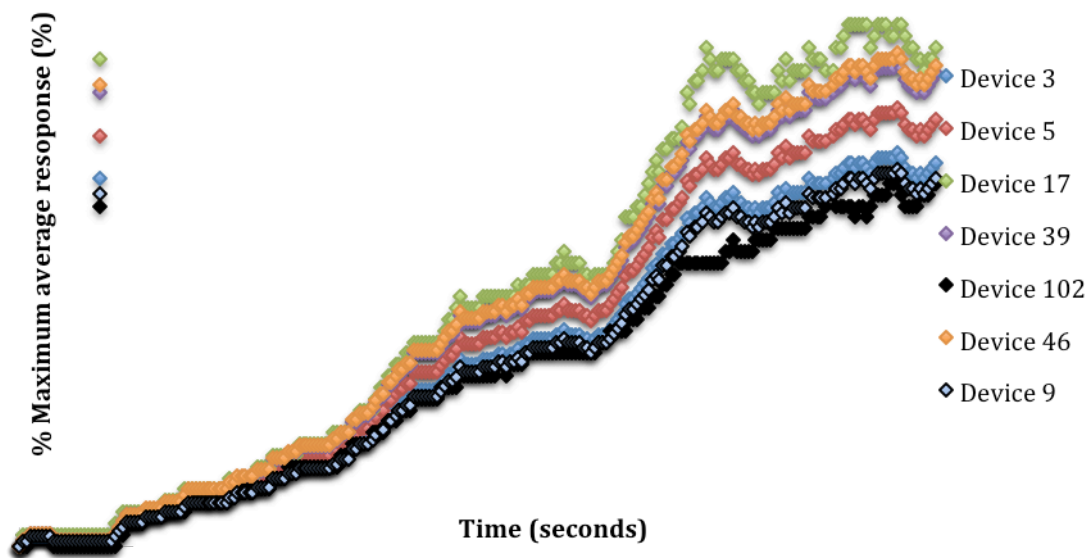


Figure 46 Example optical scatter responses from 7 TYCO fire detection devices to joss stick wad smoke for source location 5b. The data is from repeated (n=3) experiments.

Sensitivity corrected responses over the whole of each 3 tests for each of the 81 source positions were summed and averaged over test duration to give a detector response value for each position. Dividing individual position value by the maximum value and multiplying by 100 calculated a % detector response for each position. Figure 47 summarises results of such measurements and calculations.

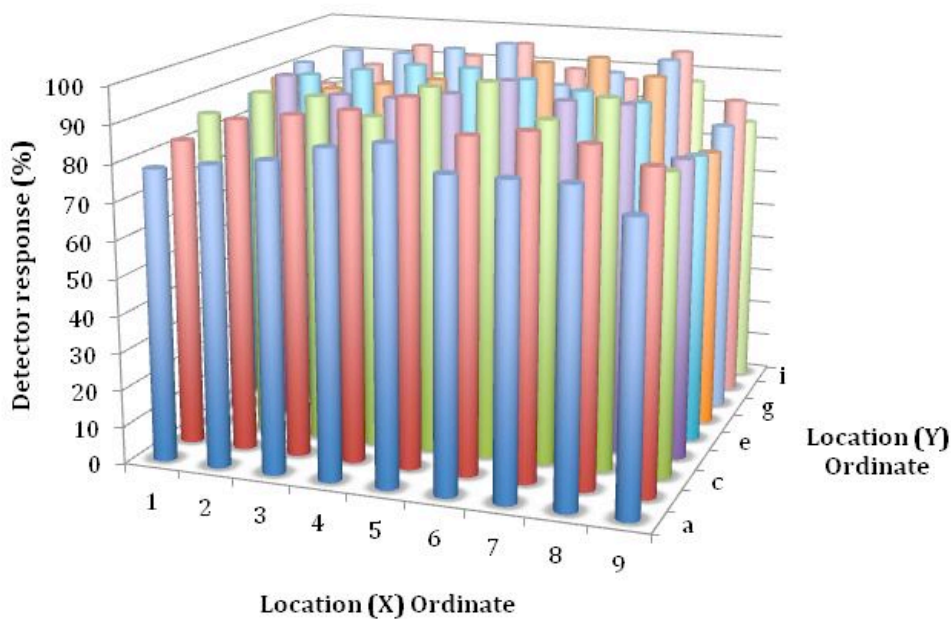


Figure 47 A graphical representation of the effectiveness of smoke generation/ transfer to detectors from each source site.

The source locations identified by number and letter combinations are represented on the plane defined by x and y axes. The % detector response calculated as described above is shown in z ordinate direction as an array of columns. Each column height is representative of an average value from repeat experiments (n=3). All readings were taken over a period of 10 days and the temperature difference between the roof and floor of the enclosure monitored before each test to check  $\Delta T < 1^{\circ}\text{C}$ .

It was apparent from results of the type shown in Figure 47 that responses were only significantly reduced when the joss wad source was positioned close to the walls. This confirmed that the source the provisional designation of the source position as shown in chapter 2 was satisfactory and that was used throughout the study.

### **3.1.2 Air Temperature Effects on UCLan Enclosure tests**

A phenomenon sometimes seen in fire enclosures, particularly for weak plume sources is stratification whereby the fire plume is prevented from reaching the ceiling. This is ascribed to presence of a temperature gradient in the enclosure with a layer of warmer air at the ceiling. This interferes with the buoyancy driven rise of a fire plume that relies on the plume temperature being higher and density lower than that of surrounding air. This issue is the reason the definitions for the standard fires specify limits on temperature differences in fire rooms, and it is to be expected that the same must apply to reduced scale enclosures. The physical limitation of the air in the enclosure is its equivalent buoyancy. In order to evaluate this effect a series of experiments were carried out to examine the impact of temperature differences in the UCLan enclosure on smoke transport.

Joss stick wads, as described in section 3.2, we placed 200 mm from the back and 500 mm from either of the walls of the fire enclosure and the smoke production measured on the optical scatter channel of an 801PC device (address 39) located at the central position of the primary detector arc connected into the MX system detector monitoring loop.

Measurements were carried out under two conditions defined by the difference between the roof and floor ( $\Delta T$ ) of the chamber being  $<1^{\circ}\text{C}$  (first condition) or  $>1^{\circ}\text{C}$  (second condition), and repeated 3 times for each condition.

Results are shown below in figure 48. It is clear that smoke levels detected for the second condition are significantly lower which is to be expected if the buoyancy driven rise of the smoke plume is impeded by a temperature and hence density gradient. This is a fairly extreme test of the effect as heat output from even 5 joss sticks is very low and so the buoyancy forces are likely to be correspondingly weak. Nevertheless it indicates the need to specify a low start of test temperature difference for valid tests. Ensuring the temperature difference is very much lower than 1°C is difficult in a general laboratory situation so for practical reasons the specification was set at 1°C for this study. The scaled fire sources used generally have a greater heat output than 5 joss sticks and so that limit is hopefully adequate.

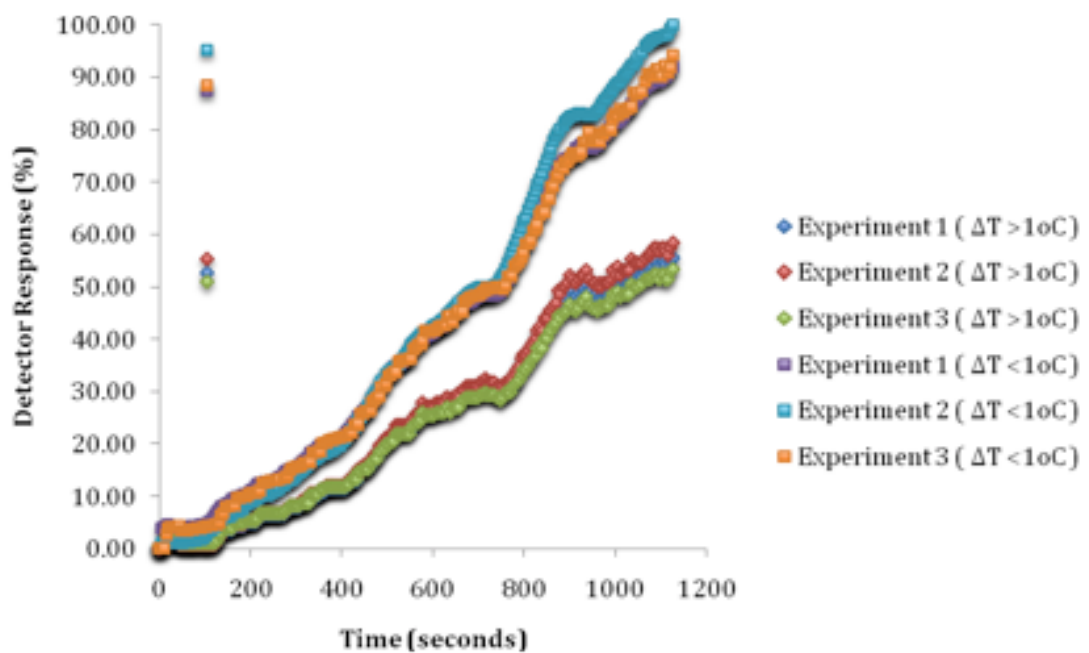


Figure 48 Effect of floor to ceiling temperature differences on joss stick wad tests in UCLan enclosure

### 3.2 Scaling requirements of specific fires (fuel geometry)

Provision of reduced scale emulations requires use of at least broadly similar fuels and fuel arrangements to those used in the full-scale standard test fires. The geometry of a fire source can significantly affect fire ignition requirements and maintenance/growth of the burn, and hence the quantity and mode of heat release and smoke production. Maintenance of a burn generally involves feedback to solid or liquid fuels of part of the heat generated to produce the required combustible vapours or gases. Fire size and geometry can affect this feedback and radiation, conduction, and convection can for small fires increase the proportionate heat loss from the fire bed. These effects, or at

least their relative importance, can be quite specific to the different fires and so some of the relevant material is dealt with for each individually in following subsections. However numerous texts have covered the subject [114][115] and some key factors are summarized below:

1. **Ignition flux:** Where ignition involves a significant heat flux (electrical heater, starter flame source) reducing the scale of fires has to be accompanied with a reduction, as far as practical, of the heat flux from ignition source.
2. **Geometry of fuel:** Burning characteristics of fires are also influenced by the thickness and geometry of fuels. The size of the fire affects how the fuel retains heat. Smaller bulk samples tend to have a greater surface area to volume ratio and larger bulk samples and can lose heat to the atmosphere quicker than larger bulks. Excessive heat loss at the point of ignition can either slow the time to ignition or prevent ignition entirely.
3. **Fire containers/enclosures.** Fires are influenced by the size, shape and geometry of the container in which they burnt as they can influence gas flow, local temperatures and heat exchange by radiation and conduction. Whether the more distant enclosure walls of reduced total air volume can affect very early stages of fire development may be doubted but generally a fire in a small enclosure can make the environment hotter than the for a larger room and this ultimately affects the combustion processes and mechanisms.

### **3.2.1 Scaled wood cribs (UL268 fire B emulation)**

Wood cribs, a simple (minimal) arrangement for which is represented in Figure 49, are typically used to study flaming wood conditions.

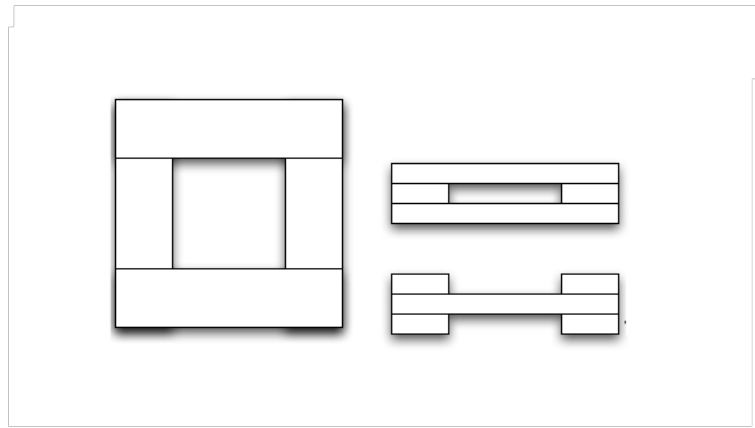


Figure 49 Example wooden crib schematic

The geometry of wood cribs has been extensively studied [116][117] Development of a wood crib fire requires significant heat retention within the core of the structure, and this depends on component dimensions and the packing and dimensions of the crib. If heat is lost from the centre too quickly, the fires can change from flaming to smouldering or even extinguish [118]. If the wood components are too thick then the heat required for ignition and to sustain the fire will be insufficient.

When scaling down the wood crib fires, the main problem encountered was keeping the wood alight. In the full scale fire the internal region of the crib is surrounded by enough wood surface to maintain feedback of heat. Heat is transferred away from the flame at a relatively slow rate while sufficient the fuel is available to allow progressive growth. Scale reductions affect the thermal thickness of the wood crib and it was observed that while the sample could be lit in the crib centre of the crib, rapid heat loss caused prevented fire development. To overcome this issue, the use of a loose foil mini enclosure around the wood crib was developed. This reflects a portion the lost heat back into the crib enabled creation of scaled fires which had a long enough burn times to produce the smoke in the appropriate quantities over a time span comparable to that of the standard fire.

### **3.2.2 Scaled smouldering wood (BS EN54/7 TF2 emulation)**

It is reported that [119] smoke production properties of smouldering, or rather pyrolysing, wood are related to the surface area exposed to the heat source. This formed the basis of the scaling experiments where size and number of wood pieces were arranged on a small heater plate maintaining as far as possible the radial arrangement of

the standard fire. These tests confirmed that the smoke production rate was primarily influenced by the surface area of wood contacting the heater surface while duration depended total amount of wood, and hence thickness.

Attempts were made to produce reduced scale heater plates for this test using cartridge heaters and metal blocks. However repeated failure of these devices led to adoption of a commercially available small cooking hob plate (~75 mm diameter) but with temperature limited to 250°C to avoid excessive heat output whilst adequate to generate wood pyrolysis product smoke.

### 3.2.3 Scaled smouldering cotton fire (BS EN54/7 TF3 emulation)

The BS EN54/7 standard describes an arrangement of 80 30cm long cotton wicks suspended together in a ring, which effectively produces a self-burning chimney. This is illustrated in

Figure 50 below where ring and flat arrangements are shown. The flat arrangement results in an uneven burning rate while in the ring orientation heat is retained round the ring with transfer between adjacent wicks.

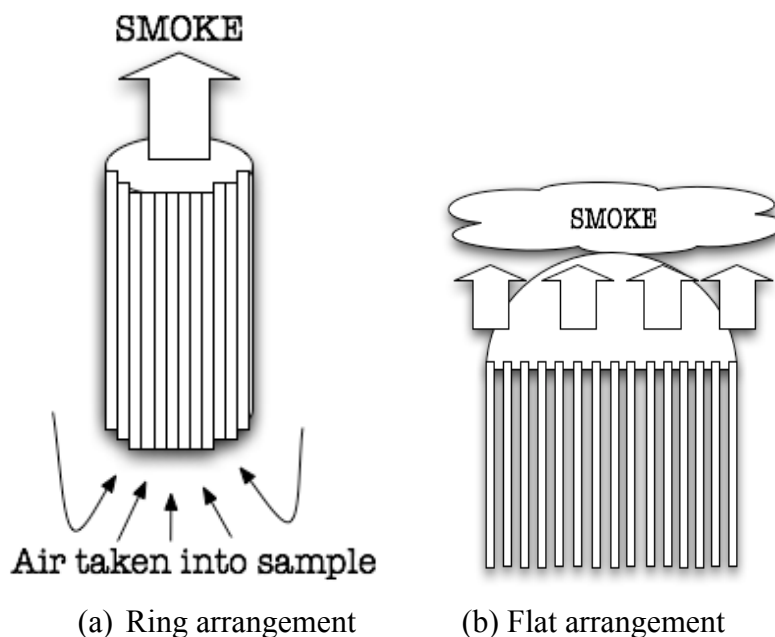


Figure 50 Orientation of cotton wick samples in a self-burning chimney orientation (a) and a flat open orientation (b).

The symmetry of the ring arrangement promotes burning at a uniform rate and the induced convection in the self-burning chimney draws air across the wick end combustion zone increasing the rate of burning as compared to that of isolated wicks. The enhancement of air supply may also affect the combustion processes, efficiency, and product mix.

It was clear therefore that a scaled test should if possible retain the ring geometry. Scaled fire development experiments consisted of reducing ring dimensions and the number and thickness of cotton wicks used until a reasonable match to the standard obscuration versus time specification was achieved.

#### **3.2.4 Scaled flaming liquid fires (EN54/7 TF5 and UL268 fire C emulations)**

The fuel and the container, which defines the pool dimensions, define the flaming liquid fires. Pool fires function in a particular way with the fuel in a pool tending to burn as a cone where the outsides of the cone are exposed to an entrained air stream and can burn in a oxygen rich environment. However air and oxygen penetration into the flame cone interior is impeded and although overall there may be excess oxygen available, the interior of a pool fire can burn in an unventilated fashion. A key aspect of pool fires is the smoke point, which is the point at the top of a flame where the conditions are most favourable for smoke production. The factors affecting this are quite complex and the size and shape of the fuel bed (pool) has a significant impact on this. In the initial stages of a fire the surface area of a fuel bed has a dominant affect on the smoke point [120] controlling the rate of combustion and affecting the mode of combustion. As the fire develops the depth of the fuel bed becomes important. [121] Normally the fuel container will determine the dimensions of the fire. However if the depth of the fuel bed is close to the depth of the container then the vapours may extend beyond the physical

confines of the container and the surface area would be larger for the initial stages of combustion [122][123].

As the pool area is crucial to the size and power output of a liquid fire, it was considered reasonable to start the scaling process by adjusting the pool area in line with the energy release rate scaling factor indicated in Table 20. The emulations developed for the BS EN57 and UL268 fires used the liquid compositions specified in the standards. As spark ignition could be used, heat output from the ignition system was not considered as sufficient to influence plume transport.

### **3.2.5 Scaled Polyurethane foam fire (BS EN54/7 TF4 emulation)**

The standard TF4 tests involve progressive burning across horizontal PU sheet material. The same geometry is appropriate for the scaled fire. It appeared likely that the power output would be related to the length of the burning line and depth of foam and the duration to the distance the fire traversed across the sheeting. The fire beds were constructed with pieces of PU foam cut and laid down to overlap so that width and length could be set. Initially the width was cut down from the TF4 specified 50 cm in line with the factors indicated in Table 20. By modifying piece size, numbers, and overlap arrangements it was possible to produce fires matching the TF4 obscuration versus time specification.

### **3.2.6 Scaled flaming paper fire (UL268 fire A emulation)**

The standard UL268 test defines a container with loosely packed shredded paper. Designs of reduced emulations adopted as similar geometry and small methanol fire to aid ignition. The quantity of shredded paper and pack aspect ratio (height to width) was varied until a reasonable match to the target obscuration characteristics was achieved.

## **3.3 Tests at scales appropriate to 2 m<sup>3</sup> UCLan Enclosure**

The process of adjustment of fuel quantities, arrangements, and containment was continued until emulations were developed showing reasonable matches to the smoke obscuration versus time characteristics to the standard fires (BS EN54/7 TF2, TF3, TF4, and UL268 fires A,B, and C) using the in house built obscuration unit in the UCLan

2 m<sup>3</sup> enclosure. These standard fire emulations are described individually below. Obscuration and some other characterisation and analysis data for many repeat burns of these fires are presented in Chapter 4, which also contains corresponding results for full-scale tests, carried out at BRE.

In addition to the standard fires a number of other fire/ false alarm stimuli tests were designed at scales appropriate for measurements in the UCLan enclosure and those tests are also described below.

### 3.3.1 Standard Test Fire Emulations for 2 m<sup>3</sup> UCLan Enclosure

The BS EN54/7 and UL 268 standards provide descriptions of standard fire tests summarised in chapter 1 with defined test room dimensions and fuel quantities, arrangements and ignition processes. Validity of individual test runs for these fires are defined in terms of the evolution and measurement of smoke usually by optical absorbance. The test fire scaling work of this study designed to provide emulations of test fires with the UCLan 2 m<sup>3</sup>. Enclosure identified reduced size fire sources where optical obscuration evolution matched the standard defined test fire validation characteristics. The reduced scale test fires described below were used in the UCLan enclosure for generation of fire products for gas sensing, GC/MS sampling, and detector studies.

### 3.3.2 Smouldering wood (BS EN54/7 TF2 scaled emulation)

Untreated non-resinous pine, free from knots or pitches was dried in an oven for 48 hours. Samples were cut from larger lengths into 20 x 10 x 10 mm wood blocks each weighing approximately 0.66g. Three blocks were arranged in a radial pattern on the hot plate (as shown in Figure 51).

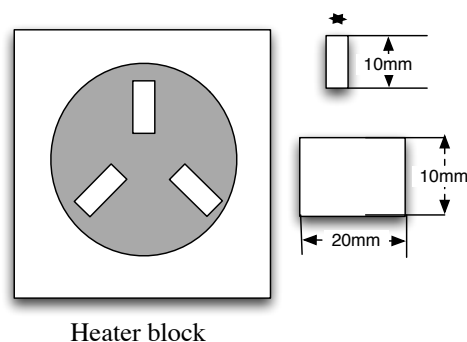


Figure 51 Schematic diagram showing the location and size of the wood blocks used in the scaled smouldering wood experiments.

The hot plate (~75 mm diameter) was heated to a temperature of 250°C. At this temperature the wood will smolder but not ignite. If glowing combustion is observed the experiment was abandoned.

Gas samples are collected on a single sorption tubes for 240 seconds (sampling was started at 60 and concluded at 300 seconds). Data was recorded for gas sensors and smoke detection/ measurement systems as described elsewhere and the test validity checked against optical absorbance characteristics based on the relevant standard. Fires are allowed to progress until the fuel was consumed or 600 seconds had elapsed.

Following these and other fire enclosure tests the enclosure was ventilated by operation of a small exhaust fan until cleared of smoke and CO. Once safe to do so the remnants of the fuel are collected and weighed, gas absorption sampling tubing replaced or cleaned where appropriate, and temperatures allowed returning to acceptable limits before further testing.

### 3.3.3 Burning wood (UL268 fire B scaled emulation)

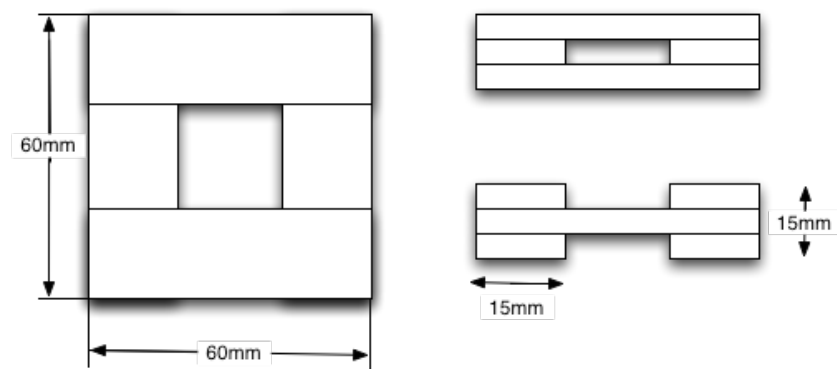


Figure 52 Schematic diagram of the construction of wood cribs used in the scaled burning wood experiments.

Wood was sourced and prepared as for the smouldering wood test (TF2 emulation) but cut to 60 x 15 x 5 mm strips and built into wooden cribs as shown in Figure 52.

The wooden crib was placed onto a small mesh platform 10 mm from the fire enclosure floor centrally within an open topped foil box 75 x 75 x 30 mm newly constructed prior to testing. The foil box with crib was positioned so that the centre of the wooden crib was 200mm from the rear fire enclosure wall and 500mm from either of the sidewalls. A small fireproof bowl (30 x 30 x 6 mm) was placed under the mesh and 1ml of methanol was added to act as an ignition source 30 seconds prior to testing. The spark generator probes were positioned near the methanol and after commencing sensor/detector operation/file recording the ignition spark was fired over the fuel bed for 5 seconds or until ignition was achieved.

Measurements and gas sampling was carried out over 60-300 seconds dependant on how the fire progressed. The fires were allowed to progress for 600 seconds or until the fire exhausts the fuel supply.

### 3.3.4 Smouldering cotton (BS EN54/7 TF3 scaled emulation)

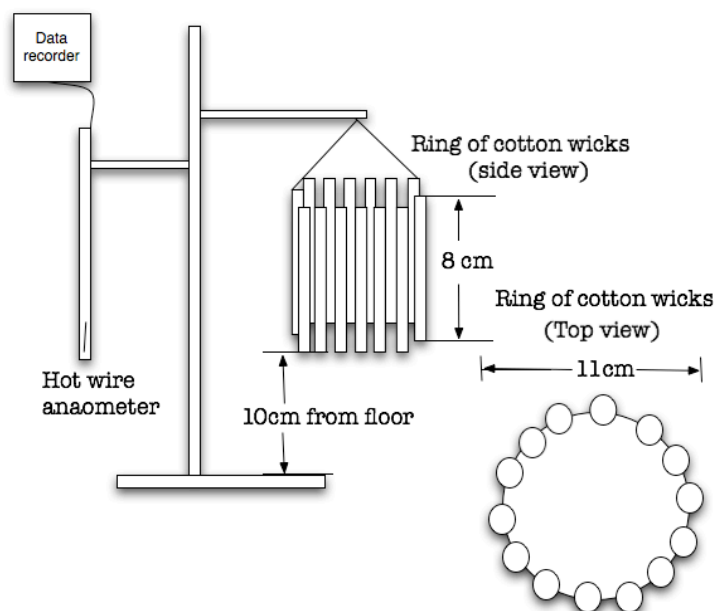


Figure 53 schematic diagrams of the cotton samples used in the scaled smouldering cotton fire experiments.

The Anemometer is used to monitor the airflow in the enclosure during each experiment.

TYCO provided untreated unbleached cotton wick. Samples for testing were prepared by cutting 14 equal 8 cm long lengths and attaching them with wire in a loop no more than 3mm apart. Once completed the loop was approximately 110mm in diameter. The total weight of the samples was approximately 7.5g.

The cotton sample was attached to retort stand as shown in Figure 53 and the stand positioned so that the center of the loop of cotton strands was 200mm from the rear wall of the enclosure and 500mm from each of the sidewalls. After commencing sensor/detector operation/file recording, all of the strands were ignited using a small butane flame lighter and then blown out so any flaming was terminated but glowing combustion was seen to continue at the tip of all strands. Fire gas sampling was continued for 60-300 seconds, and the wicks then permitted to burn to completion.

### 3.3.5 Burning polyurethane (BS EN54/7 TF4 scaled emulation)

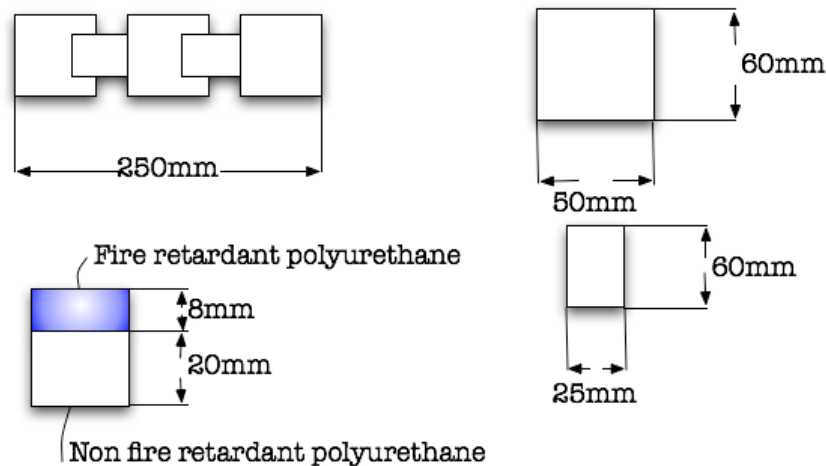


Figure 54 Schematic diagram of the arrangement of samples burnt in the scaled burning polyurethane fires. The diagram also shows the location of the fire retardant polyurethane used in the mixed fuel sample tests.

Untreated E18/Grey polyurethane foam sheets (500 x 500 x 25 mm) were sourced from Custom Foams [124]. Five sections of foam (50 x 60 x 25 mm) weighing 5 g were cut from the stock foam sheet and placed upon a foil tray 300 x 70 x 10 mm in a pattern as shown in figure 54. Each of the foam blocks except the first was overlaid at one end by 12 mm as indicated in Figure 55. This was to give an overall length of 250 mm for the sample train. This was positioned in the fire enclosure as indicated in Figure 55 with the

long axis of the sample train 500 mm from sidewalls and the rear end of the sample 100 mm from the rear wall.

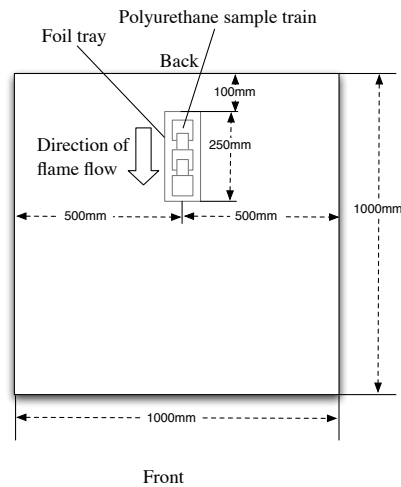


Figure 55 Schematic diagram of the polyurethane sample placement in the scaled fire enclosure test box

To examine the effect of fire retardancy on the fire gases collected a mixed fuel sample was produced where 8mm of blue commercially available halogen blown fire retardant foam was placed on top of the standard E18/Grey foam blocks in the same orientation as described. A mixed fuel bed was required to ensure combustion of the fire retardant foam.

Fire gas samples were taken over a period of 0-240 seconds. Samples were allowed to burn to completion.

### 3.3.6 Burning pool fire: Heptane: Toluene 97:3 (BS EN54/7 TF5 scaled fire)

A bulk fuel sample supply was prepared by mixing 970 ml of heptane with 30 ml of toluene (ex Sigma) and stored in a 1-liter volumetric flask. The fuel was mixed thoroughly prior to each test. A mixed sample (8 ml) was placed into an open topped welded steel container with the dimensions 70 x 70 x 30mm which was placed on the fire enclosure floor so that the centre of the container was located 200 mm from the rear wall and 500 mm from either of the sidewalls. The sample was placed in the fire enclosure no more than 30 seconds prior to the beginning of the test to prevent the build up vapors from the fuel.

The fuel is ignited using the spark generator. Fire gas samples were collected over a period of 0-240 seconds. The fuel was allowed to burn to completion, and all the fuel was consumed in the fire tests.

### **3.3.7 Flaming liquid fire II: Toluene:Heptane (75:25) (UL268 fire C emulation)**

A bulk fuel sample supply was prepared by mixing 750 ml of heptane with 250 ml of toluene (ex Sigma) and stored in a 1-liter volumetric flask. The fuel was mixed thoroughly prior to each test. A mixed sample (3ml) was placed into an open topped round bottom circular container (diameter 30mm depth 40mm). Which was placed on the fire enclosure floor so that the centre of the container was located 200 mm from the rear wall and 500 mm from either of the sidewalls. The sample was placed in the fire enclosure no more than 30 seconds prior to the beginning of the test to prevent the build up vapors from the fuel.

The fuel was ignited using the spark generator at the start of each test and fire gases collected for 240 seconds. The fuel was allowed to burn to completion and all the fuel was consumed in the fire tests.

### **3.3.8 Smouldering paper (UL268 fire A emulation)**

The fuel source for these experiments was 3 g of newspaper ( $48 \text{ g m}^{-2}$ ) or 3 g of office paper ( $80 \text{ g m}^{-2}$ ) shredded in lengths of 15-30 x 10-20 mm. This was roughly packed into a container around a spacer in an arrangement shown in Figure 56(b). The container was welded steel box (60 x 60 x 250 mm) with a wire mesh platform 10 mm from the base and ventilation slots drilled into the sides Figure 56 There was also a small fireproof bowl in the base of the container, which held 1ml of fire promoter (methanol).

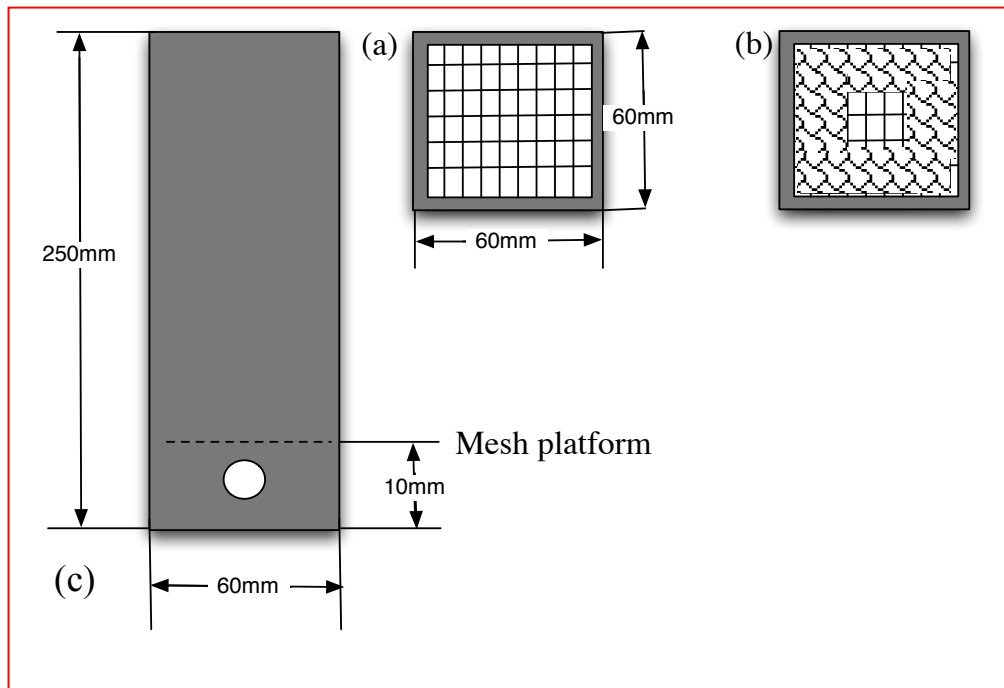


Figure 56 schematic diagrams of the scaled burning paper fire apparatus. (a) Is plan view of mesh support and (b) illustrates the packing of sample with open channel up through centre . (c) Is a side view of container showing mesh location.

To begin the tests the container with the paper and promoter was positioned so that the center of the container was 500 mm from either sidewall of the fire enclosure and 200 mm from the back wall and the spark generator was positioned to provide a spark across the surface of the promoter. The test began when white smoke was observed at the top of the container. If flames, from either the promoter or from flaming combustion, were observed, then the test was abandoned.

Samples were collected for 240 seconds between 60-300 seconds. Fires were allowed to proceed until the fuel is consumed or 600 seconds has passed from the beginning of the test.

### **3.4 Non standard fire and nuisance source tests in UCLan enclosure.**

#### **3.4.1 Burning pool fire III: Methanol**

The fuel used was commercially available analytical grade methanol. The test sample, 8ml of methanol, was placed into an open topped welded steel container 70 x 70 x 30 mm and this was positioned so the centre of the steel container was 200 mm from the rear wall and 500 mm from both of the side walls.

The sample was placed into the fire enclosure no sooner than 30 seconds prior to the start of the test. The fire conditions were monitored using the sensors and detectors in the fire enclosure. Fire gases collected for 240 seconds at a rate appropriate for the resins.

#### **3.4.2 Electrical fire scenario 1: Overheated plastic coated wire**

A 3 core electrical wire sourced from RS components (RS component No. 5093CSL005) was cut into 23 cm lengths corresponding to a sample weight of 10 g. The sample was placed in an aluminium foil tray (50 x 50mm) and then onto the centre of a hotplate (as used for TF2 emulation). The hotplate was located into the fire enclosure so that the wire was 200mm from the rear wall and 500mm from either of the sidewalls.

The wire was then heated progressively from ambient to 300°C at 11°C per minute. Gases were collected on a Carboxen resins only. Samples were captured for 240 seconds from 90 – 360 seconds. Experiments were concluded after 420 seconds and the sample was allowed to cool then reweighed.

### **3.4.3 Electrical fire scenario 2: Overheated printed circuit boards.**

Circuit boards were sourced from IT supplies (ex. computer populated hard drive daughter boards). The circuit boards were populated with a range of components and were cut into roughly equal sizes (40 x 40 mm) and sample weights 6.5 g. All samples were weighed prior to and following each test.

The samples were treated in the same way as the heated wire samples. Fire conditions and samples were monitored and collected as described elsewhere. Sample weights were monitored before and after testing.

### **3.4.4 Nuisance false fire alarm scenario 1: Toasting Bread**

A commercially available domestic 2-slice toaster was positioned in the UCLan test enclosure 200 mm from the back wall and 500 mm from the sidewalls. A single slice of thick white bread (118 x 112 x 8 mm) was selected as a fuel source. The bread was purchased freshly prior to each test.

The toaster was monitored on the highest setting and was found to heat the bread for 4 minutes at a temperature of 250°C. Initially the bread was put through a single cycle of heating at this highest setting but this did not generate alarm signals with any of the standard (801PC or 801I) TYCO fire detectors located in the enclosure. Therefore the toasted bread was put through a second, third and fourth cycles to simulate a malfunctioning toaster or reheated toast.

The bread was weighed prior to and following each stage of toasting and monitored for weight loss. Conditions in the scaled fire enclosure were monitored using the detectors and sensors as described, and samples were collected on Carboxen and Tenax samples for 240 seconds corresponding to the toasting process.

### 3.4.5 Nuisance false fire alarm scenario 2: Overheating cooking oils.

A selection of cooking oils and fats were studied in this experiment. The fuels included;

- 10g of sunflower oil.
- 10g of lard
- 10g of extra virgin olive oil.

The density provided in the literature [125] for each fuel is approximately  $0.918 \text{ g cm}^{-3}$  giving a volume of ~11 ml. Each sample was transferred into a 60 x 60 x 30 mm welded steel container (wall thickness 3.4 mm). The container was placed on the hot plate, positioned so that the centre of the container was 200 mm from the rear wall and 500 mm from either of the sidewalls of the fire enclosure.

The hot plate was heated at a rate of  $11^{\circ}\text{C min}^{-1}$ . The temperature of the oil was monitored using a type K thermocouple and the heating continued to the smoking point of the oil.

The smoking point for the various oil provided in the literature and confirmed by experimental observation are:

- Vegetable oil.  $250^{\circ}\text{C}$
- Lard  $190^{\circ}\text{C}$
- Extra virgin olive oil  $290^{\circ}\text{C}$ .

Because each type of sample has different heating properties the gas-sampling regime were modified in accordance with the smoking point of the fuel. Given the differing sample properties in terms of the smoke point, the gas sample was collected over 240 seconds to collect the main period of smoke production.

Special care had to be taken with these fires as the smoking point is very close to the flash point for some of the fuels and any test, which resulted in flaming combustion, was abandoned.

### 3.4.6 Nuisance false fire alarm scenario 3: Cigarette smoke

Simple portable smoking simulation equipment was provided for evaluation of cigarette smoke in the fire enclosure. The unit represented in Figure 57 was designed and constructed at TYCO Sunbury and holds cigarettes at the filter with a foam rubber seal. The unit incorporates a manifold accepting up to 8 cigarettes with the manifold inlets leading to a common chamber which was connected to a small fan based air pump. Electrical control (not shown in Figure 57) allowed pump duty cycle to be adjusted to simulate smoking and manifold entrances not in use were sealed with adhesive tape.

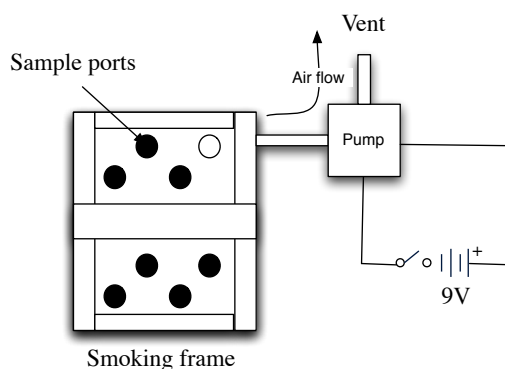


Figure 57 Schematic of the smoking machine used in the scaled fire enclosure. The diagram shows a single occupied sample port of the 8 available.

The unit was designed for up to 8 cigarettes in any one test (appropriate for small room tests), but following a series of evaluation experiments in the UCLan 2 m<sup>3</sup> enclosure it was found that one cigarette gave an appropriate amount of smoke for measurements. Smoke can come directly from the burning cigarette end (mainly when air is not being drawn through) and from the pump exhaust (when air is drawn). Some smoke is certainly lost on internal surfaces of the manifold and pump but this is presumed not to be too dissimilar to the situation with a human smoker.

The sample used for the UCLan enclosure test was a single normal strength cigarette (JPS 10mg nicotine), which held in vertical orientation by the manifold entrance seal. The unit was placed in the fire enclosure at 200 mm from the rear of the fire enclosure and 500 mm from the sidewalls. At the start of the test the cigarette was lit and the pump started. Once started the pump was activate for 5 seconds in every 20 second interval. Each time the pump was active, smoke was drawn through the cigarette and pumped into the fire enclosure. When the pump was not active smoke rose directly from the smouldering cigarette. As a result the smoke collected in the fire chamber was comprised of mainstream and side stream smoke.

The cigarette was weighed prior to and following testing. Test conditions were monitored using the sensors and detectors in the fire enclosure and gases were collected on Carboxen and Tenax sampling tubes for 240 seconds. There are however documented problems with the collection of tobacco smoke on solid phase material, including the formation of tar films over the surface of absorbents and rapid degradation of components captured by secondary reactions [126].

### **3.8 Practical and Calculated Scaling of Standard Fire Tests**

The scaling ratio calculation results presented in Table 20 indicated that the standard test fire heat outputs should be reduced by a factor of ~10 to 30 when scaled down for the UCLan 2 m<sup>3</sup> enclosure. It was unclear what that meant in terms of fuel quantity. It was considered that the fuels and fire structures might scale to power either with fuel volume or mass or with fuel surface area. No exact correspondence is to be expected but it is interesting to examine the scaling factors corresponding to the actual test fire emulations described above to see whether they fall within the calculated range.

Table 22 above shows values for the fuels in full and reduced scale versions of the standard fires. The fuel components column provides dimensions for the solid fuels and volumes and total surface areas are calculated from those. For the liquid fuels the surface area is taken as that exposed when in the container pan used for the burns. The factors shown in the two columns on the right hand are calculated from volumes or masses and areas for the full and reduced scale fires and are presented in the rows corresponding to the relevant full scale fires. Several of the scaling factor values do fall within the 10-30 range but not all and the agreements and deviations are present in both the quantity and area columns. The values for the crib fire are well outside the predicted range, which may reflect the geometrical complexity of that kind of fire.

Fire title	Fuel/ Type	Fuel Components	Volume or mass cc or g	Surface area cm <sup>2</sup>	Volume or mass factor	Area factor
Standard	Wood	10 off	50 cc	775	8	26
TF2	smoulder	7.5x2x2.5 cm				
Standard	Cotton wick	90 off 80 cm (3	270 g	10800	36	96
TF3	Smoulder	g each)				
Standard	Polyurethane	3 sheets	15000 cc	8100	40	27
TF4	foam	50x50x2 cm				
Standard	Flaming	650g (943 ml)	943 cc	1089	118	22
TF5	Heptane					
Standard	Shredded	43 g	43 g		7	
UL A	Paper					
Standard	Wood flame	1.91x1.91x15.2	333 cc	741	4	3
UL B	Crib	cm 6 off				
Standard	Flaming	40 ml	40 cc	200	13	29
UL C	Heptane					
TF2	Wood	3 off	6 cc	30		
emulation	smoulder	2x1x1 cm				
TF3	Cotton wick	14 off 8 cm	7 g	112		
emulation	Smoulder	(0.5 g each)				
TF4	Polyurethane	5x6x2.5 cm	375 cc	300		
emulation	foam	5 off				
TF5	Flaming	8 ml	8 cc	49		
emulation	Heptane					
UL A	Shredded	6 g	6 g			
emulation	Paper					
UL B	Wood flame	6x1.5x1.5 cm	81 cc	243		
emulation	Crib	6 off				
UL C	Flaming	3 ml	3 cc	7		
emulation	Heptane					

Table 22 Fuel Quantities for Standard Test Fires and UCLan Emulations showing Quantity and Area Factors

## CHAPTER 4 DATA PRESENTATION

### 4.0 Chapter overview.

Measurements described in chapters 2 and 3 on the reduced and full-scaled standard fires have generated a substantial amount of data on sensor and detector responses and samples for GC/MS analysis. The main purpose of this chapter is simply to present each of the test types (standard and non standard) a summary of characterisation data (optical obscuration %/m), with some corresponding gas sensor measurements (CO and other electrochemically oxidizable gases, CO<sub>2</sub> generation and O<sub>2</sub> consumption), and the corresponding GC/MS output presented as Ion Current versus retention time plots. Analysis of the GC/MS data identifying mass fragments and gases is not included in this chapter but follows in chapter 5.

The measurement of optical obscuration allows individual tests to be checked against the defined BS EN54/7 and UL268 test fires. The results shown in this chapter represent all of the standard fire and non-standard fire scenarios tested in the scaled fire enclosure, and additionally some data gathered for standard fires performed in the BRE fire test room.

In section 4.1 of this chapter, the fire data presented falls for each of the standard test fire emulations type into three data sets covering optical obscuration, CO and other oxidizable gases, and the major combustion related gases (CO<sub>2</sub> and O<sub>2</sub>). In each test type, the results presented are for 6 examples of the scaled fire, each of which scaled fire experiments were carried out under the same controlled conditions, as described in the experimental description for each fire in chapter 3.

In section 4.2 a limited set of sensor measurements are presented for the BRE full-scale standard test fires along with some of the corresponding reduced scale emulation data.

In section 4.3 sensor measurements are presented for non-standard fire tests carried out in the UCLan 2 m<sup>3</sup> enclosure. A summary of sensor measurements and fire data is provided in tabular form in section 4.4.

The final sections of this chapter, 4.5 onwards, comprises a series of gas chromatogram plots generated from samples collected on absorption tubes and desorbed into GC/MS equipment as described in chapters 2 and 3. The primary output from the GC/MS

equipment (Ion current versus retention time) is displayed as gas chromatogram plots. GC chromatograms deriving from Carboxen and Tenax absorption tubes are presented for each of the reduced scale (UCLan 2 m<sup>3</sup> enclosure) standard type test fires. However for some of the non standard tests only Carboxen tube related data is presented.

Hydrogen and relative humidity (%RH) data channels were also recorded throughout these experiments but the values are not presented.

In a fire where hydrogen containing fuels (most organics including all tested here) are burnt, water vapour is generated. Generally water vapour generation will correspond to the CO<sub>2</sub> increase and O<sub>2</sub> depletion. However while output from humidity measurement equipment was not inconsistent with such parallels, there were issues with the relatively poor sensitivity and response time of the humidity sensor employed. The relative humidity sensors used were not sufficiently accurate to allow good measurements of the small changes in humidity observed for small-scale fires. In view of these issues and expected correspondence with oxygen and CO<sub>2</sub> measurements, humidity sensor measurements were not continued throughout the study and results are not presented here.

The possibility of hydrogen generation in fires and its detection as a fire signature species was considered of significant interest at the start of this study. Hydrogen has been well-documented as a combustion product gas and some papers have reported hydrogen detection at concentrations which were low but above normal ambient levels as discussed in chapter 1 (Jackson and Robbins [127], Pfister[128] and Amamoto[129] .) However, throughout all of the tests in this investigation, the hydrogen concentration levels were either inconsistent or not detected. When hydrogen was detected it was always at less than 5 ppm, which is not dissimilar to some reported ambient background concentration level. Also hydrogen was detected in less than 10% of any particular type of fires making it of dubious value as a detection target. The actual measurement data is therefore not included in this presentation of data.

Some smoke detection data from output of optical scatter type detectors is presented in a later chapter, and there was an intention to include ionization detector output data. However examination of the output from the commercial ionization detector devices revealed that it was of little value due to the very limited dynamic range of such

devices. The significance of this limitation on the ionization detector outputs was not fully realized until near the end of the study and although a wider range device was deployed for a few measurements it was not felt that sufficient reliable information could be presented covering the range test fire conditions.

#### **4.0.1 Obscuration data**

The data of the greatest interest to our scaling experiments is the obscuration information. The obscuration data represents a convenient and direct method of comparing our scaled fires with an equivalent full-scale standard fire. Full scale fires tests under BS EN, UL and other international standards for fire detection, are established and documented fire events, as described previously, and offer a basis for setting smoke levels for tests on non-standard fires or nuisance sources. An obscuration of 20-30 % per meter is typical for a standard fire, and that value is used as a benchmark figure for the non-standard events. e.g. overheated electrical components, overheated cooking oil, toasted bread, and cigarettes.

All obscuration data presented in the first section of this chapter are data collected from the optical bench device installed in the roof of the fire enclosure. All data is plotted as % obscuration per metre versus time. Obscuration % per metre is calculated as described in chapter 2. Where appropriate the standard limits of compliance are also displayed on the graph taken from BS EN 54-7. The limits displayed on the scaled UL test fires are derived from UL268 but the limit conditions cannot be identified as fully in accordance with the standard and should be used for guidance only. This arises partly from the somewhat obscure descriptions given in the UL standards and the use of differently specified, and archaically designed, obscuration measurement equipment.

For initial studies of smoke generation from reduced scale fire test, optical scatter channels of TYCO commercial devices (801PC type) were used. These devices had been calibrated under reproducible conditions in the TYCO Sunbury smoke tunnel with joss stick smoke and the output related to obscuration data for the same smoke. However it was known that different smoke types result in different scatter to obscuration relationships and so this could only be used as an initial guide until the UCLan obscuration kit was brought into service. All the data on obscuration presented in this chapter, other than for measurements at BRE, is based on the output from the obscuration measurement equipment constructed at UCLan to match the BS EN54/7

specification. Obscuration data from the BRE tests was as measured by their BS EN54/7 compliant unit.

#### **4.0.2 Oxidizable gases**

The oxidizable gases data derives from measurements collected from the electrochemical 7EtO and CO sensors linked to the TYCO MX system data channels. The detector responses were converted on the basis of calibration runs against bottled reference CO concentrations carried out as described in chapter 2. The relatively selective CO channel of 801PC detectors (based on Honeywell “6<sup>th</sup> Sense” sensors) was converted to the CO concentration in ppm. The 7EtO cell output was similarly converted to a CO ppm scale but response in the tests will be to both CO and other gases oxidizable at the 7EtO device-working electrode. So while response is expressed to an equivalent CO ppm level it cannot be taken that this is a CO concentration or that the concentration of other gases can be expressed in ppm. To do the later would require knowledge of gas identities and a separate response calibration against of such gases.

In the UCLan scaled chamber we measured the CO both with electrochemical sensors and NDIR devices. There is debate as to the most suitable method of measuring the CO levels in fire products but in this study we found there was generally fair agreement in terms of the magnitude of the gas concentrations observed. Figure 58 shows the CO gas concentration as measured by NDIR measurement cell and electrochemical sensor (TYCO 801PC extended CO range device addr. 17) in three fire experiments (repeats of scaled smouldering cotton fire (TF3)).

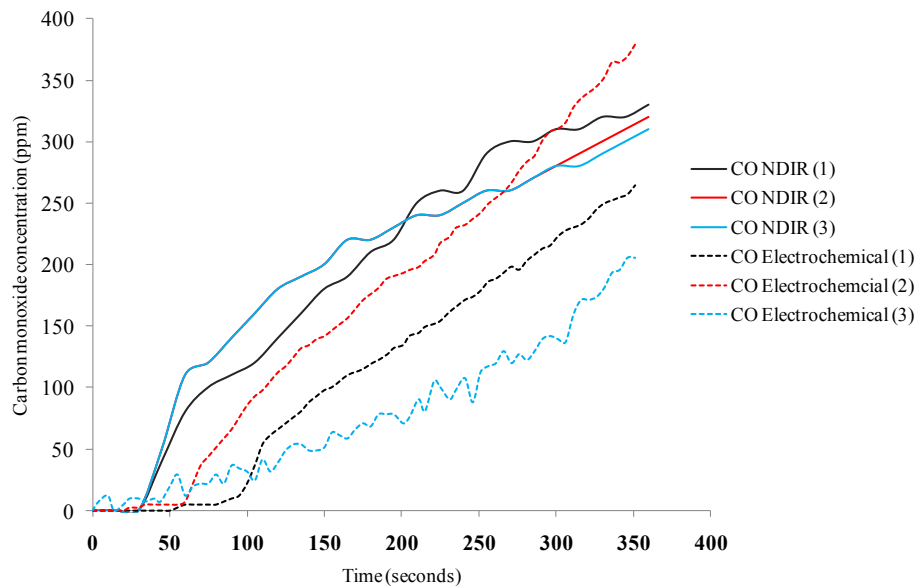


Figure 58 Measurements of CO by electrochemical (6th Sense Cell) and NDIR systems. The selected test involves 3 reduced scale TF3 type smouldering cotton experiments

There does appear some difference in response but that may reflect the different sampling arrangements and response time. The sampling response time for the NDIR unit depends on flushing time for the measurement cell and it was felt that the sampling regime for the electrochemical cells was more representative of real fire detection conditions and with a shorter effective measurement time that it gave a fuller picture of the rapidly changing concentrations of the gases in the fire enclosure. The electrochemical CO cell sampling rate could also be matched to the 7EtO devices directly as their outputs were sampled at the same (5 second) polling interval set on the MX system panel simulator equipment.

The axis on the charts give values of gas concentrations in ppm. These values are calculated against the calibration values and represent the response to a known value of carbon monoxide. For the 7EtO device the responsiveness to CO is indicated in the manufacturers information sheet is consistent with the data from calibration versus bottled gas standards.

#### 4.0.3 Major Combustion Related Gases (CO<sub>2</sub> and O<sub>2</sub>)

The term “combustion gases” as used for presentation of results below represent the increase in CO<sub>2</sub> and the depletion in O<sub>2</sub>.

The CO<sub>2</sub> was measured using a channel on the NDIR unit and the O<sub>2</sub> by an electrochemical cell as described in chapter 2. In these tests the sampling rates of the CO<sub>2</sub> and O<sub>2</sub> measurements were matched at 15 second intervals.

Expressions for stoichiometric combustion of hydrocarbons and other simple organic fuels link together CO<sub>2</sub> generation and O<sub>2</sub> consumption but there may not be a very direct link in the combustion gas measurements as presented here. Differences in fuel, combustion stoichiometry, and the effects of mixing with surrounding air are likely to obscure the connection.

The combustion gases data is presented as a percentage concentration increase or decrease versus time.

#### **4.1 Sensor Data Summary for Emulations of Standard Test Fires**

Below plots are provided summarising the primary data for replicates of each of the standard test fire types showing in order obscuration, CO and oxidizable gases, and major fire related gases CO<sub>2</sub> and O<sub>2</sub>.

### 4.1.1 Scaled Smouldering wood (BS EN 54/7 TF2 Emulations)

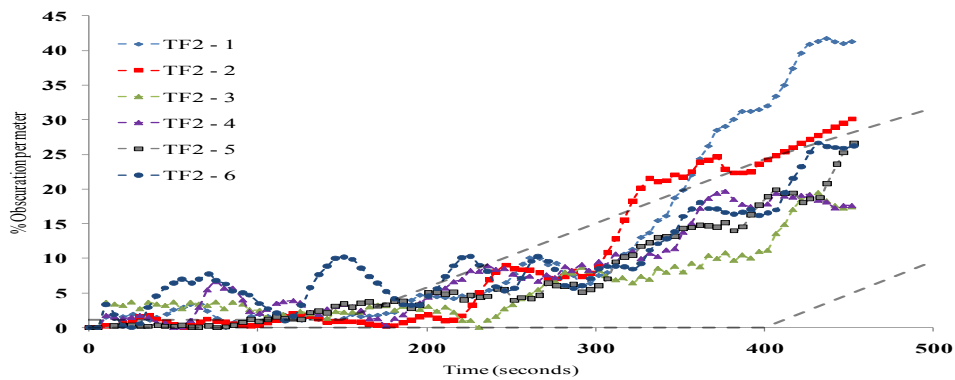


Figure 59 Obscuration versus time for 6 replications of TF2 (wood pyrolysis) Emulations in UCLan 2 m<sup>3</sup> Enclosure

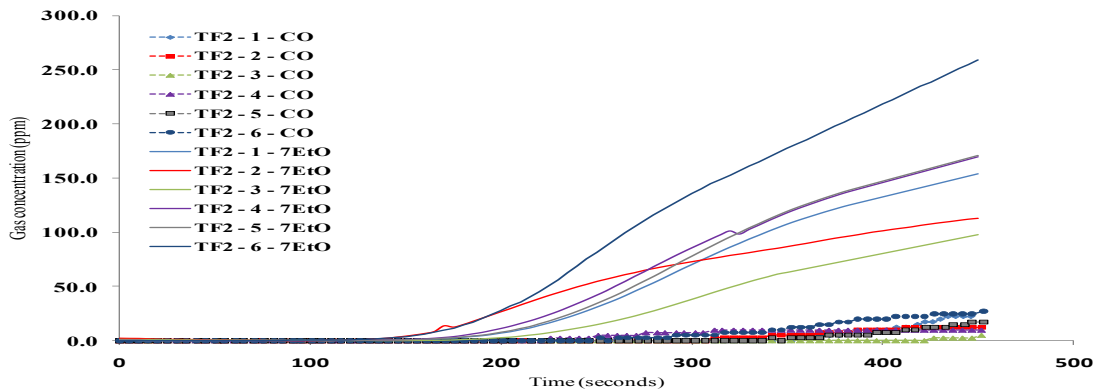


Figure 60 CO and oxidizable gas (by 7EtO) concentrations versus time for 6 replications of TF2 (wood pyrolysis) Emulations in UCLan 2 m<sup>3</sup> Enclosure

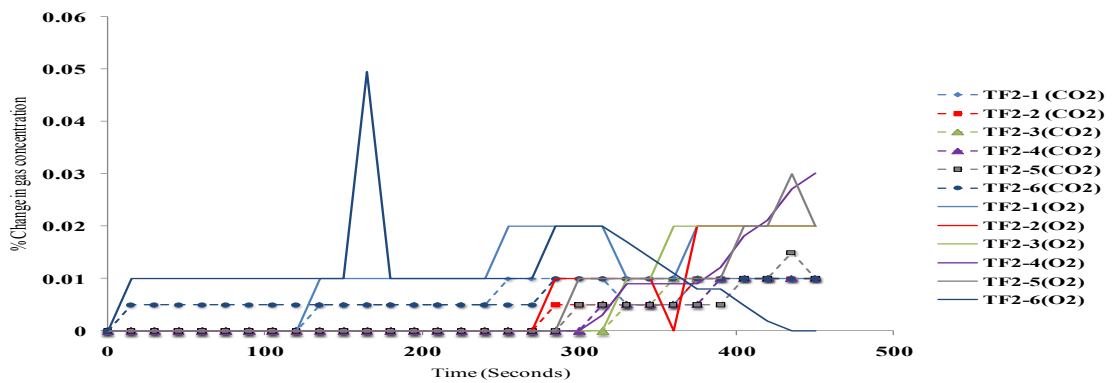


Figure 61 Changes in CO<sub>2</sub> and O<sub>2</sub> concentrations versus time for 6 replications of TF2 (wood pyrolysis) Emulations in UCLan 2 m<sup>3</sup> Enclosure

#### 4.1.2 Smouldering cotton (BS EN 54/7 TF3 Emulations)

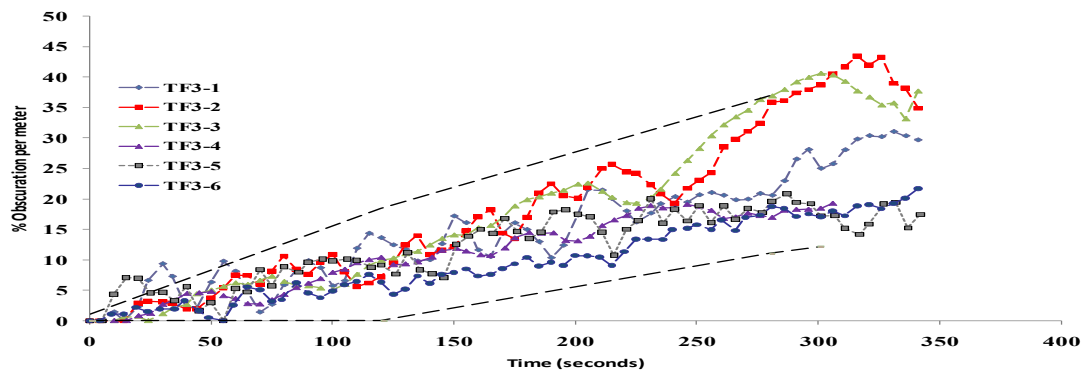


Figure 62 Obscuration versus time for 6 replications of TF3 (cotton smoulder) Emulations in UCLan 2 m<sup>3</sup> Enclosure

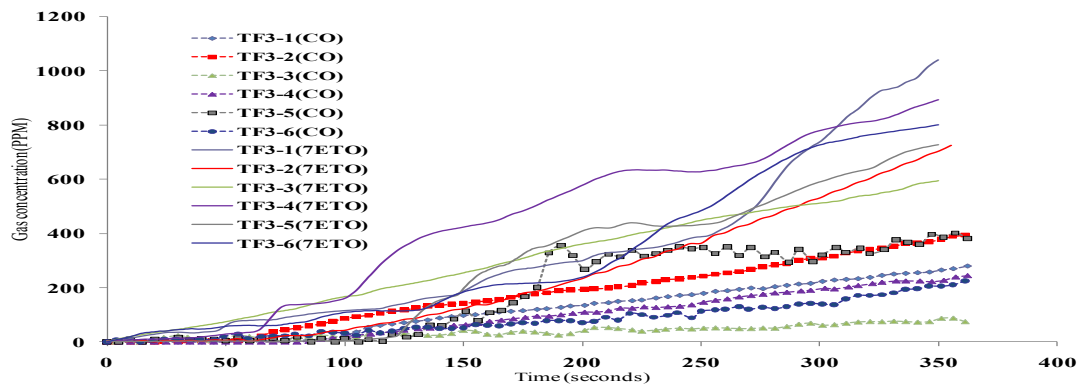


Figure 63 CO and oxidizable gas (by 7EtO) concentrations versus time for 6 replications of TF3 (cotton smoulder) Emulations in UCLan 2 m<sup>3</sup> Enclosure

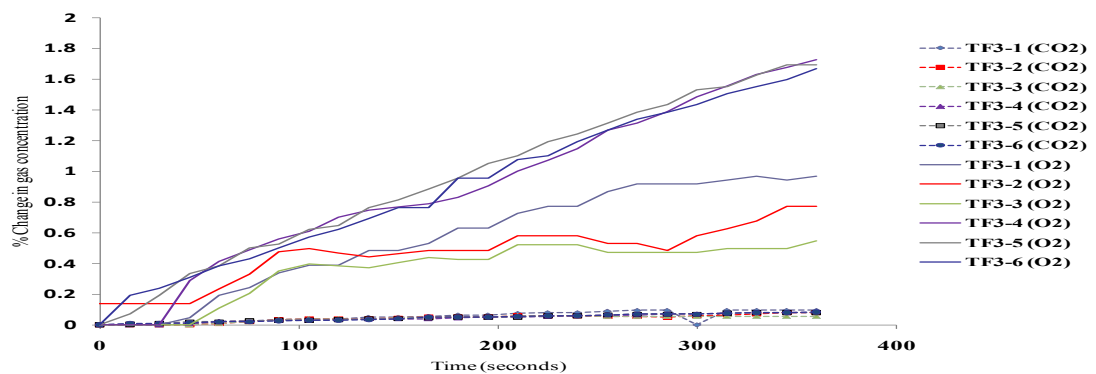


Figure 64 Changes in CO<sub>2</sub> and O<sub>2</sub> concentrations versus time for 6 replications of TF3 (cotton smoulder) Emulations in UCLan 2 m<sup>3</sup> Enclosure

### 4.1.3 Burning Polyurethane Foam (BS EN 54/7 TF4 Emulations)

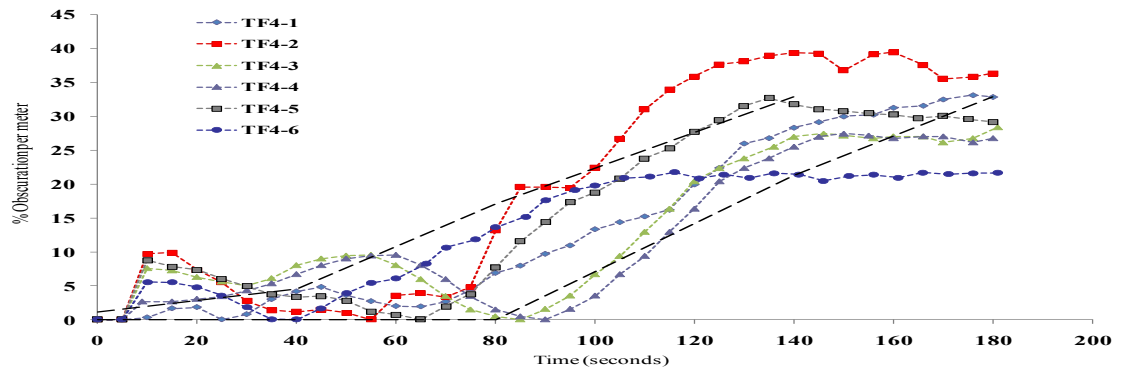


Figure 65 Obscuration versus time for 6 replications of TF4 (Polyurethane foam burn) Emulations in UCLan 2 m<sup>3</sup> Enclosure

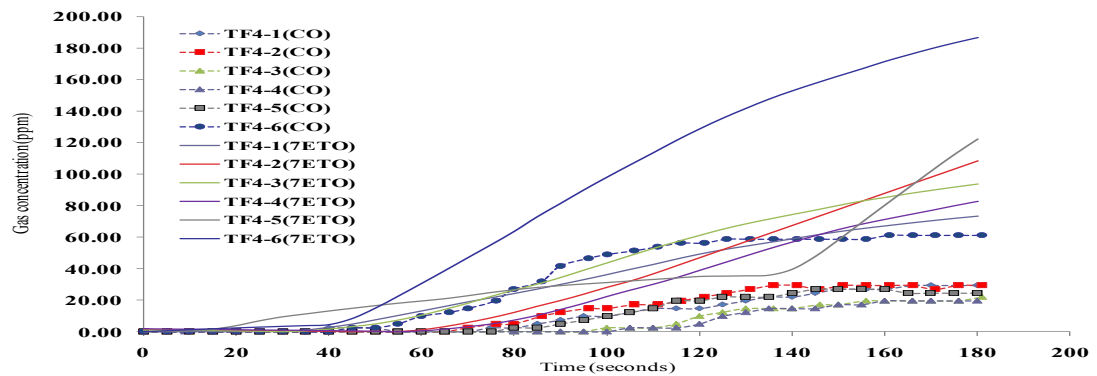


Figure 66 CO and oxidizable gas (by 7EtO) concentrations versus time for 6 replications of TF4 (Polyurethane foam burn) Emulations in UCLan 2 m<sup>3</sup> Enclosure

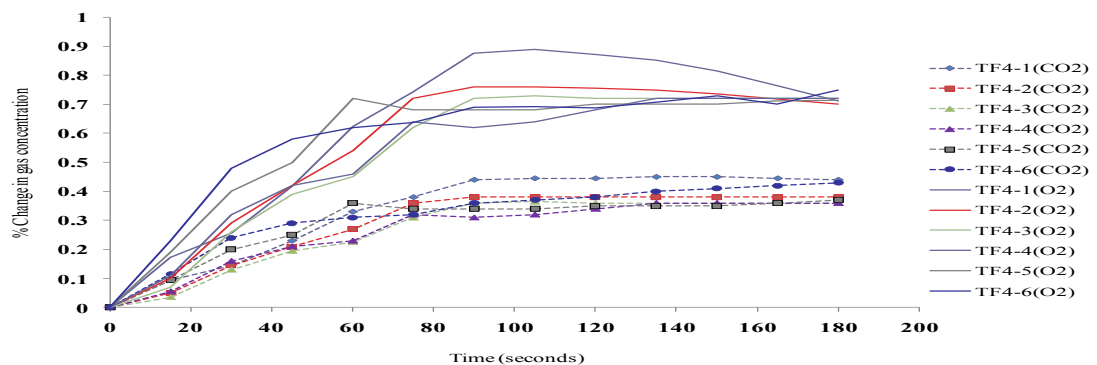


Figure 67 Changes in CO<sub>2</sub> and O<sub>2</sub> concentrations versus time for 6 replications of TF4 (Polyurethane foam burn) Emulations in UCLan 2 m<sup>3</sup> Enclosure

#### 4.1.4 Burning pool fire - Heptane (BS EN 54/7 TF5 Emulations)

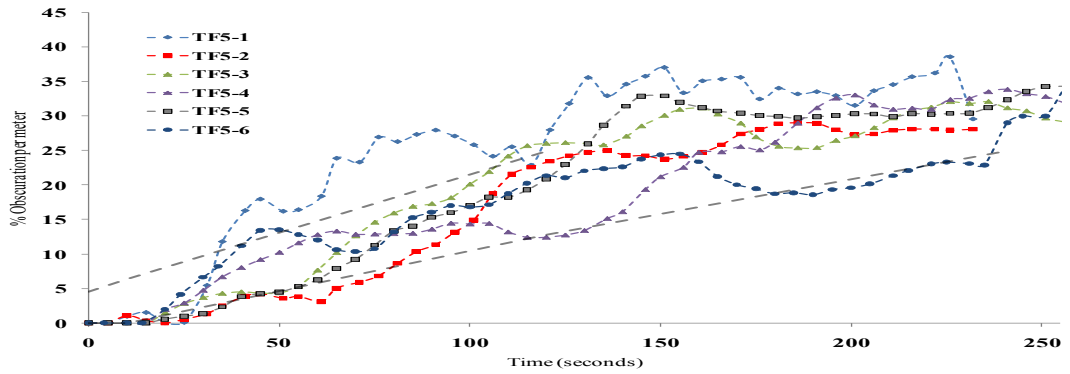


Figure 68 Obscuration versus time for 6 replications of TF5 (Flaming Heptane) Emulations in UCLan 2 m<sup>3</sup> Enclosure

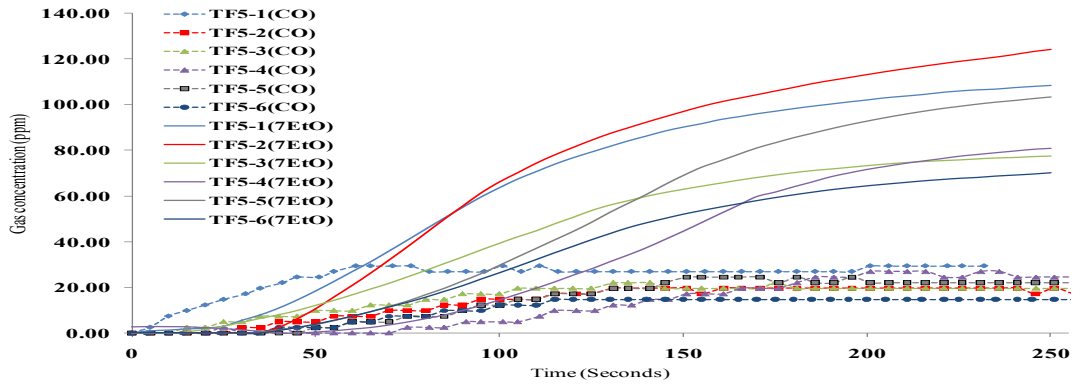


Figure 69 CO and oxidizable gas (by 7EtO) concentrations versus time for 6 replications of TF5 (Flaming Heptane) Emulations in UCLan 2 m<sup>3</sup> Enclosure

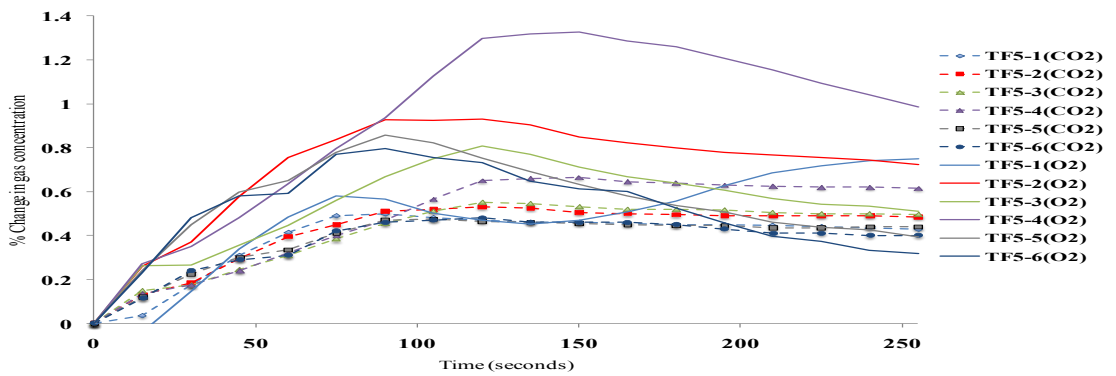


Figure 70 Changes in CO<sub>2</sub> and O<sub>2</sub> concentrations versus time for 6 replications of TF5 (Flaming Heptane) Emulations in UCLan 2 m<sup>3</sup> Enclosure

### 4.1.5 Burning pool fire - Heptane (UL268 fire C Emulation)

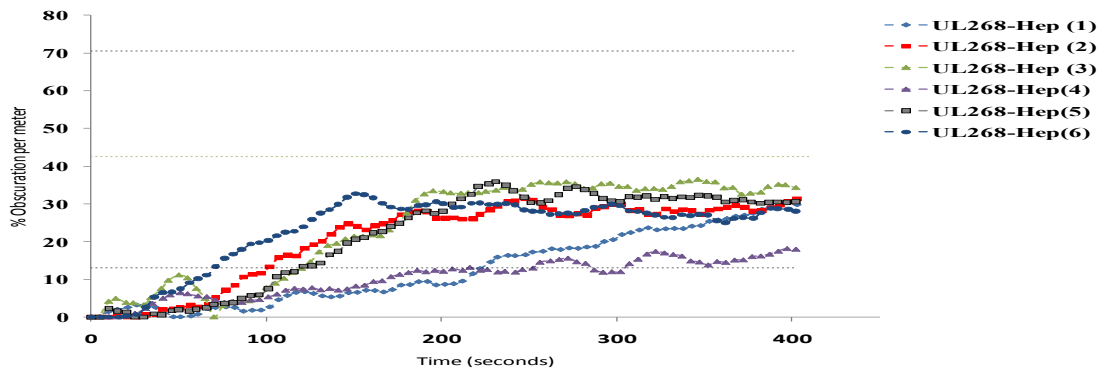


Figure 71 Obscuration versus time for 6 replications of UL fire C (Flaming Heptane) Emulations in UCLan 2 m<sup>3</sup> Enclosure

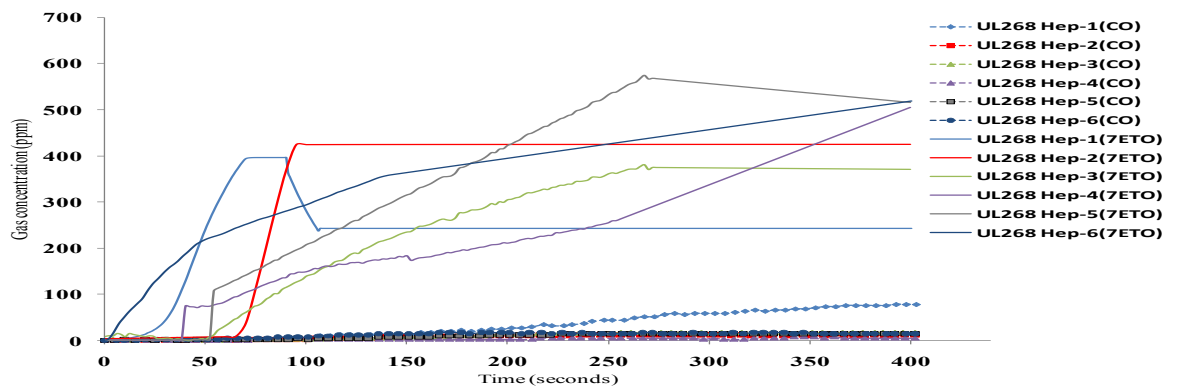


Figure 72 CO and oxidizable gas (by 7EtO) concentrations versus time for 6 replications of UL fire C (Flaming Heptane) Emulations in UCLan 2 m<sup>3</sup> Enclosure

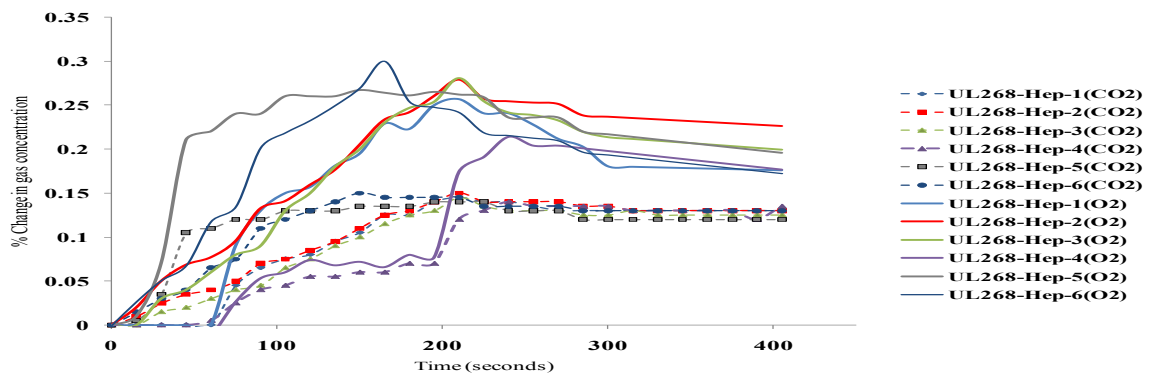


Figure 73 Changes in CO<sub>2</sub> and O<sub>2</sub> concentrations versus time for 6 replications of UL fire C (Flaming Heptane) Emulations in UCLan 2 m<sup>3</sup> Enclosure

#### 4.1.6 Burning Paper (UL268 fire A Emulation)

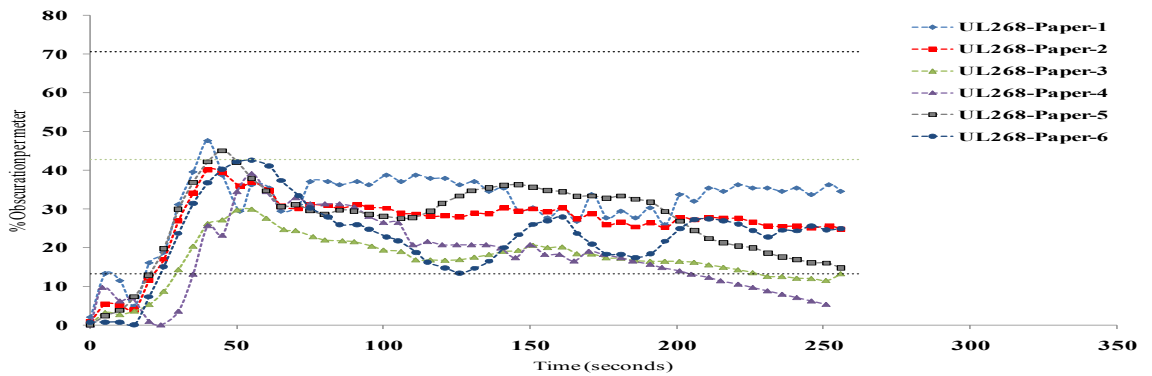


Figure 74 Obscuration versus time for 6 replications of UL fire A (Burning Paper) Emulations in UCLan 2 m<sup>3</sup> Enclosure

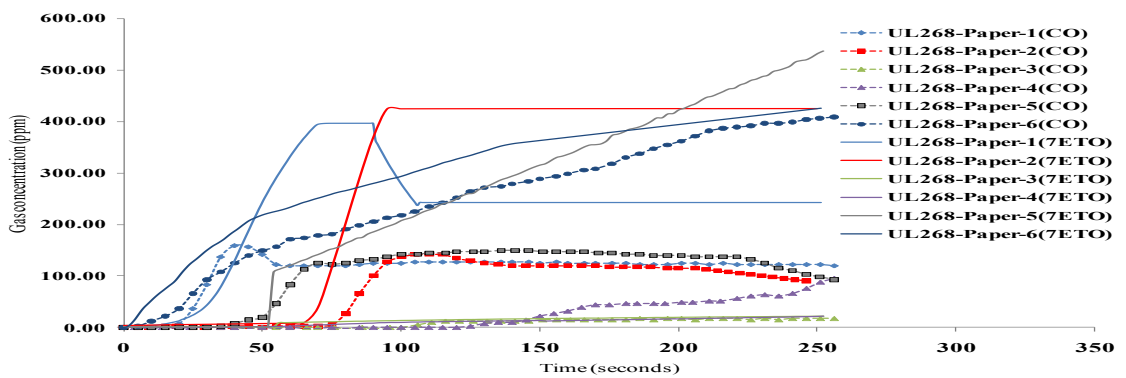


Figure 75 CO and oxidizable gas (by 7EtO) concentrations versus time for 6 replications of UL fire A (Burning Paper) Emulations in UCLan 2 m<sup>3</sup> Enclosure

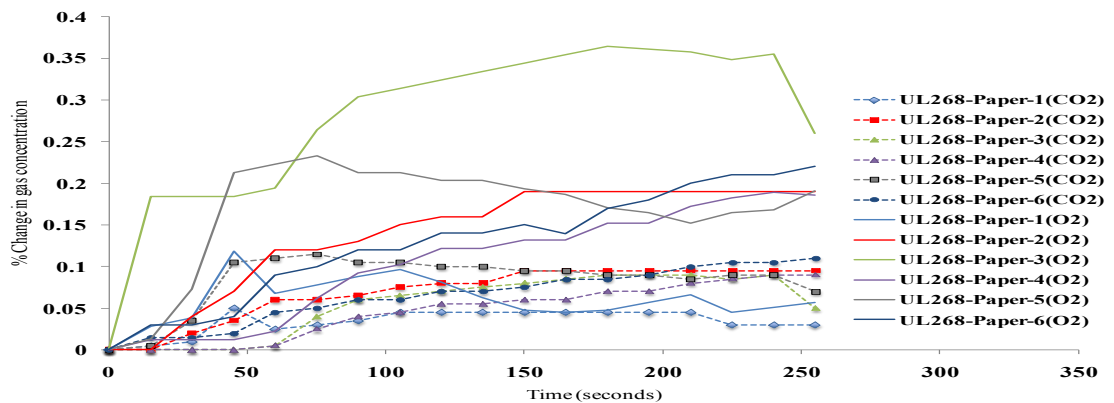


Figure 76 Changes in CO<sub>2</sub> and O<sub>2</sub> concentrations versus time for 6 replications of UL fire A (Burning Paper) Emulations in UCLan 2 m<sup>3</sup> Enclosure

### 4.1.7 Flaming wood (UL268 fire C Emulation)

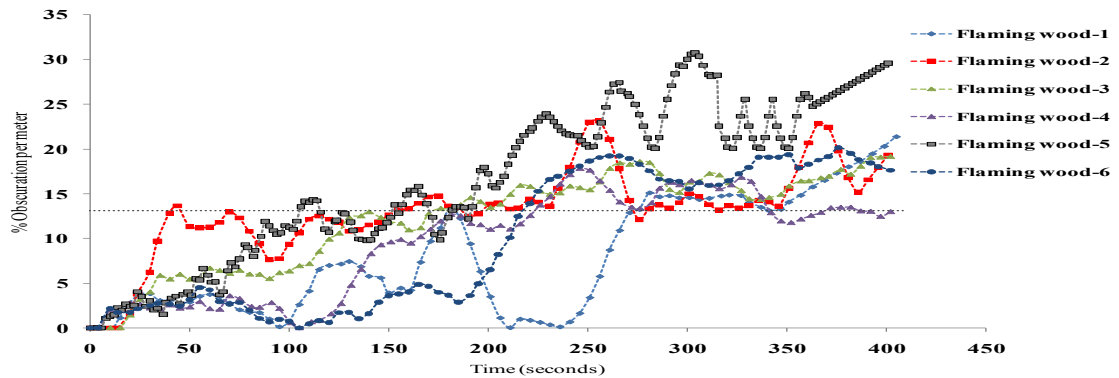


Figure 77 Obscuration versus time for 6 replications of UL fire B (Flaming Wood) Emulations in UCLan 2 m<sup>3</sup> Enclosure

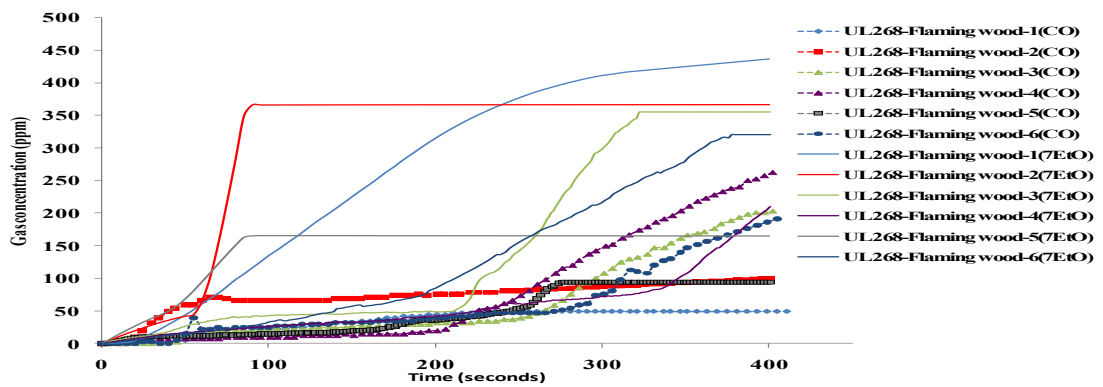


Figure 78 CO and oxidizable gas (by 7EtO) concentrations versus time for 6 replications of UL fire B (Flaming Wood) Emulations in UCLan 2 m<sup>3</sup> Enclosure

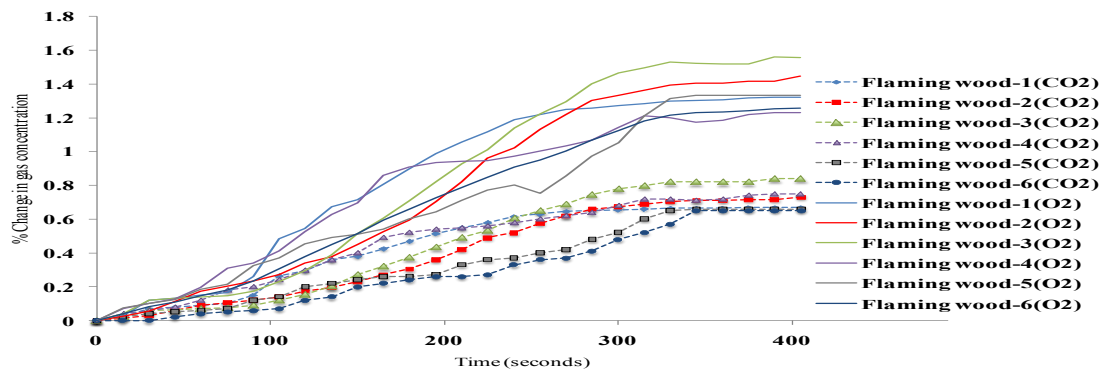


Figure 79 Changes in CO<sub>2</sub> and O<sub>2</sub> concentrations versus time for 6 replications of UL fire B (Flaming Wood) Emulations in UCLan 2 m<sup>3</sup> Enclosure

## 4.2 Standard Fire Tests at BRE and UCLan Emulations: -Sensor Data Plots

Charts below are provided summarising the sensor data for a series of the BS EN54/7 test fires carried at BRE Watford shown with a selection of corresponding data collected for emulations in the UCLan 2 m<sup>3</sup> enclosure. Only data on obscuration and CO gas levels is presented.

### 4.2.1 Smouldering Wood BS EN54/7 TF2 (BRE full scale and Emulations)

#### Smouldering wood (TF2)

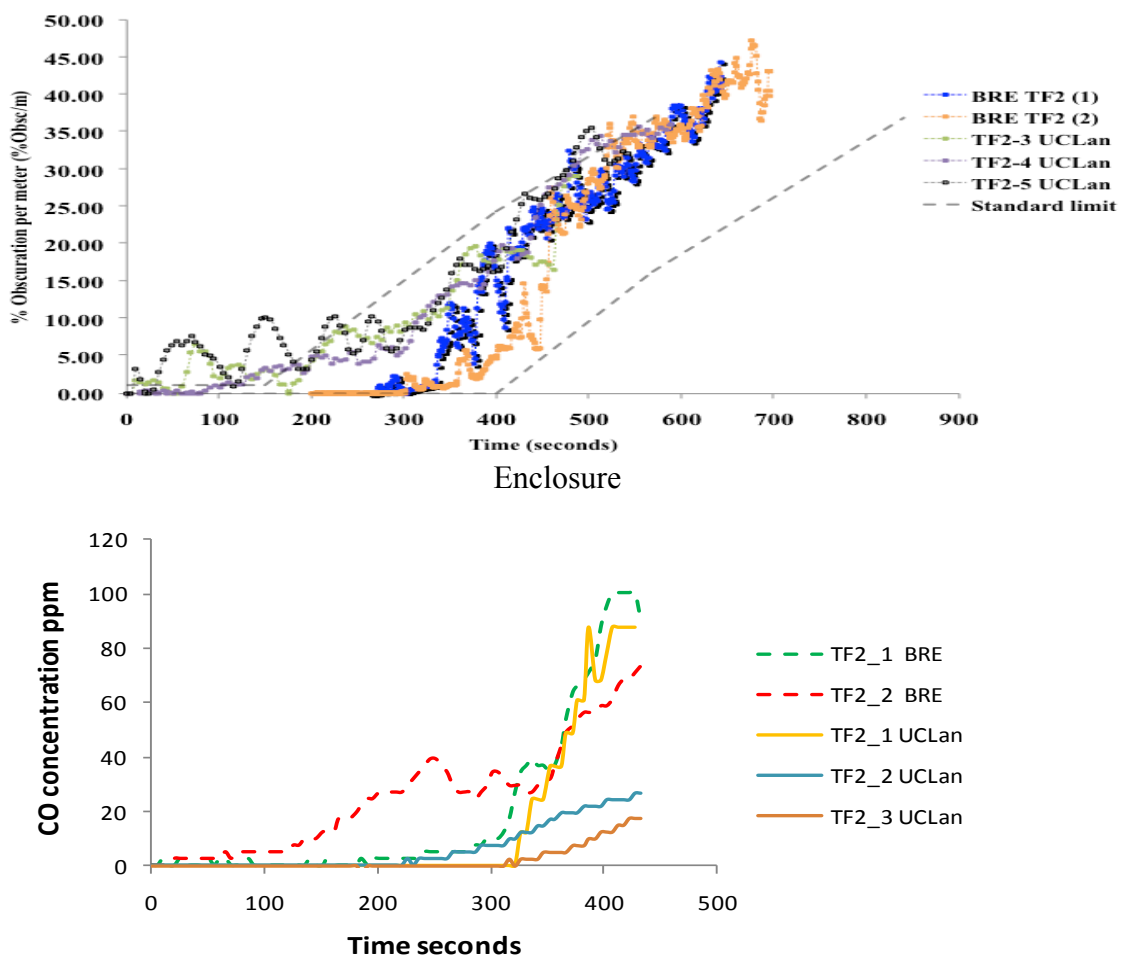


Figure 81 Carbon Monoxide (CO) versus time for standard TF2 (wood pyrolysis) at BRE (2 runs) and Emulations in UCLan 2 m<sup>3</sup> Enclosure

#### 4.2.2 Smouldering Cotton BS EN54/7 TF3 (BRE full scale and Emulations)

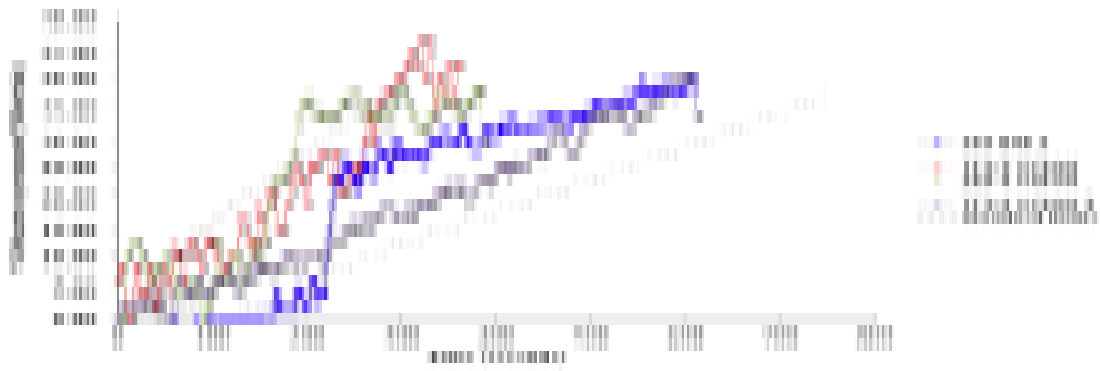


Figure 82 Obscuration versus time for standard TF3 (smouldering cotton) at BRE (2 runs) and Emulations in UCLan 2 m<sup>3</sup> Enclosure

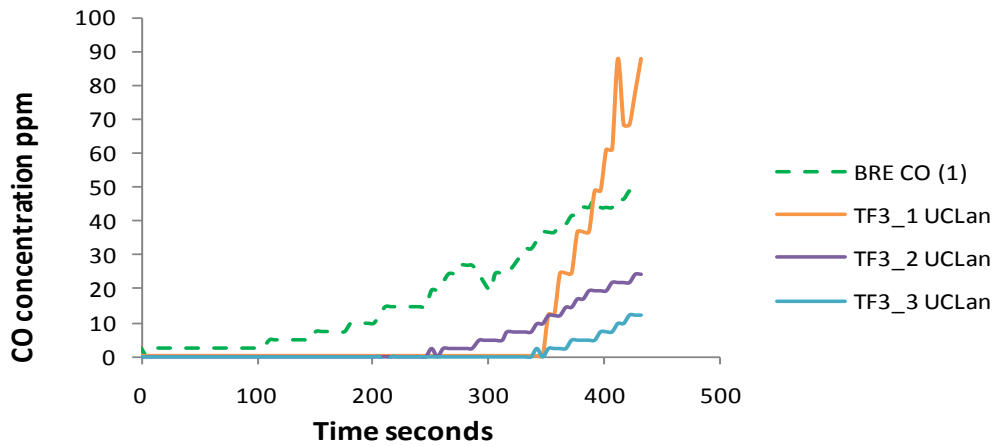


Figure 83 Carbon Monoxide (CO) versus time for standard TF3 (smouldering cotton) at BRE and Emulations in UCLan 2 m<sup>3</sup> Enclosure

#### 4.2.3 Polyurethane foam burn BS EN54/7 TF4 (BRE full scale

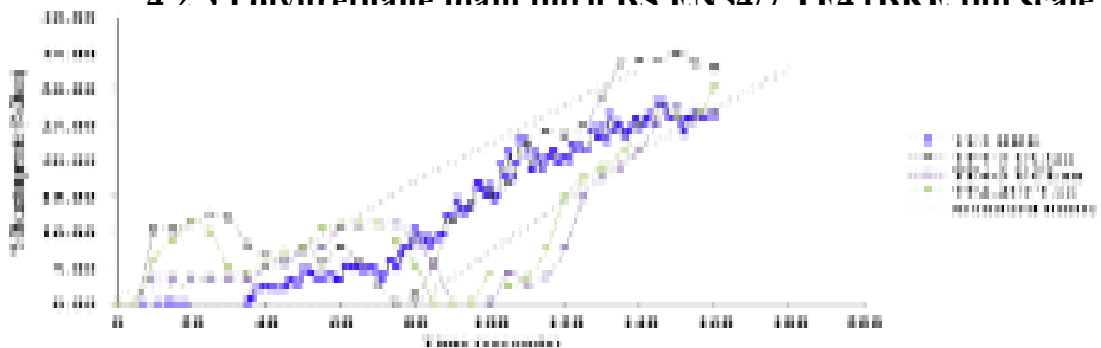


Figure 84 Obscuration versus time for standard TF4 (Polyurethane foam burn) at BRE and Emulations in UCLan 2 m<sup>3</sup> Enclosure (Polyurethane foam burn) at BRE

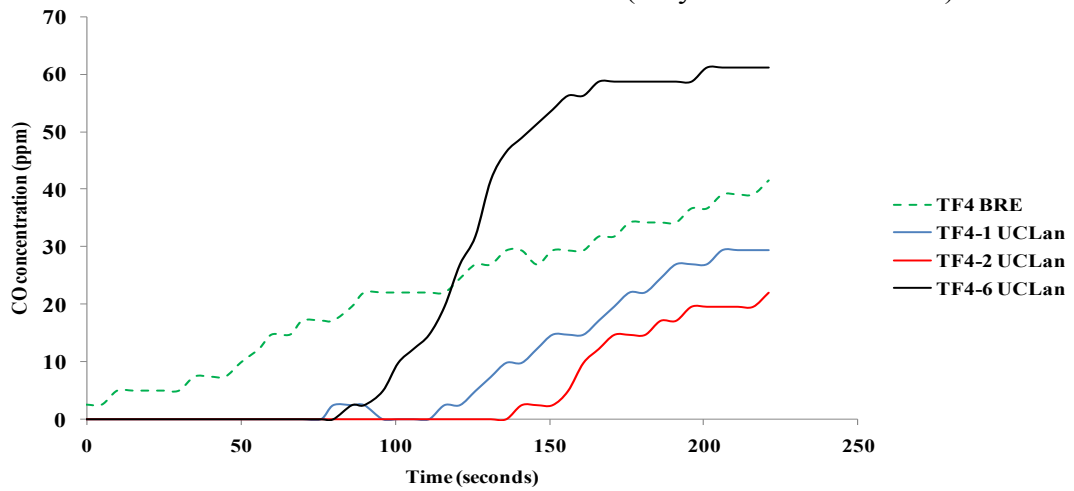


Figure 85 Carbon Monoxide (CO) versus time for standard TF4 (Polyurethane foam burn) at BRE and Emulations in UCLan 2 m<sup>3</sup> Enclosure

#### 4.2.4 Flaming Heptane BS EN54/7 TF5 (BRE full scale and Emulations)

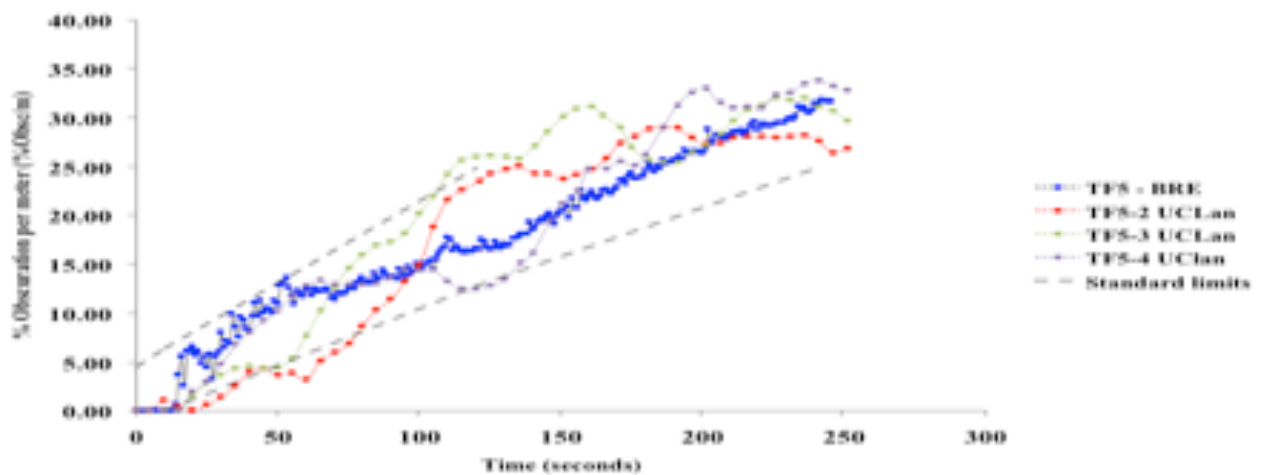


Figure 86 Obscuration versus time for standard TF5 (flaming heptane) at BRE and Emulations in UCLan 2 m<sup>3</sup> Enclosure

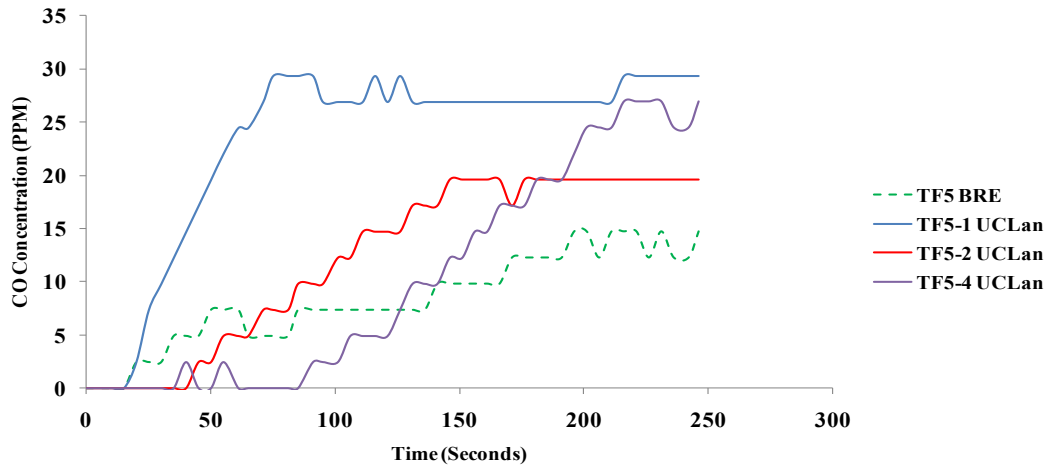


Figure 87 Carbon Monoxide (CO) versus time for standard TF5 (flaming heptane) at BRE and Emulations in UCLan 2 m<sup>3</sup> Enclosure

### 4.3 Sensor Data Summary for Non-Standard Tests in UCLan 2 m<sup>3</sup> Enclosure

Below plots are provided summarising the primary data for replicates for a series of tests carried out in the UCLan enclosure for sources other than covered in the standard based tests. Except as noted in each subsection, the results for each of the test types are shown in the order obscuration, CO and oxidizable gases, and major fire related gases CO<sub>2</sub> and O<sub>2</sub>,

#### 4.3.1 Overheating Printed Circuit Boards (PCB) in UCLan Enclosure

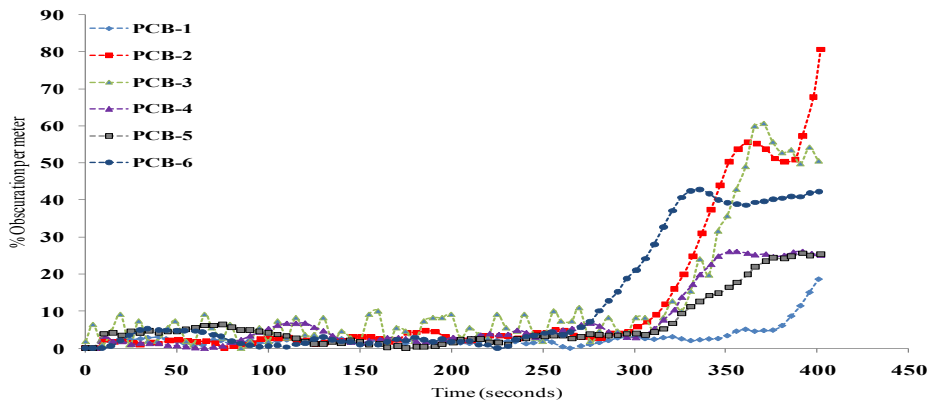


Figure 88 Obscuration versus time for 6 replications for Overheated PCBs in UCLan 2 m<sup>3</sup> Enclosure

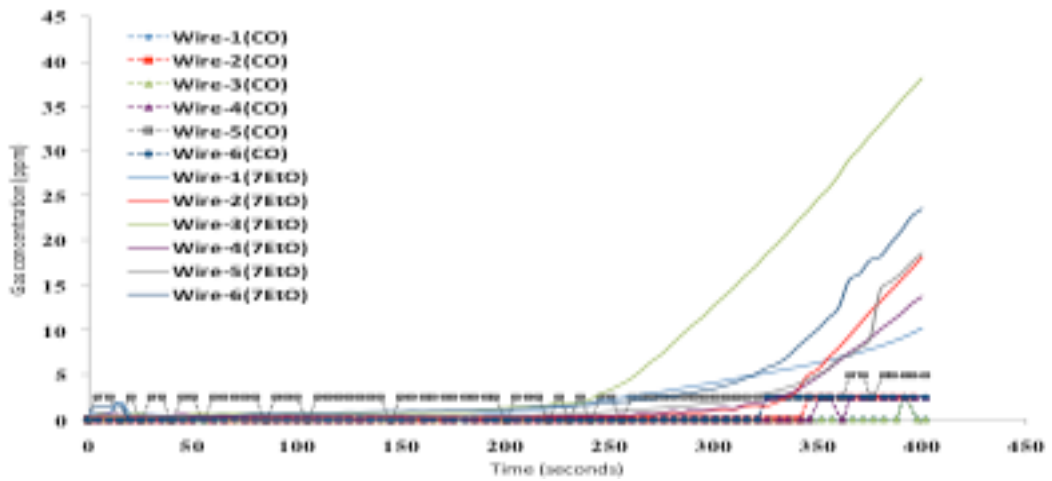


Figure 89 CO and oxidizable gas (by 7EtO) concentrations versus time for 6 replications for Overheated PCBs in UCLan 2 m<sup>3</sup> Enclosure

### Major Combustion Gases

Only very low levels of CO<sub>2</sub> and O<sub>2</sub> change were detected so the chart is not displayed here.

### 4.3.2 Burning Mixed Polyurethane Foams in UCLan Enclosure

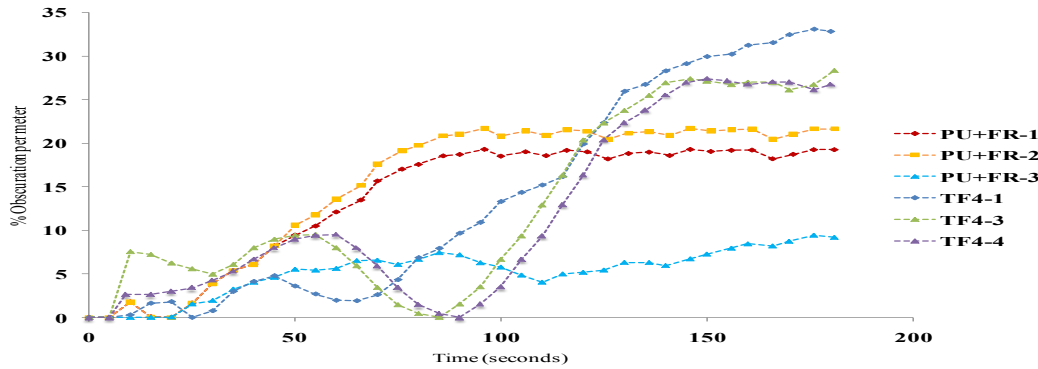


Figure 90 Obscuration versus time for 6 replications of mixed Polyurethane foam burns in UCLan 2 m<sup>3</sup> Enclosure

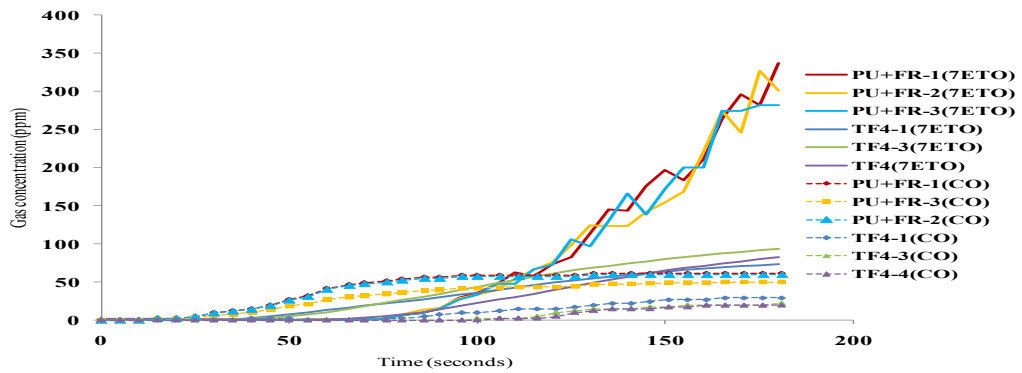


Figure 91 CO and oxidizable gas (by 7EtO) concentrations versus time for 6 replications of mixed Polyurethane foam burns in UCLan 2 m<sup>3</sup> Enclosure

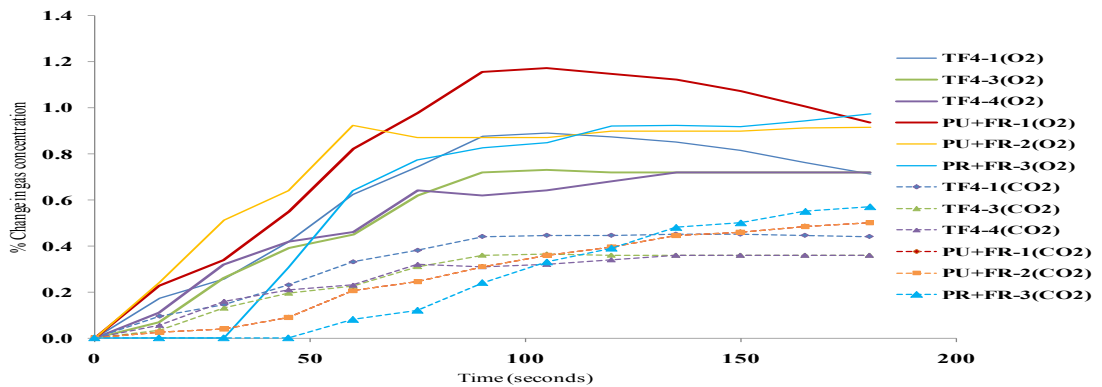


Figure 92 Changes in CO<sub>2</sub> and O<sub>2</sub> concentrations versus time for 6 replications of mixed Polyurethane foam burns in UCLan 2 m<sup>3</sup> Enclosure

### 4.3.3 Overheating Polymer Coated Wire in UCLan Enclosure

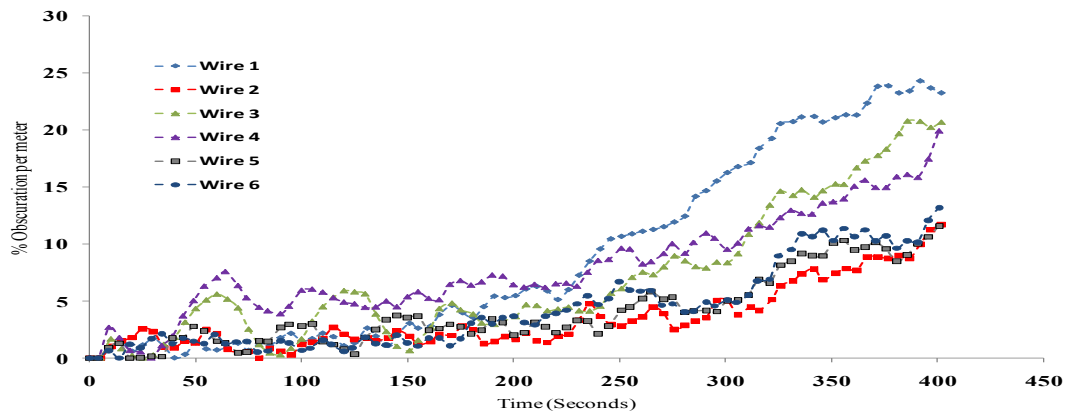


Figure 93 Obscuration versus time for 6 replications for Overheated Polymer Coated Wire in UCLan 2 m<sup>3</sup> Enclosure

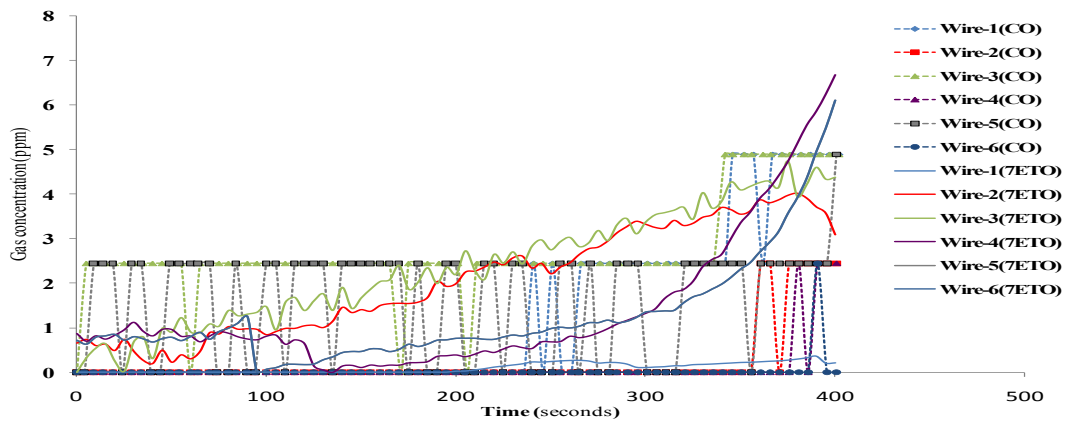


Figure 94 CO and oxidizable gas (by 7EtO) concentrations versus time for 6 replications for Overheated Polymer Coated Wire in UCLan 2 m<sup>3</sup> Enclosure

#### Major Combustion Gases

Only very low levels of CO<sub>2</sub> and O<sub>2</sub> change were detected so the chart is not displayed here.

### 4.3.4 Overheating Cooking Oils in UCLan Enclosure

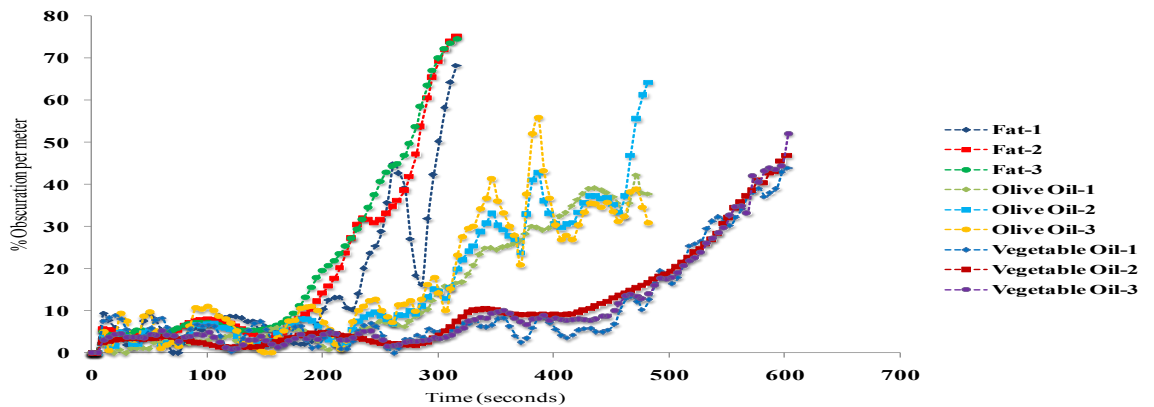


Figure 95 Obscuration versus time for Overheating of a range of Cooking Oils (3 replications each) in UCLan 2 m<sup>3</sup> Enclosure

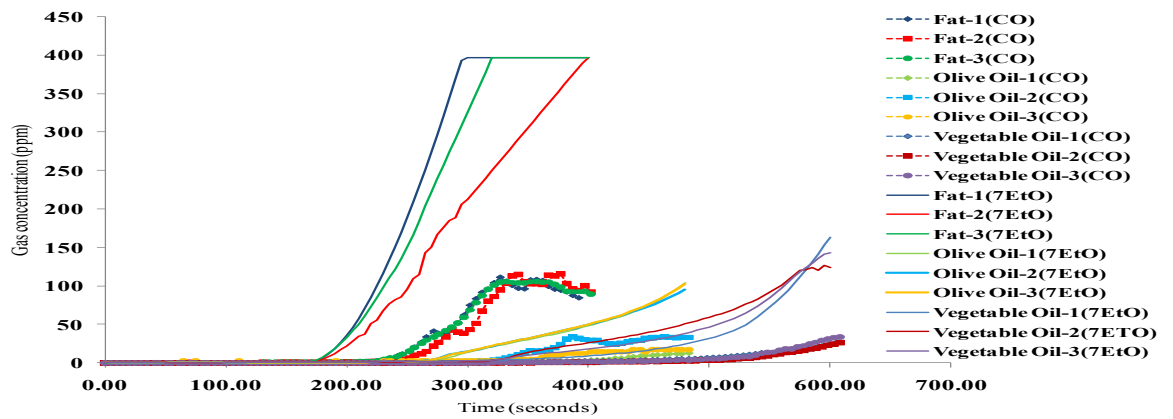


Figure 96 CO and oxidizable gas (by 7EtO) concentrations versus time for Overheating of a range of Cooking Oils (3 replications each) in UCLan 2 m<sup>3</sup> Enclosure

#### Major Combustion Gases

Only very low levels of CO<sub>2</sub> and O<sub>2</sub> change were detected so the chart is not displayed here.

### 4.3.5 Cigarette Smoking in UCLan Enclosure

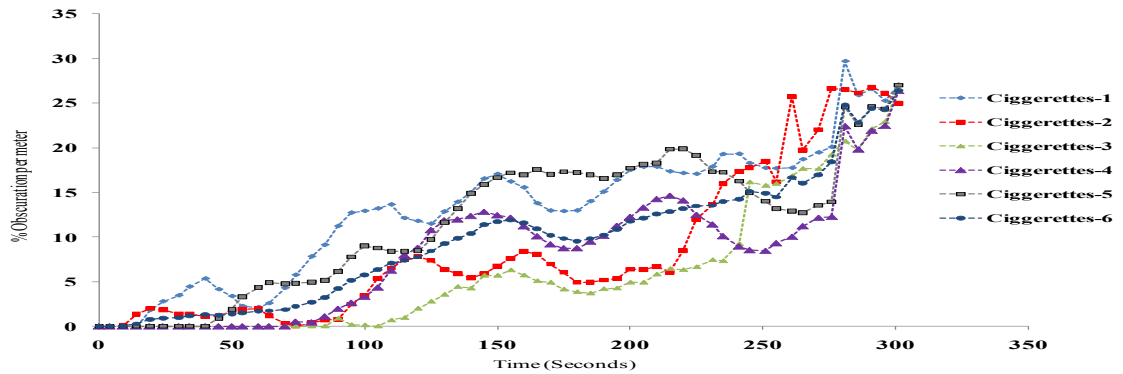


Figure 97 Obscuration versus time for 6 replications of Cigarette Smoking Tests in UCLan 2 m<sup>3</sup> Enclosure

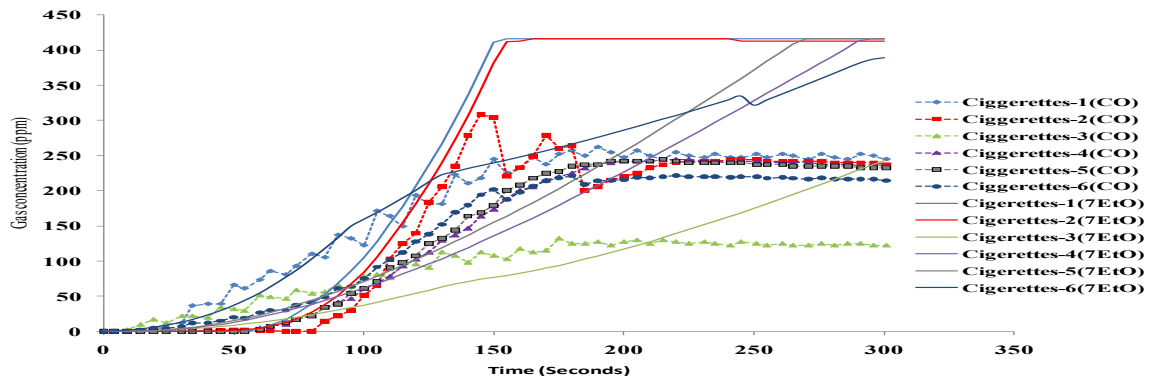


Figure 98 CO and oxidizable gas (by 7EtO) concentrations versus time for 6 replications of Cigarette Smoking Tests in UCLan 2 m<sup>3</sup> Enclosure

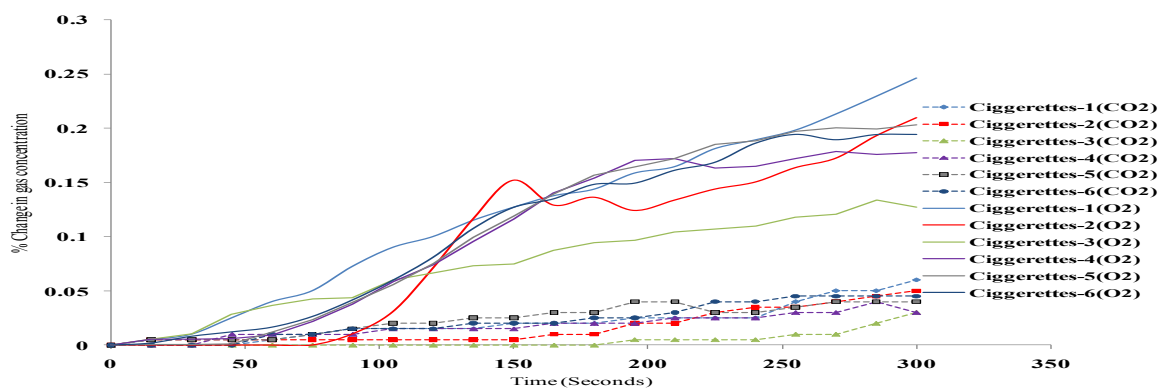


Figure 99 Changes in CO<sub>2</sub> and O<sub>2</sub> concentrations versus time for 6 replications of Cigarette Smoking Tests in UCLan 2 m<sup>3</sup> Enclosure

### 4.3.6 Bread Toasting and Re-Toasting in UCLan Enclosure

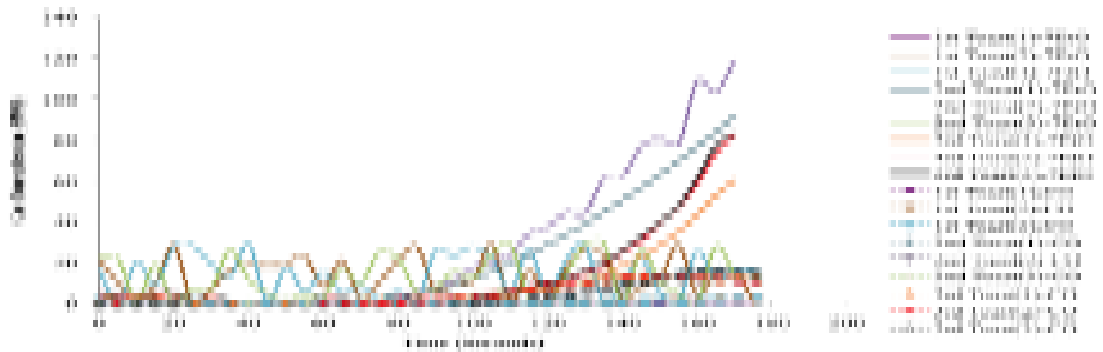
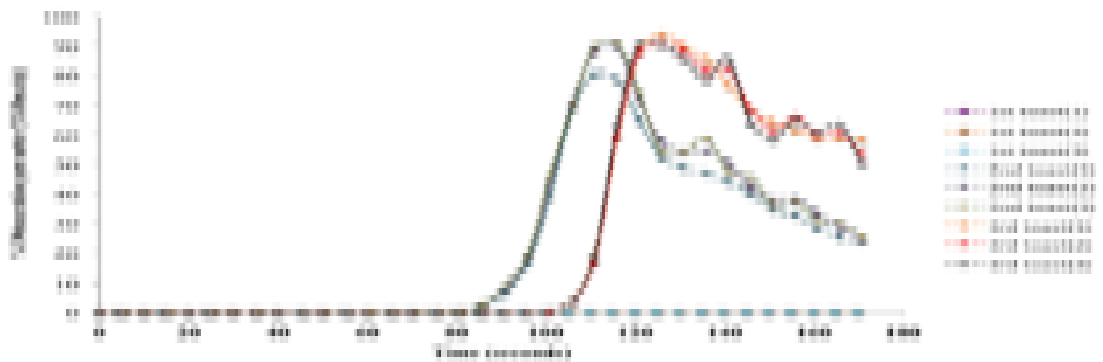


Figure 100 Obscuration versus time for 3 replications for Toasted and Re-Toasted Bread in UCLan 2 m<sup>3</sup> Enclosure



concentrations versus time for 3 replications for Toasted and Re-Toasted Bread in UCLan 2 m<sup>3</sup> Enclosure

### Major Combustion Gases

Only very low levels of CO<sub>2</sub> and O<sub>2</sub> change were detected so the chart is not displayed here.

#### 4.4 Summary of parameters for reduced scale fires

The summaries in the following tables are tabulated key fire properties presented for discussion and ease of comparison. Mass loss is a calculation of the amount of fuel consumed during the fire tests. This was calculated by measuring the fuel prior to and following experiments. The peak CO and 7EtO levels are measured electrochemically and represent the maximum amount of material produced in each of the fires. The 7EtO measurement includes CO as well as other oxidisable gases, and the difference between the measurements from the CO and 7EtO cells is a measure of the presence of organic gases and vapours.

Fuel	Smouldering wood (TF2)	Smouldering cotton (TF3)	Flaming polyurethane (TF4)	Flaming pool fire (TF5)
Mass loss (g)	1.1±0.2	4.8±0.3	6.9±0.2	8.0*
Peak CO (ppm)	12±4	258±114	31±15	22±5
7EtO response (ppm CO equiv)	161 ± 57	814 ±170	111±41	92±43
Maximum obscuration (% m <sup>-1</sup> )	26± 9	30 ± 9	29±5	29± 4

Table 23 Properties from the scaled fires based on the BS-EN 54-7 standard fired carried out in the UCLan enclosure. \* Represents a pool fire which used an accurately measured volume which is consumed during the experiment

Fuel	Fire A : Smouldering paper	Fire B : Flaming wood	Fire C : Flaming heptane
Mass loss (g)	3 ± 0.	4.6 ± 0.2	3.0*
Peak CO (ppm)	159 ±55	175 ± 92	78 ± 27
7EtO response (ppm CO equiv)	398 ± 133	443 ± 145	243 ± 101
Maximum obscuration (% m <sup>-1</sup> )	34 ± 8	15 ± 3	29 ±12

Table 24 Properties from the scaled fires based on the scaled UL268 standard fires carried out in the UCLan scaled fire enclosure.

Fuel	Polyurethane with flame retardant	Printed circuit boards	PVC heated wire	Methanol
Mass loss (g)	1.1 ± 0.2	4.8 ± 0.3	6.9 ± 0.2	8.0*
Peak CO (ppm)	12 ± 4	258 ± 114	31 ± 15	22 ± 5
7EtO response (ppm CO equiv)	161 ± 57	814 ± 170	111 ± 41	92 ± 43
Maximum obscuration (% m <sup>-1</sup> )	26 ± 9	30 ± 9	29 ± 5	29 ± 4

Table 25 Properties from the scaled fires based on the scaled non-standard polymer based fires carried out in the UCLan enclosure

Fuel	Heated vegetable oil	Heated olive oil	Heated fat
Mass loss (g)	3.2	2.9	2.1
Peak CO (ppm)	102 ± 24	58 ± 14	39 ± 19
7EtO response (ppm CO equiv)	397 ± 87	99 ± 270	55 ± 19
Maximum obscuration (% m <sup>-1</sup> )	29 ± 9	55 ± 9	69 ± 4

Table 26 Properties from the scaled fires based on the scaled non-standard sources based on cooking fuels used as false alarm scenarios. All measurements were based on the small scale fires carried out in the UCLan enclosure. For comparison the values are measured at 450 seconds.

Fuel	1 <sup>st</sup> toast	2 <sup>nd</sup> toast	3 <sup>rd</sup> toast
Mass loss (g)	7.9 ± 0.8	6.9 ± 0.8	4.5 ± 0.8
Peak CO (ppm)	2 ± 1	16 ± 1	14 ± 1
EtO response (ppm CO equiv)	11 ± 1	107 ± 17	56 ± 19
Maximum obscuration (% m <sup>-1</sup> ) <sup>1)</sup>	2.3±0.9	89 ± 9	89 ±10

Table 27 Properties from the scaled fires based on the scaled non-standard sources based on the progression of toasting used as false alarm scenarios. All measurements were based on the small-scale fires carried out in the UCLan scaled fire enclosure. Smoke from the toaster was a thick and rapidly developing grey white smoke.

#### 4.4.1 Change in temperatures

Temperature changes over the course of the experiments are illustrated in chart below.

The change in temperature was measured using the built in sensors of the TYCO devices. The chart shows an average temperature change in a range of different fire examined in the UCLan fire enclosure.

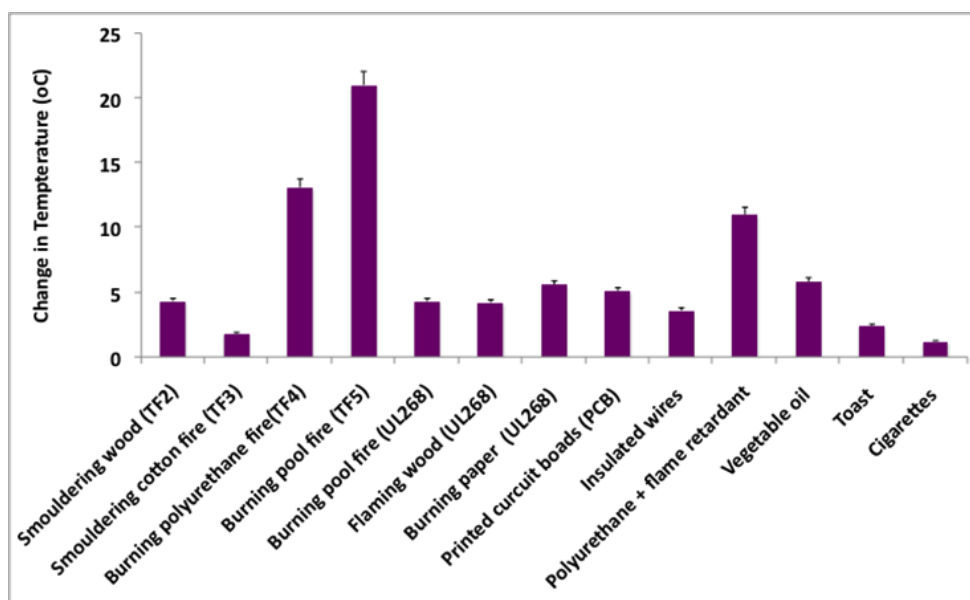


Figure 102 Example changes in temperature for a range of fuels examined in the UCLan scaled enclosure.

#### 4.5 GC-MS Data (GC Chromatograms)

This section of chapter 4 presents the GC/MS results for the range of fire tests covered in previous sections displayed as ion current versus retention time chromatograms. The GC-MS traces can generally be related to the sensor records in earlier sections by test name and number i.e. for a given test type, GC-MS traces 1-6 relate directly to the correspondingly numbered test records for sensor responses above unless otherwise stated. Because of the problems encountered using dual samples the Tenax samples labelled 7-12 are taken from separate fires that were carried out under the same conditions as fires 1-6.

In the GC/MS, the GC column separates compounds so that different compound transit the column at different speed and so reach the column exit with different retention (or elution) times. Compounds leaving the column exit are detected by the MS unit which displays an ion current value. This ion current is essentially on an arbitrary scale not readily converted to actual ion current through MS or readily to compound concentration. Ion current is expected to rise with the concentration of compound leaving the column but as different compound generate different numbers of ion fragments, a simple ratio between ion current and concentration is not expected to be maintained over a range of compounds. For each test run, the values of ion current are recorded through the GC retention time (at ~1.1 second intervals for the equipment and settings used for this work). For convenience in displaying multiple GC traces, **% ion intensity** values were calculated for each run and then displayed offset on the y axis. The parameter **% ion intensity** is calculated as indicated below:

$$\begin{aligned} \text{Ion current value recorded for } n^{\text{th}} \text{ time interval} &= I_n \\ \text{Mean ion current value } I_{\text{av}} &= (\text{Sum of all } I_n \text{ for } n = 0 \text{ to } N_{\text{max}}) / N_{\text{max}} \quad (25) \\ \text{for } n^{\text{th}} \text{ time interval, \% ion intensity} &= 100 \times I_n / I_{\text{av}} \end{aligned}$$

Equation 25 Ion intensity in GC plots

For presentation of multiple GC traces, the % ion intensity values are displayed on the y axis offset by amounts convenient for the clarity of display. The plots for each test series are intended to show the form, and consistency or variability of the chromatograms rather than data suitable for numerical interpretation. Conclusions to be based on these figures should not extend beyond comparison between samples within a set. Some degree of variability can be explained by a small sample shifts resulting from

changes in component or instrumentation characteristics or configuration, or protocols. A fuller data interpretation for typical plots from each test type is presented in chapter 5.

The figures are for comparison and do show trends in common gases and more conventionally the degree of variability between samples. Where possible data is shown for both the samples collected on Tenax sample eluted from CB5-low MS column and samples collected on the Carboxen samples eluted on the poroplot Q columns. Late in the project it was decided that the gases of interest would most likely be the low MW samples so for some of the non standard fire samples only Carboxen/poroplot Q data was recorded.

The data presented first (sections 4.6.1 to 4.6.7) is for samples collected on Carboxen and Tenax during emulations of standard EN54/7 and UL 268 test fires carried out in the UCLan 2 m<sup>3</sup> enclosure.

A series of chromatograms derived for samples collected on Carboxen at the EN54/7 standard tests at BRE are presented in section 4.7 and these are reproduced in greater detail in chapter 5.

GC data from samples collected for non-standard tests conducted in the UCLan enclosure is presented in sections 4.8 onwards. These are for Carboxen absorbed samples only except for some measurements for toasted bread. This GC data series does not include a replication series for burning cigarettes as very complex poorly reproducible chromatograms were found for this source.

## 4.6 GC Chromatograms for UCLan. Emulations of Standard Fires

### 4.6.1 Scaled Smouldering wood (EN 54/7 TF2 Emulations)

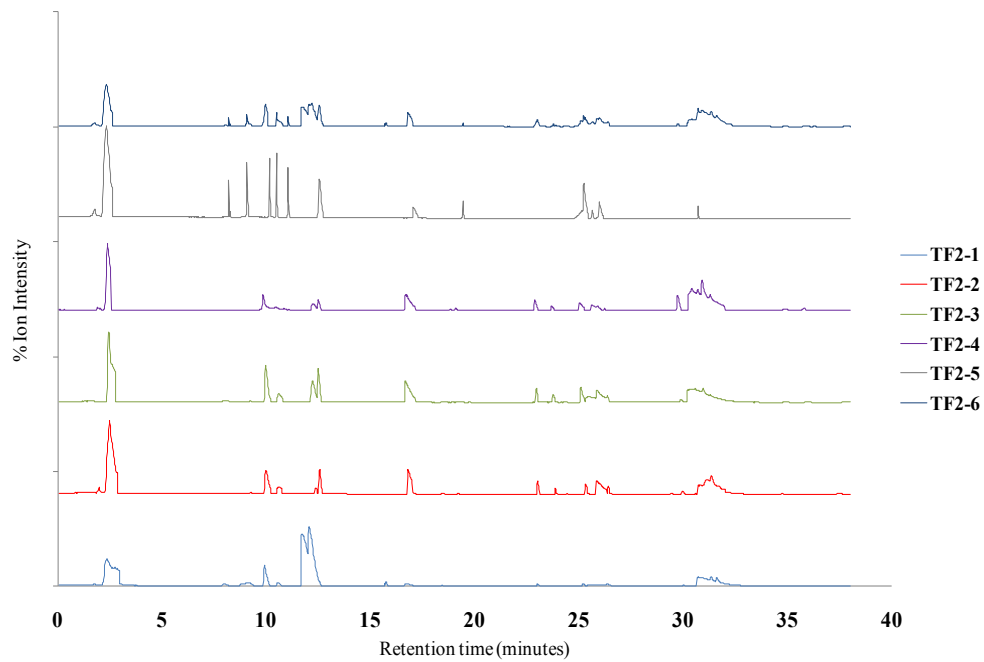


Figure 103 GC/MS Chromatograms for material from Carboxen tubes used for 6 replications of TF2 (wood pyrolysis) Emulations in UCLan 2 m<sup>3</sup> Enclosure

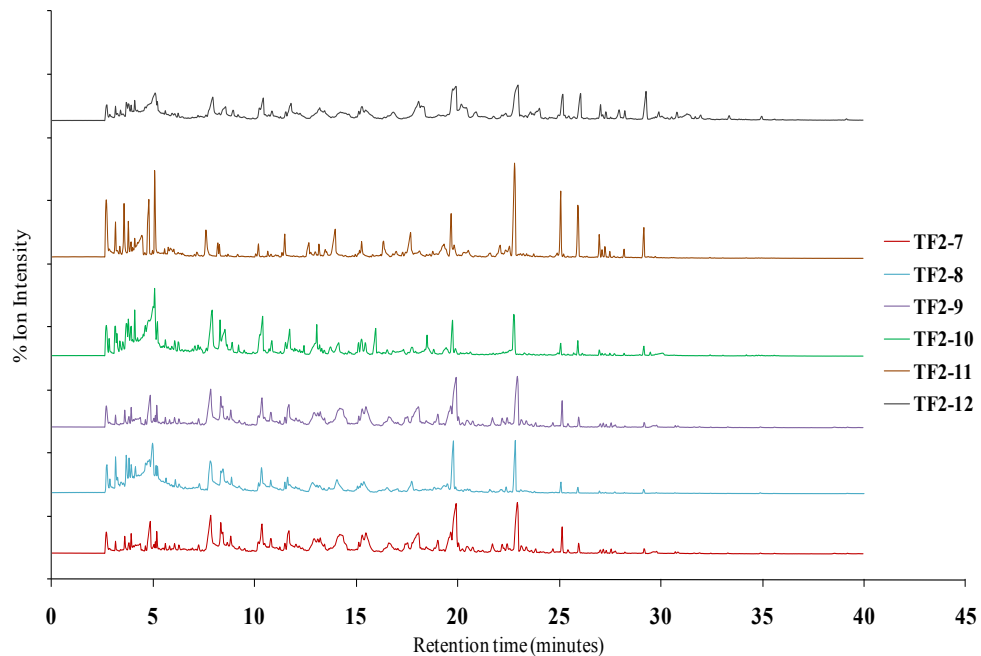


Figure 104 GC/MS Chromatograms for material from Tenax tubes used for 6 replications of TF2 (wood pyrolysis) Emulations in UCLan 2 m<sup>3</sup> Enclosure

#### 4.6.2 Smouldering cotton (EN 54/7 TF3 Emulations)

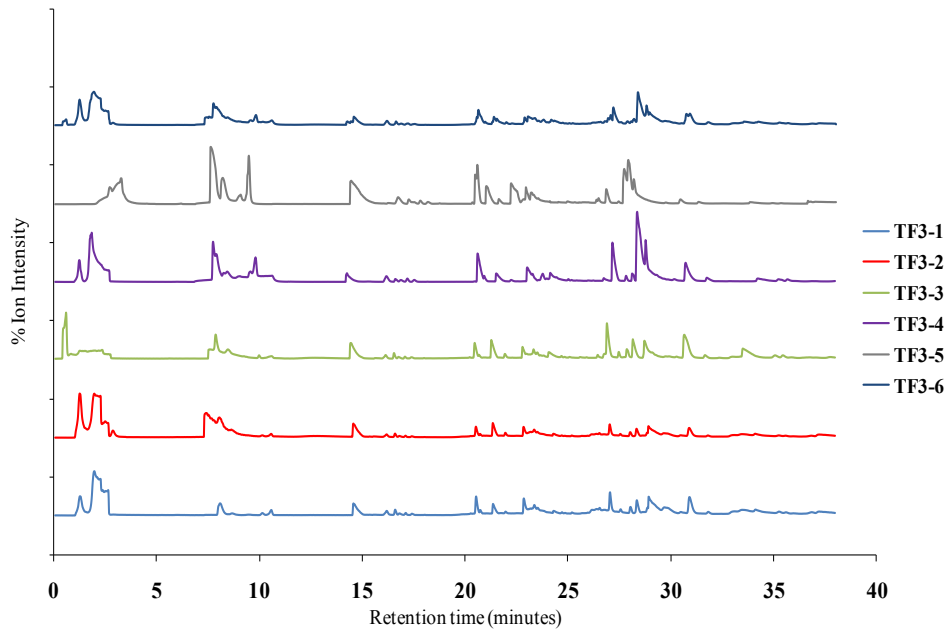


Figure 105 GC/MS Chromatograms for material from Carboxen tubes used for 6 replications of TF3 (cotton smoulder) Emulations in UCLan 2 m<sup>3</sup> Enclosure

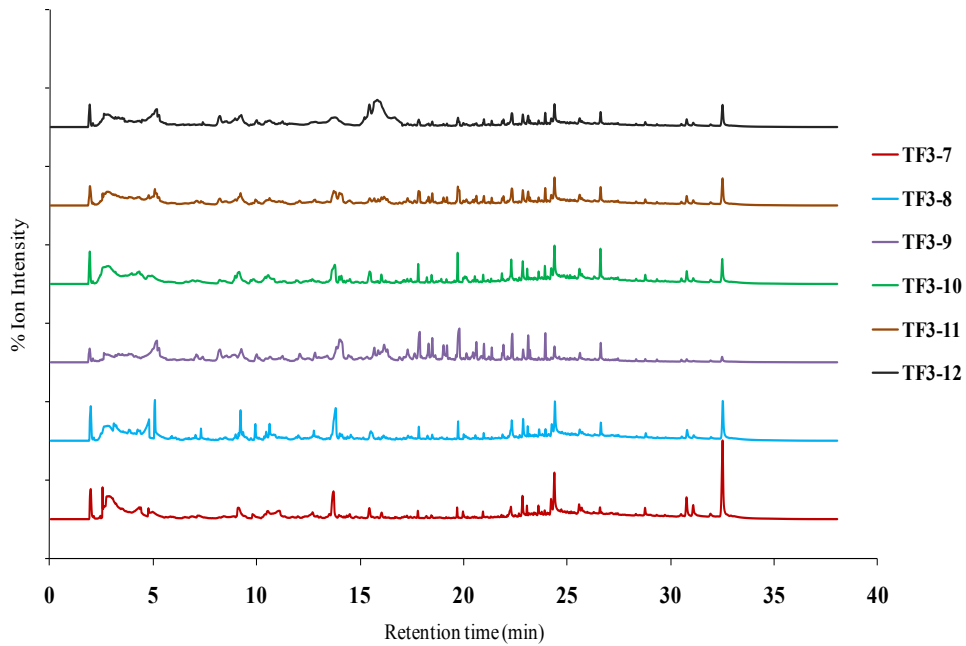


Figure 106 GC/MS Chromatograms for material from Tenax tubes used for 6 replications of TF3 (cotton smoulder) Emulations in UCLan 2 m<sup>3</sup> Enclosure

### 4.6.3 Burning Polyurethane Foam (BS EN 54/7 TF4 Emulations)

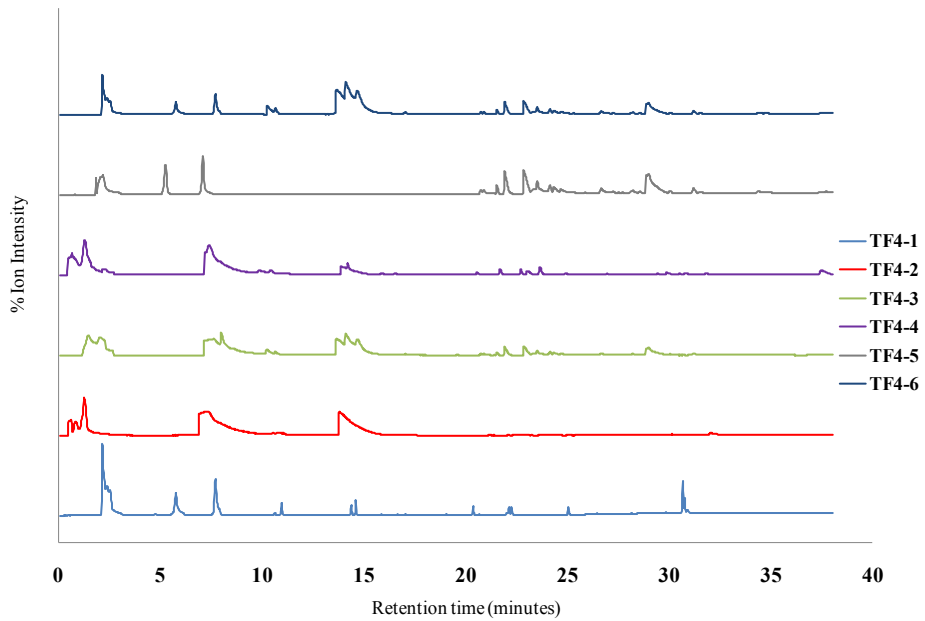


Figure 107 GC/MS Chromatograms for material from Carboxen tubes used for 6 replications of TF4 (Polyurethane foam burn) Emulations in UCLan 2 m<sup>3</sup> Enclosure

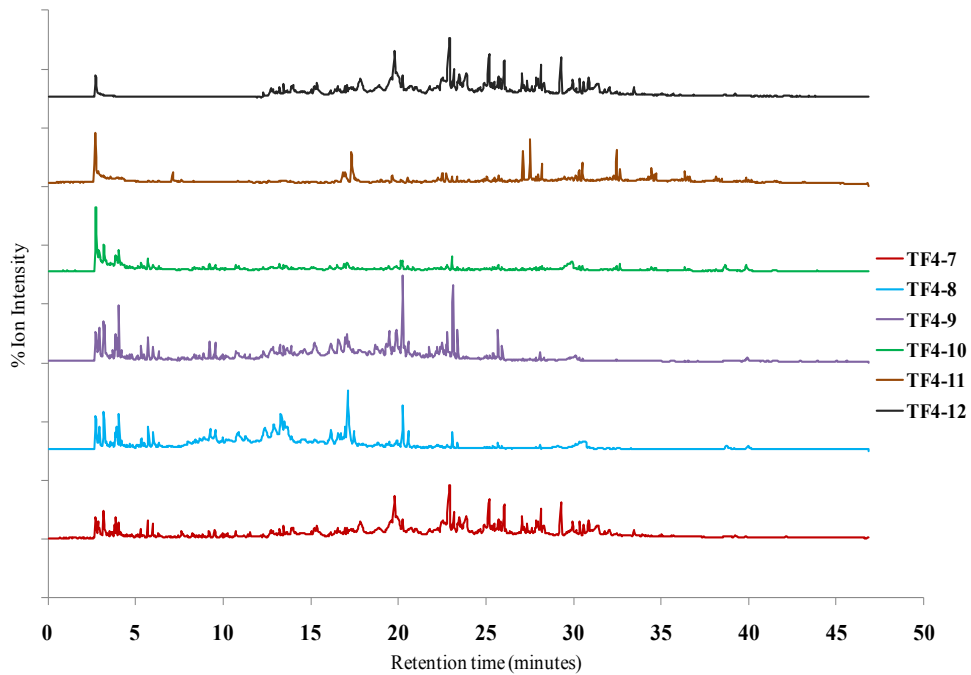


Figure 108 GC/MS Chromatograms for material from Tenax tubes used for 6 replications of TF4 (Polyurethane foam burn) Emulations in UCLan 2 m<sup>3</sup> Enclosure

#### 4.6.4 Burning pool fire - Heptane (BS EN 54/7 TF5 Emulsions)

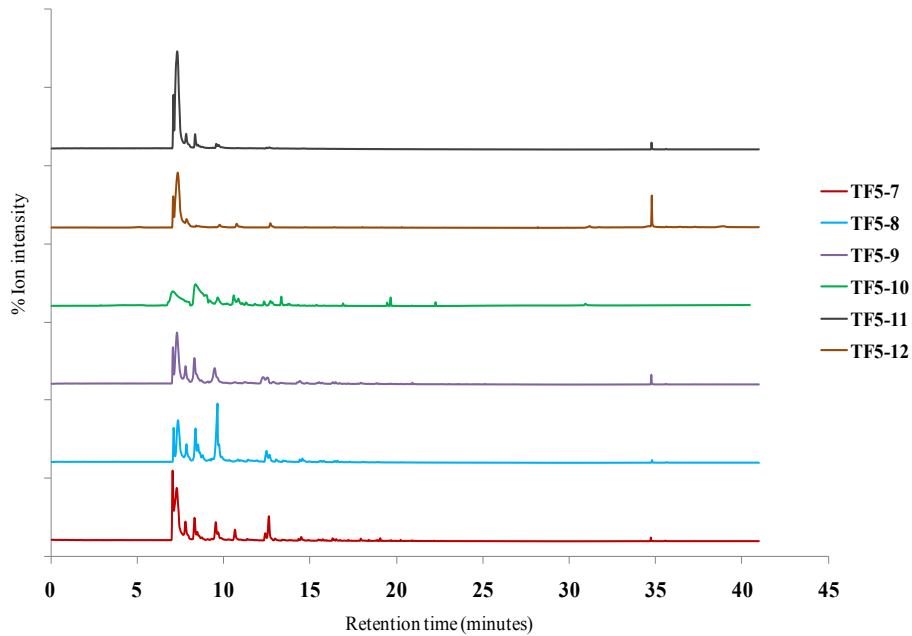


Figure 109 GC/MS Chromatograms for material from Carboxen tubes used for 6 replications of TF5 (Flaming Heptane) Emulsions in UCLan 2 m<sup>3</sup> Enclosure

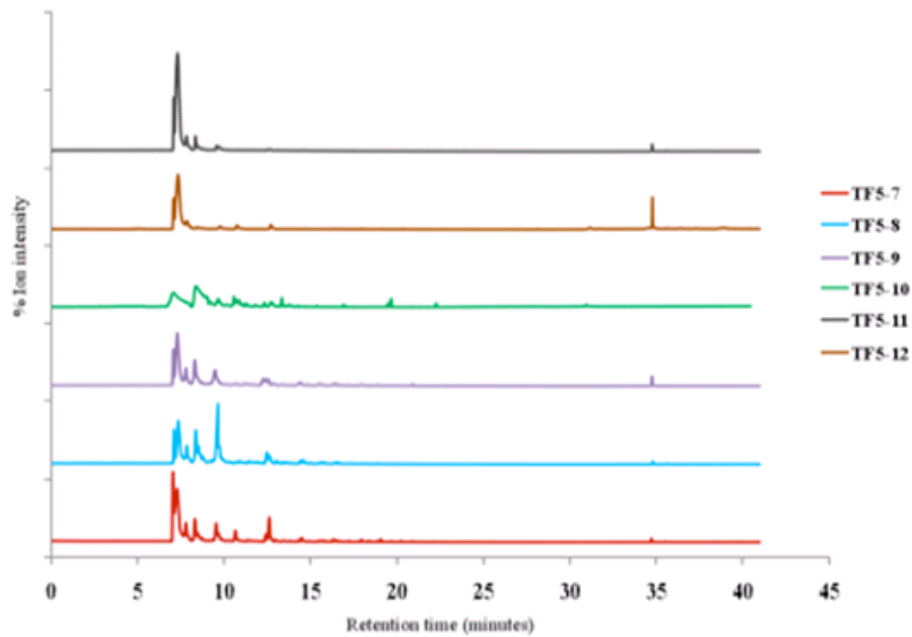


Figure 110 GC/MS Chromatograms for material from Tenax tubes used for 6 replications of TF5 (Flaming Heptane) Emulsions in UCLan 2 m<sup>3</sup> Enclosure

#### 4.6.5 Burning pool fire - Heptane (UL268 fire C Emulation)

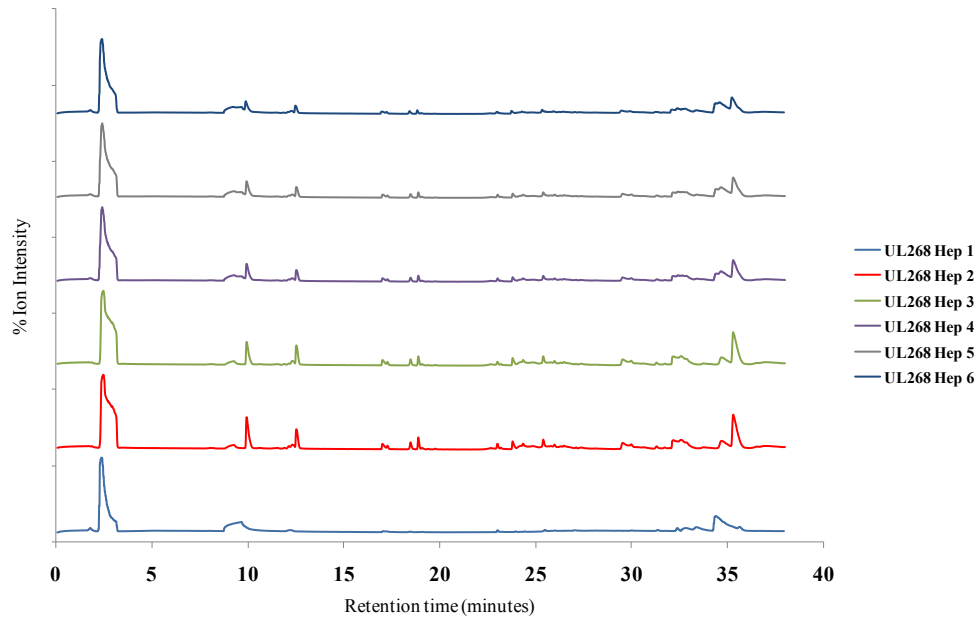


Figure 111 GC/MS Chromatograms for material from Carboxen tubes used for 6 replications of UL fire C (Flaming Heptane) Emulations in UCLan 2 m<sup>3</sup> Enclosure

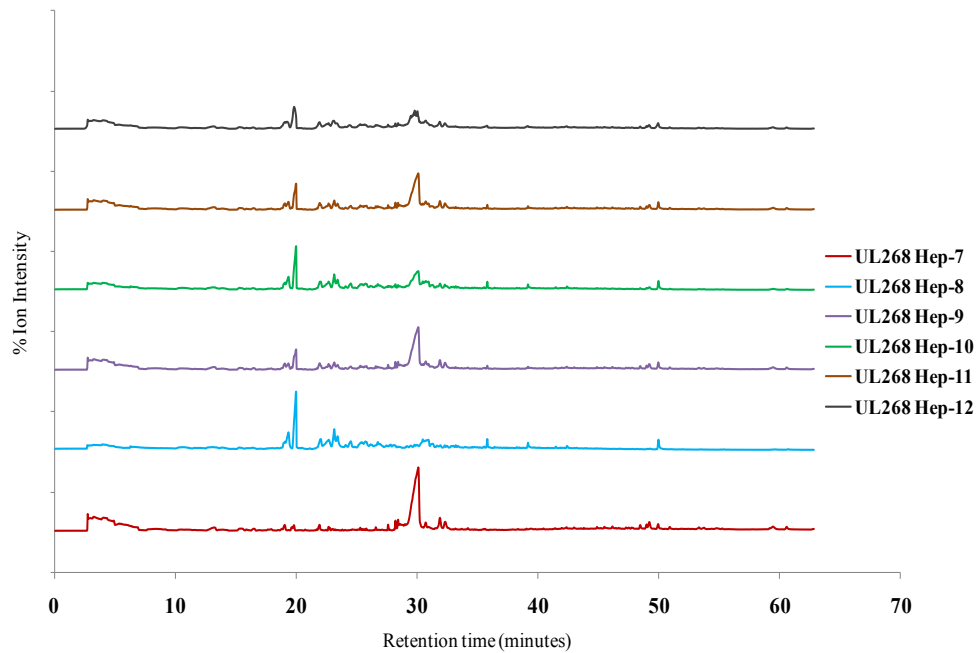


Figure 112 GC/MS Chromatograms for material from Tenax tubes used for 6 replications of UL fire C (Flaming Heptane) Emulations in UCLan 2 m<sup>3</sup> Enclosure

#### 4.6.6 Burning Paper (UL268 fire A Emulation)

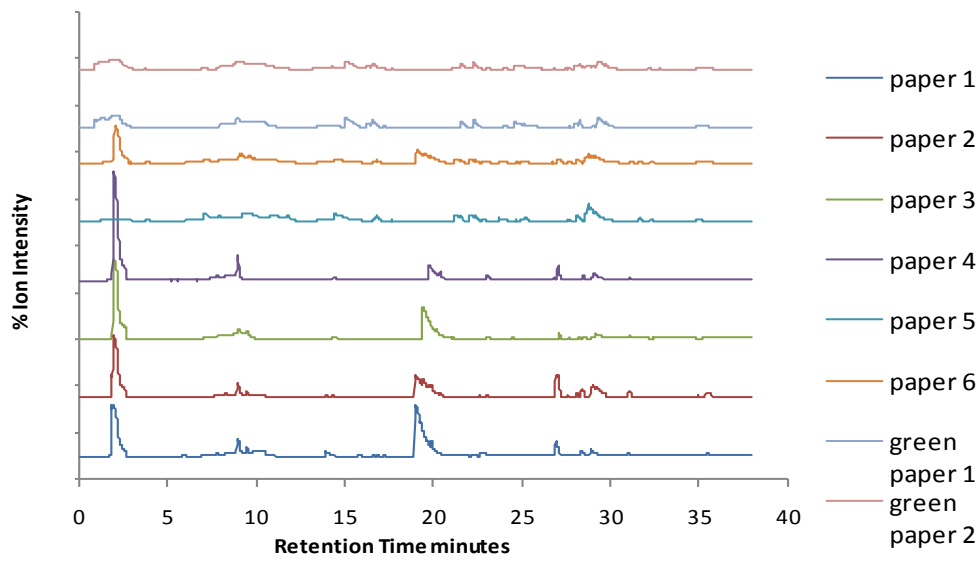


Figure 113 GC/MS Chromatograms for material from Carboxen tubes used for 6 replications of UL fire A (Burning Paper) Emulations in UCLan 2 m<sup>3</sup> Enclosure. Also shows results for green paper of type that may be found in washroom litterbin.

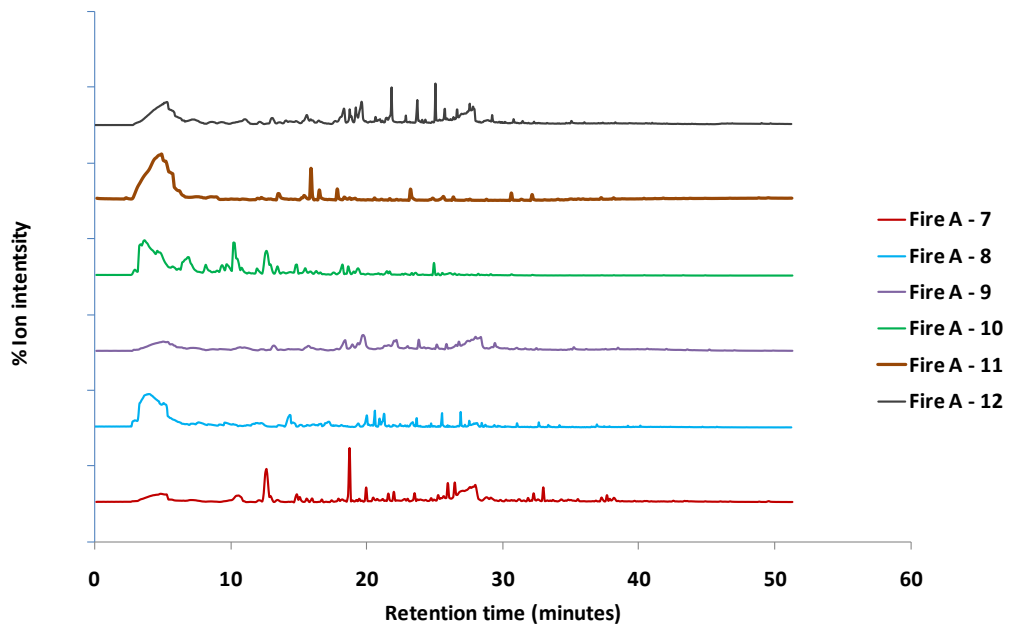


Figure 114 GC/MS Chromatograms for material from Tenax tubes used for 6 replications of UL fire A (Burning Paper) Emulations in UCLan 2 m<sup>3</sup> Enclosure

#### 4.6.7 Flaming wood (UL268 fire B Emulation)

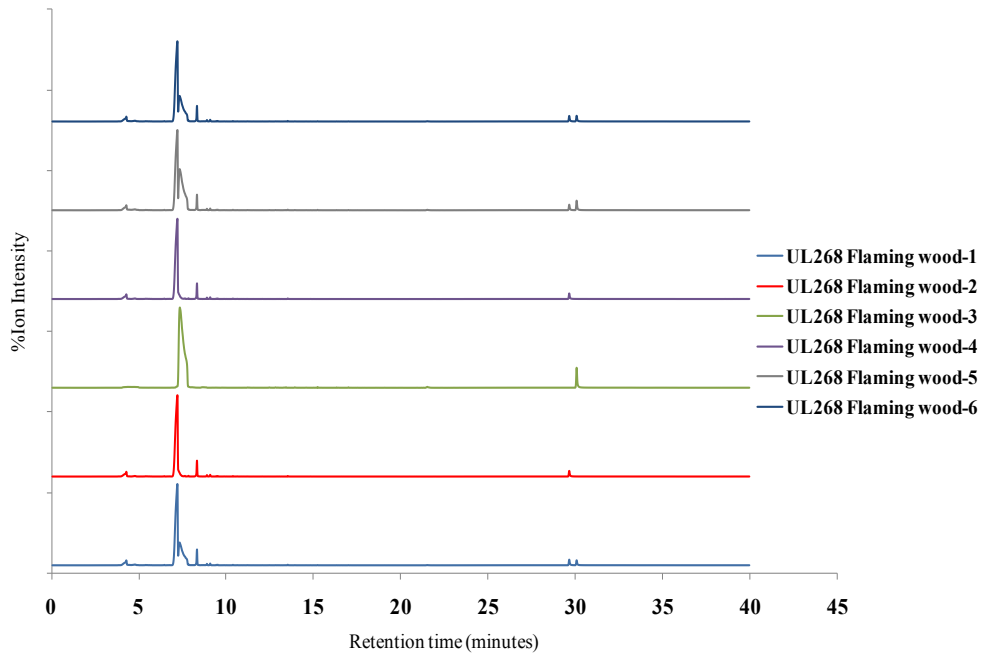


Figure 115 GC/MS Chromatograms for material from Carboxen tubes used for 6 replications of UL fire B (Flaming Wood) Emulations in UCLan 2 m<sup>3</sup> Enclosure

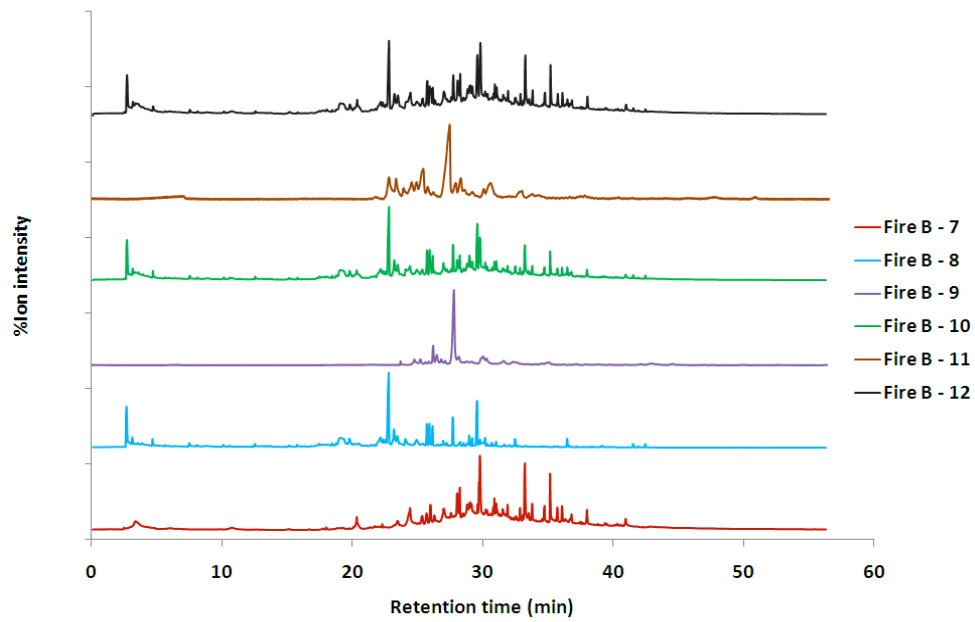


Figure 116 GC/MS Chromatograms for material from Tenax tubes used for 6 replications of UL fire B (Flaming Wood) Emulations in UCLan 2 m<sup>3</sup> Enclosure

#### 4.7 GC Chromatograms for EN54/7 fires conducted at BRE

The GC chromatograms below are for samples collected on Carboxen absorption tubes at full scale fire tests carried out in the test room at BRE Watford in May 2010.

As only there is only one plot for each test, ion current (arbitrary units) was not converted to ion intensity scale as for the groups of UCLan enclosure tests.

It is apparent that the forms of the chromatograms for samples from the BRE tests do not show a close resemblance to corresponding tests in the UCLan enclosure.

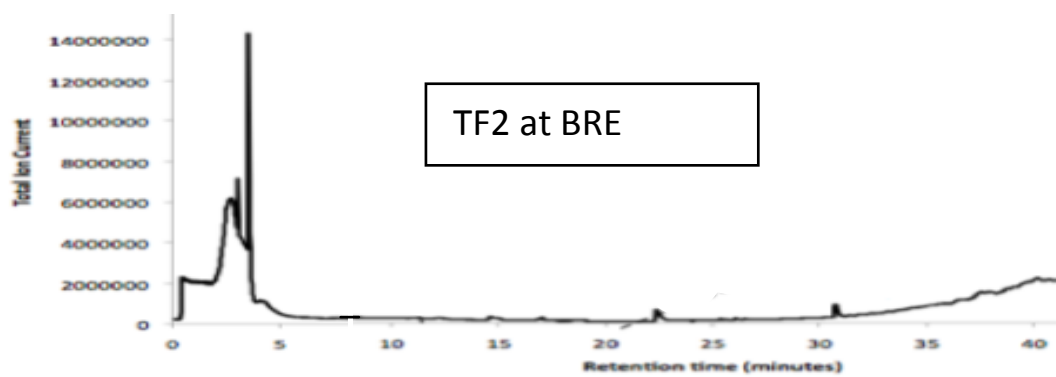


Figure 117 GC/MS Chromatograms for material from Carboxen tube used EN54/7 TF2 (smouldering wood) fire at BRE

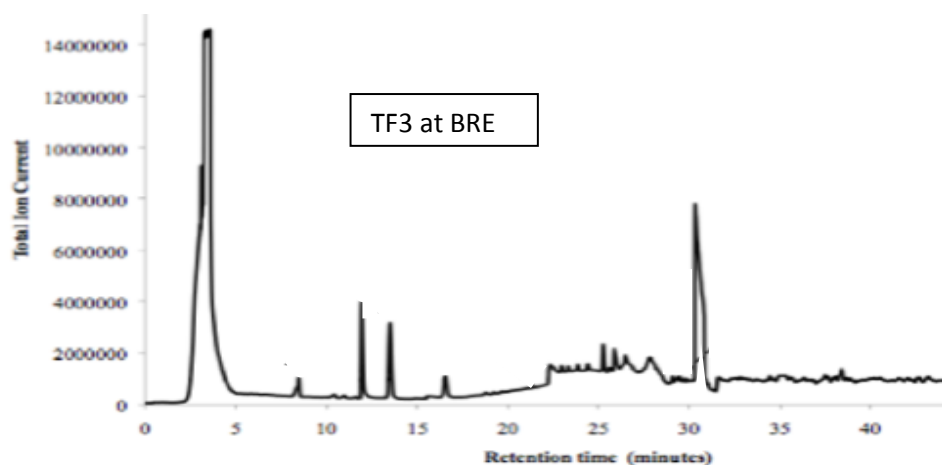


Figure 118 GC/MS Chromatograms for material from Carboxen tube used EN54/7 TF3 (smouldering cotton) fire at BRE

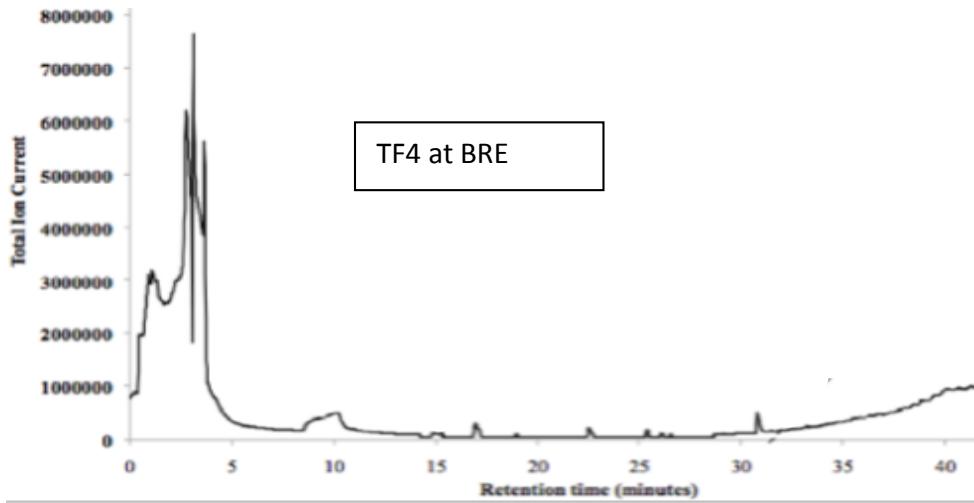


Figure 119 GC/MS Chromatograms for material from Carboxen tube used EN54/7 TF4 (Polyurethane foam burn) fire at BRE

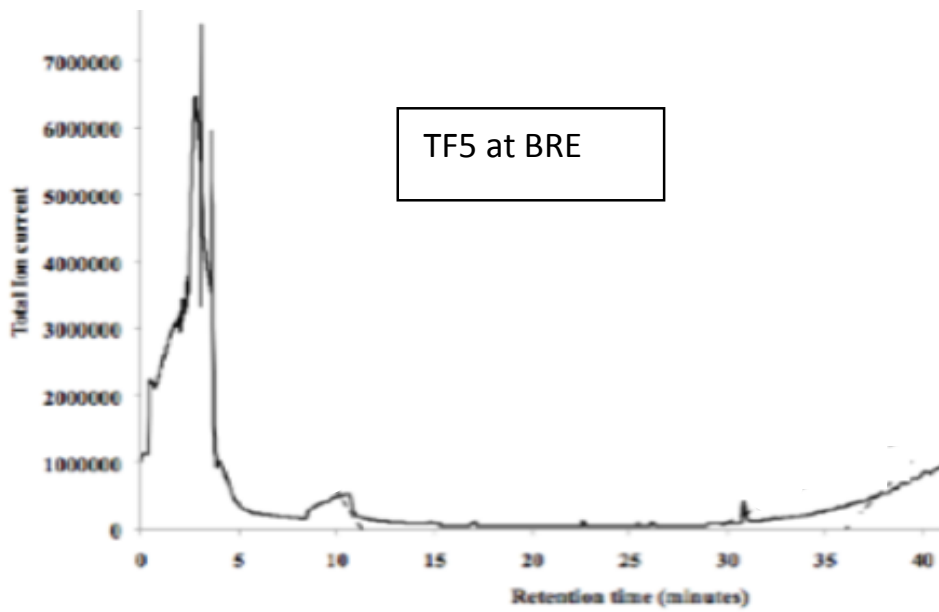


Figure 120 GC/MS Chromatograms for material from Carboxen tube used EN54/7 TF5 (Flaming Heptane) fire at BRE

## 4.8 GC for Non-Standard Tests in UCLan. Enclosure

### 4.8.1 Burning Mixed Polyurethane Foams in UCLan Enclosure

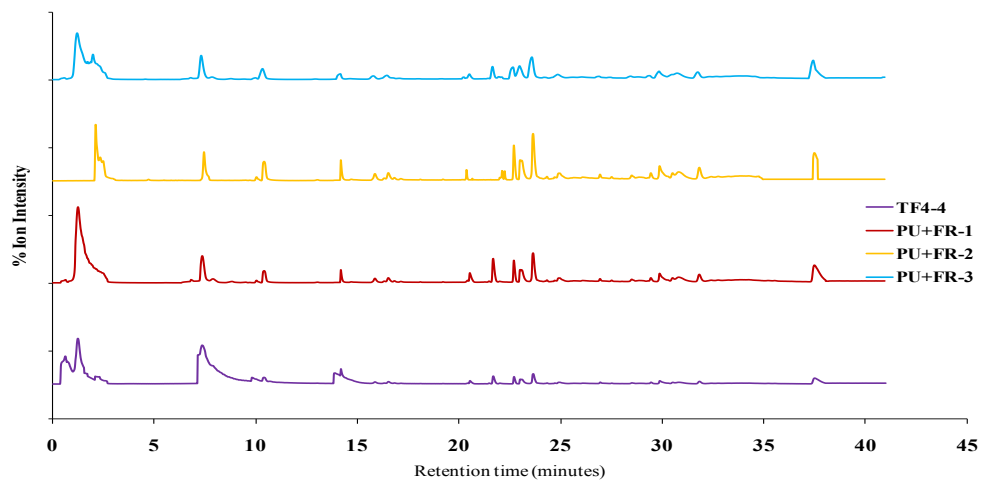


Figure 121 GC/MS for material from Carboxen tubes used for 3 replications of mixed Polyurethane foam burns and a TF4 Emulsion in UCLan 2 m<sup>3</sup> Enclosure

### 4.8.2 Overheating PCBs in UCLan Enclosure

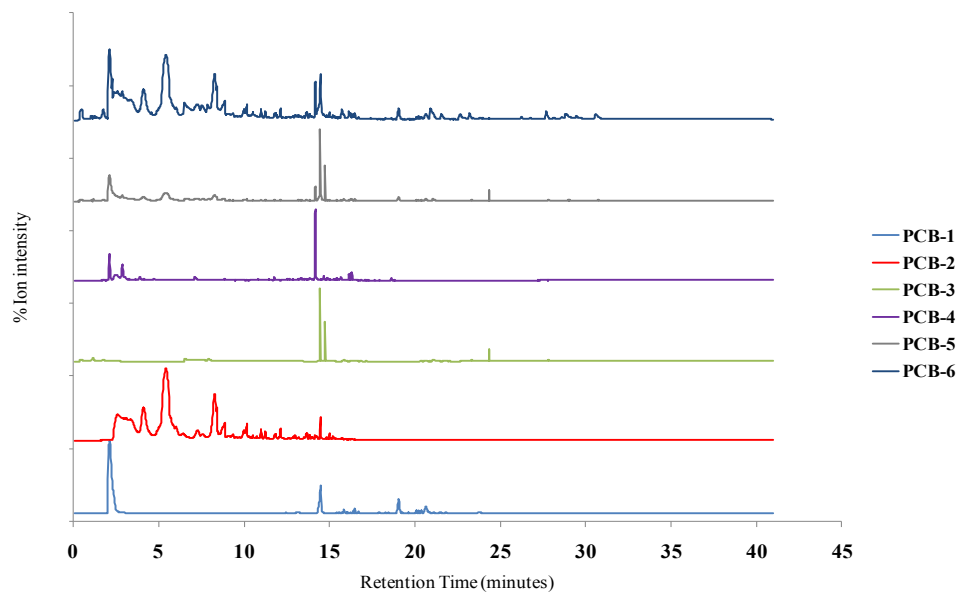


Figure 122 GC/MS Chromatograms for material from Carboxen tubes used for 6 replications for Overheated PCBs in UCLan 2 m<sup>3</sup> Enclosure

### 4.8.3 Overheating Polymer Coated Wire in UCLan Enclosure

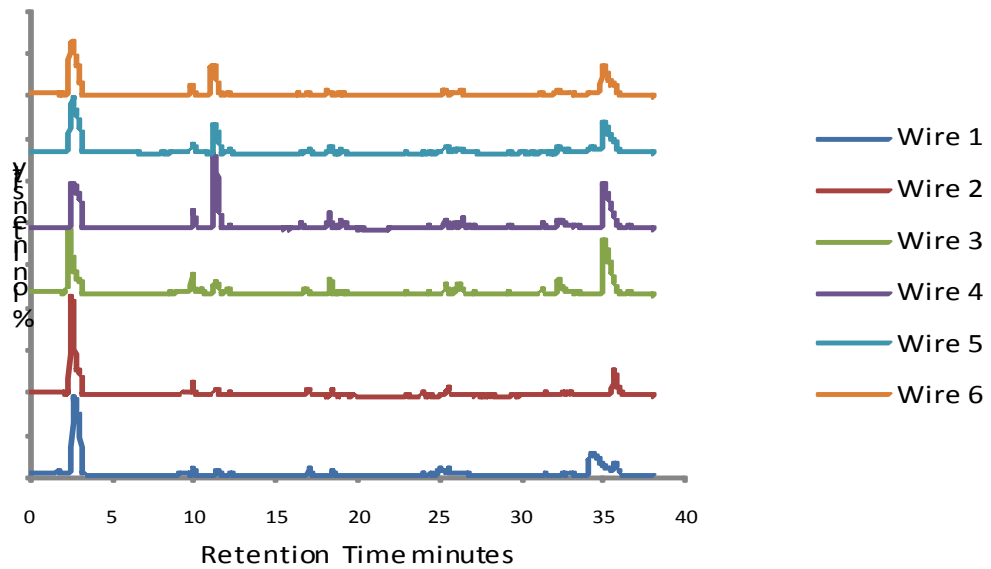


Figure 123 GC/MS Chromatograms for material from Carboxen tubes used for 6 replications for Overheated Polymer Coated Wire in UCLan 2 m<sup>3</sup> Enclosure

### 4.8.4 Overheating Cooking Oils in UCLan Enclosure

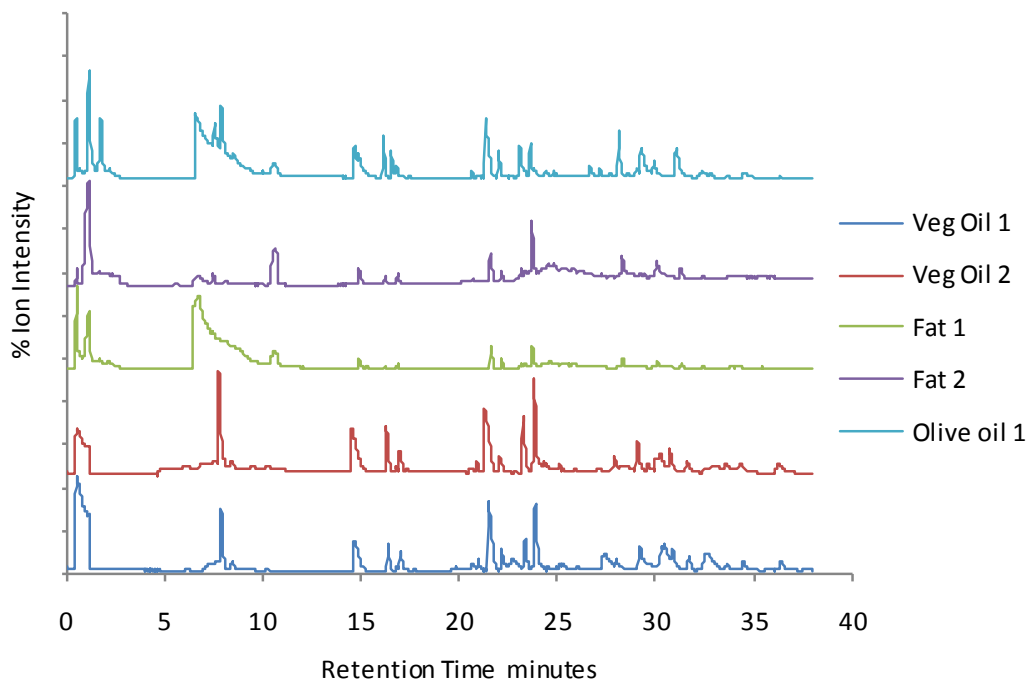


Figure 124 GC/MS Chromatograms for material from Carboxen tubes used for overheating Cooking Oil tests in UCLan 2 m<sup>3</sup> Enclosure

#### 4.8.5 Bread Toasting and Re-Toasting in UCLan Enclosure

As described in chapter 3, experiments on toasting single slices of bread were carried out in a commercially available domestic toaster and as a single toasting operation did not yield sufficient smoke to cause any detector alarms, each slice was subjected to a second and third toasting operation. Samples were collected on absorbent media for each toasting and Figure 126 below shows the results for GC of Carboxen absorbed samples from 1<sup>st</sup>, 2<sup>nd</sup>, and 3<sup>rd</sup> toasting on three slices of bread. It was apparent that water emissions from the bread were a significant factor and further tests were carried out where the content of the absorption tubes was dried by passing through dry nitrogen for 15 seconds. Figure 126 shows GC results for 2<sup>nd</sup> toasting of six slices where the Carboxen containing absorption tubes for three had been treated as normal (not dried) and for another three which had been subjected to the drying process. Figure 127 shows results for Tenax absorption tubes used for sample collection from 2<sup>nd</sup> toasting of six slices.

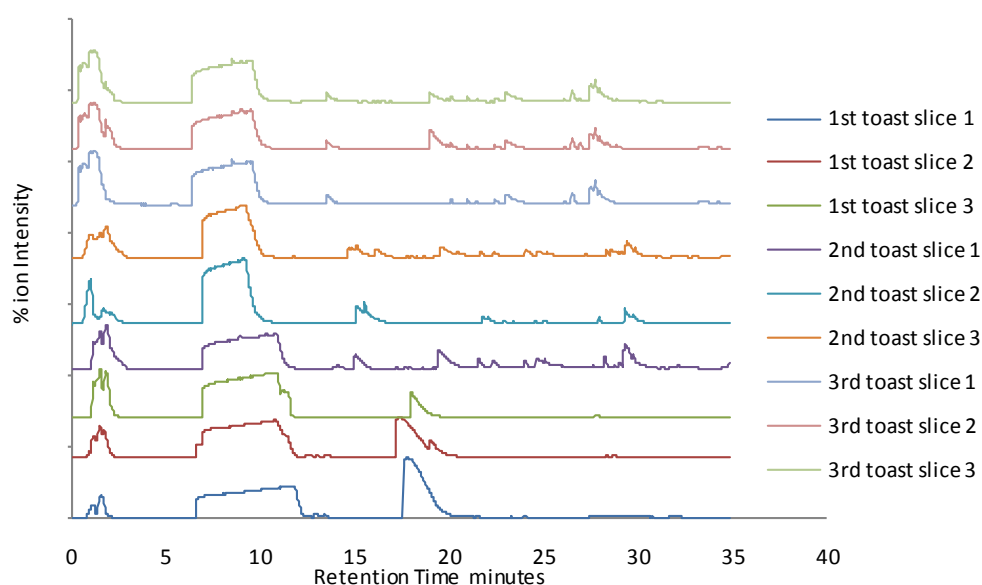


Figure 125 GC/MS Chromatograms from Carboxen tubes used for 1<sup>st</sup>, 2<sup>nd</sup>, and 3<sup>rd</sup> Toasting operations replicated with 3 bread slices in UCLan 2 m<sup>3</sup> Enclosure

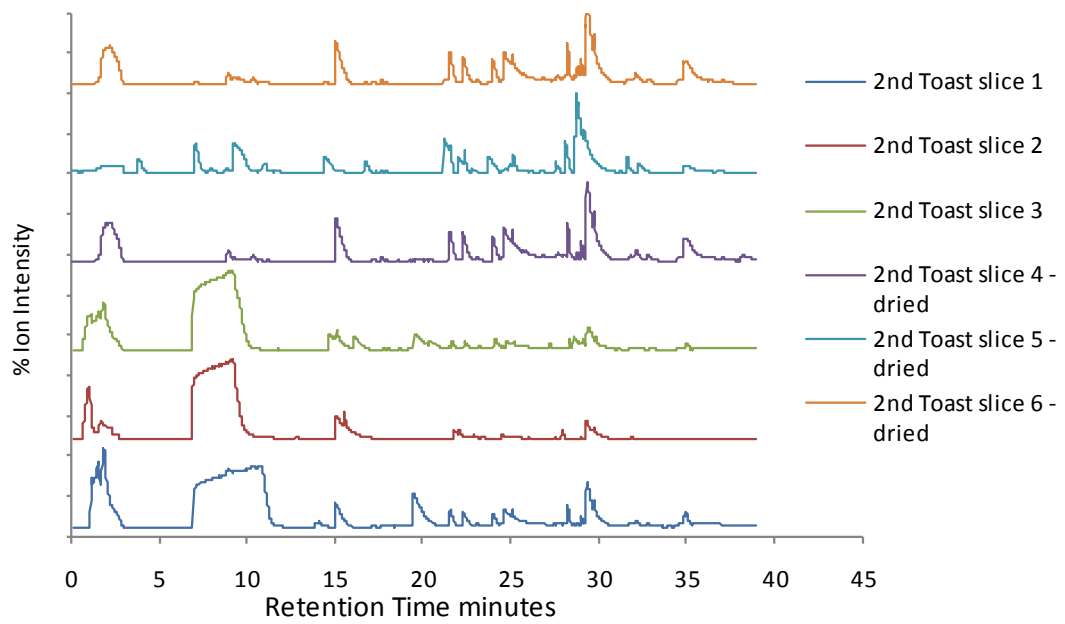


Figure 126 GC/MS Chromatograms from Carboxen tubes used for 2<sup>nd</sup> Toasting operation in UCLan 2 m<sup>3</sup> Enclosure, with drying applied to absorbent media for slices 4, 5, and 6

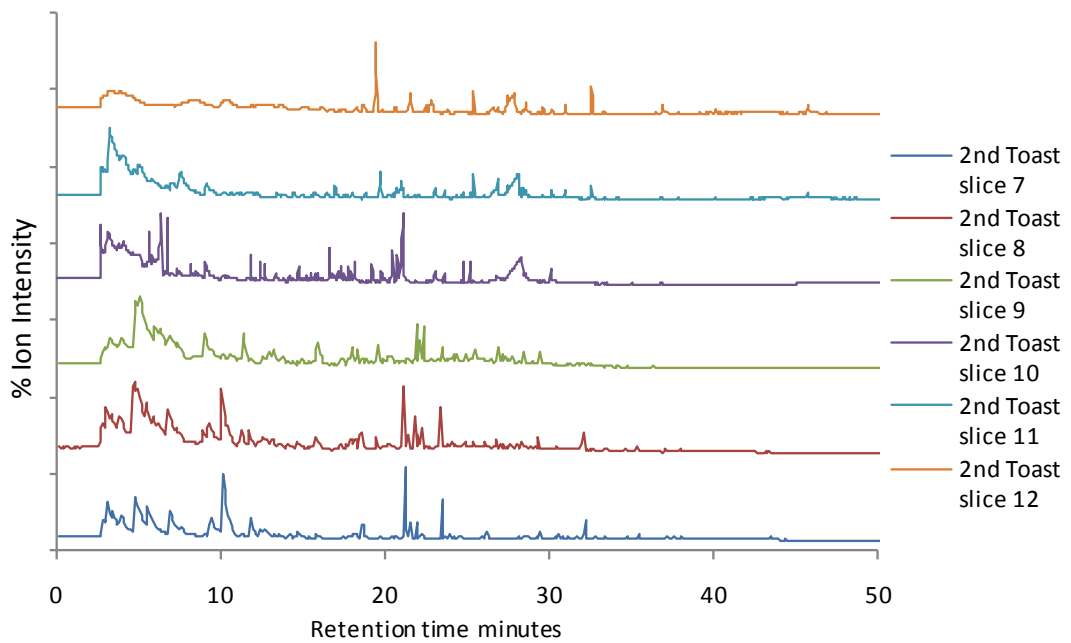


Figure 127 GC/MS Chromatograms for Tenax tubes used for 6 replications of 2<sup>nd</sup> Toasting of Bread Slices in UCLan 2 m<sup>3</sup> Enclosure

## CHAPTER 5 INTERPRETATION OF GC-MS RESULTS

### 5.1 MS Spectra Analysis Processes

The GC/MS chromatograms yield retention time peaks, which if well defined against background may correspond mainly to a single species or at least a non complex mixture. A number of techniques can be applied to mass spectrometer spectra to derive information from the spectra as to the amounts and identities of the species separated by GC. Selecting a well-defined elution peak and viewing the corresponding mass/ charge spectrum can allow identification of species from the ion masses and fragmentation pattern. This section briefly covers how methods applied to the MS data acquired in this study and how produced the species identifications shown in tables provided for a number of fire tests. Further the section covers why some elution peaks were not susceptible to analysis and so have not been labelled or discussed in detail.

Firstly some of the terms used in this chapter and that are prevalent in the literature are covered. Figure 128 represents a typical mass spectrum providing a visual representation of a probability distribution of ions arising from one source species.

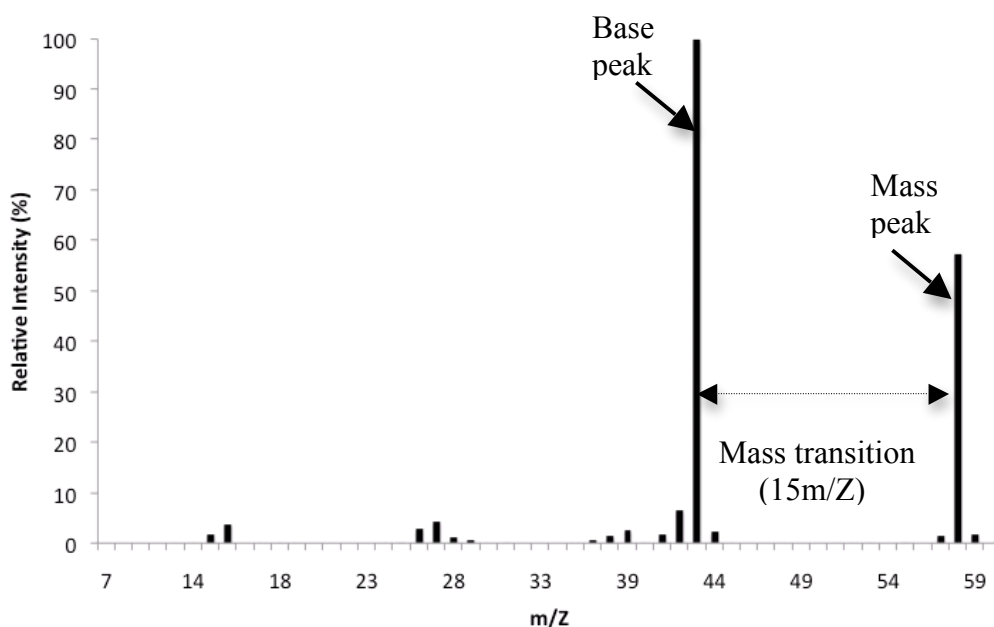


Figure 128 Example chromatogram

The axes are the mass to charge ratio of the ions and the relative intensity of the total ion current.

Given that all the experiments in this study were carried out in typical electron ionization conditions (-70eV), then it is normal to expect to see only singular charged ions so  $m/Z$  is taken used as the mass of the ion.

The other terms used in figure 128 and in tables within this chapter are the base ions and the mass ions.

The mass ion is the parent ion of the molecule being analyzed. These are typically the largest ion though in EI spectra the mass ion commonly not seen in high abundance as the parent is decomposed in the ionization process. This is particularly true where the analyte molecule contains oxygen or other hetero ions as decomposition into fragments is more energetically favorable. This study involves oxidation of hydrocarbons and so compounds containing oxygen molecules are to be expected. However based on the range of processes and pathways in fuel pyrolysis and combustion it is also to be expected that a range of saturated and unsaturated hydrocarbons may present.

The base ions represent the most common fragment favorably produced in the ionization process. The base peak provides information about the type of analyte present. Where the base peak is the same as the mass peak then the parent ion is typically a heterocyclic or conjugated system, which is difficult to ionize.

The occurrence of particular ions and distribution in spectra also give clues as to the typical composition of an unknown by the size and regularity of the transitions. For example:

- Clusters between  $m/Z$  36-43 are indicative of 3 carbon groups in fuels consisting mostly of carbon and hydrogen.
- Fully saturated hydrocarbons are indicated by mass ions at 15 ( $\text{CH}_3$ ) 29 ( $\text{C}_2\text{H}_5$ ), 43( $\text{C}_3\text{H}_7$ ), 57( $\text{C}_4\text{H}_9$ ) etc.
- Molecules with benzene at the core will typically produce an ion at 77 and 51 $m/Z$ , which corresponds to phenylium ion and resulting loss of acetylene. The addition of Alkyl chains to the benzene core will result in a major peak at 91 $m/Z$ , which is a mixture of benzylium and tropylium structures. The loss of the alkyl chain in this instance results in a fragment at 65 $m/Z$ .
- Transitions of 15 $m/Z$  units is indicative of the loss of a  $\text{CH}_3$  group, a difference between two ions of 29 $m/Z$  units would indicate the loss of a  $\text{C}_2\text{H}_5$  ion etc .  
Small mass losses may be explained by occurrence of simple rearrangements.

The formation of fragments occurs as a result of one of 5 fragmentation rearrangements that occur following ionization as proposed by McLafferty [130] proceeding in accordance to specific energy rules [131]. There are however impossible or forbidden transitions that do not correspond to the loss of any reasonable fragments from a given species. The presence fragments corresponding to apparently forbidden transitions, especially between prominent mass peaks, suggest there is a mixture of analytes. Where there are mixtures of more than a few co eluting analytes it is very difficult to obtain a positive identification for any of the components and this is a major issue in fire gases analysis, especially for the larger molecular weight samples where significant co-elution of captured species occurs.

There are a number of tools available to aid GC/MS analysis. The main methods used in this chapter involved library matching using the NIST 05 [132] data library, software manipulation with AMDIS [133], elemental mass analysis, fragmentation analysis, isotope analysis and examination of the structural properties.

### **5.1.1 Unlabeled and unknown peaks**

The initial peak in the chromatographs equivalent to the dead volume are unretained components. In the Tenax fire analysis samples the unretained peak make up many of the gases (<C6). This is the cut off for the resin and consists of permanent and semi

permanent gases, although Tenax is has a very low affinity for moisture. Carboxen samples on the poroplot Q column have a lower cut off (<C2) but the permanent gases are too volatile to be resolved at normal operating conditions. Cryo focusing may have allowed us to look closer at the high volatility gases, many are already known and well studied in fire systems (e.g. CO/CO<sub>2</sub>), but in the case of Carboxen samples would have provided more problems in terms of the removal of moisture.

Results presented for bread toasting shows how moisture can significantly affect the chromatograms and the ability to identify components in smoke. This can be countered by some post sampling manipulation including passing dry gas through the resin.

Given the range of possible mixtures arising in uncontrolled and incomplete combustion processes, the occurrence of elution peaks yielding MS spectra that cannot be reasonably de-convoluted to provide identification is not surprising. Background, contamination and artifact peaks and mixtures are responsible for these peaks. However ion mass ranges observed at least put some limits on the likely range of components. Simple mixtures and samples with significant background contamination can be resolved using mass spectra tools such as AMDIS. AMDIS (Automated Mass Deconvolution and Identification System) is an automated program provided by NIST as an compliment to their mass spectra tools which is an advanced library matching. AMDIS scans and removes a mathematical algorithm that relates to the background in any given spectra. AMDIS then matches the resultant spectra with the NIST library. AMDIS was used extensively in the analysis of Tenax samples.

### **5.1.2 Library matching acquired spectra**

Where peaks are not too difficult to resolve a library matching procedure may be used as follows. This is used for identification of some of the major components of standard and non standard fires. Library matching is one of the most commonly utilized tools in mass spectra analysis. Because mass spectra are generated in standard conditions under a high vacuum a series of standard libraries of spectra for compounds has been generated and distributed by standards, instrumentation and publishing organizations. The library used for this study was the Wiley NSIT 05 library but others are available.

Library matching works by describing the molecule mathematically based on the intensity of the largest peaks. The mathematical expression is then compared to the unknown, and the match is rated to how close the unknown is to the standard. The unknown is then ranked by two values the F, or forward fit number and the R or reverse fit number. The F fit is a measure of how well the unknown fits into the standard spectra and the R fit is a measure of how well the standard fits in the unknown spectra. The R fit is sometimes preferentially used in complex mixtures because it discounts more of the background.

Most of the discussion thus far has focused on the identification of the components observed in the low mass range. The same principles were used for the Tenax samples and the data is presented in the tables in chapter 5. Library matching is more important for larger molecules as the spectra become more and more complex, especially in mixtures.

### **5.1.3 Mass analysis**

Mass analysis is based on the exact masses of the elements concerned. By knowing the exact mass of an ion the elemental composition or empirical formula can be derived. Typically there are calculators [134] that can be used to calculate the formula based on known information of masses and expected composition. For example we consider the fuels used in TF3 fires have a composition of C, H and O. Using this information the mass ion the chromatograph displayed as peak V may be identified with benzene.

The exact mass of the peak listed at 78m/Z taken from the instrument listing is 78.118. The elemental composition calculated from this mass can be calculated as the possibilities in table 28 below:

<i>Elemental composition</i>			<i>PPM</i>
<i>C</i>	<i>H</i>	<i>O</i>	
6	6	0	271.0
5	6	1	714.1
4	2	2	1157.3
3	4	1	456.8
2	0	2	900.0
0	8	3	1343.2

Table 28 Elemental analysis based on the exact masses of the elements involved in the potential structure 78 m/Z ion in peak C . The best match is C<sub>6</sub>H<sub>6</sub> with the smallest deviation from the theoretical mass. The PPM in this case does not relate to gas concentration but is a parameter related to the deviation of the measured mass from the expected mass.

With information available on the empirical formula further information may be derived concerning the number of saturations. If the number of hydrogen atoms in a hydrocarbon (x) can be expressed as ;

$$x = 2n+2-2N_i \quad (26)$$

Equation 26 Where N<sub>i</sub> is the number of saturations and n is the number of carbons.

This can be rearranged to give:

$$N_i = (2n+2-x)/2 \quad (27)$$

Equation 27 re-arrangement of equation 26

Hetero atoms like oxygen and sulfur both replace hydrogen atoms and reduce the hydrogen by the same effect and so do not factor into the calculations. Substituting the values from table 26 in equation 26 generates the results shown in Table 28.

Empirical formula	Number
Carbon	6
Hydrogen	6
<b>Number of saturations (Ni)</b>	<b>4</b>

Table 29 Calculated number of saturations + ring structures in the empirical formula derived from the analysis of the exact mass in table 4 using the formula

With this additional information the proposed identification can be referred back to the

library match and this can be used to validate the observations. Ni 4 is equivalent to 3 saturations and 1 ring structure or numerical algorithm thereof, which is not conclusive evidence the peak identified as peak V is benzene but is consistent given the other evidence. Linear C<sub>6</sub>H<sub>6</sub> molecules with two triple bonds or one triple bond and two double bonds can meet the criteria but are less likely and more reactive candidates.

#### **5.1.4 Fragmentation analysis**

The formation of fragments occurs as a result of one of 5 fragmentation rearrangements that occur following ionization. These are most commonly associated with McLafferty [135] and proceed in accordance to specific energy rules.

Looking at the chromatograms, one of the more common peaks occurs around 31 minutes has been identified as peak V, benzene in the scaled BS EN standard fires and several of the other scaled fires and in the full scale fire room tests. Comparing the acquired spectrum from TF3 fire, the ions represent specific transitions in an ionization fragmentation reaction. For benzene the fragmentation reaction is given in figure 129.

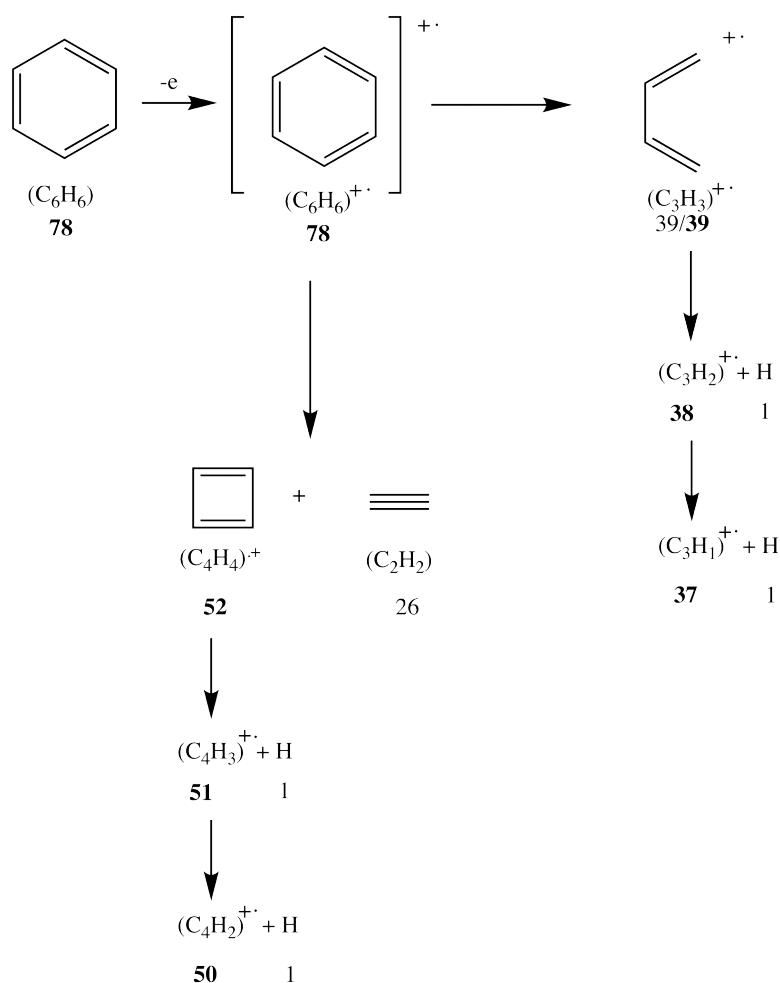


Figure 129 Fragmentation pattern for benzene

### 5.1.5 Isotope analysis

Sometimes the library match throws up matches, which we struggle to explain. For example the peak identified as peak D in TF2 fires produces a strong sulfur dioxide identification match (figure 130). Given what we know of the wood used in the experiment it is unlikely to be an element produced by the thermal decomposition of the fuel. The immediate response was it could quite simply be contamination but we took several steps to eliminate any potential contamination root. These included changing the collection resin, sample tubing and other checks. But it was found that it only appeared in specific fuel tests and it was a persistent peak in the analysis of those fuels. Therefore we considered it could be an oxidation of environmental sulfur.

We can check the identity of the peak by examining the isotope ratio. Each ion is related to the mass of the elements that it is composed of. In some cases elements are present in

more than one isotope such sulfur which is present in  $^{32}\text{S}$  and  $^{34}\text{S}$ . Using this in sulfur dioxide we would see peaks at 64 ( $^{32}\text{S} + ^{16}\text{O} + ^{16}\text{O}$ ) and 66 ( $^{34}\text{S} + ^{16}\text{O} + ^{16}\text{O}$ ) in approximate 97:4 ratio.

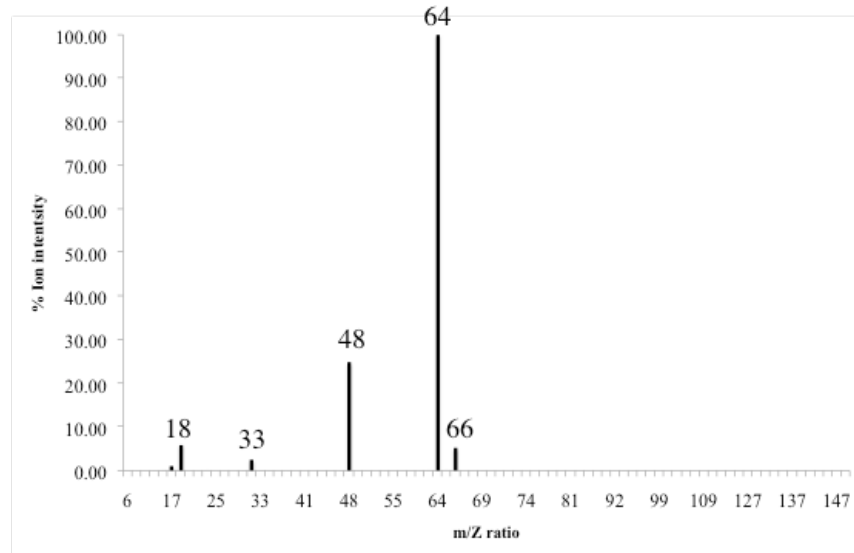


Figure 130 Example of chromatogram taken from flaming polyurethane fire peak

Examining the intensity of the ions in the spectra at 64 and 66 the ion ratio is given as 95.9:4.9 , which is comparable to the desired ratio in the limitations of the measurement equipment .

## 5.2 Analysis of GC/MS from Test Fires

The purpose of this chapter is to identify the key components identified from each fire conditions studied both in the scaled fire enclosure at UCLan and where appropriate in other environments including full scale fire experiments at BRE.

As shown in chapter 4 there are some fires, which seem to show a great deal of reproducibility with clear patterns being observed. In other experimental conditions there is an apparent lack of commonality between fires and the purpose of chapter 4 was to highlight these patterns or lack there of.

In this chapter a single representative chromatogram is presented for each fire condition along with some identification of components. Where appropriate each fire condition is represented by two chromatograms for large and small fire components. The small components were captured on Carboxen 1000 air sampling tubes and eluted onto a poroplot Q column and these represent the gases we had the most interest. The Carboxen results are presented first in section 5.3 and the Tenax results are presented in section 5.4.

### **5.3 Examples of Carboxen and poroplot Q chromatograms**

This section presents chromatograms from different test fires and tabulated data showing masses of major ions corresponding to identified and labelled GC peaks. Unlabelled peaks are typically unresolved and suffer from high background levels and are therefore not discussed further.

The methods used for identification of each best match as described in section 5.1. Where possible within a section common gases share common identification letters. For example for the TF2 fire, peak H has the best match of furan, and this is also true for TF3 fires. However the nomenclature does not carry between sections because of the large number of components. The tables hold the mass ions of the most dominant species identified in the peaks labelled. Unlabelled peaks are typically unresolved and suffer from high background levels and are therefore not discussed further.

## 5.3.1 BS EN 54-7 Standard fires – products captured on Carboxen

### 5.3.1.1. Smouldering wood (TF2 Emulation)

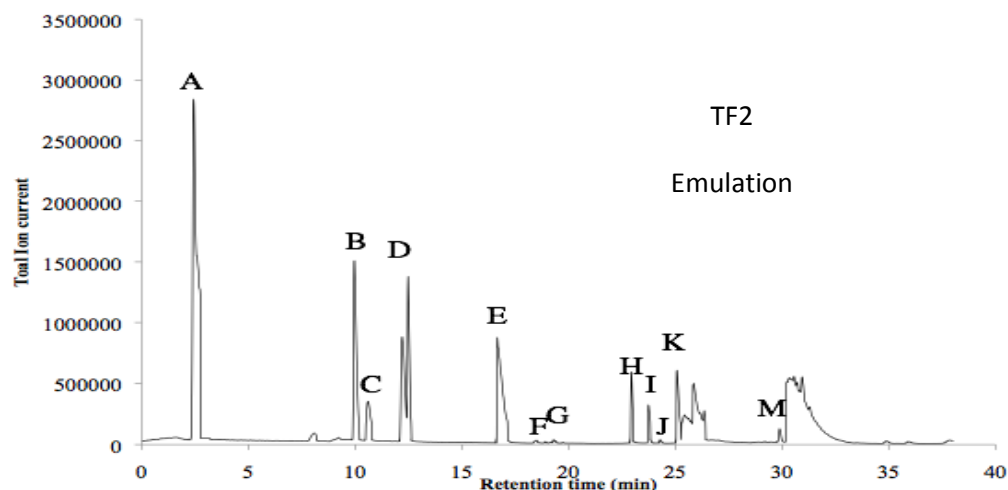


Figure 131 Representative chromatogram for Carboxen captured sample from smouldering wood TF2 emulation in UCLan enclosure. Corresponds to sect. 4.6.1, TF2-2.

Peak ID	Base Peak	Other mass ions (m/Z)	Best match
A	45	40,32,28,18	Unretained
B	41	44,43,29,28,15	Propene
C	44	46,45,31,29,27	Ethylene oxide
D	64	66,48,32,28	Sulphur dioxide
E	28	44,32,31,14	Acetaldehyde
F	41	56,55,53,51,39,28,19	Cyclobutene
G	68	80,64,56,53,49,41,39,30,29,28,19	Unknown
H	41	68,40,39,38,32,28	Furan
I	43	93,72,53,52,51,43,42,29,26,19,16,15	Butanal *
J	43	58,42,29,28,27,26,19,16,15	Acetone
K	28	58,43,32,15	Propene oxide
L	43	74,59,46,45,29,15	Methyl acetate
M	78	79,77,52,51,50,39	Benzene

Table 30 The Mass ions corresponding to peaks A-M from the chromatogram for smouldering wood fire (TF2 Emulation) displayed in Figure 131 .

### 5.3.1.2 Smouldering cotton (TF3 Emulsion)

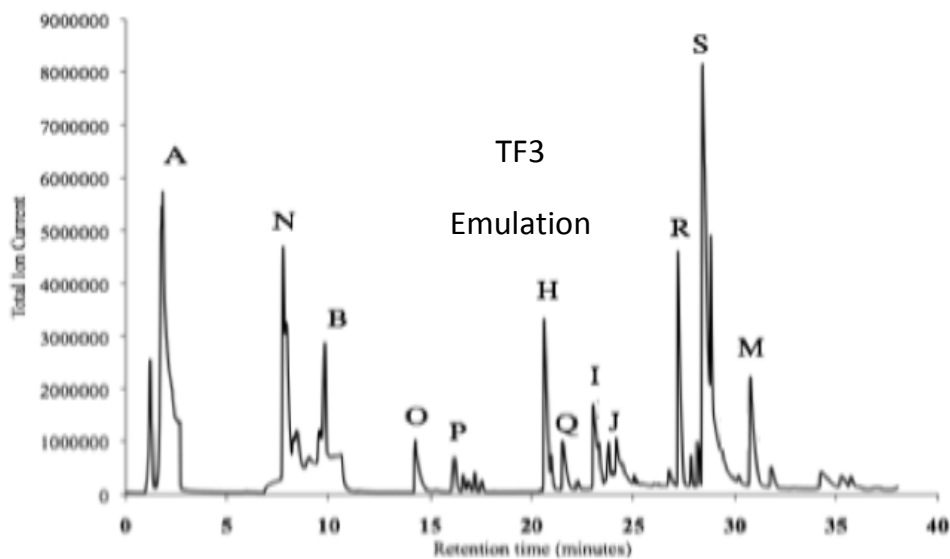


Figure 132 Representative chromatogram for Carboxen captured sample from smouldering cottonwood TF3 emulsion in UCLan enclosure. Corresponds to sect. 4.6.2, TF3-4.

Peak ID	Base Peak	Other mass ions (m/Z)	Best match
A	28	47,45,46,44,43	Unretained
N	41	43,42,40,39,27	Cyclopropane
B	41	44,43,39,40,15	Propene
O	41	40,39,27,26,12,11	1,2-Propadiene
P	41	56,55,39,28,27	Butene
H	41	68,41,39,27	Furan
Q	56	55,53,37,29,28,27,19	2-Propenal
I	28	72,53,52,51,43,29,26,16	Butenal *
J	43	58,42,29,27,16	Acetone
R	82	83,81,53,39,27	2 Methyl furan
S	87	68,67,45,44,42,41,39,27,26,16	2-Butanoic acid*
M	54	79,77,52,51,50,39	Benzene

Table 31 The peaks IDs in the table represents the mass ions corresponding to the peaks A-O from Figure 132

### 5.3.1.3 Flaming Polyurethane (TF4 Emulation)

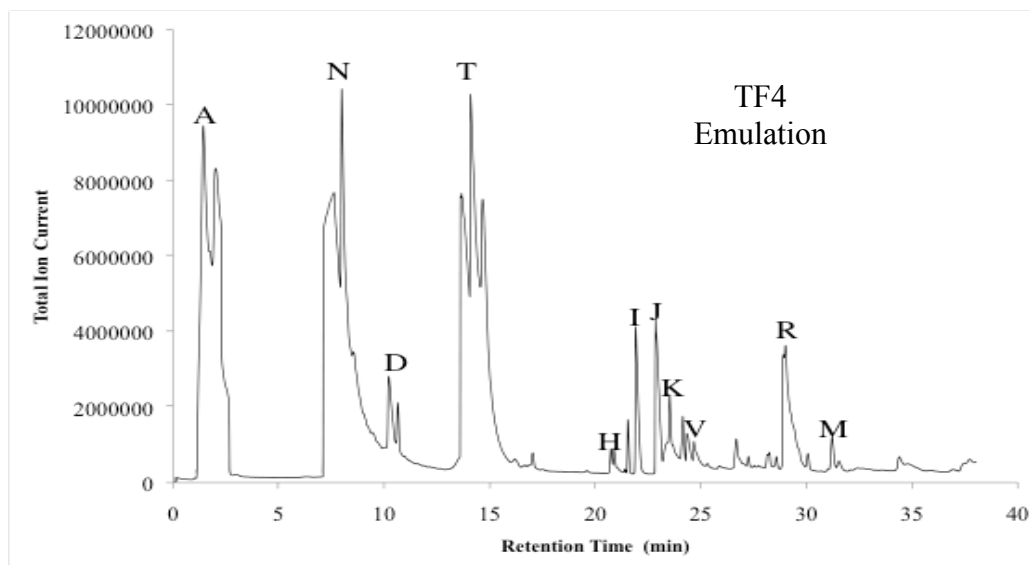


Figure 133 Representative chromatogram for Carboxen captured sample from polyurethane foam burn TF4 emulation in UCLan enclosure. Corresponds to sect. 4.6.3, TF4-3.

Peak ID	Base Peak	Other mass ions (m/Z)	Best match
A	28	45,47,46,44,43	Unknown
N	41	43,42,40,39,27	Cyclopropane
D	64	66,48,32,28	Sulphur dioxide
T	16	40,26,17	Unknown
H	41	68,41,39,27	Furan
I	56	55,53,37,29,28,27,19	2-Propenal
J	43	58,42,29,27,16	Acetone
U	43	74,59,51,29,16	Acetol
V	46	45,44,29,18	Formic acid
R	82	83,81,53,39,27	2 Methyl furan
M	78	77,52,51,50,	Benzene

Table 32 The peak ID corresponds to the peaks in the chromatogram shown in Figure 133, relating to the scaled flaming polyurethane fire (TF4)

### 5.3.1.4 Flaming heptane (TF5 Emulation)

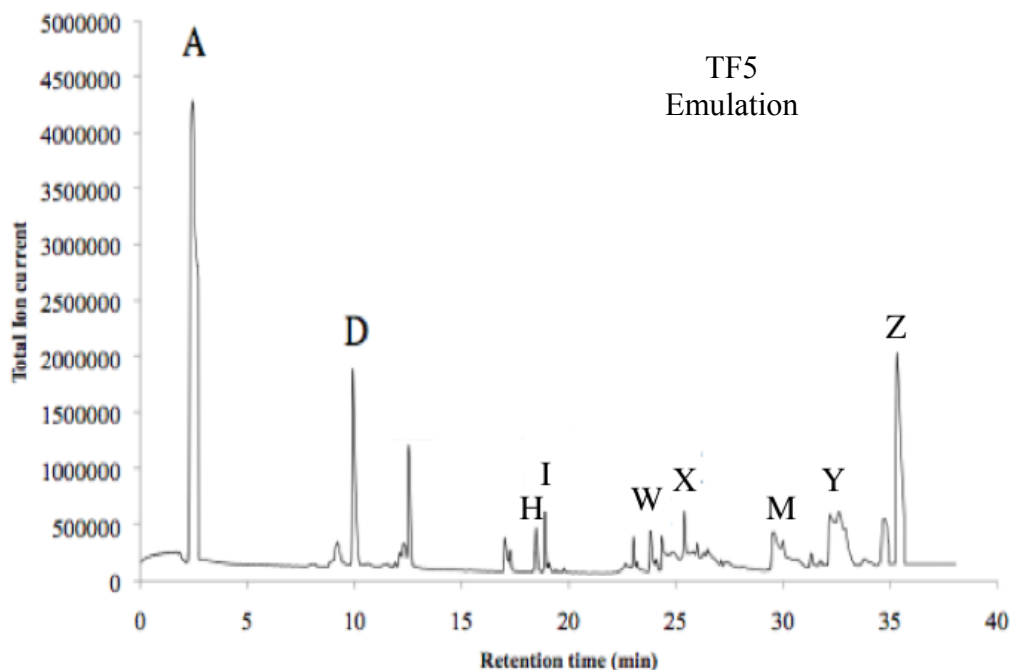


Figure 134 Representative chromatogram for Carboxen captured sample from flaming heptane TF5 emulation in UCLan enclosure. Corresponds to sect. 4.6.4, TF5-2.

Peak ID	Base Peak	Other mass ions (m/Z)	Best match
A	28	45,47,46,44,43	Unretained
D	64	66,48,32,28	Sulphur dioxide
H	41	68,39,27	Furan
I	29	56,55, 39,38,37,29,27	2-Propenal
W	43	70,58,55,42,32,28	Unknown
X	28	72, 68,67,57,55,43,42,41,32	Pentane
M	54	79,77,52,51,50,39	Benzene
Y	29	71,57,56,41,32,28	Unknown
Z	28	72,68,67,57,55,43,42,41,39,32,29,27	2-Butanal

Table 33 The peak ID corresponds to the peaks in the chromatogram shown in Figure 134, relating to the scaled flaming pool fire (TF5)

## 5.3.2 UL268 Scaled fires – products captured on Carboxen

### 5.3.2.1 Smouldering paper fires (UL268 fire A Emulation)

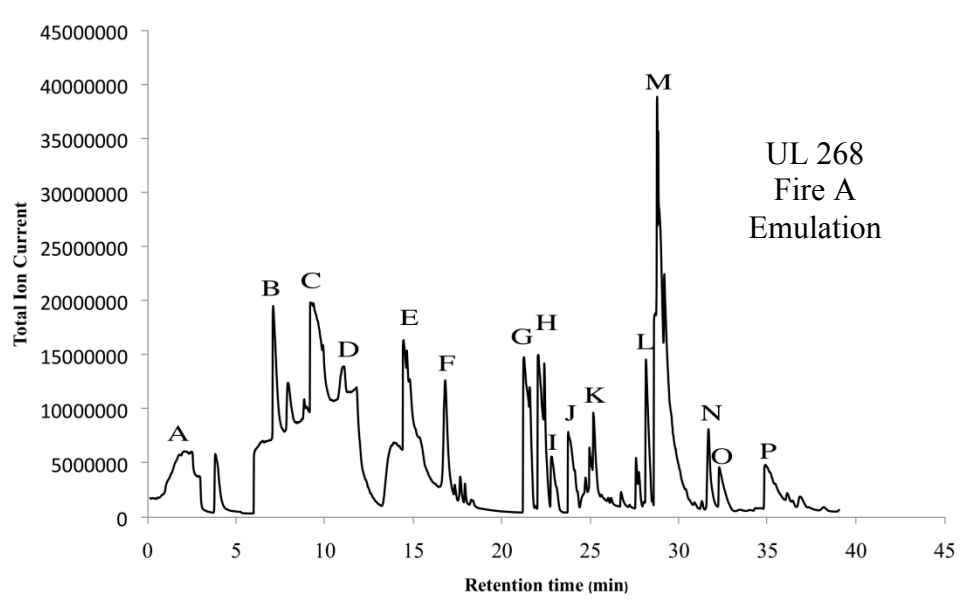


Figure 135 Representative chromatogram for Carboxen captured sample from paper fire UL268 fire A emulation in UCLan enclosure. Corresponds to sect. 4.6.6. The paper used in this experiment was sourced from the local UCLan free newspaper and the paper density was given as 48gsm. The peaks A-P are identified in table 32.

Peak ID	Base Peak	Other mass ions (m/Z)	Best match
A	60	44,32,30,28	Unretained
B	41	44,42,40,39,38,27	Propene
C	48	66,64,50,32	Unknown
D	19	66,64,48,39,32	Sulphur dioxide
E	44	43,42,41,30,29	Propane
F	31	56,55,41,39,32,29	Butene
G	39	69,68,54,42,40,29	Furan
H	56	55,37,29,28,27,26	2-Propenal
I	78	76,63,52,52,50,44,39,38,32,27	Butadienykacetylene
J	41	70,69,42,40,39,38,37,29	Methyl propenal
K	82	81,54,53,43,39,38,29,28,27	2-Methyl furan
L	55	82,81,70,53,39,27	Unknown
M	78	86,77,48,52,51,50,39,30,29	Divinylacetylene
O	78	77,58,52,51,50,39,30,29	Benzene
P	41	69,41,39,29	Unknown

Table 34 The peak ID correspond to the peaks in the chromatogram shown in Figure 135, relating to the scaled representation of the smouldering paper fire based on the UL268 standard fire (Fire A)

### 5.3.2.2 Flaming wood fire (UL268 fire B Emulation)

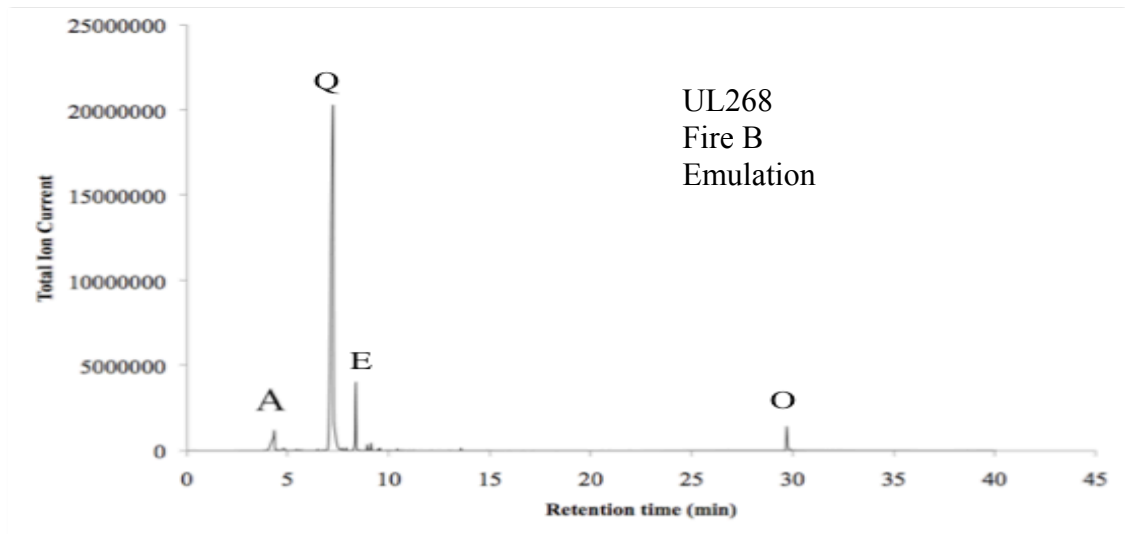
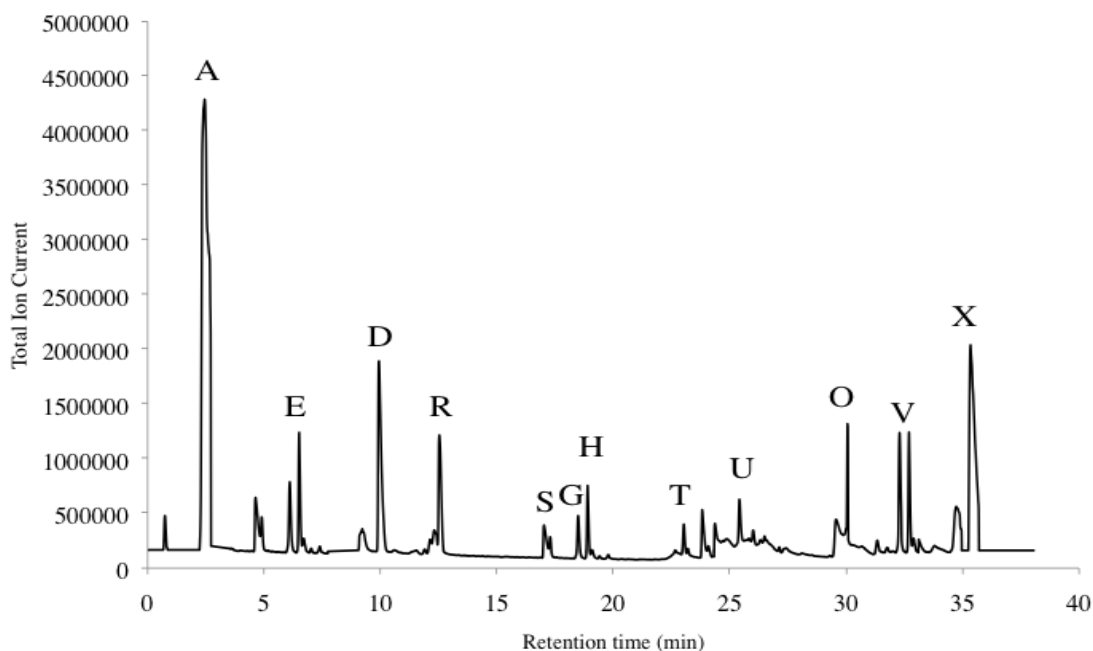


Figure 136 Representative chromatogram for Carboxen captured sample from flaming wood UL268 fire B emulation in UCLan enclosure. Corresponds to sect. 4.6.7.

Peak ID	Base Peak	Other mass ions (m/Z)	Best match
A	44	28,22	Unretained
Q	41	42,40,39,27,26	Cyclopropane
E	41	42,40,39,38,37	Propene
O	78	77,52,51,50	Benzene

Table 35 The peak ID correspond to the peaks in the chromatogram shown in Figure 136, relating to the scaled representation of the flaming wood fire described in the UL268 standard (Fire B)

### 5.3.2.3 Burning pool fire : Heptane (UL268 fire C emulation)



Peak ID	Base Peak	Other mass ions (m/Z)	Best match
A	44	45,47,46,44,43	Unretained
D	64	66,48,32,28	Sulphur dioxide
R	68	44,43,42,26,15	Ethylene oxide
S	28	46,45,28,17,16	Formic acid
E	29	45,44,42,41,39,29,18	Propane
G	39	69,68,54,42,40,29	Furan
H	28	56,55,41,40,29,27,26	2-Propenal
T	43	58,42,49,29,27,16	Acetone
U	28	72, 68,67,57,55,43,42,41,32	Pentane
O	78	77,58,55,42,41,40,32,28	Benzene
V	44	102,98,77,63,52,51,28	Unknown
X	64	72,68,67,57,55,43,42,41,39,32,29,27	2-Butenal

Table 36 The peak ID corresponds to the peaks in the chromatogram shown in Figure 137, relating to the scaled representation of the flaming pool heptane fire of the UL268 standard fire (Fire C)

### 5.3.3 Full scale BS EN 54 Fire tests– products captured on Carboxen

#### 5.3.3.1 Smouldering wood (TF2)

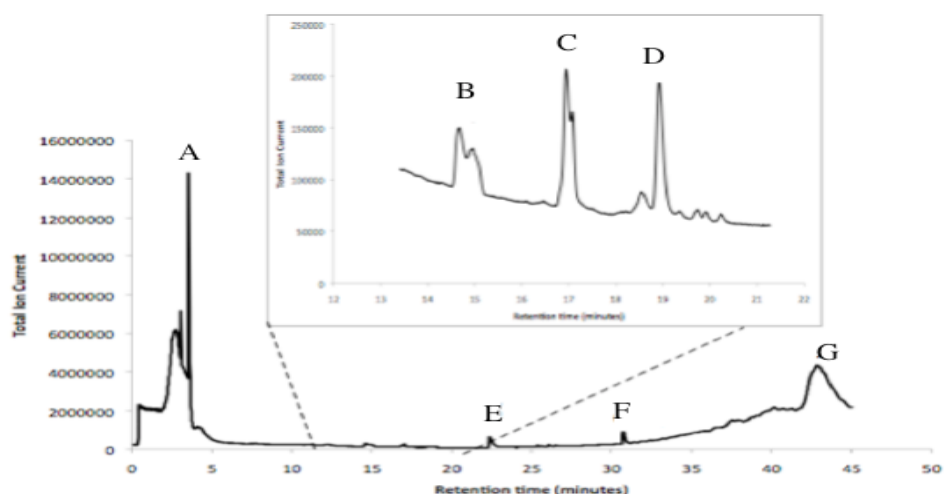


Figure 138 Chromatogram for Carboxen captured sample from smouldering wood TF2 fire at BRE.

The sample collected included a series of small peaks that are included in the magnified section, highlighting the above baseline significance.

Peak ID	Base Peak	Other mass ions (m/Z)	Best match
A	29	28,40,32,18	Unretained
B	31	31,32,29,15	Methanol
C	29	44,43,42,15,28	Acetaldehyde
D	68	42,40,38,27,29	Furan
E	43	60,45,42,29,15	Acetic acid
F	78	77,58,55,42,41,40,32,28	Benzene
G	74	75,73,55,56,57,45,30,29,58	Propionic acid

Table 37 Identified components from the spectra shown in figure 138 taken from the full scale BRE smouldering wood fire (TF2) .

In the magnified section there are a series of small gases that could be clearly observed above the baseline which are identified here.

### 5.3.3.2 Smouldering cotton fire (TF3)

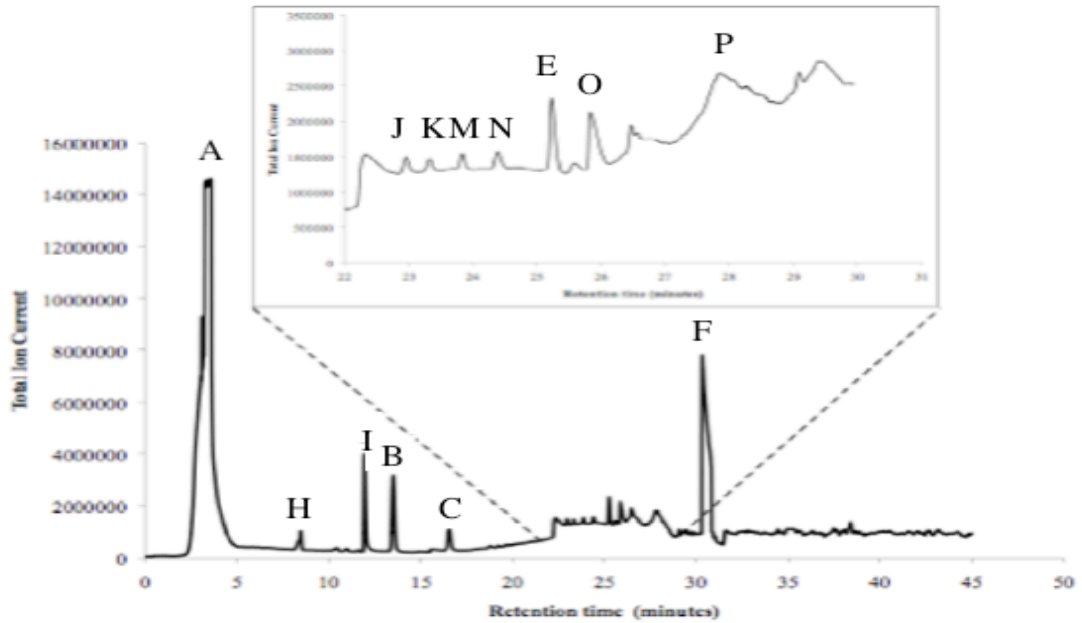


Figure 139 Chromatogram for Carboxen captured sample from smouldering cotton TF3 fire at BRE.

The magnified section between 22 and 28 minutes show the minor hydrocarbon peaks present in the cotton smoke.

Peak ID	Base peak	Other mass ions (m/Z)	Best match
A	32	28,40,32,18	Unretained
H	41	44,42,40,39,38,27	Propene
I	64	66,48,32,28	Sulphur dioxide
B	31	32,29,15	Methanol
C	29	44,43,42,15,28	Acetaldehyde
J	31	45,44,43,29,27	Ethanol
K	41	40,39,27,28,18,15,14	Acetonitrile
M	43	58,42,29,27,16	Acetone
N	29	46,45,44,43,28,17,16	Formic acid
E	43	60,45,44,42,41,29,15	Acetic acid
O	43	88,73,70,61,45,29,27	Ethyl acetate
P	41	42,45,60,29,15	Unknown
F	78	77,58,55,42,41,40,32,28	Benzene

Table 38 Identified components from the spectra shown in Figure 139 taken from the full scale BRE smouldering cotton fire based on the BS EN 54 standard fire (TF3).

### 5.3.3.3 Flaming polyurethane (TF4)

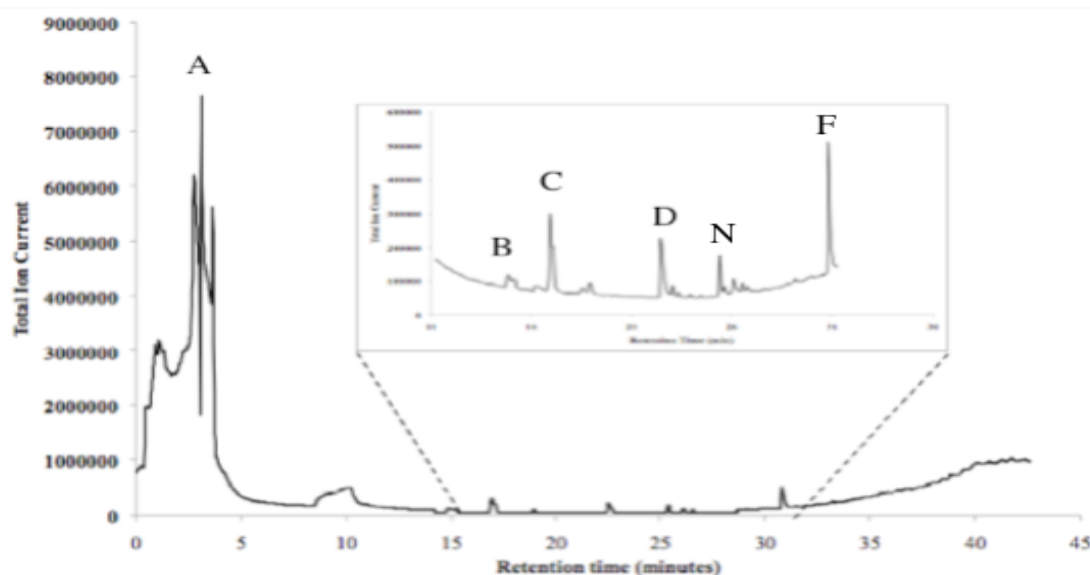


Figure 140 Chromatogram for Carboxen captured sample from polyurethane foam burn TF4 fire at BRE

The gases were collected on Carboxen sample tubes and the section between 15 and 31 minutes was expanded to show the above baseline significance of the peaks A-F and N.

Peak ID	Base peak	Other mass ions (m/Z)	Best match
A	28	28,40,32,18	Unretained
B	31	32,29,15	Methanol
C	29	44,43,42,15,28	Acetaldehyde
D	68	42,40,38,27,29	Furan
N	29	46,45,44,43,28,17,16	Formic acid
F	78	79,77,52,51,50,39	Benzene

Table 39 Identified components from the spectra shown in Figure 140 taken from the full scale BRE flaming polyurethane based on the standard BS EN 54 fire (TF4).

### 5.3.3.4 Flaming heptane pool fire (TF5)

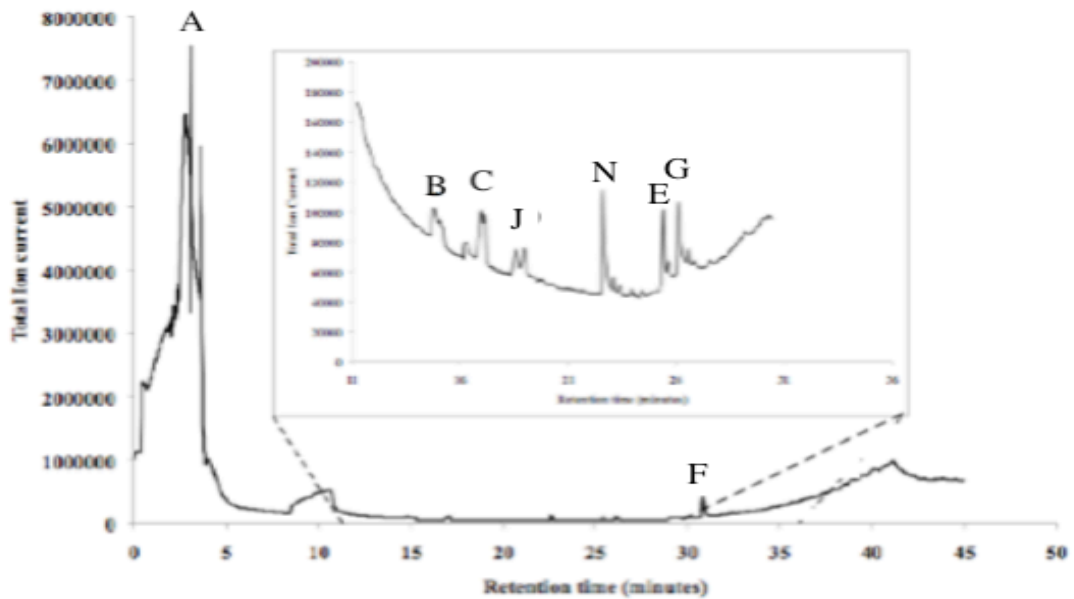


Figure 141 Chromatogram for Carboxen captured sample from flaming heptane TF5 fire at BRE .

The magnified section between 11 minutes and 31 minutes represent the minor components captured during the test.

Peak ID	Base peak	Other mass ions (m/Z)	Best match
A	41	40,32,18	Unretained
B	31	32,29,15	Methanol
C	29	44,43,42,15,28	Acetaldehyde
J	31	45,44,43,29,27	Ethanol
N	29	46,45,44,43,28,17,16	Formic acid
E	43	60,45,42,29,15	Acetic acid
G	74	75,73,55,56,57,45,30,29,58	Propionic acid

Table 40 The identified components from the spectra shown in Figure 141.

The chromatogram is representative of the gases collected from a full-scale fire test based on the BS-EN 54 TF5 flaming heptane fire.

### 5.3.4 Non-Standard fires with polymer fuels– products captured on Carboxen

#### 5.3.4.1 Overheated Printed circuit boards

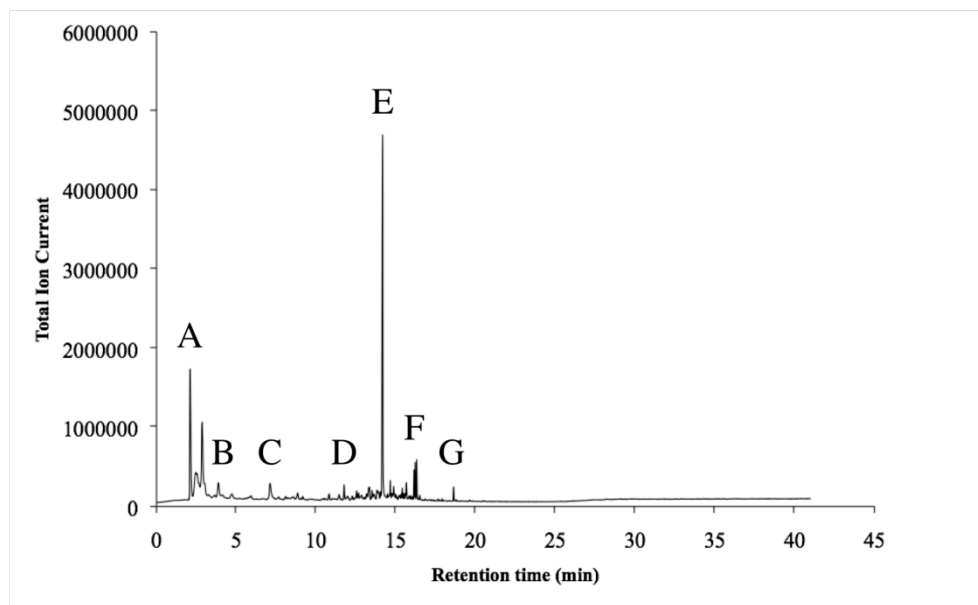


Figure 142 Representative chromatogram for Carboxen captured sample from PCB heated on hotplate in UCLan enclosure. Corresponds to sect. 4.8.2. The peaks are identified in table 41.

Peak ID	Base Peaks	Other ions (Fragments)	Best match
A	43	40,32,28,18	Unretained
B	64	66,48,32,28	Sulphur dioxide
C	43	128,99,85,71,70,57,56,55,43,41,39,29,28,27	Unknown
D	117	131,132,102,78,77,74,63,62,52,51,50,39,27	1-phenyl,2-butene
E	134	133,117,107,91,89,79,78,77,66,65,51,43,39,27	2-Chloro-1-phenylacetylene
F	43	58,55,43,41,39,29,27,18	Butane
H	121	136,122,107,103,93,91,77,63,60,56,43,42,41,39	Methyl 2-chlorobutyrate
I	94	66,65,55,53,50,47,40,41,39,38	Phenol
G	43	86,60,28,15	Unknown

Table 41 The table represents the data from the peaks identified in the spectra shown in Figure 142.

### 5.3.4.2 PVC Wire

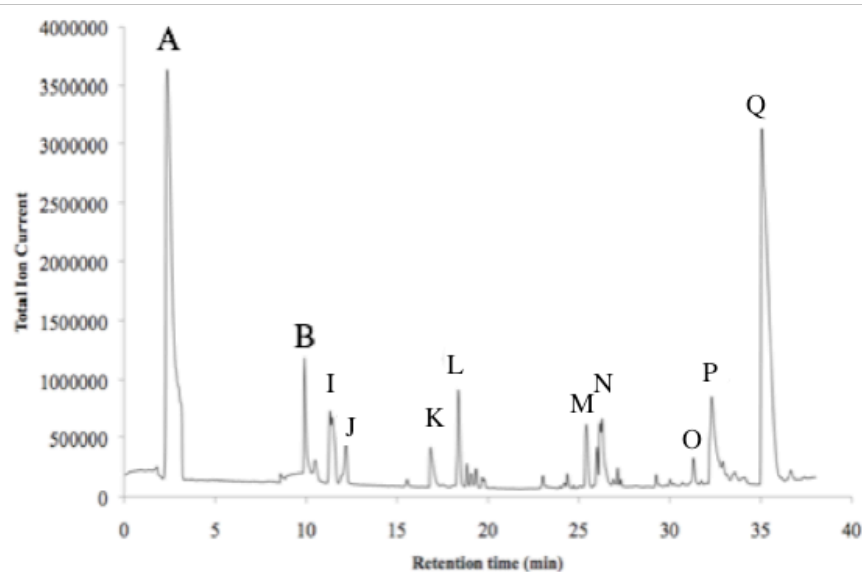


Figure 143 Representative chromatogram for Carboxen captured sample from PVC covered wire heated on hotplate in UCLan enclosure. Corresponds to sect. 4.8.3. The peaks from this chromatogram are identified on table 42.

Peak ID	Base Peak	Other mass ions (m/Z)	Best match
A	16	46,45,44,28,22,12	Unretained
B	64	66,48,32,28	Sulphur dioxide
I	41	40,39,27,26,12,11	1,2-Propadiene
J	60	36,35,26,25,24	Chloroethyne
K	29	44,43,29,16	Propane
L	41	56,55,39,32,29,28,27	2-Butene
M	54	53,51,50,39,32,28,27,26	Acetone
N	42	78,68,53,51,50,43,42,41,39,32,29,27	n-Propyl chloride
O	39	68,67,53,41,40,38,37,29,18	2 Butynal
P	43	72,71,57,56,42,41,39,29,27,18	2 Methyl butane
Q	78	77,52,51,39,32,28	Benzene
R	64	72,68,67,57,55,43,42,41,39,32,29,27	2-Butenal

Table 42 This table shows the mass ion data collected from analysis of the spectra shown in Figure 143.

### 5.3.4.3 Mixed Polyurethane

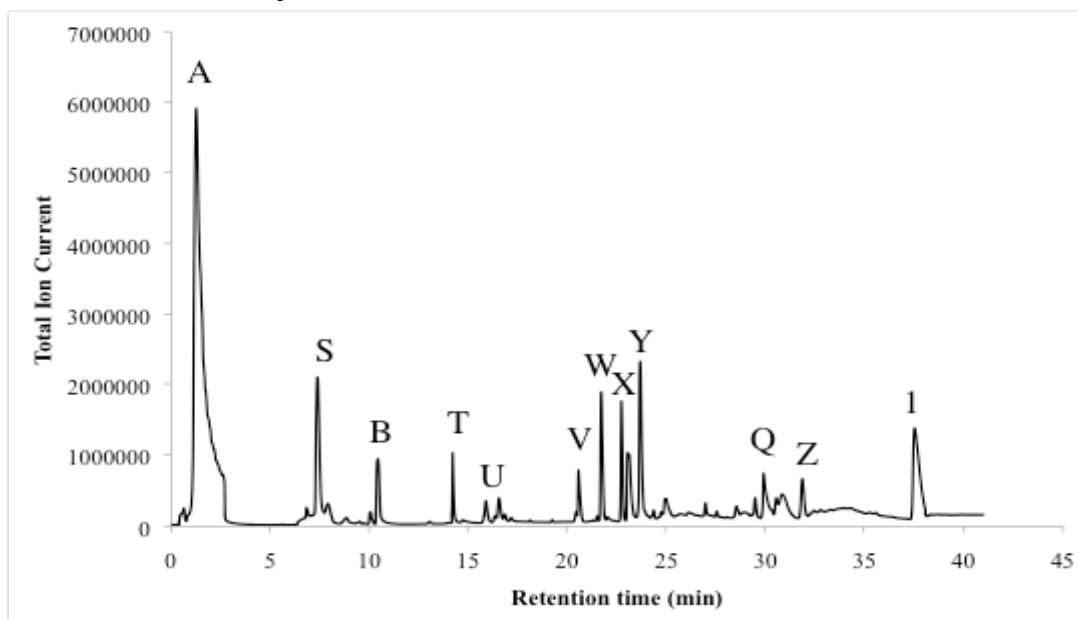


Figure 144 Representative chromatogram for Carboxen captured sample from a flaming polyurethane foam fire in UCLan enclosure.

The fire was arranged as TF4 emulsion but with 25% of fuel being fire retardant. Corresponds to sect. 4.8.1, PU+FR-2. The peaks from this chromatogram are identified on table 43.

Peak ID	Base Peak	Other mass ions (m/Z)	Best match
A	44	46,45,32,28,22,26	Unretained
S	41	44,42,40,39,38,27	Propene
B	64	66,48,32,28,28	Sulphur dioxide
T	64	66,50,48,32,28,18	Unknown
U	29	44,43,42,41,32,31,18,16,15	Acetaldehyde
V	28	68,42,40,39,38,37,32,29,18,14	Furan
W	41	78,77,61,58,43,42,39,28,15	Propene-2-chloro
X	36	78,77,76,48,35,34,29,27,18	1 Propene-1-chloro
Y	60	74,59,46,45,43,41,29,28,18,15,14	Butanoic acid
Q	45	82,81,78,72,53,39,27,18,15	Benzene*
Z	63	82,81,78,77,76,65,64,62,52,41,39,28	Dichloro-1,2-propane
1	43	86,60,28,15	Unknown

Table 43 Table of the mass ions and potential identifications from the flaming mixed polyurethane fires. These peaks correspond to the peaks shown in the Figure 144.

\*The Benzene peak in this spectra is difficult to resolve from the background and co-eluting compounds but there is enough evidence to suggest an identification on the base of retention time, presence of dominant ions and library matching compared with other samples,

### 5.3.5 Non-Standard Fires –cooking oils -products on Carboxen

The fumes from cooking oils and fats and cooking in general can be a significant cause of false alarm signals. There are many different kinds of cooking oils and this study looked at three of the most common types to check whether the gasses from overheating were common or differed.

#### 5.3.5.1 Vegetable oil

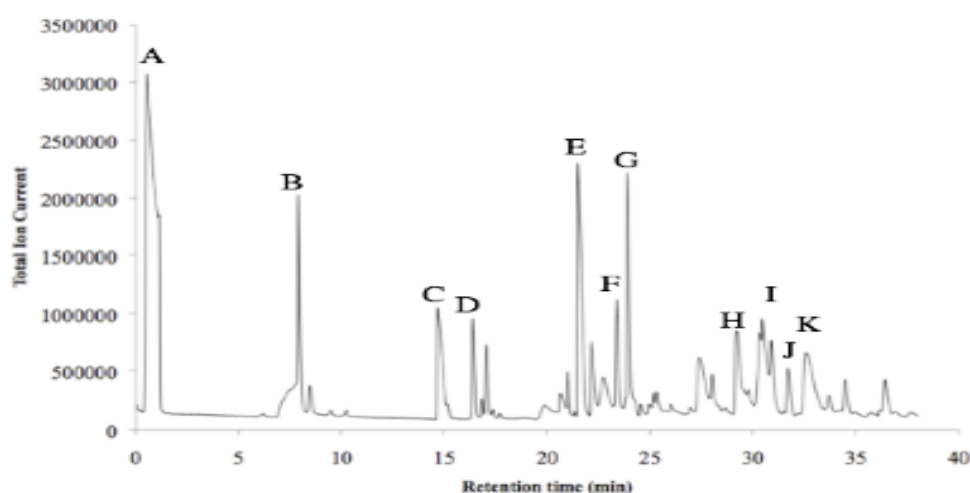


Figure 145 Representative chromatogram for Carboxen captured sample from overheated vegetable oil in UCLan enclosure. Corresponds to trace in sect. 4.8.4, The labelled peaks A-K are described in table 44.

Peak ID	Base Peak	Other mass ions (m/Z)	Best match
A	44	46,45,43,28,22,17,13	Unretained
B	41	70,43,42,40,39,38,27	2-Methyl Propen-1-one
C	41	44,42,40,39,38,27	Propene
D	41	56,55,53,50,39,32,29,28,18,15,14	Butene
E	68	69,42,40,38,39,37,34,29	Furan
F	56	57,55,53,52,40,39,38,37,36,29,28,27	2-Propenal
G	43	72,71,57,56,42,41,39,29,27,18	2 Methyl butane
H	82	83,81,54,53,39,28,27	2 Methyl Furan
I	56	84,83,70,69,55,43,42,41,39,29,27	Hexene
J	78	77,64,53,39,29	Benzene
K	43	72,71,60,57,42,41,32,29,27,18,15	2 Methyl Furan

Table 44 These ions represent the peaks from the chromatogram traces identified in Figure 145, are the most dominant ion patterns in each identified peak.

### 5.3.5.2 Olive Oil

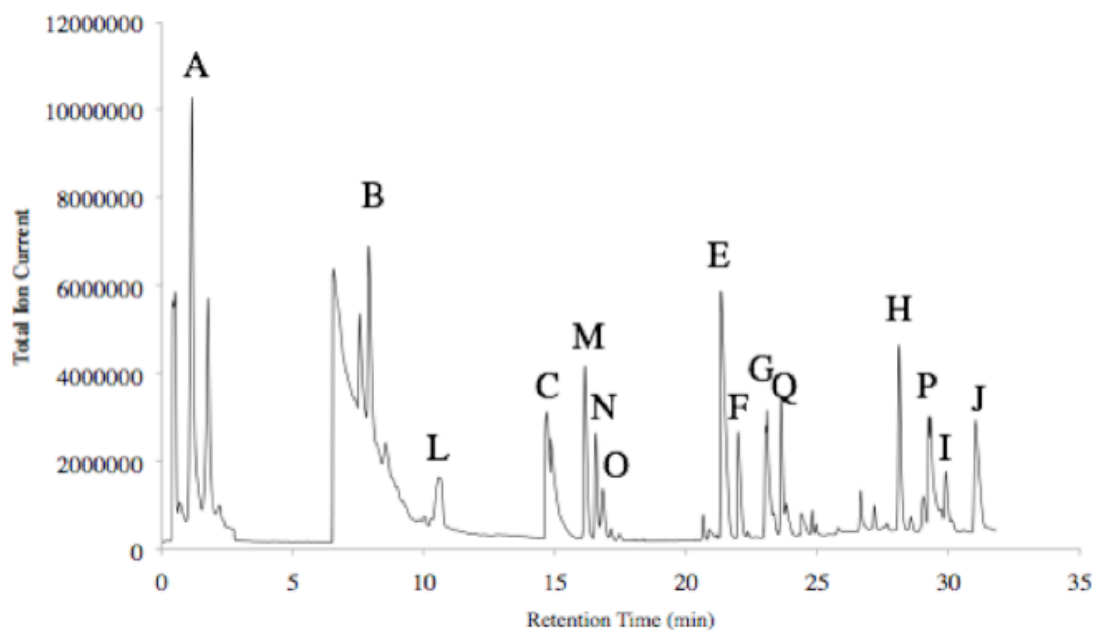


Figure 146 Representative chromatogram for Carboxen captured sample from overheated olive oil in UCLan enclosure. Corresponds to trace insect. 4.8.4. Ions corresponding to the peaks A-N are represented in table 45.

Peak ID	Base Peak	Other mass ions (m/Z)	Best match
A	44	46,45,43,28,22,17,13	Unretained
B	29	44,42,40,39,38,27	Propene
L	64	66,48,32,28,28	Sulphur dioxide
D	41	70,43,42,40,39,38,27	2-Methyl Propen-1-one
L	41	56,55,39,29,28,27,26	2- Butene
M	54	53,51,50,39,28,27,26	2 Butyne
N	43	58,42,41,29,28,27	Isobutane
E	68	69,42,40,39,38,29,28,27,26,25	Furan
F	29	58,57,28,27,26	2-Propenal
G	43	72,71,57,56,42,41,39,29,27,18	2 Methyl butane
Q	41	71,70,69,55,43,42,40,39,38,29	2-Methyl-2-Propenal
H	82	83,81,54,53,39,28,27	2 Methyl Furan
P	56	84,69,55,42,41,39,29,27	Cyclohexane
I	57	86,71,56,43,42,41,39,29,27	Hexane
J	78	79,77,52,51,50,39,38	Benzene

Table 45 These ions represent the peaks from the chromatogram traces identified in Figure 146 are the most dominant ion patterns in each identified peak.

### 5.3.5.3 Solid Cooking fat (lard)

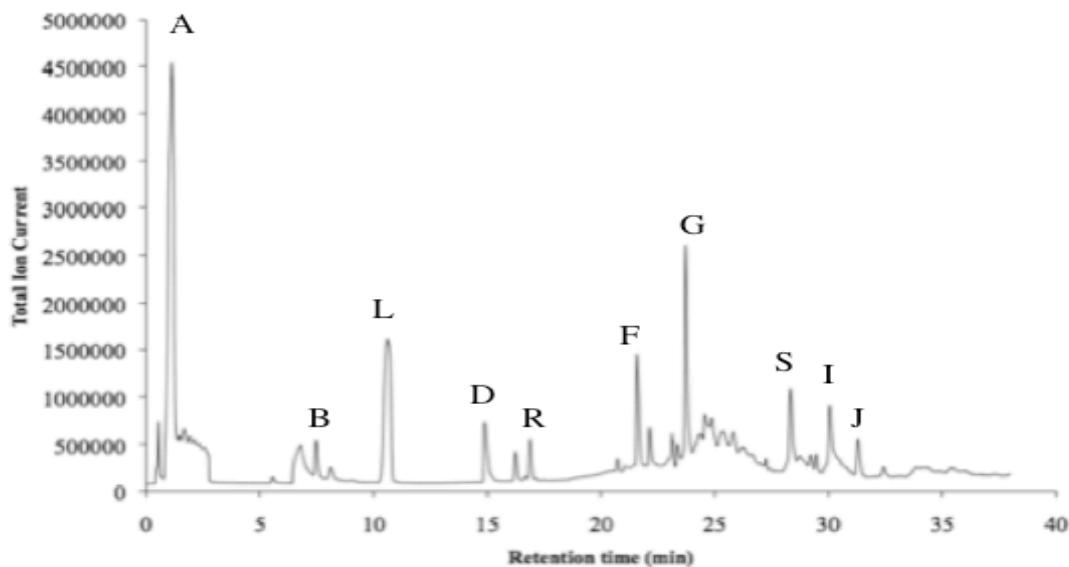


Figure 147 Representative chromatogram for Carboxen captured sample from overheated cooking fat in UCLan enclosure. Corresponds to trace in sect. 4.8.4. The peaks A-J are described in table 46.

Peak ID	Base Peak	Other mass ions (m/Z)	Best match
A	44	45,46,43,28,22,17	Unretained
B	41	70,43,42,40,39,38,27	2-Methyl Propen-1-one
L	64	66,50,58,32,18	Sulphur dioxide
R	29	44,43,42,15,28	Acetaldehyde
D	43	56,55,53,50,39,32,29,28,18,15,14	Butene
F	29	56,55,53,39,38,37,29,28,27,26,25	2-Propenal
G	43	72,70,57,55,42,41,39,29,27	2 Methyl butane
S	44	72,71,57,43,42,41,39,29,27,26,16	Butenal
I	57	86,70,60,58,57,56,45,42,41,29,27,18	Hexene
J	78	77,76,64,57,42	Benzene

Table 46 These ions represent the peaks from the chromatogram traces identified in Figure 147, are the most dominant ion patterns in each identified peak.

## 5.3.6 Toasting Bread

### 5.3.6.1 Progression of toasting

Experiments on the progression of toasting were to determine the vapours present as the bread progressed through stages of toasting to burnt, and identify changes as the toast becomes more carbonized as indicated in Figure 148

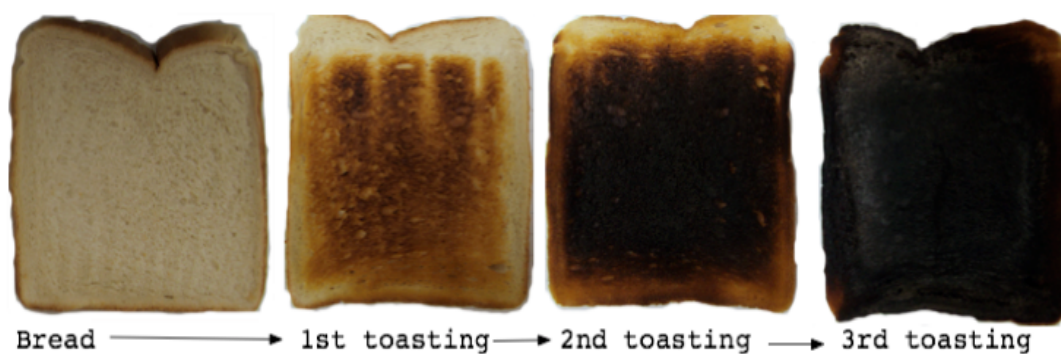


Figure 148 Images of toast representing 0-3 toasting experiments

Example results for experiments conducted in the UCLan enclosure with Carboxen sample tubes are presented below. No steps to reduce the moisture in samples for the first three experiments and consequently a peak around 10 minutes swamps many of the minor components.

The following chromatograms (figure 149-151) in the progression of toasting experiments represent the different stages of toasting discussed in chapter 2. The initial stage of toasting rarely produces a fire signal and the types of gasses collect are thought consistent with dehydration. Where moisture has been left in the sample tubes it demonstrate how large signal water can be in many of the fires compared to the other components.

Results for pure nitrogen dried sample are presented in Figure 152.

## Progression of toasting: 1<sup>st</sup> toasting

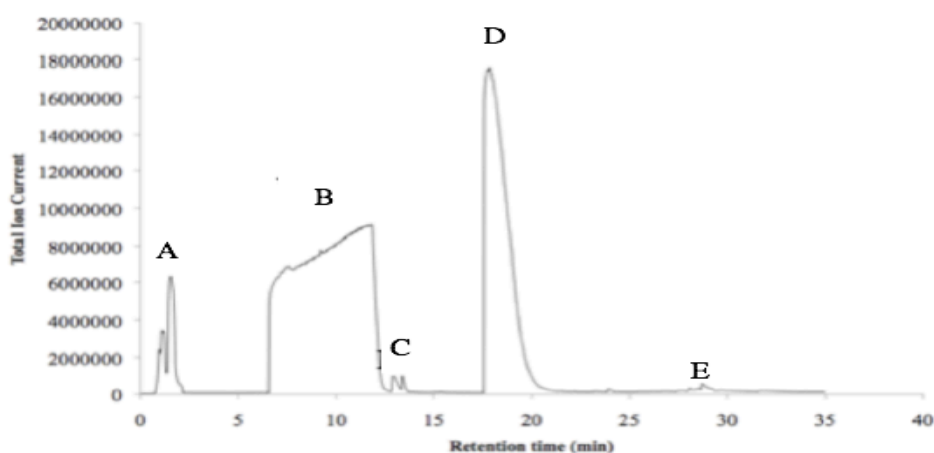
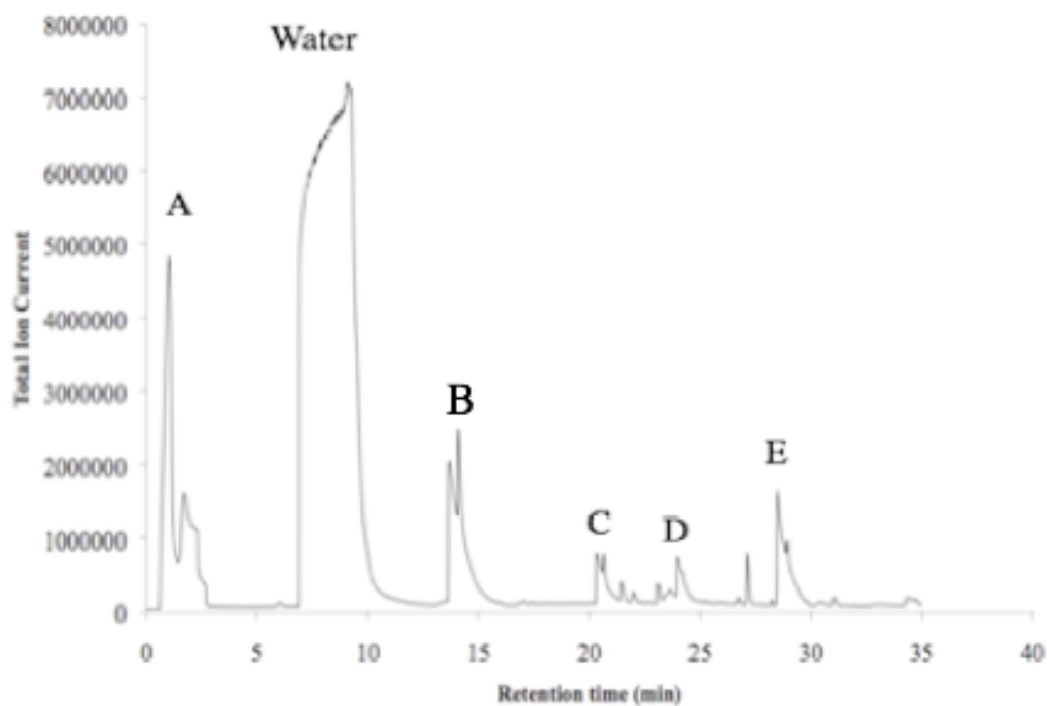


Figure 149 Representative chromatogram for Carboxen captured sample from first toasting of bread slice in UCLan enclosure. Peaks A-E are described in table 47.

Peak ID	Base Peak	Other mass ions (m/Z)	Best match
A	18	40,32,28,14	Unretained
B	64	66,48,32	Sulphur dioxide/Water
C	44	46,45,31,29,27	Ethylene oxide
D	31	45,44,43,29,27	Ethanol
E	43	60,45,44,42,41,29,15	Acetic acid

Table 47 These ions represent the peaks from the chromatogram traces identified in Figure 149, are the most dominant ion patterns in each identified peak

## Progression of toasting: 2<sup>nd</sup> toasting



Peak ID	Base Peak	Other mass ions (m/Z)	Best match
A	18	40,32,28,15,16	Unretained
B	41	44,42,40,39,38,27	Propene
C	31	45,44,43,29,27	Ethanol
D	45	56,55,46,44,39,38,28	Oxalic acid
E	43	60,45,44,42,41,29,15	Acetic acid

Table 48 These ions represent the peaks from the chromatogram traces identified in Figure 150, are the most dominant ion patterns in each identified peak.

## Progression of toasting: 3rd toasting

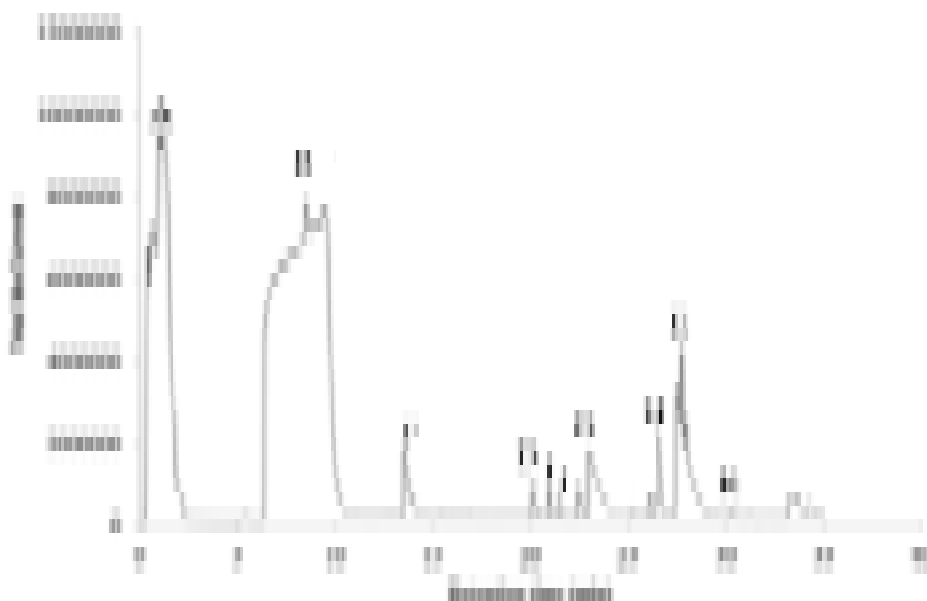


Figure 151 Is a representative chromatogram for Carboxen captured sample from third toasting of bread slice in UCLan enclosure.. Peaks A-J are described in table 47.

Peak ID	Base Peak	Other mass ions (m/Z)	Best match
A	32	40,39,28,27,18,17,16	Unretained
B	44	46,45,31,29,27	Ethylene oxide
F	43	56,5,50,39,32,29,28,18,15,14	Butene
D	31	45,44,43,29,27	Ethanol
I	43	58,57,28,27,26	2 Propanal
J	68	69,42,40,39,38,29,28,27,26,25	Furan
G	43	58,42,29,27,16	Acetone
H	82	83,81,70,54,53,39,28,27	2 Methyl Furan
E	43	60,45,44,42,41,29,15	Acetic acid
K	78	79,77,64,52,51,50,39,38	Benzene

Table 49 These ions represent the peaks from the chromatogram traces identified in Figure 151, are the most dominant ion patterns in each identified peak.

As the effect of water was particularly evident on the GC/MS chromatograms for toast, measurements were also carried out on samples where the Carboxen was dried by flushing through with dry nitrogen before carrying out desorption and GC analysis.

## Bread 2<sup>nd</sup> toasting, Carboxen dried by gas flow

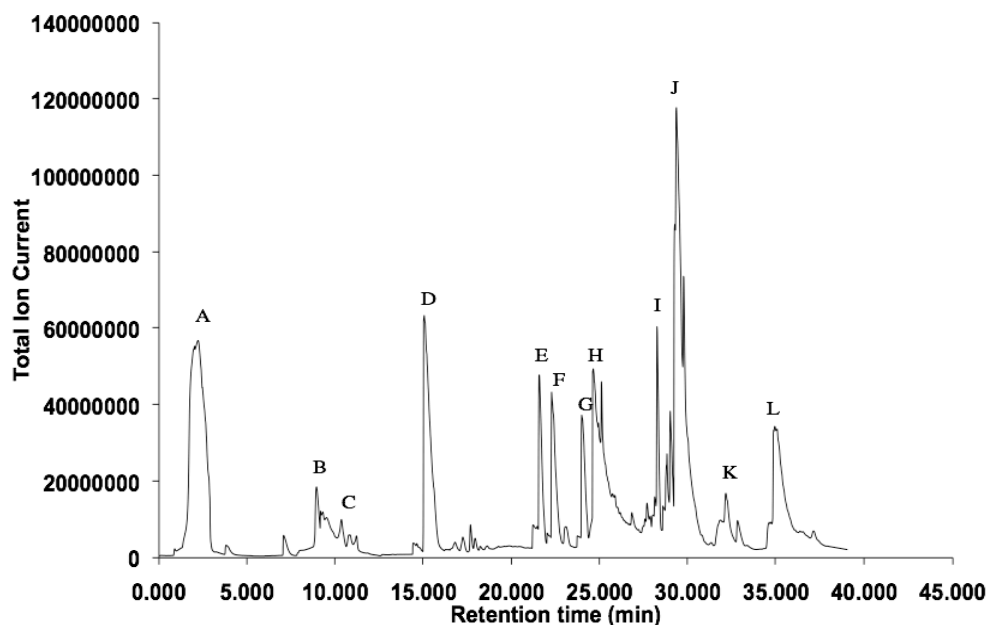


Figure 152 Is a representative chromatogram for Carboxen captured sample from second toasting of bread slice in UCLan enclosure.

This chromatogram is for absorption tube contents flushed with dry nitrogen before GC. Was collected . Peaks A-L are described in table 50.

Peak ID	Base Peak	Other mass ions (m/Z)	Best match
A	28	40,32,28,14	Unretained
B	41	44,42,40,39,38,27	Propene
C	64	66,48,30	Sulphur dioxide
D	44	43,42,29,28,27	Propane
E	56	57,55,38,37,36,29,28,27,26,25	2-Propenal
F	43	59,58,42,41,40,39,38,37,27,26,16,15	Acetone
G	43	60,45,42,29,18,17,15	Acetic acid
H	43	72,54,41,39,29,27	Pentane
I	82	81,54,53,51,50,43,39,27	3 Methyl Furan
J	78	77,76,64,52,51,50,39,38	Benzene
K	45	73,72,70,69,60,43,42,41,39,27	Butanal 3-Hydroxy
L	64	72,68,67,57,55,43,42,41,39,32,29,27	2-Butenal

Table 50 These ions represent the peaks from the chromatogram traces identified in Figure 152, are the most dominant ion patterns in each identified peak

### 5.3.7 Methanol Flaming Liquid Fire

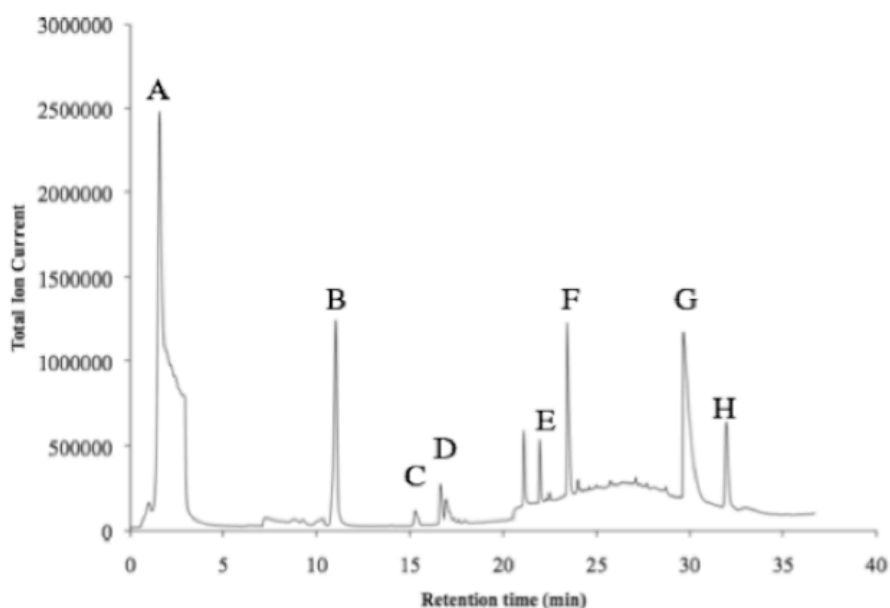


Figure 153 The figure represents those components captured and eluted from Carboxen sample tubes. Peaks A-H are described in table 51.

Despite burning for the most part with clean blue flame the burning methanol fire clearly did produced fire components other than CO<sub>2</sub> and water.

Peak ID	Base Peak	Other mass ions (m/Z)	Best match
A	28	40,32,29,28,14	Unretained
B	64	66,48,32	Sulphur dioxide
C	31	32,29,15	Methanol
D	41	56,55,39,29,28,27,26	2- Butene
E	68	69,42,40,39,38,29,28,27,26,25	Furan
F	43	59,58,41,40,39,37,27,26,16,15	Acetone
G	43	60,45,29,18,15	Acetic acid
H	78	77,52,51,50,39,38	Benzene

Table 51 These ions represent the peaks from the chromatogram traces identified in Figure 153, are the most dominant ion patterns in each identified peak.

### 5.3.8 Non standard smouldering paper

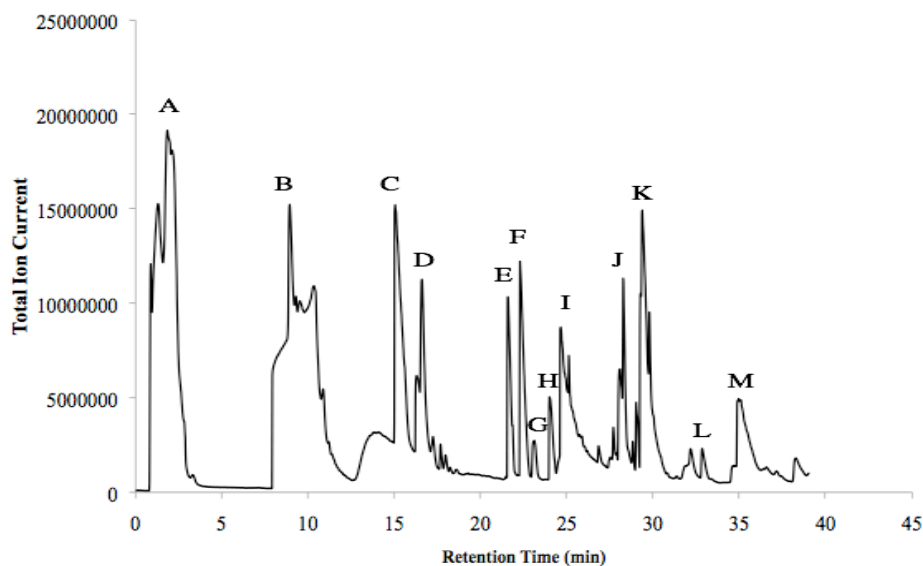


Figure 154 Representative chromatogram for Carboxen captured sample from green paper (wash room hand towel type) under conditions as for UL268 fire A emulsion in UCLan enclosure . The peaks are described in table 52.

Peak ID	Base Peak	Other mass ions (m/Z)	Best match
A	28	60,32	Unretained
B	29	44,43,41,39,28,27,15	Propane
C	29	48,44,43,30,29,16	Unknown
D	32	57,56,55,41,32,31	Unknown
E	68	69,40,39,29	Furan
F	56	55,39,38,37,36,28,27,26	2-Propenal
G	29	46,45,44,28,17	Formic acid
H	41	70,42,40,39,29,27	Methacrolein
I	82	81,54,53,39,28,27	2 Methyl Furan
J	82	70,65,55,53,27	Unknown
K	41	70,69,42,39,38,29,27	2-Butenal
L	78	77,64,53,39,29	Benzene
M	70	69,41,39,27	Unknown

Table 52 These ions represent the peaks from the chromatogram traces identified in Figure 154, are the most dominant ion patterns in each identified peak.

### **5.3.9 Cigarettes**

There is a very extensive literature on identification and measurement of components of cigarette smoke. However analysis involving direct collection on absorbent media is recognized to be difficult as solid media as used in most environmental sampling and in this study, rapidly becomes poisoned by the light tar associated with cigarette smoke. It was found in this study that cigarette smoke generated complex and poorly reproducible GC/MS chromatograms, for both Carboxen and Tenax absorption, though particularly for the former. It was not considered useful for this document to include an example trace for cigarette smoke captured on Carboxen.

### **5.4 Example chromatographs from Tenax samples**

This section presents chromatographs from different test fires collected on Tenax, and tabulated data showing masses of major ions corresponding to identified GC peaks.

The way the data is presented for the Tenax samples is slightly different from the Carboxen samples. The main reason behind this is that a range of relatively large and complex molecules are captured on the Tenax samples often giving ill defined peaks while for the Carboxen samples a series of simpler and more clearly resolved compounds are collected. Instead of labelling each of the peaks, peaks are identified by their retention times. Where possible product identities are suggested but the complexity of the samples with unresolved mixtures makes identification rather problematic. Where the peaks cannot be accurately identified or resolved the major mass ions are presented for information.

## 5.4.1 Scaled EN 54 fires at UCLan – products captured on Tenax

### 5.4.1.1 Smouldering wood (TF2 Emulation)

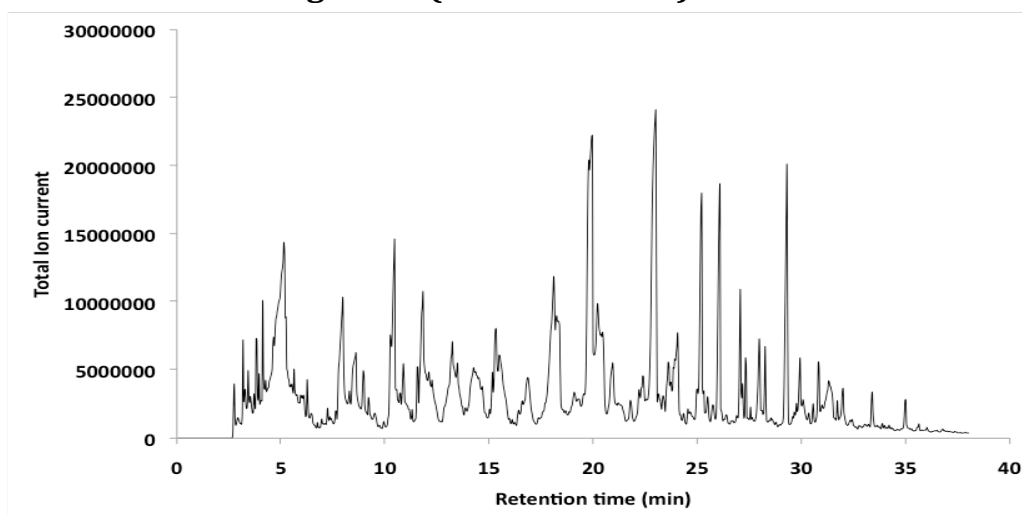


Figure 155 Representative chromatogram for Tenax captured sample from smouldering wood TF2 emulation in UCLan enclosure.

Retention Time	Base peak	Other ions (Fragments)	Best fit Match
5.1	43	83,74,60,45,44,43,42,32,31,29,28	3-Butan-2-one
7.9	29	88,74,73,44,43,42,39,31,29,28,27	3 Butene 1-2-Diol
8.6	43	85,84,55,54,42,29,15	2(5H) Furanone
10.6	72	58,57,56,43,41,39,39,29,27	3-Furaldehyde
11.8	98	97,81,70,69,53,52,51,50,49,42,41,39,31,29,27	2-Furan Methanol
13.2	67	96,91,84,81,70,68,67,57,55,53,44,43,42,41,39,29	
14.2	70	107,100,85,44,43,42,41,39,73,29,27	3 Methyl 2 Cyclopenten-1-one
15.9	43	130,110,109,101,96,81,73,67,57,53,51,43,29,27	2 Methyl 1-Propene-1-one
18.1	60	121,,113,112,87,73,69,57,56,55,45,43,42,41,39	
19.9	81	124,109,65,63,53,52,51,39,27	Mequinol
22.9	138	123,107,95,77,67,66,65,55,53,51,41,39	Unknown
22.0	41	138,126,110,97,81,73,71,69,68,55,53,51,50,42,41,39,38,31,29,27	Unknown
25.2	137	152,122,109,94,91,79,77,65,55,53,51,43,41,39,29	Unknown
26.1	150	166,135,107,91,89,79,78,77,65,63,55,53,51,43,39	Unknown
27.0	164	149,137,133,131,121,105,104,103,93,91,79,78,77,65,64,63,55,51,43,41,39,27	Unknown
28.0	151	164,152,137,123,109,91,81,79,77,65,63,55,53,52,51,50,39,38,29,27	Unknown
29.3	164	149,137,133,131,121,115,103,102,91,77,65,63,55,53,51,43,39,27	Unknown
30.8	137	180,122,,94,77,65,64,51,43,39	Unknown
32.0	151	194,180,123,108,97,77,74,65,55,52,51,43,41,39	Unknown
33.4	137	190,182,175,163,147,137,123,124,106,105,94,91,79,77,65,55,53,51,43,39,31,27	Unknown
35.0	178	190,189,163,161,147,145,135,124,118,117,109,107,105,91,89,78,77,65,63,61,55,51,39,29,27	Unknown
39.2	43	239,227,213,199,185,171,157,143,129,115,111,101,97,87,85,83,72,71,69,60,57,55,45,43,41,39,29	Unknown

Table 53 These ions represent the peaks from the chromatogram traces identified in Figure 155, are the most dominant ion patterns in each identified peak.

### 5.4.1.2 Smouldering cotton (TF3 Emulation)

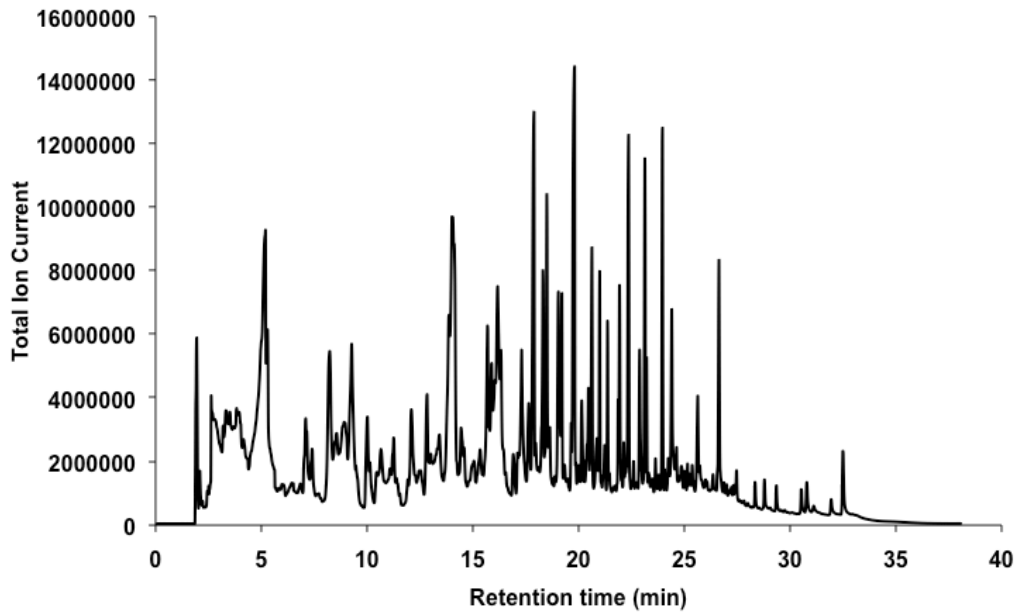


Figure 156 Representative chromatogram for Tenax captured sample from smouldering cotton TF3 emulsion in UCLan enclosure.

Retention Time	Base peak	Other ions (Fragments)	Best fit Match
5.0	43	79,78,77,42,32,31	Benzene
7.8	29	58,57,42,31,27	Unknown
8.3	43	102,44,42,32,31	Unknown
10.4	96	97,71,67,53,41,40,39,38,26	Unknown
11.1	98	97,81,70,69,53,52,51,50,49,42,41,39,31,29,27	2-Furan Methanol
12.7	55	86,84,54,42,41,39,29,28,27,26,	
13.9	98	111,110,109,98,85,70,57,50,43,42,39,29	Furfural
15.3	53	99,98,70,69,56,55,43,42,41,39,28,27,26	5 – Methyl furanone
17.6	112	84,83,69,56,55,43,41,39,28,27	Unknown
20.2	41	132,131,98,82,70,57,55,43,29,27	
25.1	121	132,131,115,104,103,95,89,78,77,76,63,57,51,50,39,27,26	3-Phenyl-2-Propen-1-ol
22.0	28	128,115,70,69,57,55,43,42,41,29	Unknown
22.9	69	144,114,98,86,70,57,41,39,31,29	Unknown
23.1	41	131,126,97,82,69,57,43,41,39,29	Unknown
23.4	57	170,146,145,94,85,77,71,43,41,29	Unknown
27.2	71	173,143,98,89,83,56,55,43,41,27	Unknown
27.5	71	173,143,89,71,57,56,55,43,41,28	Unknown
27.8	154	155,153,152,77,76,64,63,51,50,39	Biphenyl
30.2	169	168,167,165,153,152,139,121,111,94,83,69,63,54,51,39	Diphenylmethane
30.4	60	144,98,97,73,70,60,57,43,42,29	Unknown
32.5	71	243,159,155,111,83,56,55,43,41,27	Unknown
34.8	178	179,177,176,152,151,89,88,76,57,43	Anthracene

Table 54 These ions represent the peaks from the chromatogram traces identified in Figure 156, are the most dominant ion patterns in each identified peak.

### 5.4.1.3 Flaming polyurethane (TF4 Emulation)

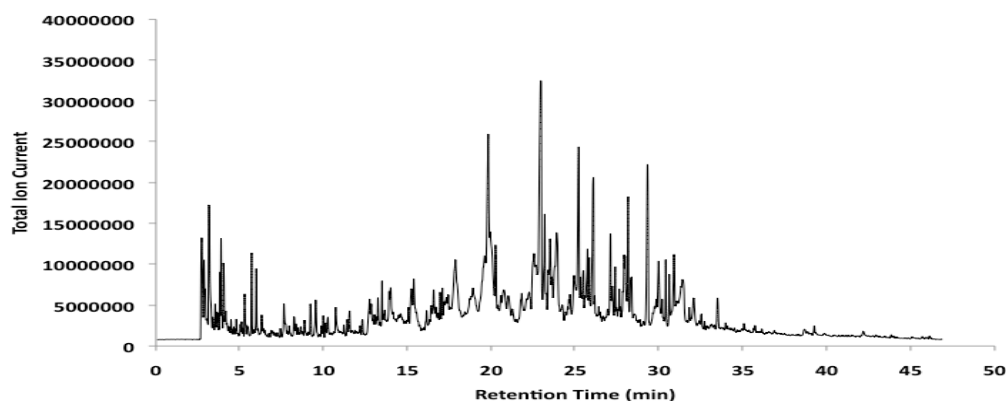


Figure 157 Representative chromatogram for Tenax captured sample from polyurethane foam burn TF4 emulsion in UCLan enclosure. Corresponds to sect. 4.6.3. TF4/12.

Retention Time	Base peak	Other ions (Fragments)	Best fit Match
2.7	32	44,40,34,30,29,28	Unretained
3.1	27	72,68,67,58,57,56,55,43, 29,28,27,26	Unknown
3.8	55	86,70,43,27	Unknown
3.9	44	72,57,43,42,41,39,29,27	2-Buten-1-ol
4.0	41	84,72,69,56,55,43,44,39,29,27	Hexene
5.3	71	86,56,55,45,43,42,41,39,29,27	Furan, tetrahydro-2-methyl-
5.7	57	58,45,44,41,39,29,27	Pental
6.0	41	98,86,83,71,70,69,57,56,55,43,42,39,31,29,28,27	Unknown
6.3	100	98,71,57,43,41,29,27,24	Unknown
9.2	100	82,72,67,57,56,45,44,43,41,40,29,27,19	Hexenal
9.5	112	85,83,70,69,57,56,55,43,41,39,29,27,26	Octene
17.8	112	124,97,84,83,69,56,55,43,42,41,39,29,27	Unknown
19.8	109	124,81,65,63,53,52,51,39,38,37,27	Unknown
22.9	138	168,140,138,123,107,95,85,79,78,77,69,68,67,66,65,55,53,51,41,39,29,27	1 Dodecene
25.2	132	182,125,112,111,98,97,85,84,83,71,70,69,56,55,54,43,41,39,29,27	Cis - tridecene
26.6	150	166,135,91,90,79,78,77,65,63,53,51,39,27	Unknown
27.8	164	173,149,138,137,133,131,121,104,103,91,85,77,65,55	Unknown
28.1	43	140,125,112,111,98,97,83,82,70,69,67,57,55,54,43,41	Unknown
29.2	164	164,149,137,133,131,121,103,91,77,65,55,53,51,43,41,39,27	Unknown
29.9	151	166, 123,108,80,77,73,65,60,43,29	Unknown
30.4	41	211,180,151,137,125,111,97,83,69,57,55,43,29,27	
30.9	137	180, 122,105,94,77,66,65,51,43,39	9H-Fluorene, 2-methyl-
32.1	109	190, 180,123,108,91,83,74,55,43,41,29	5,9-Tetradecadiyne
33.5	137	190, 182, 175,164,149,122,107,94,91,77,65,55,51,43,39,31,27	Cyclopropa[b]anthracene

Table 55 These ions represent the peaks from the chromatogram traces identified in Figure 157, are the most dominant ion patterns in each identified peak.

#### 5.4.1.4 Flaming pool fire (TF5 Emulation)

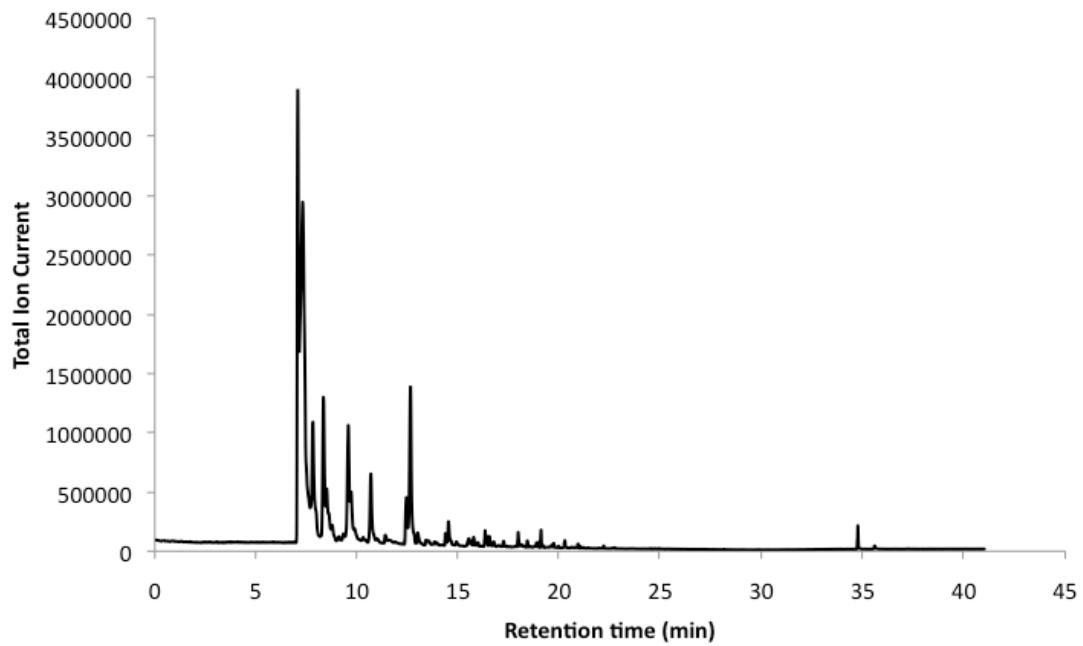


Figure 158 Representative chromatogram for Tenax captured sample from flaming heptane TF5 emulation in UCLan enclosure. Corresponds to sect. 4.6.4 . TF5/7.

Retention Time (min)	Base peak	Other ions (Fragments)	Best fit Match
4.3	44	28,22	Unretained
7.1	43	100,71,57,42,41,39,29	Hexene
8.4	91	92,65,63,51,50,45,39	Pentenal
10.6	71	114,55,56,43,39,29	Benzoic acid
12.8	57	128,99,94,66,65,41,39	Unknown
14.6		98,74,73,61,57,56,55,45,43,42,41,39,29	Hexanoic acid
16.7	41	42,40,39,38,37	Unknown
34.8	178	179,177,176,152,151,89,88,76,57,43	Anthracene

Table 56 These ions represent the peaks from the chromatogram traces identified in Figure 158, are the most dominant ion patterns in each identified peak

## 5.4.2 Scaled fires based on UL268 standard fires – products captured on Tenax

### 5.4.2.1 UL268 Fire A Emulation – Burning paper

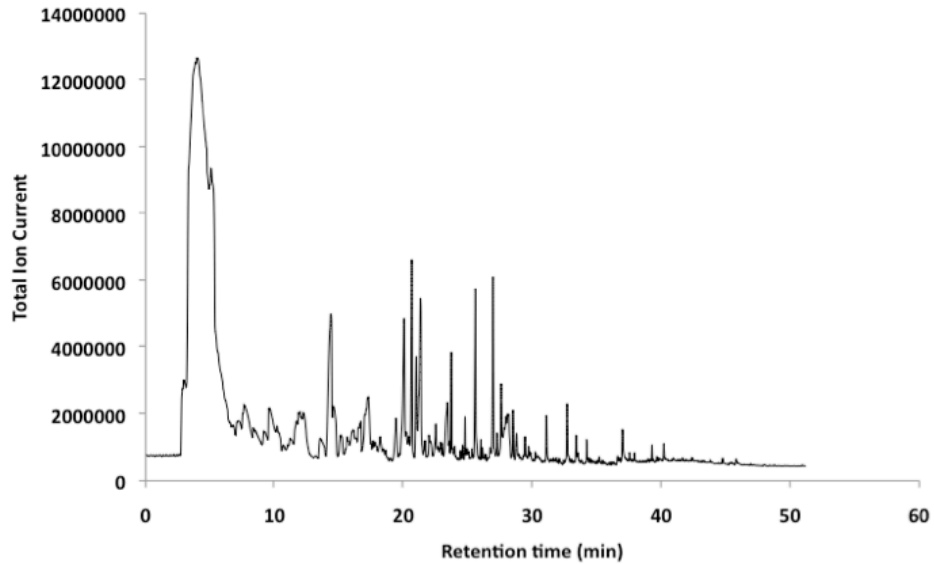


Figure 159 Representative chromatogram for Tenax captured sample from burning paper UL268 fire A emulation in UCLan enclosure. Corresponds to sect. 4.6.6.

Retention Time	Base peak	Other ions (Fragments)	Best Fit
4.0	29	57,45,43,41,31,29	Unretained
14.4	103	76,75,51,50	Benzonitrile
20.1	43	116,85,82,70,69,57,43,41,39,29	Unknown
20.5	128	142,102,98,74,64,51,43,39,29	Napthalene
21.0	110	144,98,85,81,69,64,57,41,29,27	Unknown
21.3	41	126,120,109,97,69,53,39,31,29,27,	Unknown
23.7	150	135,107,77,65,63,53,52,51,39,27	Unknown
25.6	151	152,137,123,109,81,65,63,53,51,39	Vanalin
26.9	164	149,137,131,121,103,91,77,65,55,39	Unknown
27.6	152	153,151,150,126,76,75,74,63,51,50	Acenaphthylene
28.5	137	180,122,94,77,66,65,51,43,39	Unknown
28.8	43	168,139,115,102,98,73,70,60,57,29	Unknown
31.1	137	182,165,149,122,107,91,77,65,51,39	Unknown
32.7	178	161,147,135,124,118,107,89,77,63,51	Unknown
33.4	43	204,185,164,149,137,129,73,60,41,29	Unknown
34.2	178	179,177,176,152,151,89,88,76,57,43	Anthracene
37.0	43	213,185,129,97,83,73,69,60,57,56,43,41,29	Pentadecanoic acid
37.5	204	205,203,202,102,101,89,88,76,63,51,39,28	Unknown
37.9	134	206,177,167,166,139,107,79,57,41,29	Unknown
39.3	202	203,201,200,174,101,100,88,87,75,74	Pyrene
40.2	202	203,201,200,174,101,100,88,87,75,74	Fluoranthene

Table 57 These ions represent the peaks from the chromatogram traces identified in Figure 159, are the most dominant ion patterns in each identified peak.

### 5.4.2.2 UL268 Fire B Emulation- Flaming wood

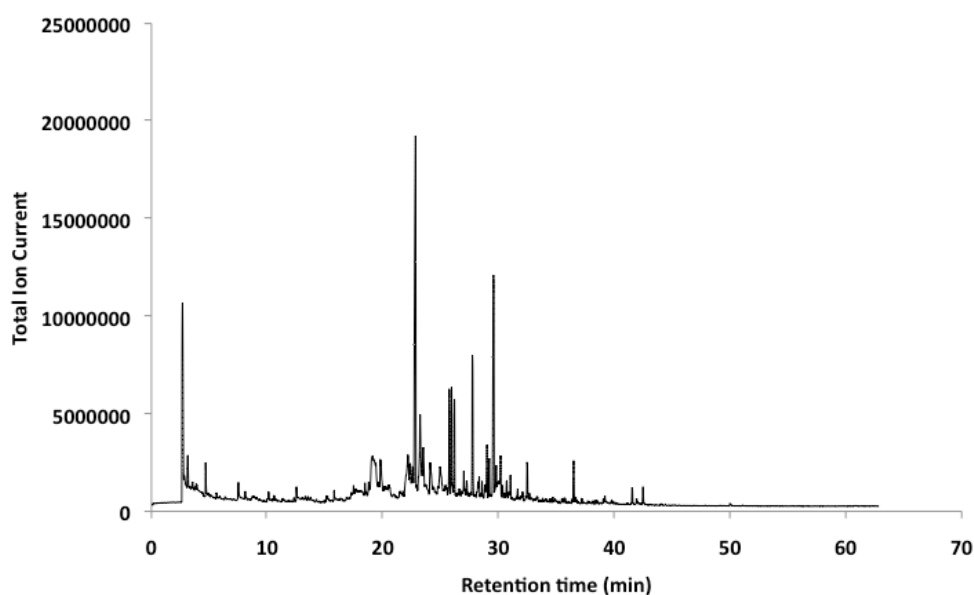


Figure 160 Representative chromatogram for Tenax captured sample from flaming wood UL268 fire B emulation in UCLan enclosure. Corresponds to section. 4.6.7.

Retention Time	Base peak	Other ions (Fragments)	Best Fit
2.69	32	44,40,29,28	Unretained
19.10	43	71,45,44,42,41,27	Pentane
19.77	68	116,98,97,96,70,53,42,41,39,29	Heptene
22.88	128	129,127,126,102,77,75,64,63,51,39	Napthalene
25.72	142	141,122,115,89,75,71,63,58,51,39	Naphthalene, 2-methyl-
25.93	150	151,135,107,91,77,63,53,51,39,27	Unknown
26.17	142	143,141,139,115,89,71,63,58,51,39	1H-indene, 1-ethylidene-
27.71	154	155,153,152,77,76,64,63,51,50,39	Biphenyl
29.53	152	153,151,150,126,76,75,74,63,51,50	Acenaphthylene
30.16	153	168,167,154,126,76,75,63,51,50,39	Unknown
32.46	166	167,165,139,83,82,71,63,55,43,41	Fluorene
36.46	178	179,177,176,152,151,89,88,76,57,43	Anthracene
41.50	202	203,201,200,174,101,100,88,87,75,74	Pyrene
41.89	202	203,201,200,174,101,100,88,87,75,74	Fluoranthene
42.47	202	218,203,201,200,174,101,100,88,87,76	Unknown

Table 58 These ions represent the peaks from the chromatogram traces identified in Figure 160, are the most dominant ion patterns in each identified peak.

### 5.4.2.3 UL268 Fire C Emulation- Flaming pool fire

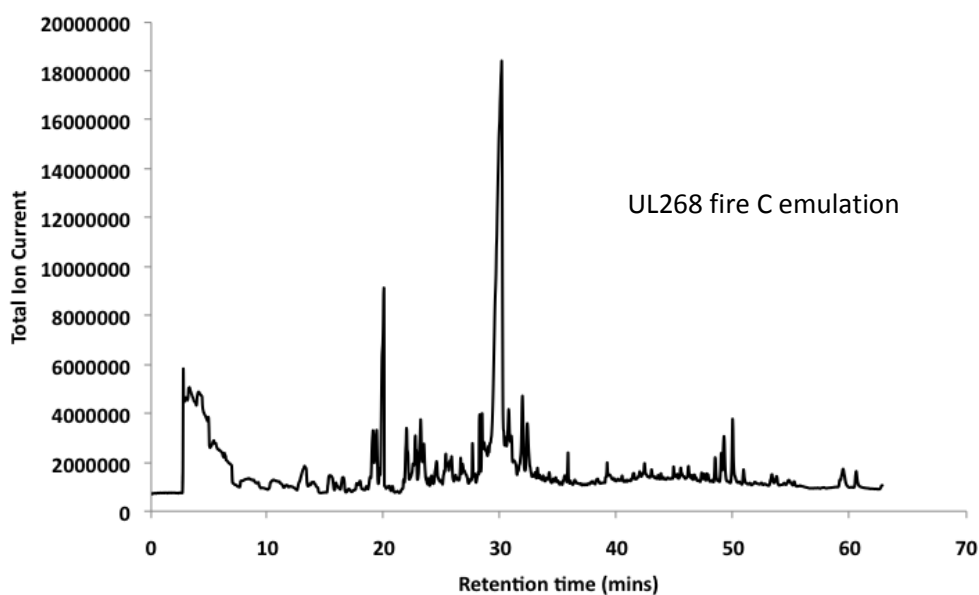


Figure 161 Representative chromatogram for Tenax captured sample from flaming heptane UL268 fire C emulation in UCLan enclosure. Corresponds to sect. 4.6.5.

Retention Time	Base peak	Other ions (Fragments)	Best Fit
1.3	48	44,40,39,28,18	Unretained
12.4	55	86,84,54,,41,39,29,26	Unknown
23.0	128	129,127,126,102,77,75,64,63,51,39	Napthalene
23.9	132	107,77,65,63,39,27	Unknown
25.4	132	125,112,98,97,85,84,83,71,70,69,65,43,41	Unknown
26.0	151	152,137,123,109,81,65,63,53,51,39	Vanalin
30.3	153	168,167,154,126,76,75,63,51,50,39	unknown
35.2	178	179,177,176,152,151,89,88,76,57,43	Anthracene

Table 59 These ions represent the peaks from the chromatogram traces identified in Figure 161, are the most dominant ion patterns in each identified peak.

## 5.4.3 Other fires

### 5.4.3.1 Toasting Bread

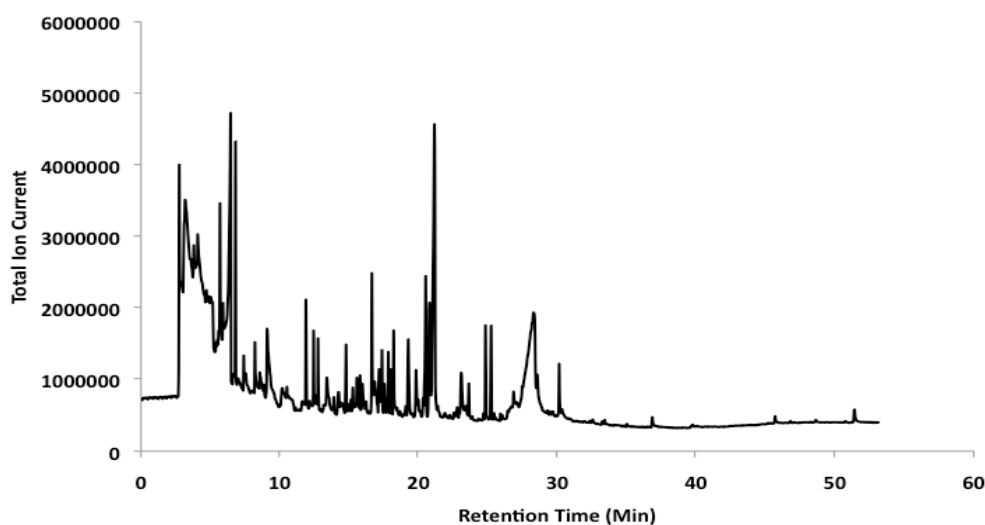


Figure 162 Representative chromatogram for Tenax captured sample from 2<sup>nd</sup> Toasting of bread in UCLan enclosure.

Retention Time	Base peak	Other ions (Fragments)	Best fit Match
4.8		82,74,58,	Unretained
6.2	43	100,71,57,42,41,39,29	Hexene
7.6	43	85,84,55,54,42,29,15	2(5H) Furanone
9.8	91	92,65,63,51,50,45,39	Pentalen
10.8	71	114,55,56,43,39,29	Benzoic acid
12.8	98	97,81,70,69,53,52,51,50,49,42,41,39,31,29,27	2-Furan Methanol
14.3	103	76,75,51,50	Benzonitrile
16.7	124	123,95,67,53,51,39,38,37,29	Unknown
17.4	43	127,82,71,57,44,43,38,29	Unknown
16.6	137	136,121,107,93,79,68	Unknown
18.9	97	95,67,68,56,55	Unknown
19.9	43	71,45,44,42,41,27	Pentane
23.3	128	129,127,126,102,77,75,64,63,51,39	Napthalene
24.3	71	173,144,112,97,88,83,56,43,41,27	Unknown
25.0	43	143,89,71,56,41,29,27	Unknown
26.6	151	152,137,123,109,81,65,63,53,51,39	Vanalin
27.9	178	177,173,172,,60,57,55,43	Unknown
29.0	152	153,151,150,126,76,75,74,63,51,50	Acenaphthylene
34.4	178	177,152,151,150,97,98,83,70,60,57,55,39	Phenanthrene
35.8	228	263,262,233,229,227,226,215,184,165,139,128,15,102,89,78,77,76,63,51	Benz[a]anthracene

Table 60 These ions represent the peaks from the chromatogram traces identified in Figure 162, are the most dominant ion patterns in each identified peak.

### 5.4.3.2 Cigarettes

As indicated earlier, cigarette smoke generated complex and poorly reproducible GC/MS chromatograms (figure 163). An example traces for a Tenax absorbed sample is provided below for illustrative purposes but cannot be considered truly representative.

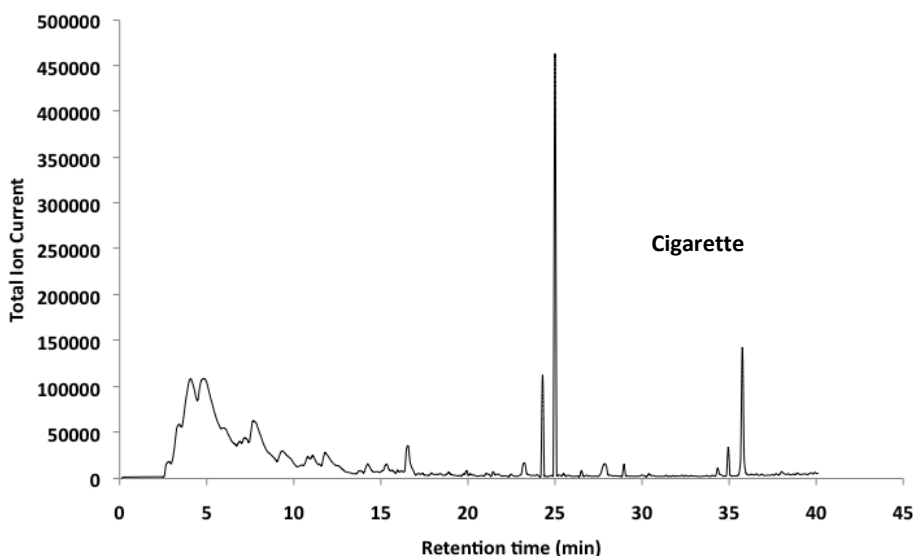


Figure 163. Example chromatogram for Tenax captured sample from cigarette carried out in UCLan enclosure.

The early part of the elution indicated that the complexity of the gas mixture of gases is sufficient to render adequate resolution with the systems in use barely possible. With over 4000 components reported in cigarette smoke this is perhaps not surprising. Analysis of cigarette smoke using solid absorbent media is recognized to be difficult due to media becoming poisoned by associated light tars. As indicated above for this study, cigarette smoke generated complex and poorly reproducible GC/MS chromatograms.

## 5.5 Summary of Product Identification for BS EN 54/7 Test Fires

For the standard scaled fires a series of common gases have been identified using the library matching program with gases being assessed as good or poor fits compared to the standard spectra from the library. These species and fit parameters are listed in table 61 below.

Peak identity	TF2		TF3		TF4		TF5	
	F	R	F	R	F	R	F	R
B : Propene	730	901	850	788			769	758
E : Acetaldehyde	809	893						
H : Furan	855	876	933	897	720	766	777	789
I : 2 – Propanal			867	803	830	733	959	942
J : Acetone	906	933	750	775	761	722		
R: 2 Methyl furan			910	899	717	906		
V : Benzene	877	923	902	899	891	901	801	855

Table 61 Common gasses observed in the scaled standard fires in the UCLan enclosure with the library match values presented.

While anything with a match value above 750 is considered a good match, but the library match should only be considered as a jumping off point and not a definitive identification. Other information which can be obtained from mass spectra where the MW <150AMU can help confirmation of an identification.

Standard fragmentation spectra for some of the more interesting components are shown in Figure 164 below.

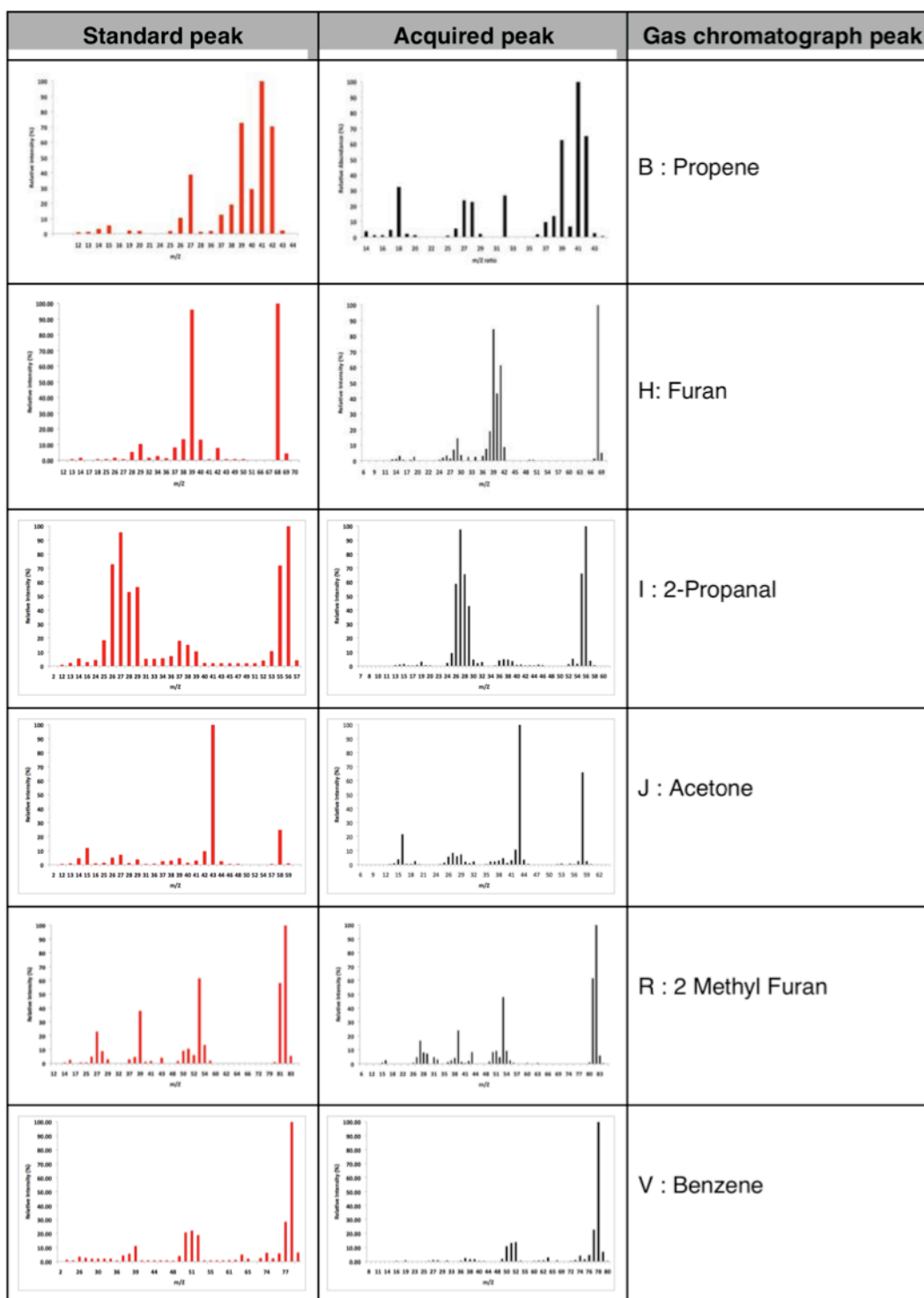


Figure 164 Example plots of the mass spectra acquired from experimental results compared to the GC-MS spectra from standard library taken from NIST web book [136]

## **CHAPTER 6 DISTINGUISHING FIRES WITH ADDITIONAL FIRE CHARACTERISTICS**

Over the course of this study we have been mostly interested in looking at the identities of the fire gases in the early stages of combustion. The main reason for doing so is to identify potential targets for new fire detection systems as ways to distinguish between different types of fires and non-fires commonly associated with false alarms.

This chapter looks at other fire related characteristics which have been studied in the UCLAN scaled fire enclosure, TYCO smoke tunnel and the BRE full scale test rooms. These characteristics include particle size analysis and the effect on scatter and ion mobility patterns of smoke emissions.

### **6.1 Distinguishing fires by scatter**

There has been some work looking at differentiating different types of fire based on the light scattering behaviours of smoke particulates. Weinerts [137] group looked at the effects of light polarisation on scattering angles from particulates generated from a series of flaming and non-flaming fires and nuisance signals (e.g. toast) and concluded while it was possible to distinguish between smouldering and flaming combustion, it was not possible to distinguish smoke originating from smouldering fires and nuisance sources. A study by Keller [138] concurred with Weinerts conclusions, and also examined the relationship between fire type and smoke aerosol particle size distribution as well as connections to optical scatter.

It is generally considered that the span of smoke particle sizes is comparable with wavelength of light over the UV to near IR range and that therefore the most appropriate theoretical basis for understanding light scattering by smoke is that for Mie scattering. Mie scattering is described in detail in a number of texts [139], but briefly, is based on the solution of the Maxwell equations for homogeneous spheres. The mathematical formula governing Mie scattering is complex and are most conveniently applied in computer program form but generally scattering by smaller particles is

expected to increase at shorter wavelengths. The response of optical scatter devices is therefore expected to be dependant on particle size and optical wavelength and in principle operation at shorter wavelengths should have potential to improve optical scatter detection for some smokes where ionisation type devices have been favoured.

Modern optical scatter devices employ LED light sources and silicon photodiode sensors. Most such detectors employ LEDs operating in the near infra red region (~800-950 nm) as these are established long life products with good stability, are well matched to the broad sensitivity peak of silicon photodiodes, and are available at low cost. In recent years LEDs emitting in the blue and even near UV regions have become commercially available and some optical fire detector products are beginning to be supplied which incorporate blue LED technologies. It has been suggested in patents [140] and some commercial publications that use of dual wavelengths (blue and IR) could improve discrimination between smoke and fire types and between smoke and other aerosols which may generate false alarms. Bosh are one of the companies which are offering detectors incorporating multiwavelength to the fire detection market. A group from Bosh have published supporting literature at the AUBE`09 [141] conference. Bergman published work on a Mie theory based predictive analysis related to fire detection devices and a series of experimental tests. There is a little other work published in the open literature tending to support claims of improved discrimination potential and some exploratory work at TYCO has shown that effects are discernable under well controlled conditions as in smoke tunnels [142]

The output levels for optical scatter devices depend on a large number of factors including light source type and power, optical sensor responsivity, the geometry of the detector chamber and lensing structures, and electronic amplification of the photosensor output. A two point calibration check as used for obscuration devices can not be employed for optical scatter detectors and so such detectors are generally set up with reference to reproducible scatter (smoke) levels and their output signal and consequent alarm notification validated against standard fire tests. As part of this study a series of optical scatter detectors both conventional (NIR ~850 nm) and modified to use other wavelengths (especially blue ~465 nm) were deployed. The work by Bergman indicated that different fires could yield discernibly different blue: near IR scatter response ratios and the data gathered in this study is analysed to determine whether that could be confirmed for fires in the UCLan enclosure and BRE test room.

The TYCO conventional and modified devices used are tabulated below (Table 62).

**Table of devices**

Address	Ser. No.	Type	Details
3	12019CBEE	801PC	Conventional NIR 850 nm LED
9	92019CC09	801PC	Conventional NIR 850 nm LED
12	20382805	experimental	465 nm (blue) LED with NIR phosphor (main emission ~870nm)
17	1200C0C9C	801PC	Conventional NIR 850 nm LED
32	20382815	experimental	Dual LED (blue 465 nm and NIR ~850 nm)
38	12019CC13	experimental	Near UV LED (~370nm)
47	12019CBFF	experimental	Longer NIR LED (~1070 nm)
102	120049EA8	801PC	Conventional NIR 850 nm LED
<b>170</b>	9200002A4	801PH	Conventional NIR 850 nm LED (higher sensitivity setting than 801PC)

Table 62 List of devices used in the standard fire tests indicating the wavelengths of the associated components used in the detectors.

Conventional TYCO optical scatter smoke detectors with near IR LEDs (~850 nm) and some experimental devices incorporating blue LEDs (~465 nm) were deployed for fire tests in the UCLan fire test box and for tests in the standard test room at BRE. Additional devices with LEDs operating in the near UV (~370 nm) and longer near IR (~1075 nm) were also deployed. Devices operating with near IR only were constructed with silicon photodiodes having inbuilt filters not passing visible light (as in conventional detectors to avoid sensitivity to external light). The devices operating with blue or UV have similar photodiodes without filtering so that radiation down to about 320 nm is detected. Selections of the detectors in Table 62 were employed for fire tests in the UCLan 2 m<sup>3</sup> enclosure, in the Sunbury fire tunnel and in the standard fire test room at BRE. Measurements of obscuration and gas analyses for most of the same test series are provided in chapter 4. Although the devices were deployed for measurements on false alarm stimuli (e.g. cooking toast) the material covered in this chapter is limited

to the BS EN54/7 BRE test fires (TF2 – pyrolysing wood, TF3 – smouldering cotton, TF4 – flaming polyurethane foam, TF5 – flaming heptane) and emulations of those fires in the UCLan enclosure, and measurements in the TYCO Sunbury smoke tunnel.

All the optical scatter devices have output collected using the TYCO MX panel simulator as 8 bit digital signals (0 to 255 bits) in log files, which are subsequently processed in excel. Each device has a small output, the pedestal value, corresponding to clear air (most probably from light scattering/reflection from smoke chamber walls). The signal value in presence of smoke is given by the bit output with smoke minus the pedestal value (output in clean air), which is expressed in shortened forms as below.

□

$$\begin{aligned}\text{Device signal} &= \text{raw output bytes in smoke} - \text{Output bytes in clean air} && (28) \\ &= \text{output in smoke} - \text{pedestal output} \\ &= \text{output} - \text{ped.}\end{aligned}$$

Equation 28 Device signal from raw output and clean air (pedestal) value

As constructed the devices have somewhat different sensitivities, even where devices are of same type). This is shown in Figure 165 below which shows an example run with joss sticks in the Sunbury tunnel for some of the devices.

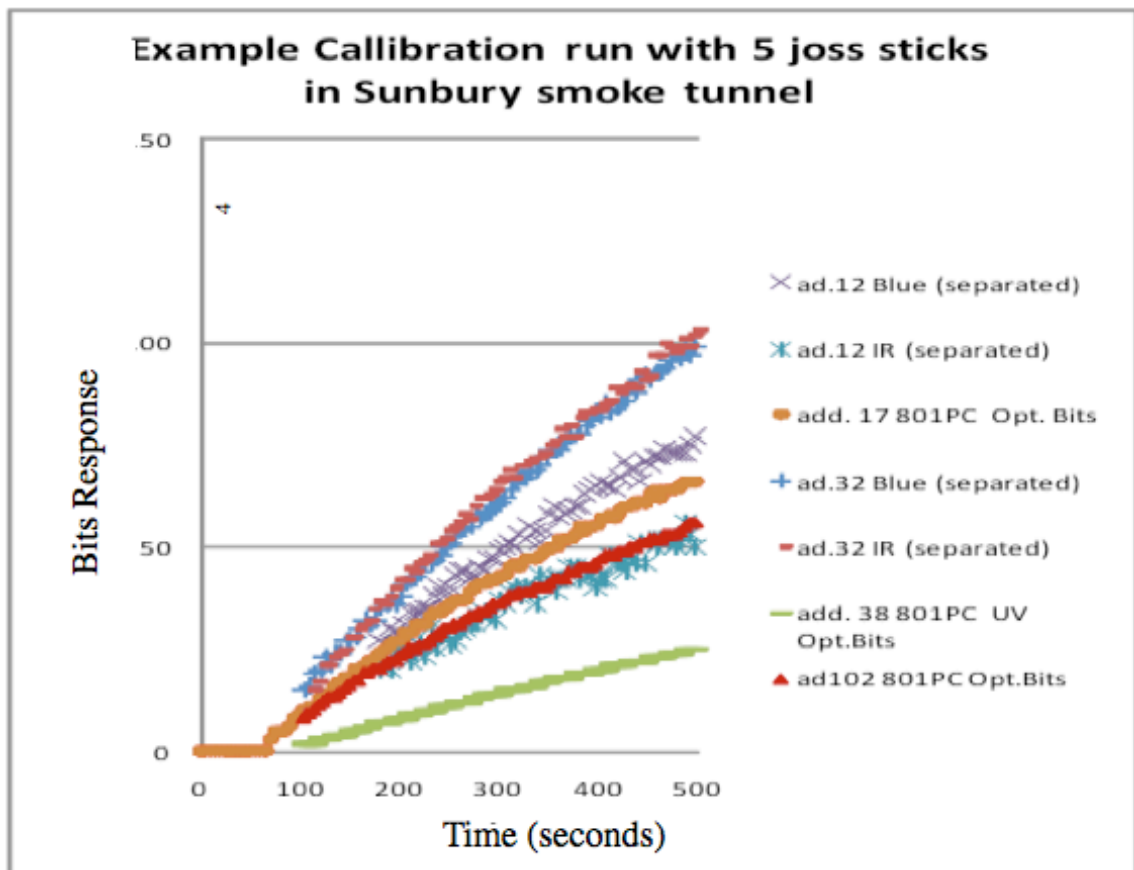


Figure 165 Response of different types of detectors described in table 62 to 5 joss sticks and 0.2m/s airflow in TYCO smoke tunnel.

165 shows composite results from a series of test runs with joss sticks in the Sunbury tunnel plotted against the scatter signal for 801PC device address 17 which is taken as a reference device for the following data processing. A ratio of response for any device may be calculated by the expression below:

$$\text{Response Ratio} = \frac{\text{Device signal}}{\text{Device signal for standard (add.17)}} \quad (28)$$

Equation 28 Device Response ratio calculation

166b shows a plot of Response Ratios for the devices obtained by processing the data shown in Figure 166a for the joss stick test in the Sunbury smoke tunnel.

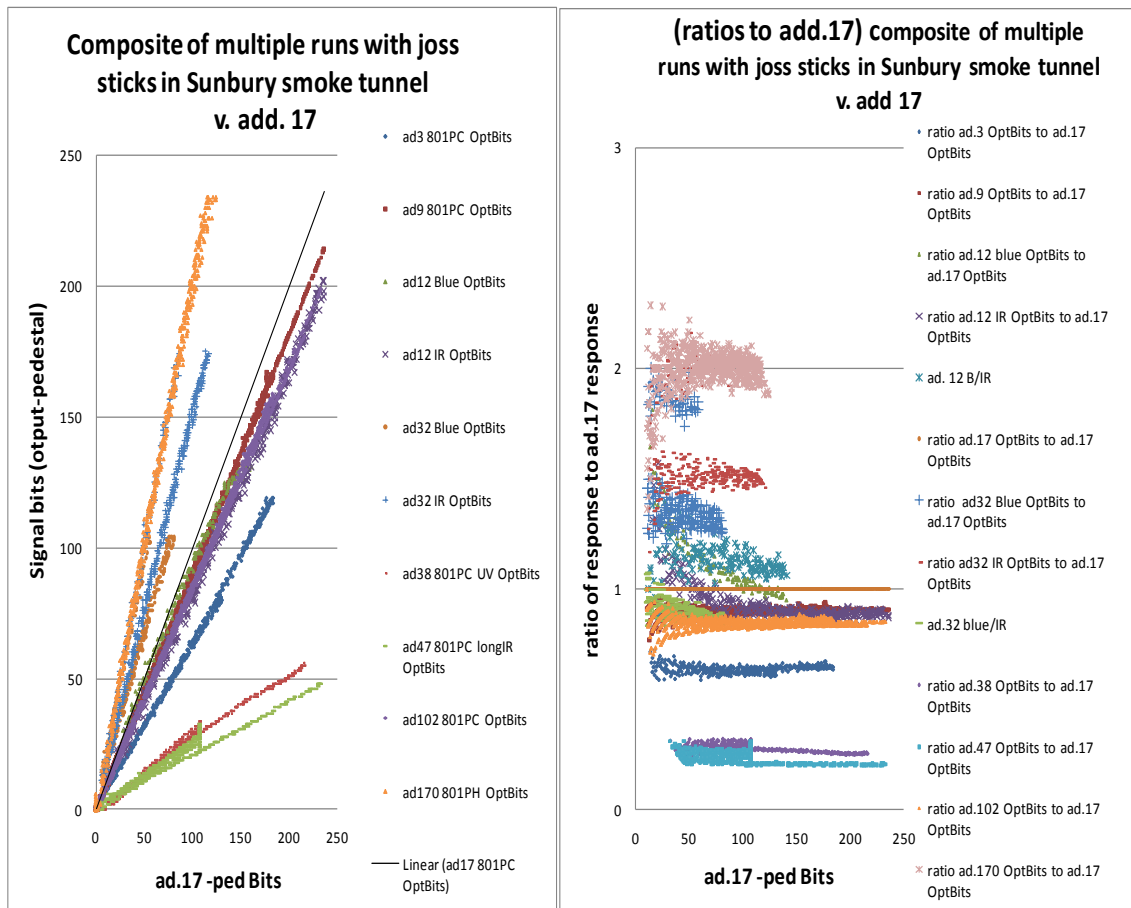


Figure 166 Composites of calibration runs carried out in the Sunbury smoke tunnel  
 (a) Signal from the experimental devices plotted versus signal from TYCO device (add. 17)  
 (b) Ratios of signals (signal for each device / signal for NIR device ( generally add. 17)) is plotted against the output signal from the standard device ( add. 17)

For experimental dual wavelength devices add. 12 and add. 32 which incorporate both blue and IR sources in the same chamber the separate blue and IR contributions are first calculated from the values on two output channels corresponding to IR and blue together and IR alone using factors determined by the circuit design and validated by other tests carried out at Sunbury before these units were supplied for use in this study. Ratios for blue to IR signals in devices add. 12 and add. 32 are also shown in Figure 166.

The differences in slope shown in Figure 165 and Figure 166(a) and ratios in Figure 166(b) are set by the combinations of components used and amplification settings. The purpose of this section of the study is to determine whether changes of smoke or aerosol type consistently affect the blue or UV to IR response ratios. To aid such comparison normalisation factors were determined to adjust the slopes and corresponding ratios to

match the values for a standard near IR optical device (type 801PC add. 17) for joss stick smoke .i.e. to bring the slopes in Figure 167 together to that of device add.17. The determined normalisation factors are given in Table 61 below.

Normalised signals for each device are obtained by dividing the Device Signal (equation 27 above) by the device normalisation factor. As applied in excel this is calculated from raw data output using the formula:

$$\text{Normalised bit signal} = \frac{\text{Integer ((raw bit output – pedestal bit output))}}{\text{normalisation factor} + 0.5} \quad (29)$$

Equation 29 Excel calculation normalised signal values

The corresponding Ratio of Normalised Responses is calculated according to equation 30 below:

$$\text{Ratio Normalised Response} = \frac{\text{Normalised bit signal}}{\text{Device signal for standard.(add.17)}} \quad (30)$$

Equation 30 Device Response ratio calculation

Values used for data shown in Figures 167 to 185 were determined by applying these calculations and the normalisation factors from Table 63 to raw results from a series of tests at Sunbury, UCLan and BRE.

<b>Address</b>	<b>Wavelength nm</b>	<b>Device type/description</b>	<b>Normalisation factor</b>
<b>3</b>	850	801PC	0.627
<b>9</b>	850	801PC	0.903
<b>12</b>	465	Experimental (blue LED)	0.956
<b>12</b>	840	Experimental (NIR phosphor)	0.829
<b>17</b>	850	801PC	1
<b>32</b>	465	Experimental (blue LED)	1.347
<b>32</b>	850	Experimental (NIR LED)	1.526
<b>38</b>	370	Experimental (near UV LED)	0.26
<b>47</b>	1070	Experimental (longer NIR LED)	0.21
<b>102</b>	850	801PC	0.848
<b>170</b>	850	801PH	2.031

Table 63 Normalization factors for each of the TYCO devices used in Figures 165 and 166 .

The result of applying selected factors to the Sunbury tunnel joss stick test data is shown in 167a and 167b below:

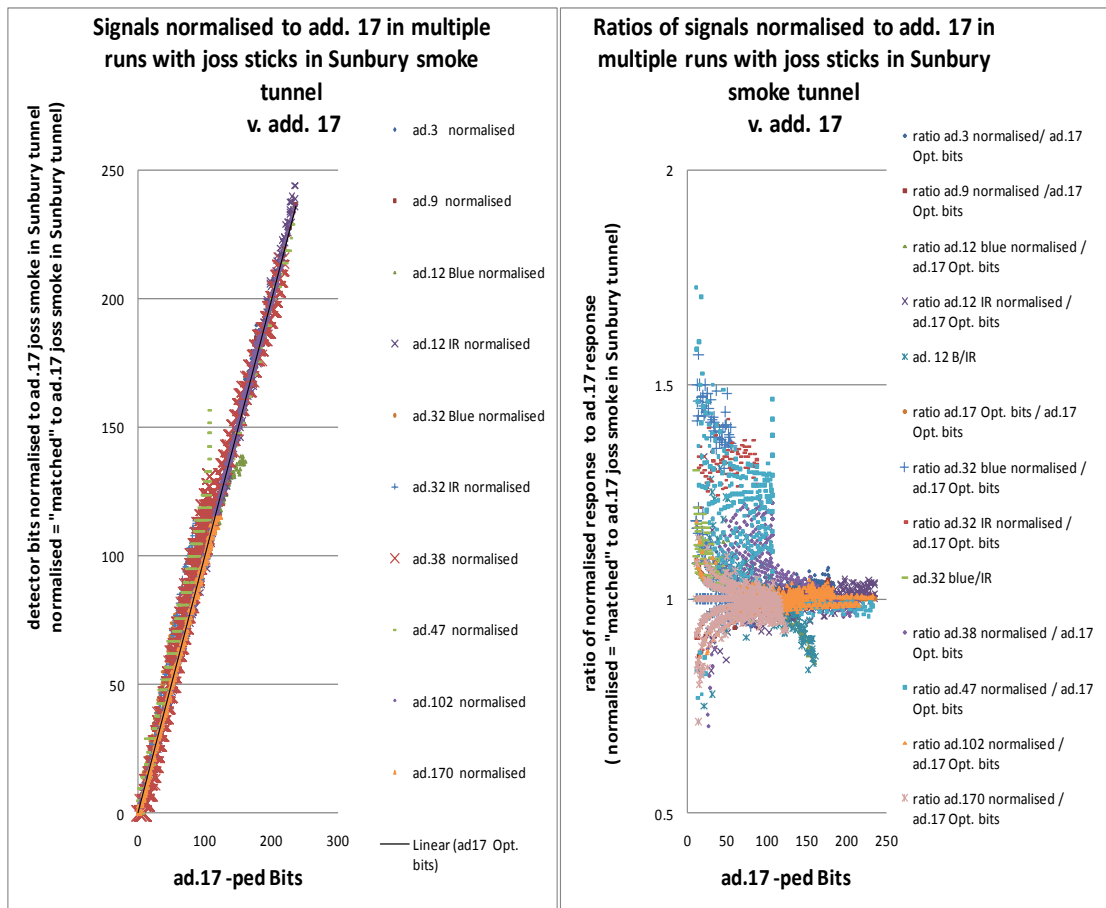


Figure 167

a) Composite of calibration runs. The “normalised” signal was plotted versus signal from TYCO device (add. 17).

b) Composite of calibration runs. The ratio of “normalised” output was plotted versus signal from TYCO device (add. 17).

(The ratio of “normalised” signal = normalised signal for device/signal for device add.17 , equal to 1 if normalisation is perfect)

Values for the ratio of blue or UV to IR signals using data from devices with addresses 12, 17, 32, and 38 are provided again in Figure 168. It is immediately clear that signal ratios vary with smoke level, unsurprisingly showing larger variations at low levels of smoke but tending towards steady values at higher smoke concentrations. Linear dynamic range on some of the devices (especially the blue/near IR device add. 32) limit the range of smoke concentrations over which the data processing can be applied.

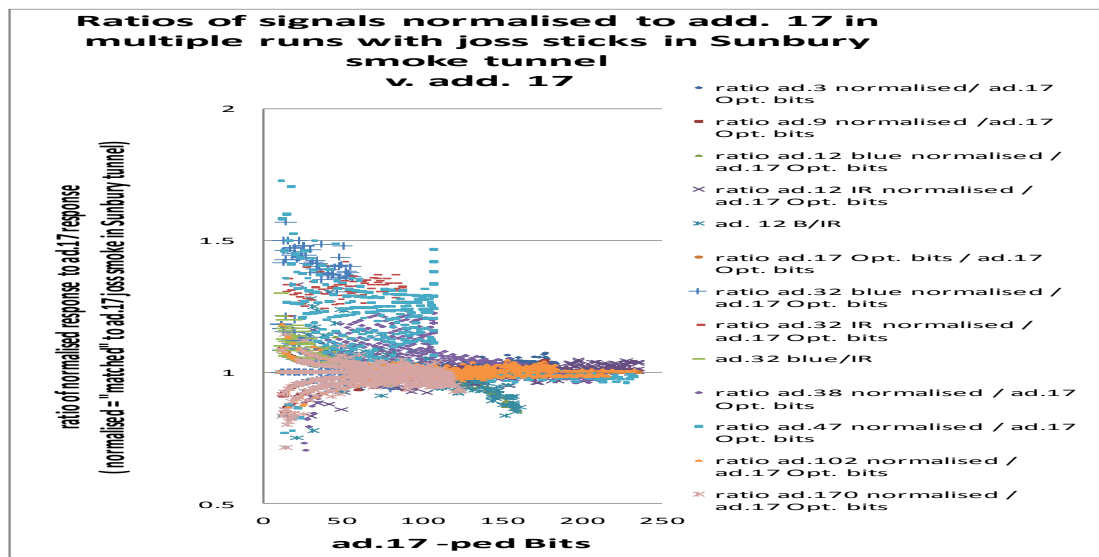


Figure 168 Multiple calibration values from blue, UV LEDs fire detection devices . The ratio of “normalised” output to the output from a standard TYCO device ( add. 17) signals Vs. standard output add. 17

Data from a series of BS EN54/7 test fire emulations carried out in the test box at UCLan and the Sunbury smoke tunnel was processed to give outputs normalised to device add. 17 in joss stick smoke and the results for collections of such tests (~4-8 for each test type) plotted below showing normalised output, ratios of normalised output to add. 17 signal, and ratios for the subgroup with blue or UV LEDs, all plotted against add.17 signal values. For the UCLan enclosure data, Figures 169-170 are for the TF2 emulation, Figures 171-172 for the TF3 emulation, 173-174 for the TF4 emulation, and Figures 175-176 for the TF5 emulation.

A similar process was carried out from data collected from smouldering wood and cotton experiments carried out in the Sunbury smoke tunnel and this data is shown in Figure 177.

Data from a series of tests in the full scale fire test room at BRE have processed in the same way. These tests were BS EN54/7 tests TF2, TF3, TF4, and TF5. Data for the individual tests subject to the same normalisation procedure as for the UCLan tests is plotted in Figures 178-185.

It is immediately obvious that some of the data in these plots shows much scatter or at least wide deviation from what might be expected for simple shifts in relative response in going from one fire test to another. Devices with the same construction, LED and

photodiode types as the standard device (add.17) often do not track or match its response well.

### 6.3.1 UCLan Smouldering wood (TF2)

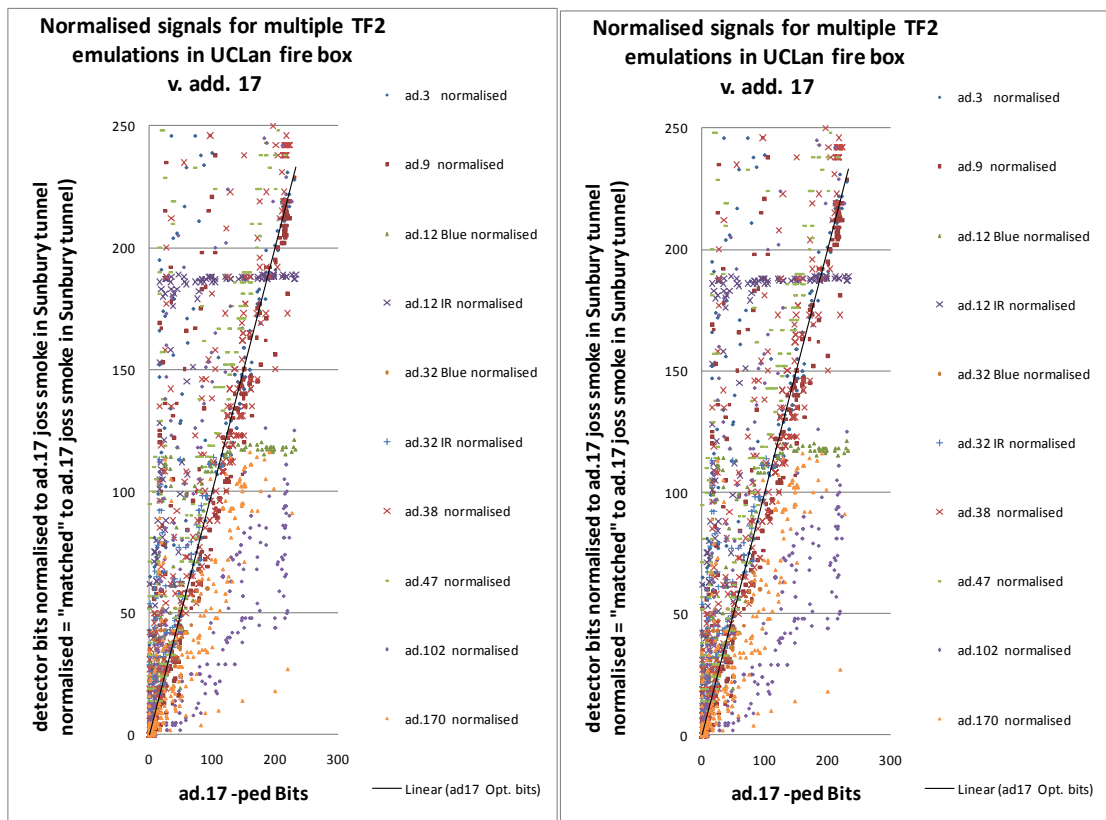


**Figure 169** (a) Multiple TF2 in UCLan enclosure “normalised” signal V. std. signal (add. 17),  
 (b) Ratio normalised signal : std. signal ( add. 17) Vs std. signal ( add. 17)

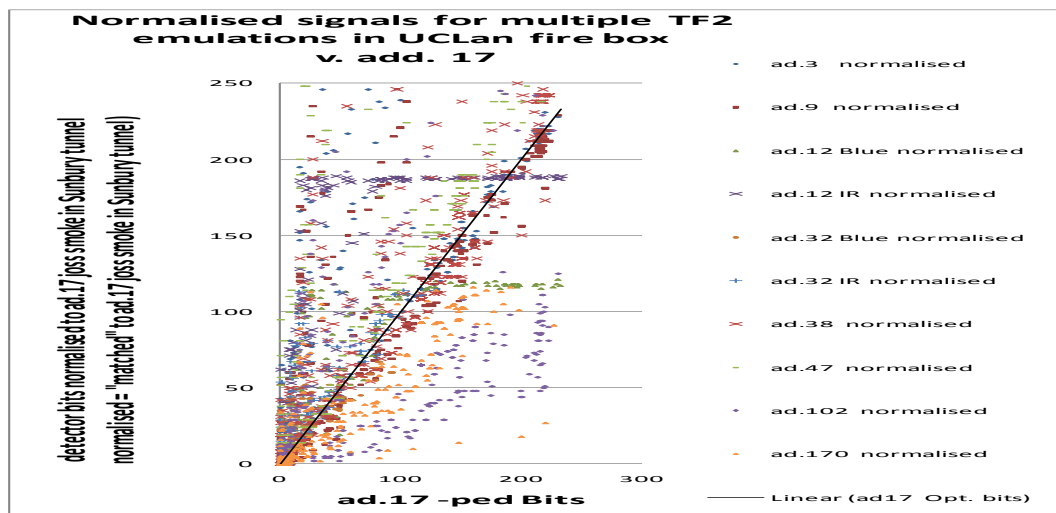


**Figure 170** TF2 emissions collected during scaled UCLan experiments .The Blue, UV LEDs detector output is converted into a ratio of “normalised” output: TYCO Standard device (add. 17) signals Vs. Output-Ped from standard TYCO device( add. 17)

### 6.3.2 UCLan Smouldering cotton (TF3)

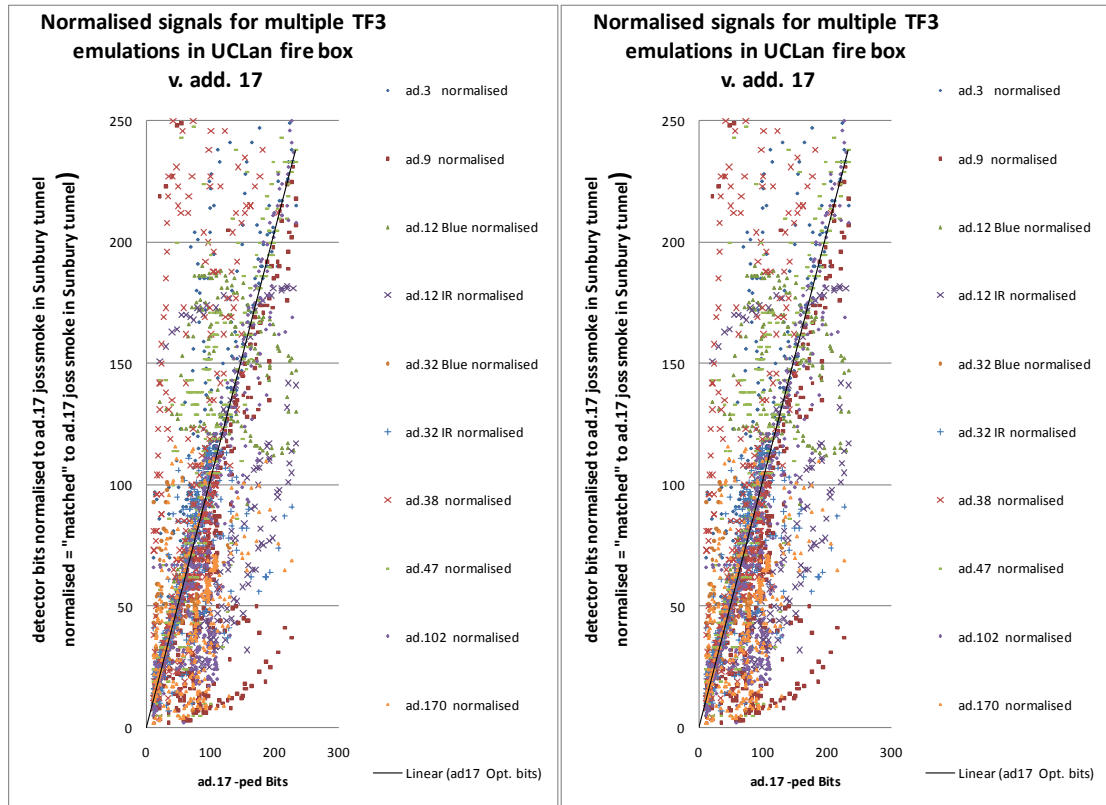


Figure 171

a)

b)

a) Multiple TF3 UCLan emulations “normalised” signal versus signal from standard TYCO device (add. 17), (b) Ratio of normalised UCLan output data:output from standard TYCO device (add. 17) Vs. Standard TYCO device bit-ped output (add. 17)

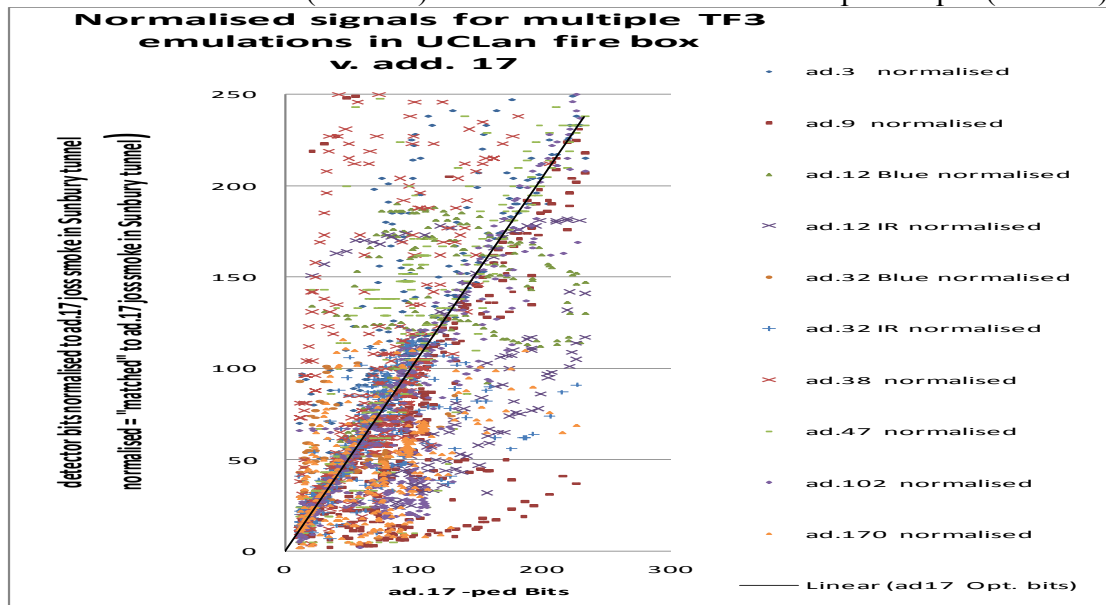


Figure 172 TF3 emissions collected during scaled UCLan experiments. The Blue, UV LEDs detector output is converted into a ratio of “normalised” output: TYCO Standard device (add. 17) signals Vs. Output-Ped from standard TYCO device (add. 17)

### 6.3.3 UCLan Flaming polyurethane (TF4)

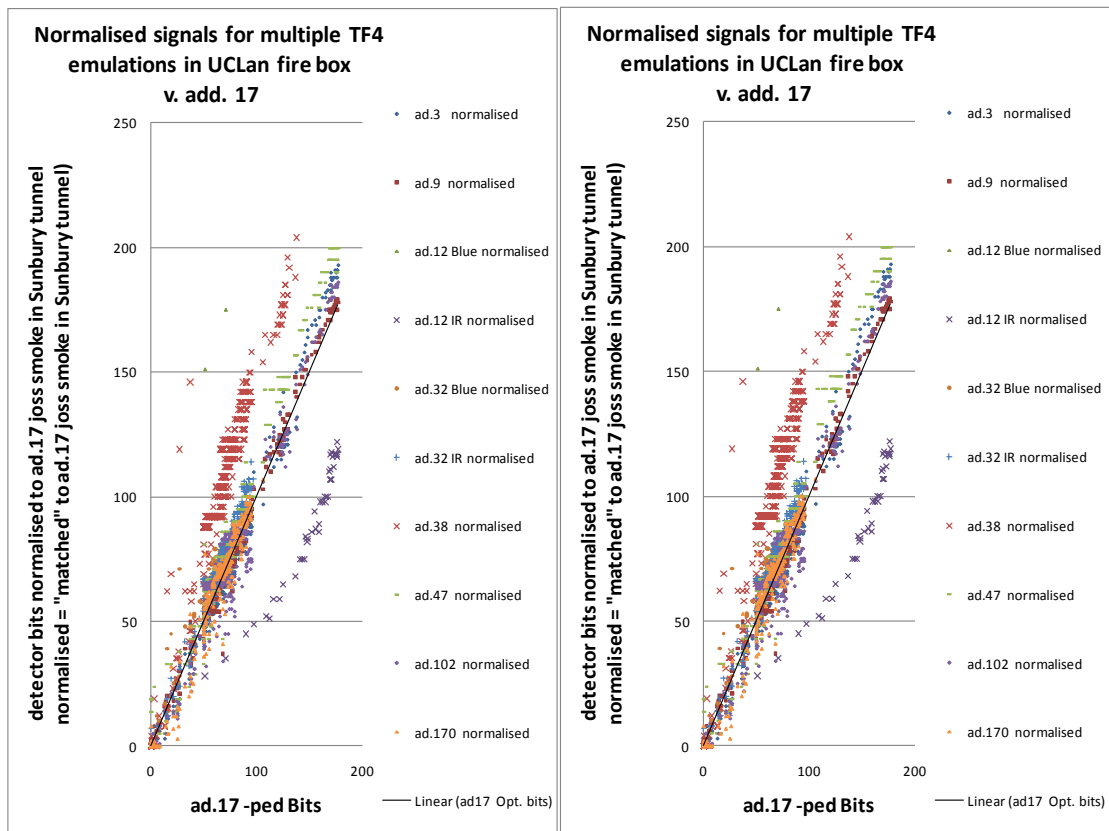


Figure 173 a) Multiple TF4 UCLan emulations “normalised” signal versus signal from standard TYCO device (add. 17), (b) Ratio of normalised UCLan output data:output from standard TYCO device (add. 17) Vs. Standard TYCO device bit-ped output (add. 17)

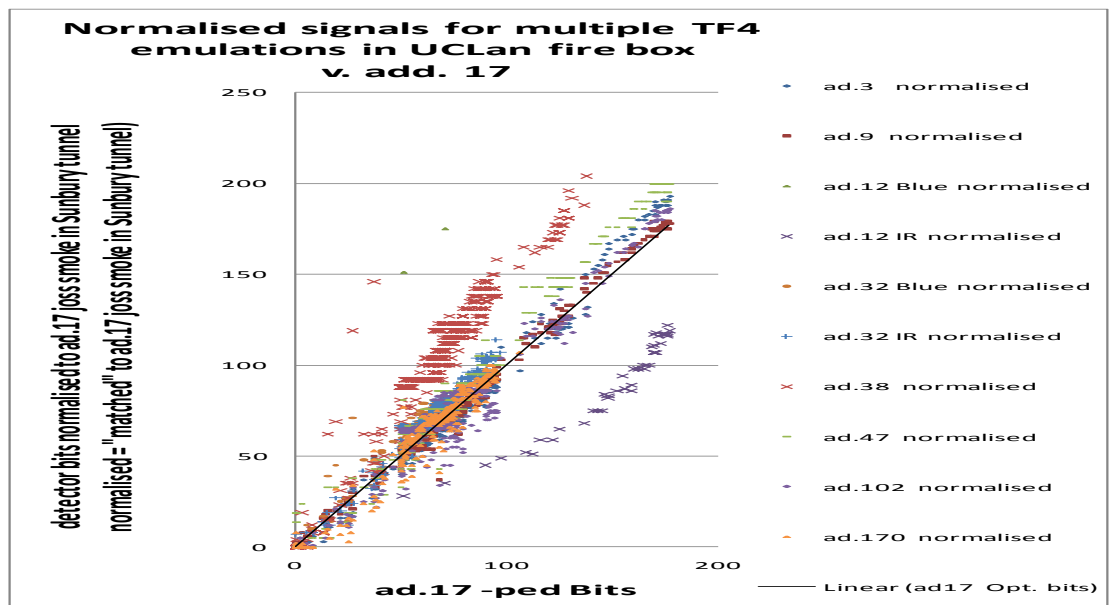


Figure 174 Multiple TF4 emissions collected during scaled UCLan experiments. The Blue, UV LEDs detector output is converted into a ratio of “normalised” output: TYCO Standard device (add. 17) signals Vs. Output-Ped from standard TYCO device (add. 17)

### 6.3.4 UCLan Flaming pool fire – Heptane (TF5)

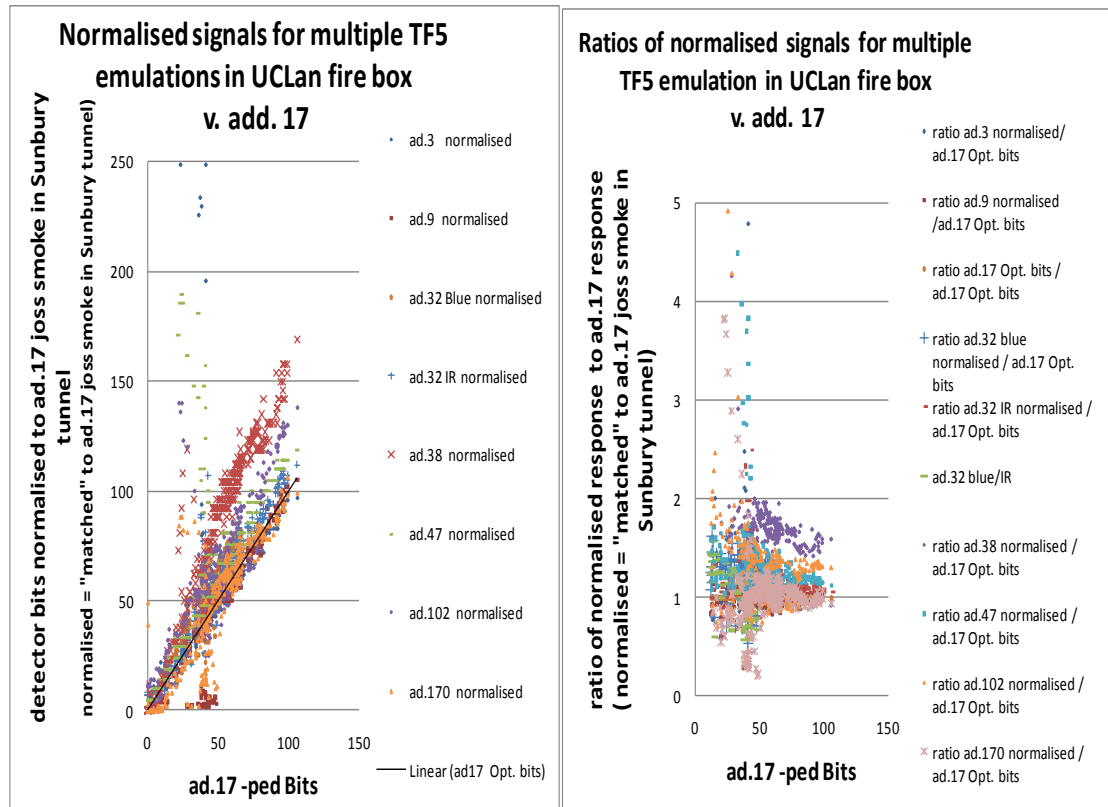


Figure 175 a) Multiple TF5 UCLan emulations “normalised” signal versus signal from standard TYCO device (add. 17), (b) Ratio of normalised UCLan output data: output from standard TYCO device (add. 17) Vs. Standard TYCO device bit-ped output (add. 17).

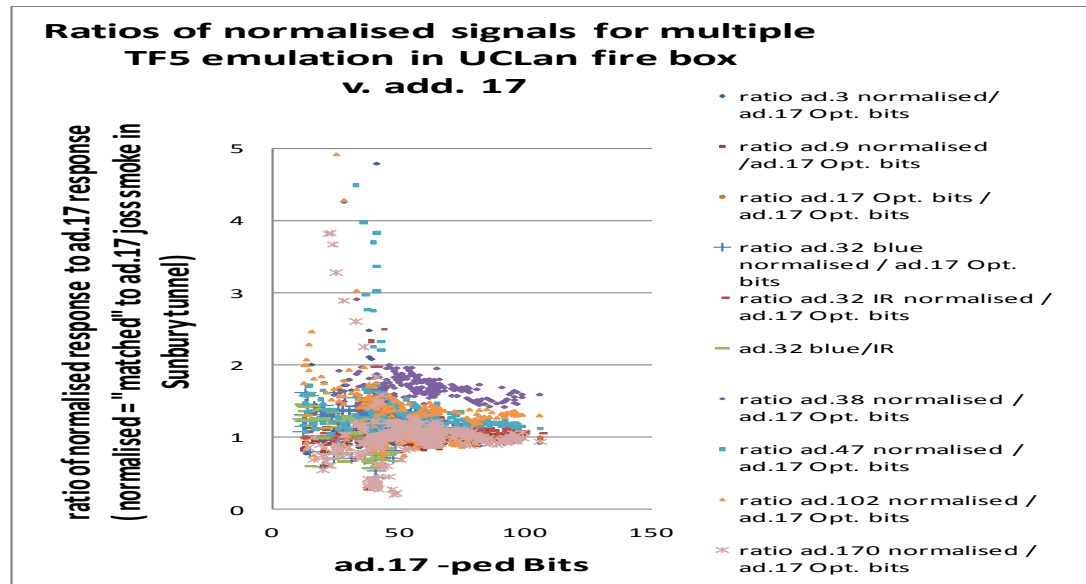


Figure 176 Multiple TF5 emissions collected during scaled UCLan experiments. The Blue, UV LEDs detector output is converted into a ratio of “normalised” output : TYCO Standard device (add. 17) signals Vs. Output-Ped from standard TYCO device (add. 17)

### 6.3.5 Sunbury smoke tunnel tests

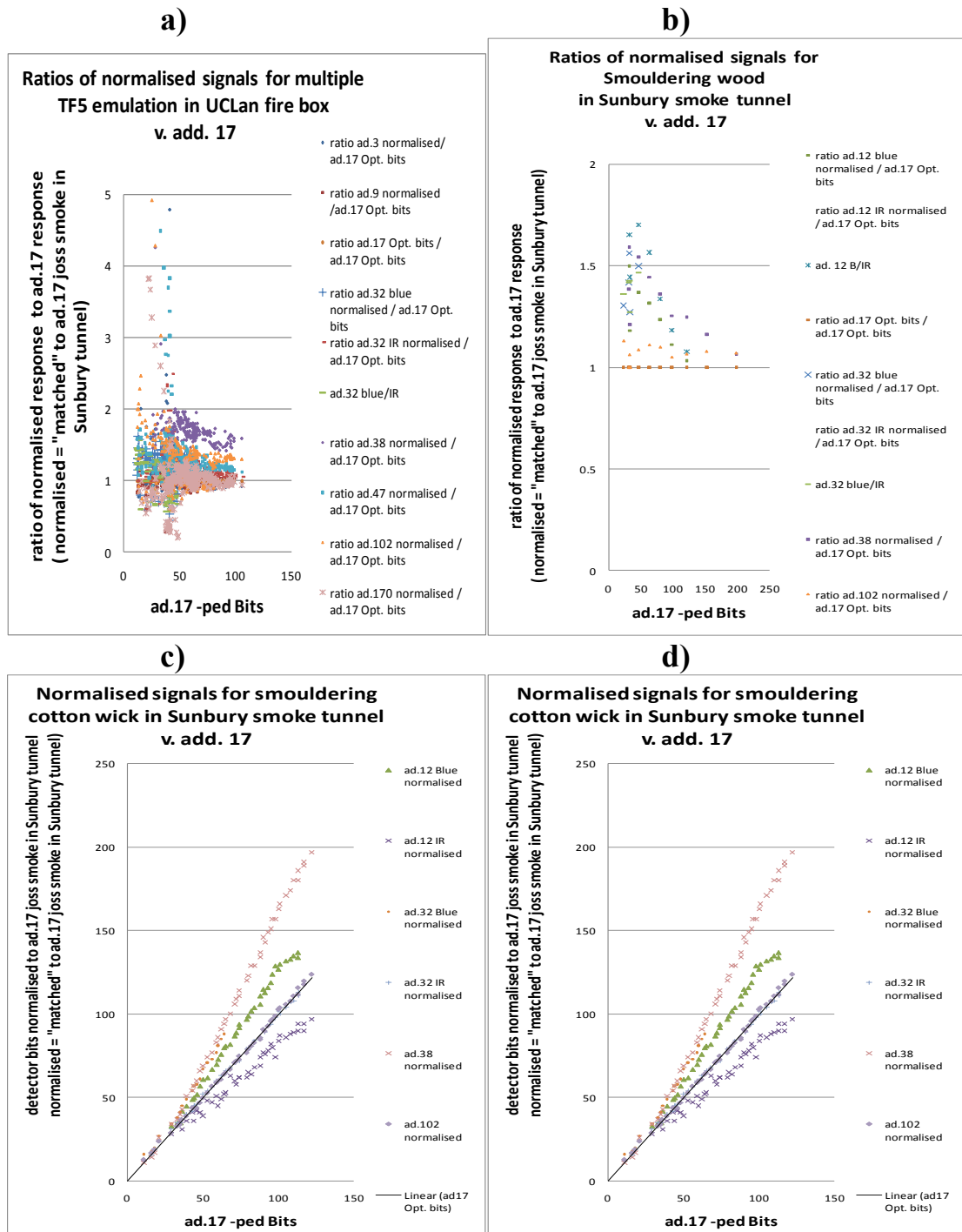


Figure 177 Pyrolysing Wood (TF2 emulation in smoke tunnel). (a) “Normalised” signals versus signal from add. 17, (b) Ratio “normalised”/ add. 17 versus signal from add. 17 Smouldering Cotton (TF3 emulation in smoke tunnel). (c) “Normalised” signals versus signal from add. 17 (d) Ratio “normalised”/ add. 17 versus signal from add. 17

### 6.3.6 BRE full scale Smouldering wood (TF2)

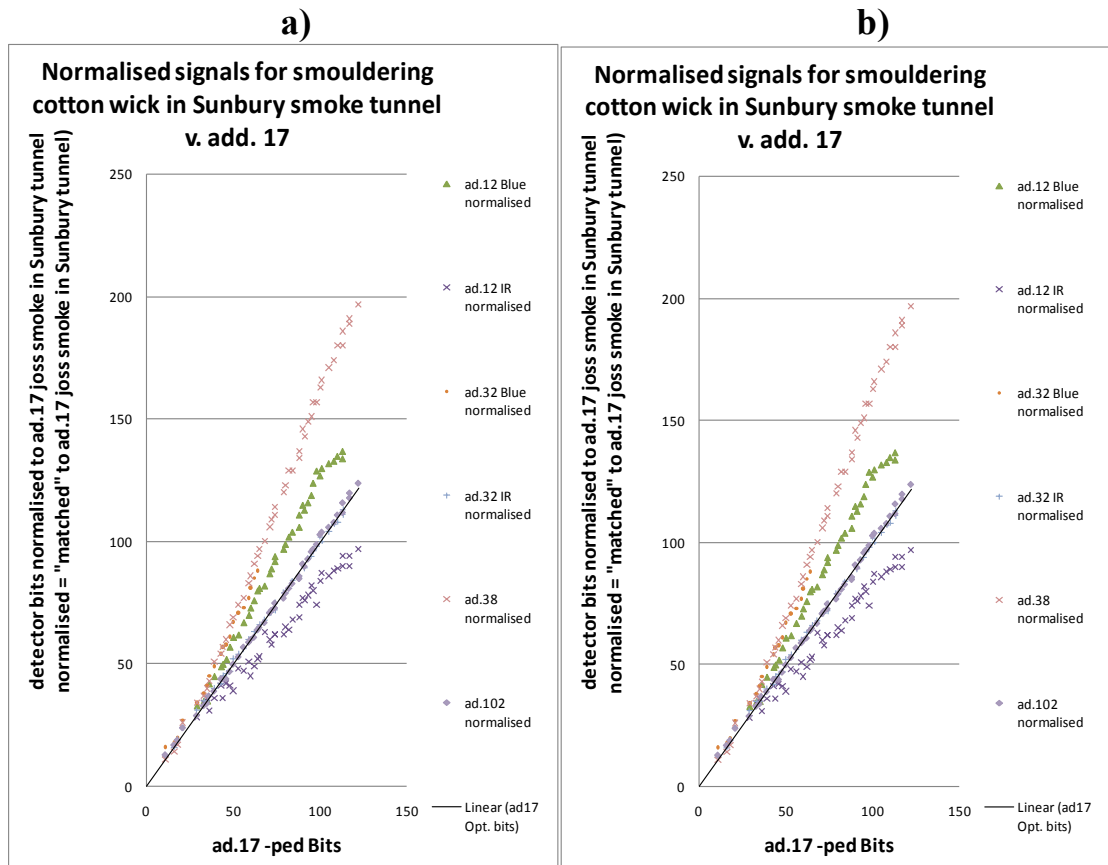


Figure 178 Full scale smouldering wood TF2 experiment carried out at BRE  
 (a) “normalised” signal versus signal from standard TYCO device(add. 17),  
 (b) Ratio of normalised UCLan output data:output from standard TYCO device( add. 17) Vs standard TYCO device (bit-ped) output ( add. 17)

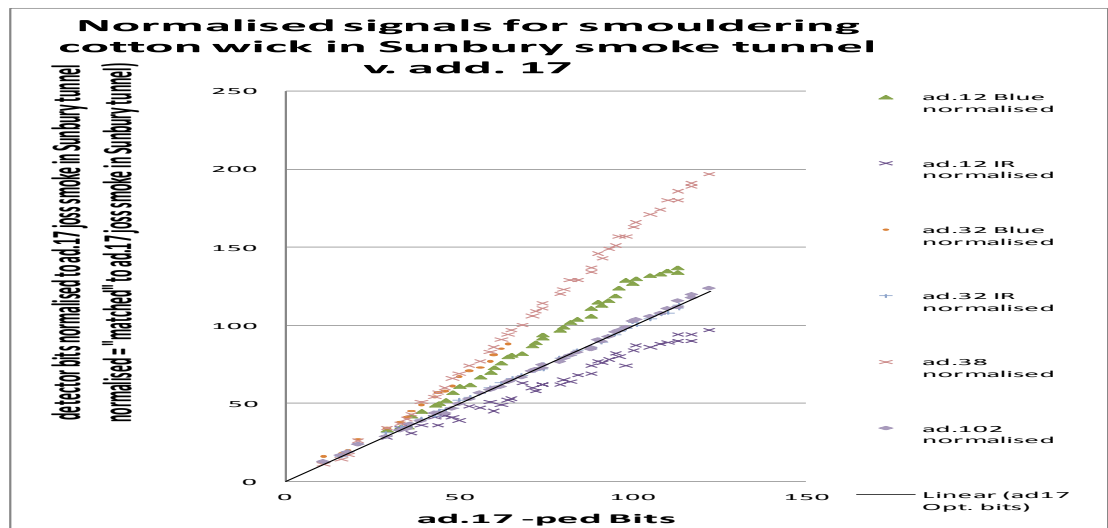


Figure 179 An example smouldering wood fire (TF2) data collected during BRE experiment . Blue & UV LED detector outputs are converted into a ratio of “normalised”output : TYCO standard device (add. 17) signals Vs. (bit-ped) from standard TYCO device( add. 17)

### 6.3.7 BRE Smouldering cotton (TF3)

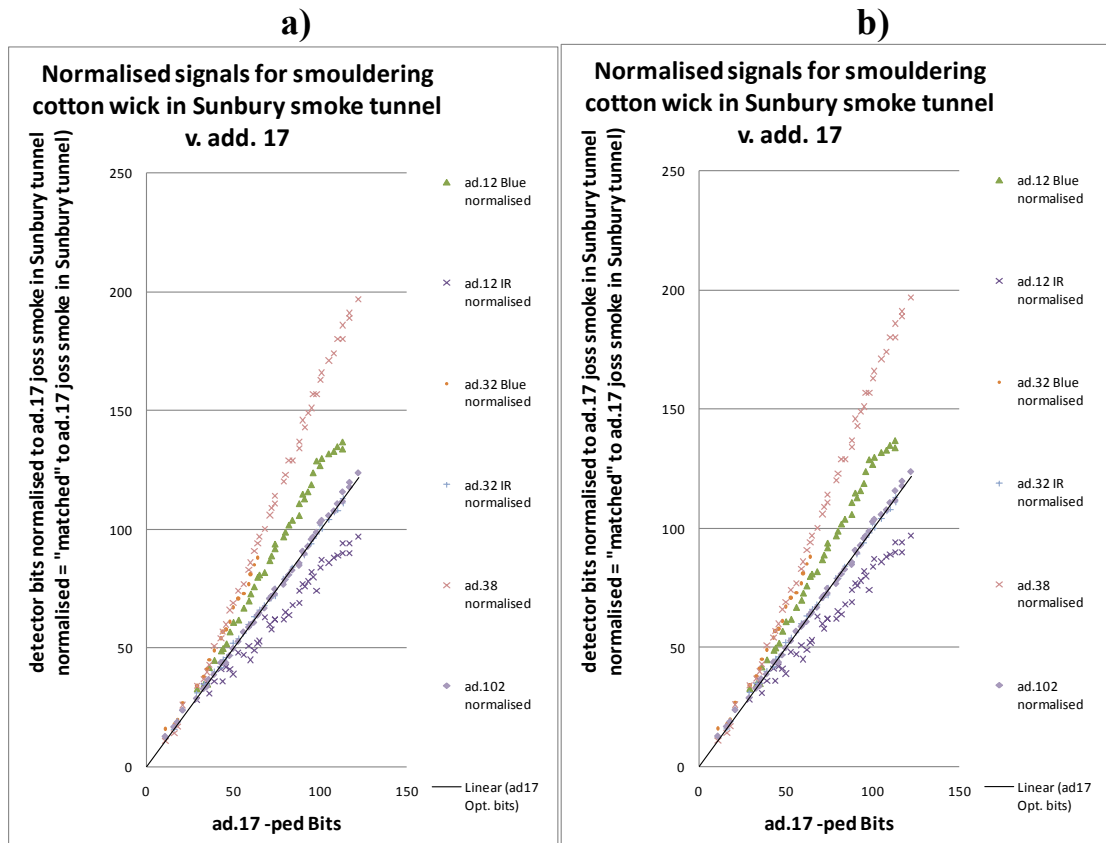


Figure 180a) Full scale smouldering cotton TF3 experiment carried out at BRE “normalised” signal versus signal from standard TYCO device (add. 17), (b) Ratio of normalised UCLan output data:output from standard TYCO device ( add. 17) Vs. standard TYCO device (bit-ped) output ( add. 17)

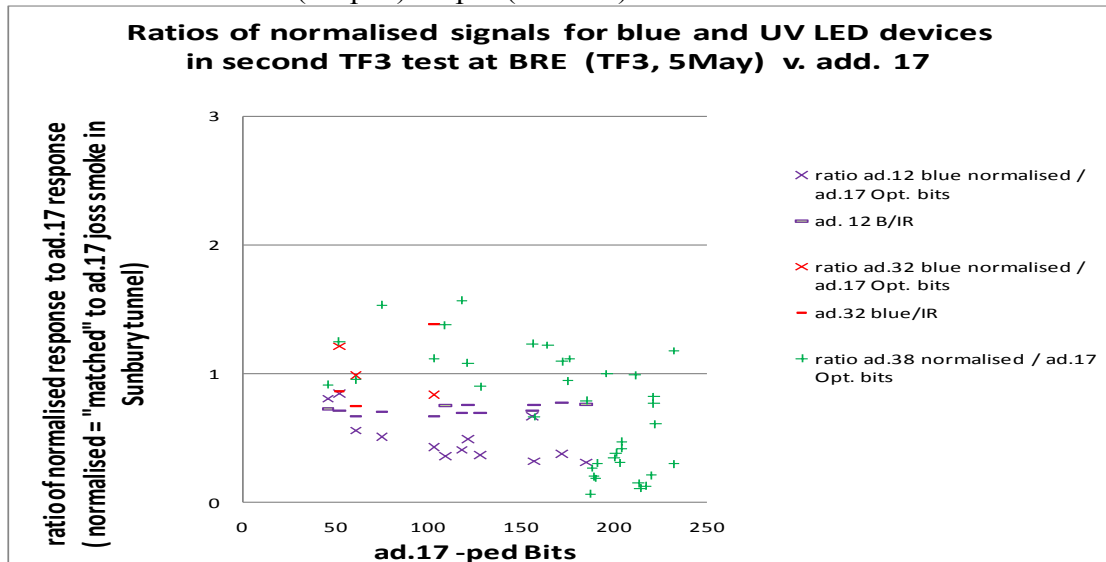


Figure 181 An example smouldering cotton fire (TF3) data collected during BRE experiment .The Blue & UV LEDs detector outputs are converted into a ratio of “normalised”output : TYCO Standard device (add. 17) signals Vs. (bit-ped) from standard TYCO device( add. 17)

### 6.3.8 BRE Flaming polyurethane (TF4)

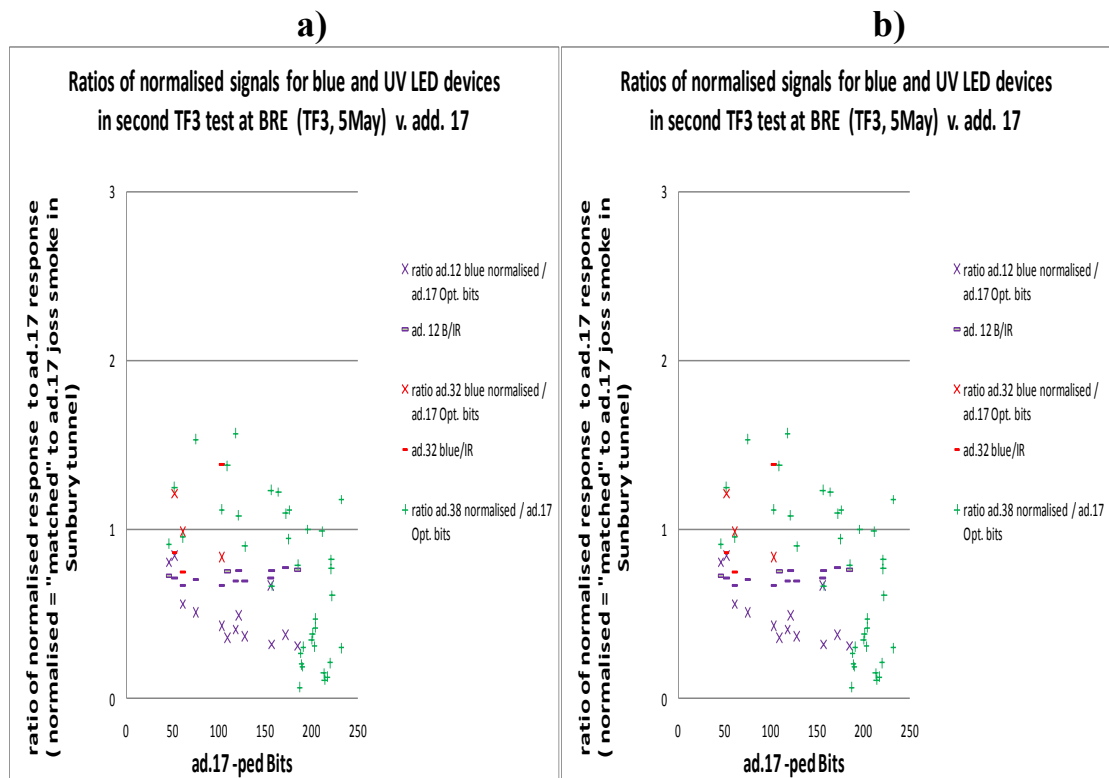


Figure 182 a) Full scale smouldering cotton TF4 experiment carried out at BRE “normalised” signal versus signal from standard TYCO device (add. 17), (b) Ratio of normalised UCLan output data:output from standard TYCO device ( add. 17) Vs standard TYCO device (bit-ped) output ( add. 17)

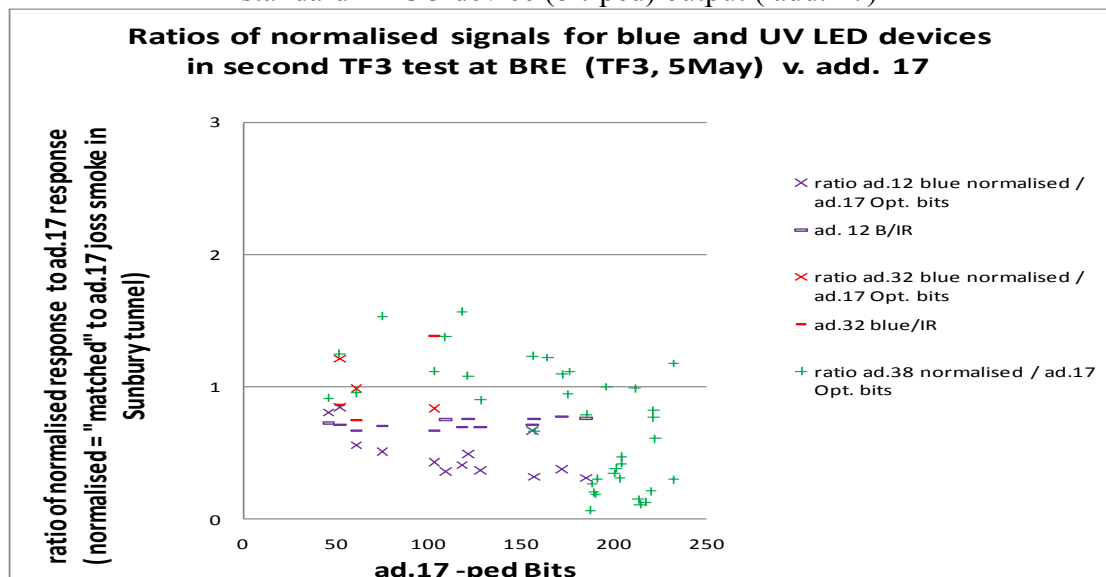


Figure 183 The recorded data collected during BRE a single experiment flaming polyurethane (TF4) fire .The Blue & UV LED detector outputs are converted into a ratio of “normalised” output: TYCO Standard device (add. 17) signals Vs. (bit-ped) from standard TYCO device( add. 17)

### 6.3.9 BRE Flaming Pool fire – Heptane(TF5)

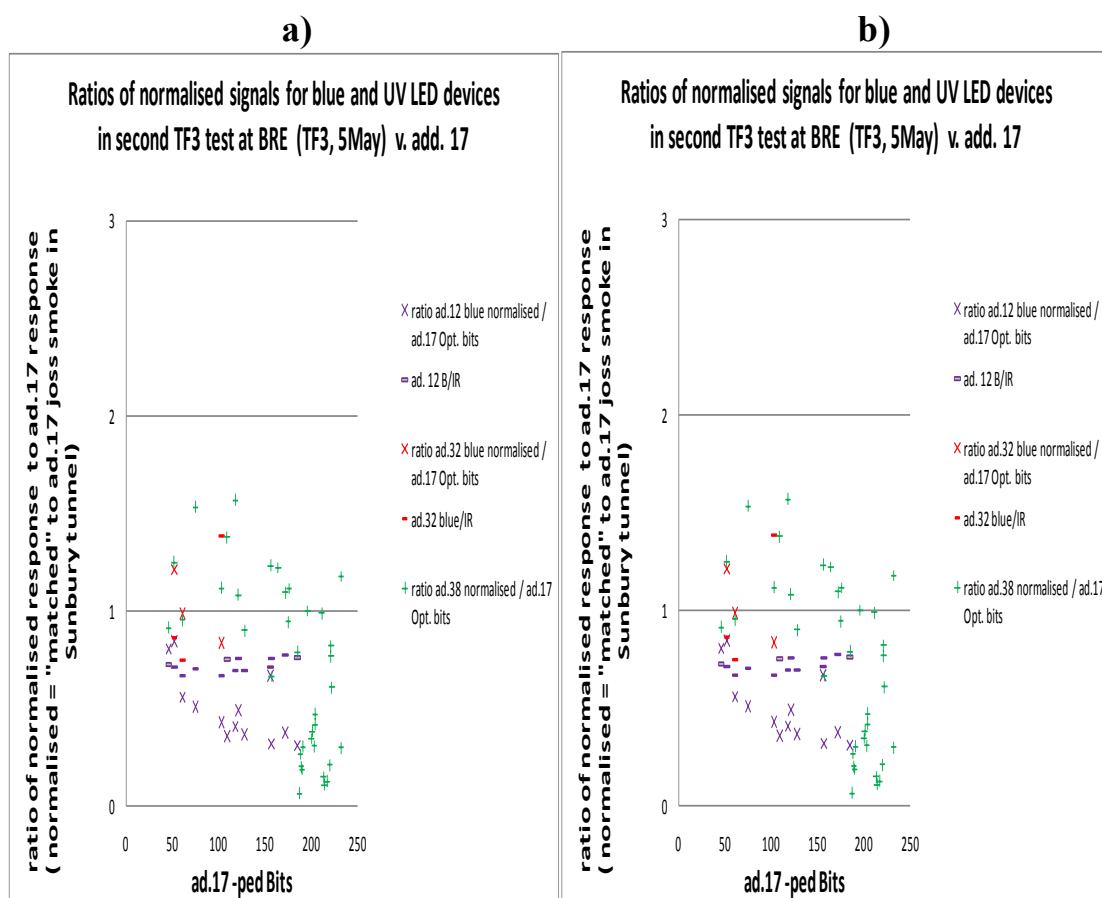


Figure 184(a) Full scale smouldering cotton TF5 experiment carried out at BRE “normalised” signal versus signal from standard TYCO device (add. 17), (b) Ratio of normalised UCLan output data:output from standard TYCO device ( add. 17) Vs. standard TYCO device (bit-ped) output ( add. 17)

The scatter seen in the results shown in Figures 164 to 185 is substantial and it is probable that at least some of this reflects differences in transport to and into detectors in different locations. This is always likely to be worst for the UCLan enclosure where there is no forced convection as in the tunnel and where detector to detector distances constitute a larger proportion of source to detector distance than for the standard test room. In reality this confirms that to get a reasonable measure of any wavelength effect on response, the measurements need to apply to the same smoke sample i.e. in the same detector. It is therefore reasonable to pay greatest attention to the results for devices with address 12 and 32 which are so constructed, and particularly to the ratio calculated from device signals alone (not involving add. 17 except in use of normalisation factors).

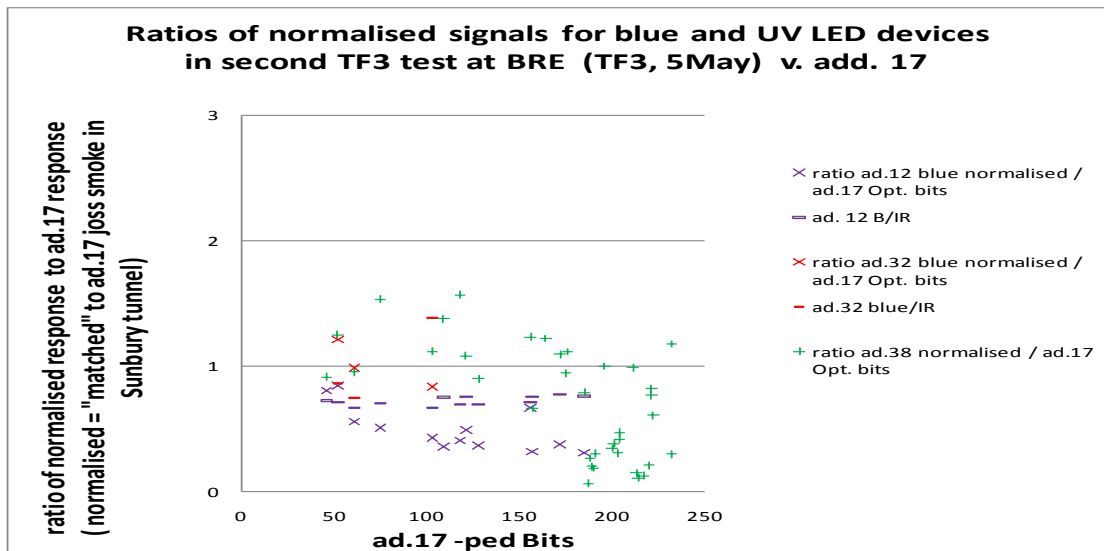


Figure 185 The recorded data collected during BRE a single experiment flaming heptane pool fire (TF5) . Blue & UV LED detector outputs are converted into a ratio of “normalised” output: TYCO standard device (add. 17) signals Vs. (bit-ped) from standard TYCO device( add. 17)

Examining the BRE test results in Figures 179-185 one may discern a trend in the normalised response ratios for the blue/near IR devices from fire to fire which may approximate to:

Normalised response ratio  $\sim 0.6$  for TF2  $< \sim 0.8$  for TF3  $< \sim 1$  for TF4  $\approx \sim 1$  for TF5.

However the scatter even in these results is such that it would not be possible to rely on such data to recognise fire type. The TF2 and TF3 emulations in the Sunbury smoke tunnel do not show agreement with results from the BRE tests. This may reflect the effects of forced air movement on the fire sources changing the smoke characteristics. The UCLan enclosure results are not inconsistent with the BRE tests but there is greater spread and again no reliable fire identification could be achieved from such results.

It is interesting to re-examine the paper by Bergmann in the light of these results. It is difficult to determine how much spread was observed in that work but it is clear that as there were only moderate changes in ratio between the TF2, TF3, TF4 and TF5 fires. A more substantial shift was observed with a burning crib fire (rarely used EN 54 Standard fire TF1) and it is perhaps unfortunate in retrospect that the emulation of flaming wood UL267 test fire was not included in this analysis. However such wood crib fires are very easily detected and so not generally considered of very great interest to detector development.

Overall the multiwavelength optical scatter results indicate that the variability in real fire situation may interfere significantly with discrimination. There may be utility with respect to some nuisance sources such as steam (not investigated in this study) but there are probably better technical solutions available.

#### **6.4 Smoke Particle Size Analysis by Cascade Impactor**

As optical scatter is expected to have some dependence on particle size it is reasonable to ascribe at least part of the differences in response to different fires to differences in the particulates generated by different fuels and fire types. A series of particle size measurements were undertaken as part of the study on the basis that these could possibly supplement and perhaps clarify the optical scatter data obtained with smoke detector devices described above and establish some independent measure of smoke parameters by using a cascade impactor particle size measurement system. The operation of cascade impactors for measurement of aerosol particle size distributions was described in general terms in chapter 1.

A New Star LLC Series 290 Marple Personal Cascade Impactor developed by McCauley based on the Marple and Rubow theory [143] regarding cascade impactors was used for these measurements. The impactor is made up of 8 different stages each with a stainless steel perforation substrate on which particulates may be collected. The impactor aerodynamically separates particles by invoking a flow through the chamber accelerating through the 6 radial slots on the initial impactor stage. Particles with sufficient momentum will impact on the substrate beneath each slot while smaller particles pass to the next stage. The slots get smaller at successive stages, and as the flow is maintained at a fixed rate, the jet velocity increases. This allows progressively smaller particles to accumulate enough momentum to impinge upon a substrate and be removed from the flow. At the end of the different stages all the remaining particulates are collected on a built in 0.34 micron filter.

The New Star LLC cascade impactor shown in Figure 186 was available for measurements on smoke from fires in the UCLan enclosure. The impactor consists of a series of metal filters and stainless steel substrates, which prior to impactor assembly

were cleaned with acetone in an ultrasonic bath to remove grease and dust particles. After drying each of the substrates was weighed and placed with the respective filter stages of the impactor assembly. The impactor was then assembled in accordance with manufactures instructions.

A calibrated pump with flow controller was connected to the impactor base and flow was set at  $2 \text{ l min}^{-1}$ . The impactor was then placed in position in the scaled fire chamber to capture fire gas plume components from each of the scaled standard and non-standard fires described below. Each fire test was monitored in triplicate.

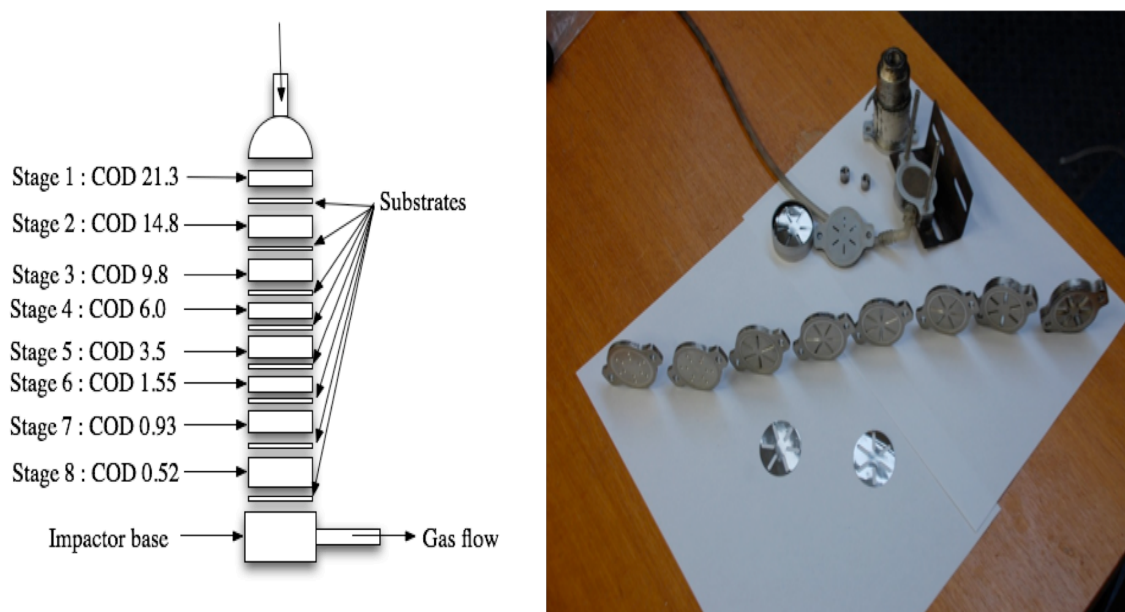


Figure 186 Diagram shows how the stages of the cascade impactor are constructed.

The image on the right is an image of a deconstructed LCC cascade impactor. On the left is a schematic of the impactor. In the schematic diagram the stage COD is the cut off diameter (in micrometers) of each of the substrate filters, which limits the size of the particulate populations, which are captured.

Following the collection of samples the impactor is carefully dismantled and each substrate is weighed a second time. These weights are then used to calculate the differential and cumulative particle size distributions. The particulate populations are calculated using the following equations.

Use of cascade impactor data requires knowledge of the cut-points of the impactor stages. This depends on the filter structure dimensions and the flow rate but the

equipment manual provides tabulated values reproduced below (Table 64) for the cut off point parameter  $D_p$  for the design airflow rate of 2 litre/minute used in this work. Inlet restrictions are taken as setting an upper limit of 50  $\mu\text{m}$  for collected material. A geometric mean value GMD calculated from successive  $D_p$  values, is taken as representing each collected fraction, ( $\text{GMD} = (D_i * D_{i-1})^{1/2}$ ).

Cut-point  $D_p$  is aerodynamic equivalent particle diameter for spherical particle of unity mass density in air at 25°C and 1 atm. Soot particle densities and indeed shape may not be fully consistent this aerodynamic equivalent specification. However the likely range of constituent materials and forms make the density assumption at least not too unreasonable.

Stage Number	$D_p$ $\mu\text{m}$	GMD $\mu\text{m}$
1	21.3	32.6
2	14.8	17.8
3	9.8	12
4	6	7.7
5	3.5	4.6
6	1.55	2.33
7	0.93	1.20
8	0.52	0.70

Table 64 Cut of Point  $D_p$  and Geometric Mean Diameter GMD for the New Star Cascade Impactor with 2L./minute air flow rate.

The flow rate, collection times, and weight accumulations allow calculations of mass concentration in air ( $\mu\text{g m}^{-3}$  of particles) corresponding to each of the eight size fractions. In Figure 187 data for three each of the BS EN54/7 fire emulations carried in the UCLan enclosure are plotted as mass concentration versus particle size (GMD value  $\mu\text{m}$ ).

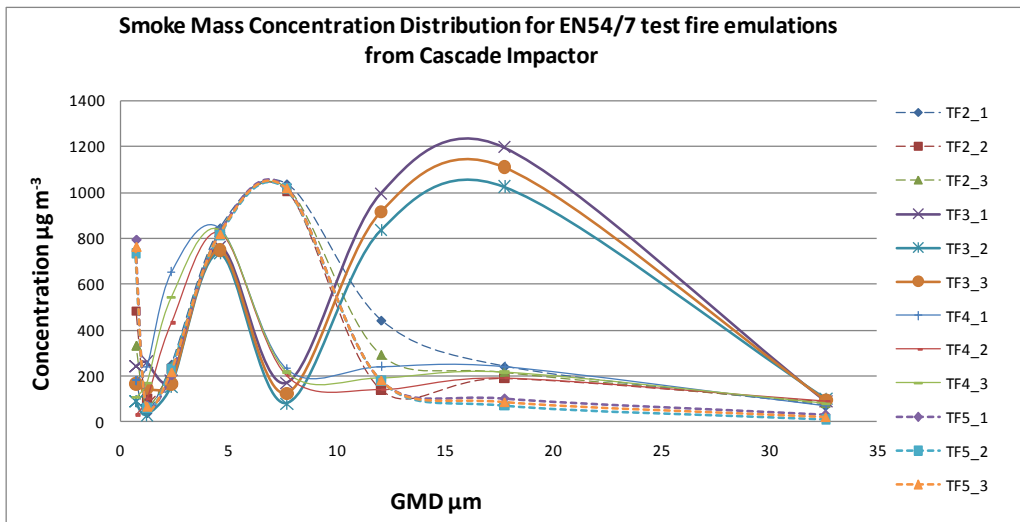


Figure 187 Particulate mass concentrations versus size For BS EN54/7 fire emulations. Concentrations are calculated from mass collected on each filter and total air volume filtered.

Results for a series of UL268 fire emulations and bread toasting experiments (2<sup>nd</sup> toasting) are shown in Figure 188 below.

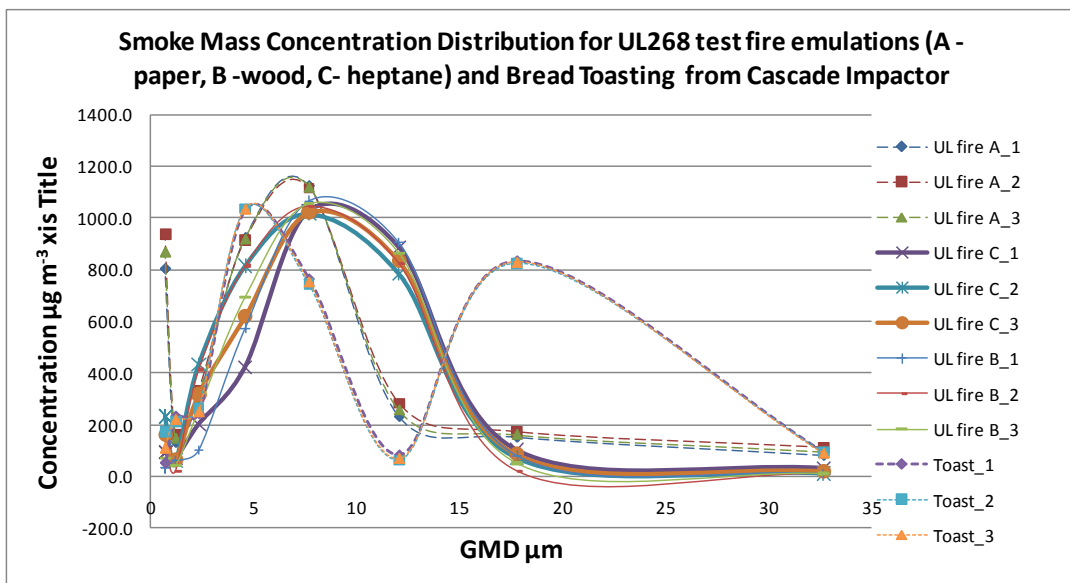


Figure 188 Particulate mass concentrations versus size For UL268 fire emulations and bread toasting

There are many ways of representing particle distributions and the representation, as mass concentration versus particle size as above may not be the most informative. Continuing with the assumption of spherical particles of unit density allows estimates of number concentrations to be calculated for each size interval by dividing mass concentration by the mass of a sphere with diameter of the relevant GMD value.

Applying this to the BS EN54/7 emulation results produces a distribution shown in Figure 190 below where the concentration is expressed on a logarithmic scale.

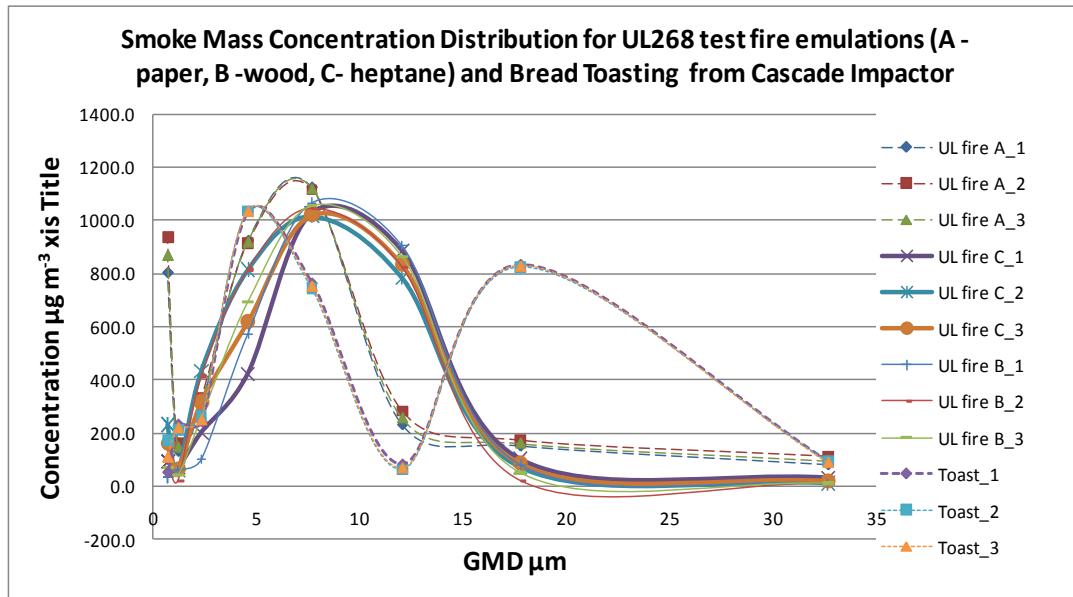


Figure 189 Particulate number concentrations versus size For BS EN54/7 fire emulations.

Viewed in this form it is fairly clear that the smallest particles are overwhelmingly the most numerous. Particle numbers are particularly important in the response of fire detectors, both ionisation and optical scatter based devices. Give the range restrictions of the impactor cascade measurements it is probable that these cannot be relied upon to generate data allowing useful comparisons with detector performance and the effects of fire type on multiwavelength optical scatter devices.

## 6.5 FAIMS measurements (High Field Asymmetric Ion Mobility Spectrometry)

### 6.5.1 Principles and Background

Ion mobility spectroscopy (IMS) and its variant FAIMS were described in general terms in chapter 1 section 1.9.6. An OWLSTONE FAIMS device was made available by UCLan towards the end of the project and applied to set of full scale BS EN54/7 fire tests carried out at BRE in May 2010 and to some tests carried out in a smoke tunnel at

TYCO in Sunbury. The interest in FAIMS measurements arises from claims by the manufacturers that it may have fire gas recognition capability, that the active device is compact being based on a small micromachined chip, and that costs can potentially become low enough for future incorporation in fire detection equipment. The system presently available is an analytical device with a Windows enabled computer incorporated to control device operation and data collection.

The operation of a Owlstone FAIMS unit may be understood in terms of Figure 190a and 190b below reproduced from Owlstone publications [144][145] As for conventional ion mobility spectrometry (IMS), FAIMS measurements rely on differences in mobility of ionized species in air, however IMS operates with relatively low field gradients where the mobilities of the ions in air show little or no field dependence (to left in Figure 190a) while FAIMS also uses the higher field gradient region (to right in Figure 190a) where mobility varies with field and different molecules can show different variability (molecule A, B, C). Application of a pulsed asymmetric field (higher field in one direction, lower in other) between filter electrodes as shown in Figure 190b acts on ions passing towards a collection electrode.

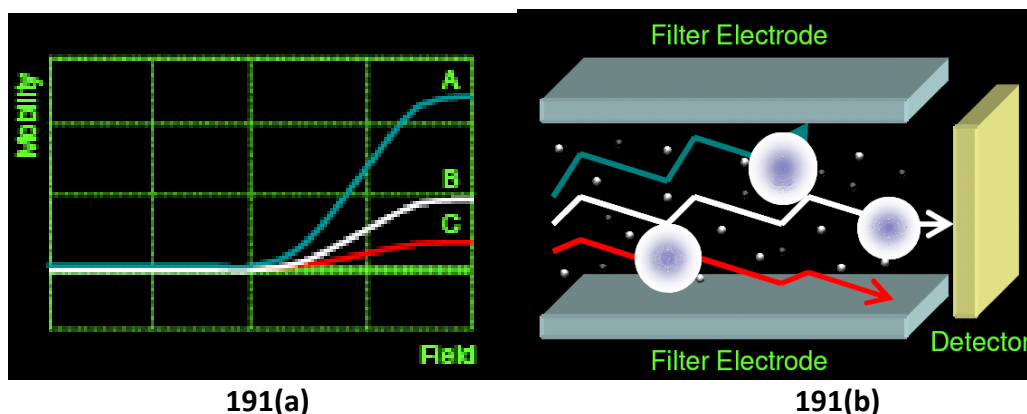


Figure 190 Principle of FAIMS Operation (a) effect of field on mobility, (b) application of pulsed asymmetric field to selectively deflect ions to filter electrodes.

Only ions suitable mobility characteristics reach the collection electrode to produce a signal and others are lost to the filter electrode. This selectivity is further modified by application of DC bias fields between the filter electrodes.

Sample air is subjected to ionisation, most commonly Ni 63 Beta emitter as for this study. A substantial advantage of FAIMS is ability to sample untreated but filtered air directly and units may be operated with photo-ionisation and possibly with corona

based units. Ions, usually associated with water molecules, are then moved by an applied electric field towards a current measuring collection electrode passing through a filter electrode assembly where some ions are selectively removed as indicated above. Etching silicon forms the filter electrode assembly in an Owlstone chip ~0.5 mm thick to provide inter-digitated comb electrodes and its operation is illustrated in Figure 191.

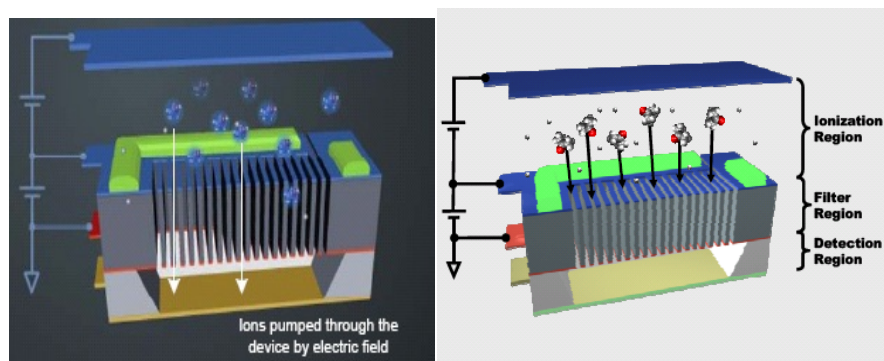


Figure 191 Representation of FAIMS Filter Operation.

The field parameters (pulsed field, and DC bias or compensating voltage) operating at the filter can be varied with time and the collected ion current plotted against those variables. This may be displayed as in Figure 192a and 192b below reproduced from the unit operation manual showing results for benzene in air.

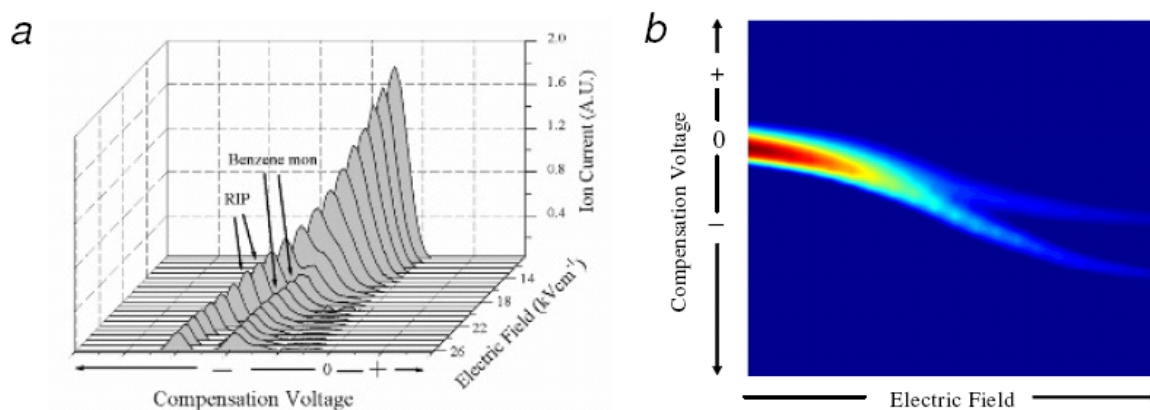


Figure 192 Representation of Display of FAIMS Spectra with Ion current shown on 3d graph or as false colour scale(b) .

### 6.3.2 Experimental Work with FAIMS equipment

The short FAIMS study within this work was directed at measurements on standard BS EN54/7 fires in the full-scale standard test room at BRE. This was supplemented by a series of measurements in the Tyco smoke tunnel. The unit was operated in “Lab User” mode where the range of mobility parameters accessible to the unit are scanned over a period of ~2 minutes to build up a display image of a mobility spectra which may

provide a “finger print” of the gas types present. It was not expected that identification of particular gaseous components would be possible although such capability is claimed for the kit under controlled conditions. These tests were intended to demonstrate whether FAIMS could reliably distinguish between clean air and air containing fire products, and whether the different tests fire types could be distinguished one from another. The unit is equipped with an aspiration system and was provided with pre-filters (~0.2  $\mu\text{m}$ ) to remove particulates. The ionisation of gases generates both positive and negative ions.

The unit was operated in “Lab User “ mode the unit, which displays mobility dispersion spectra as false colour images for both positive and negative ions. The “spectra” are built up as a series of parameter line sweeps (varying dispersion fields and compensating voltages affecting ions transiting the detector chip) and these are recorded as data files (matrices of data taking ~2 minutes for each scan ) which can be further processed in excel to generate lines scans and plots showing changes in going from clean to contaminated air. This can aid data analysis and inspection. Although this was carried out, such plots are not shown here.

Figure 193 shows the FAIMS kit mounted on the TYCO fire tunnel with a pumped system provided to present part of the tunnel air stream to the instruments gas inlet.



Figure 193 FAIMS Instrument operating to collect spectra for gases in TYCO smoke tunnel.

The build up of dispersion spectra can be seen on the display. For the BRE tests a line with glass filter was simply inserted through one of the ceiling detector mounting ports.

Prior to each test a clean air spectra is acquired before air containing fire products is sampled. The unit is designed to respond to gases not particulates and in addition to the external filter there is an inbuilt unit. The FAIMS devices give close to real time updates of the smoke sampled and displays a trace every 8 seconds and full scan in ~2 minutes. Inherent response time is fast but in scan mode the fire gases may change very substantially within one sweep period.

The unit was operated throughout the tests with standard optical scatter detectors in operation, for Sunbury and BRE, and optical absorption measurements at BRE. The FAIMS files could be correlated with recorded fire times and fire detector and BRE obscuration meter file records.

Owlstone staff were consulted about operation of the kit, data analysis and some of the initial results obtained. Software for analysing the data files was also provided by Owlstone. Following examination by Owlstone staff of files obtained for clean air input, it was suggested that the equipment had been subjected to some significant and persistent contamination prior to these tests. Improvements to the sample inlet system alleviated this issue and it was not felt that the overall results were very significantly affected. Figure 194 below reproduces a display for clean air.

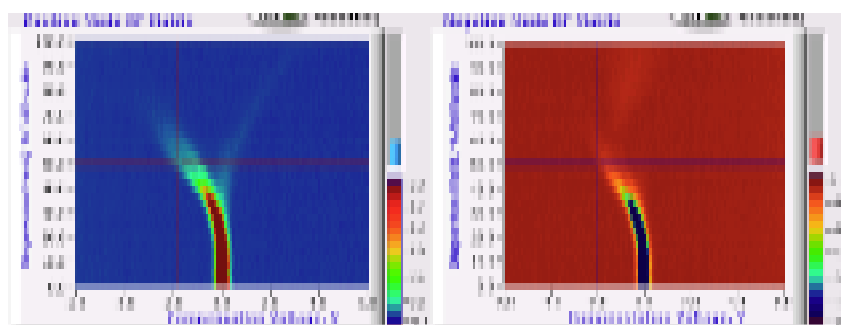


Figure 194 Example clear air plot from capillary file prior to the collection of smoke from standard fire . The blue background display is the positive ion trace and the red background image on the right represents the negative ions produced after the gas is passed through the ionization source.

Prior to each test a clean air spectra is acquired, (an example is given in Figure 194) before smoke is sampled. The FAIMS devices give close to real time updates of the smoke sampled and displays a trace every 8 seconds. The presence of organic material is expressed by the shifting of the elevated ion current “tendrill” from the left to the right

representing a change in compensation voltage for which ions generate an ion current (reach the detection electrode). The amount of organic material present is represented by the intensity of the colour of the “tendrils”.

#### 6.4.1 Smouldering wood (TF2)

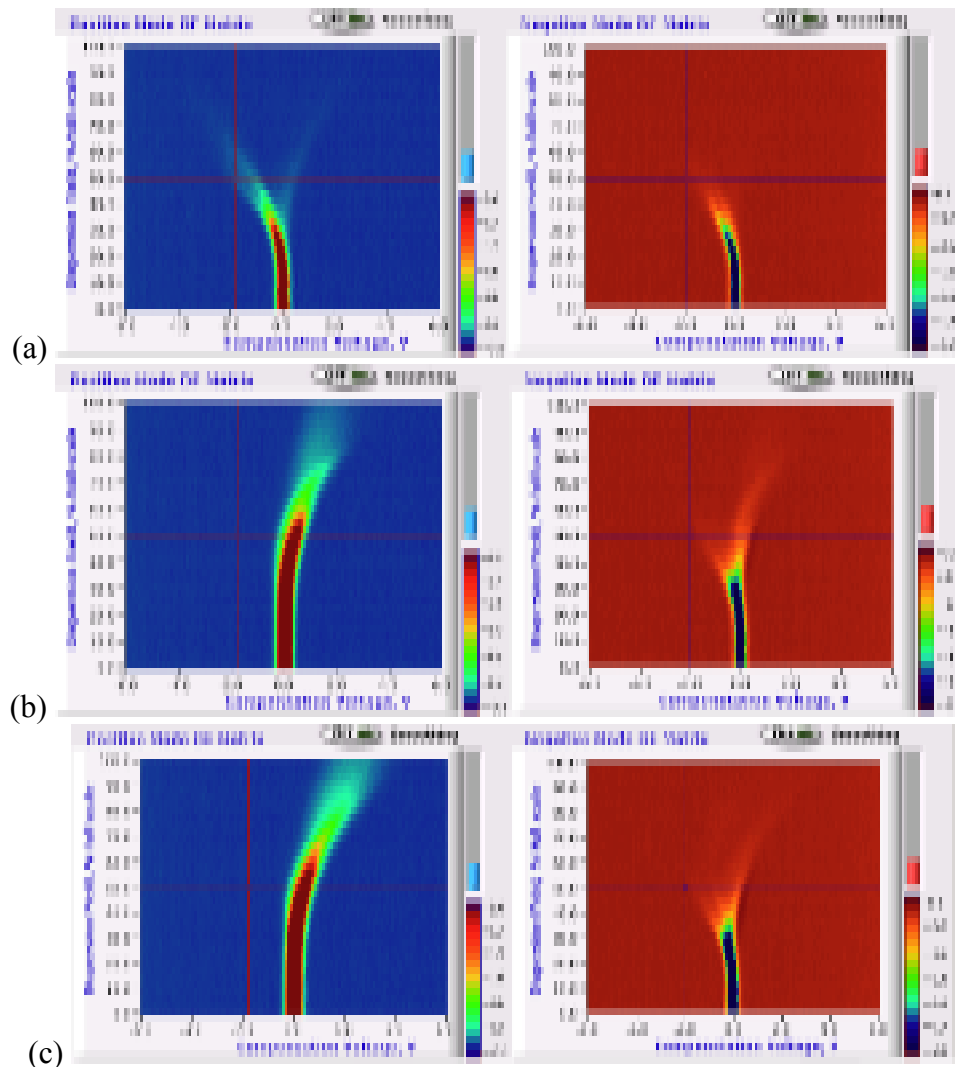


Figure 195 The figure represents the FAIMS response (a) to clear air, (b) to material in smoke during a pyrolysing wood fire in the Sunbury smoke tunnel, and (c) to a full scale TF2 fire in the BRE test room.

In Figure 195(a), the clean air trace signal arises from ionised water and oxygen clusters probably with some low levels made up of organic vapours present in the atmosphere as a natural background. As ionizable material enters the FAIMS inlet the trace bend to the right (Figures 195(b) and (c)). The displacement of the positive and negative ion trace to the right and ion currents values is comparable in the different scale fires and represents a significant amount of material.

## 6.4.2 Smoldering cotton (TF3)

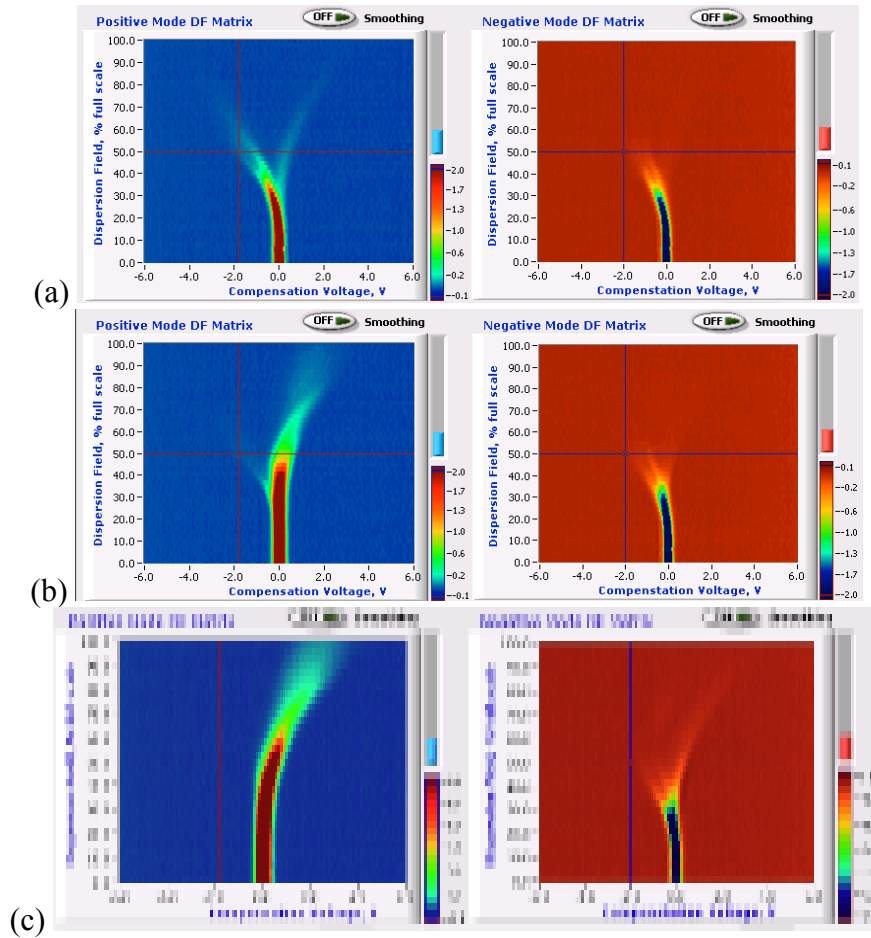


Figure 196 The figure represents the FAIMS response (a) to clear air, (b) to material in smoke during a smoldering cotton wick fire in the Sunbury smoke tunnel, and (c) to a full scale TF3 fire in the BRE test room.

As in Figure 195 the displacement angle of the ion traces in Figure 196 is comparable in the two different scale fires. However the intensity appears smaller in the Sunbury tunnel compared to the BRE full-scale fire test room, which suggests a higher concentration in the BRE test. The other noticeable difference is the presence of a shift negative ion trace for the BRE test, which is not discernable for the Sunbury tunnel test.

### 6.4.3 Flaming polyurethane (TF4)

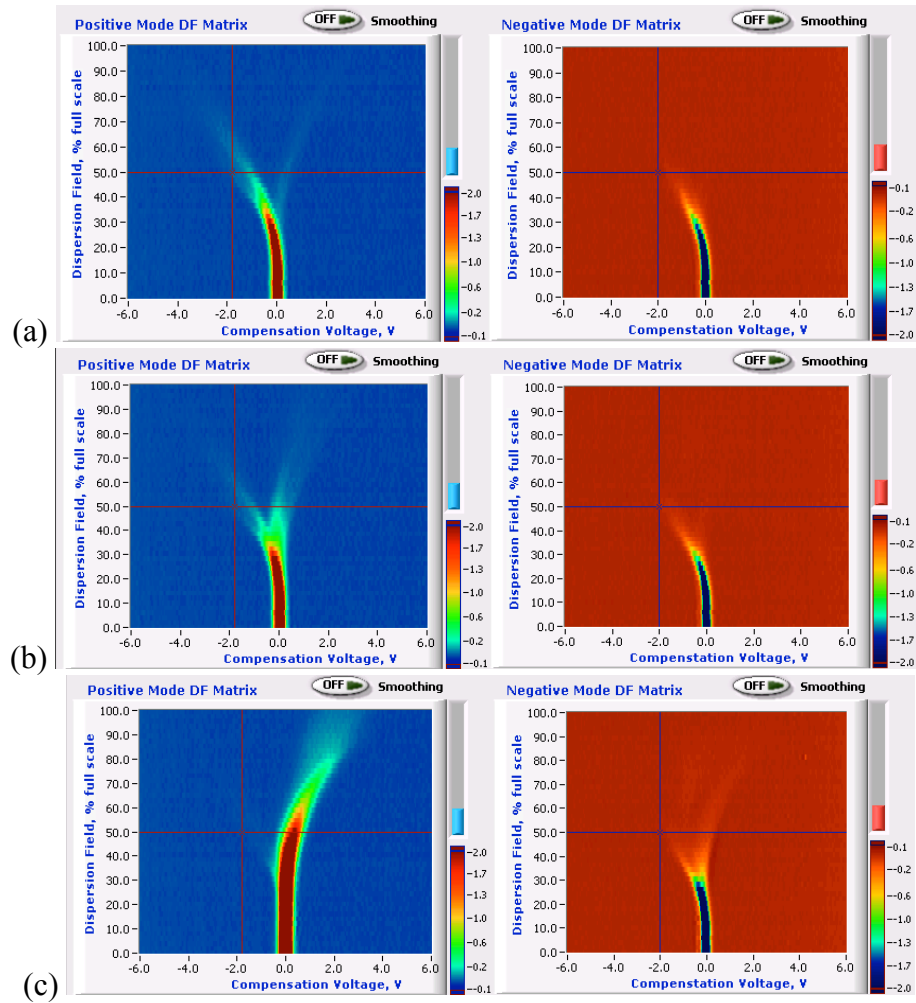


Figure 197 The figure represents the FAIMS response (a) to clear air, (b) to material in smoke during a polyurethane foam burn in the Sunbury smoke tunnel, and (c) to a full scale TF4 fire in the BRE test room.

As for Figures 195 and 196, the shifts are seen for both the smoke tunnel and the BRE tests but appear more substantial for the latter suggesting a higher product concentration.

## 6.4.4 Flaming Pool fire (TF5)

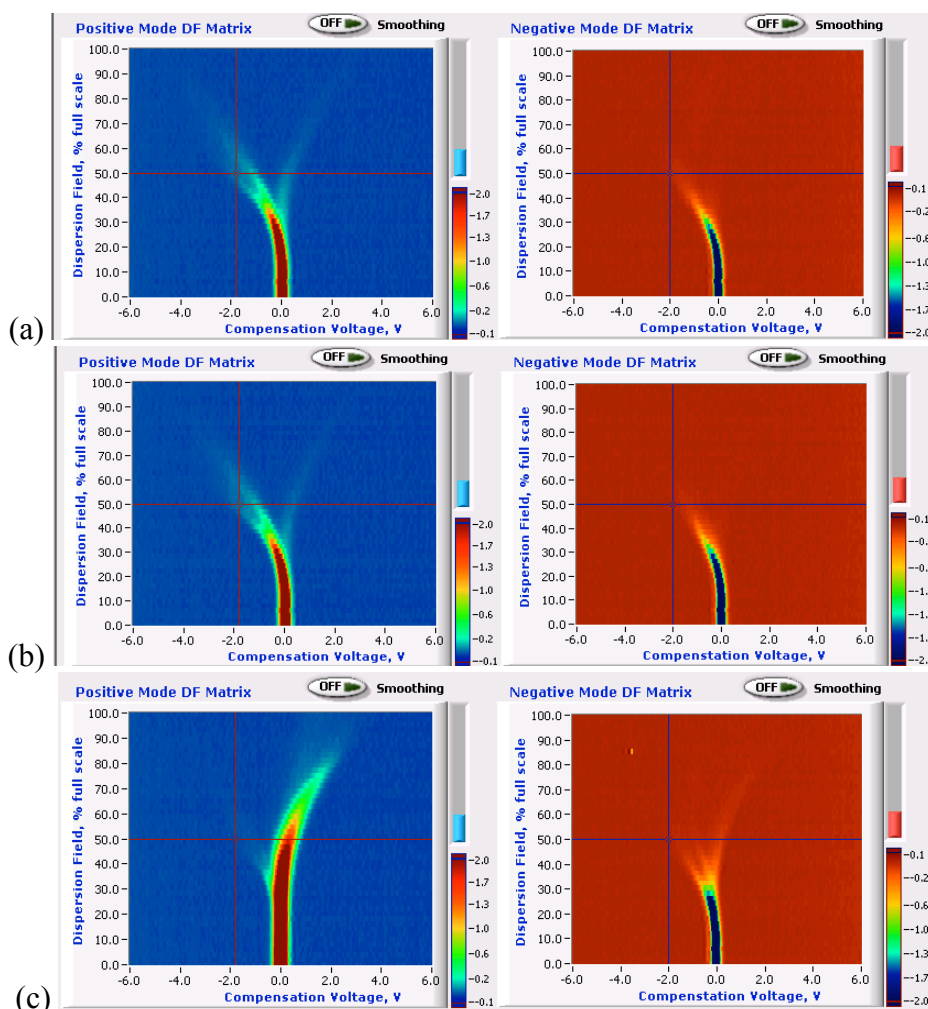


Figure 198 Results from regulated inlet to a FAIMS device in clean air (a) and smoke from a flaming polyurethane fire in the Sunbury smoke tunnel (b). Figure C is the FAIMS response from a full scale TF4 test at BRE.

Figure 198 figure represents the FAIMS response (a) to clear air, (b) to material in smoke during a flaming heptane fire in the Sunbury smoke tunnel, and (c) to a full scale TF5 fire in the BRE test room.

As for Figures 195 to 197 the shifts are seen are significantly more substantial for the BRE tests than for the smoke tunnel test. In fact for the Sunbury tunnel test almost no shift is discernable. This may reflect the fact that most vapour from these tests is simply fuel evaporation and the heptanes molecule is not very readily ionised under the prevailing conditions and may not generate a good signature.

## **CHAPTER 7 DISCUSSION AND CONCLUSION**

This study was directed at characterising airborne (gas, aerosol) emissions for fires at the early stage relevant to detection. A primary target is characterisation of standard test fires used for detector approvals (BS EN 54-7:2001 [1] and UL 217/268 [2],[3]) but interest extended to scenarios beyond test standards including electrical pyrolysis events, and identified false alarm stimuli e.g. cooking fumes. While products from well developed fires have previously been well documented, relatively little research has been directed at identifying products other than smoke and CO from early stage fires or for the standard test fires. This is an impediment to rational innovation in fire detection.

When conceived it was envisaged that the project would be primarily directed at characterising fire gases. However aerosol (smoke) generation is an important aspect of nuisance fires and a major factor in their detection [146], and many possible fire gases may be involved in exchange with smoke particles. The study therefore includes some measurements related to smoke detection and characterisation.

### **7.1 Review of Work and Results**

#### **7.1.1 Development of Reduced Scale Test Fires**

While a target of the study included measurements on full scale standard test fires, it was recognised that the study had to involve development of reduced scale emulations both to provide scope for development of measurement protocols and to accumulate at acceptable cost a significant data set on variable fire conditions. The study has thus required development of an enclosure and equipment for performing reduced scaled test fires, and deployment of sensor, fire detector, and analytical systems to carry out measurements on both a reduced scale enclosure and on full scale fire test environment.

Initially it was thought that an existing standard enclosure (NBS smoke box) could provide an environment in which reduced scale tests could be performed but early work revealed that this was not suited to development of fires with characteristics comparable to the target test fires. A larger (2 m high by 1 m<sup>2</sup>) enclosure was constructed at UCLan,

and with sensors mounted at the enclosure ceiling, as for standard tests, a series of test fire emulations were developed. This development eventually produced reduced scale tests which matched the smoke generation characteristics of the full scale test fire standards in terms of obscuration versus time. Although this development was informed by some existing understanding of fire scaling, the actual development of sources was largely empirical limited only by matching fuel and combustion type. Development of reduced scale test sources involved in some cases provision of structures partially enclosing fires to limit radiative heat loss and prevent small fires from self-extinguishing. With the exception of a flaming crib fire, the designed emulations were broadly consistent with scaling expressions despite the fact those were developed for much larger fire environments.

The reduced scale enclosure and fire test emulations are certainly more capable of matching real test fire than forced draft tunnel type units such as FE/DE device proposed by Grosshandler [82] which have been used as the basis for much detection research.

### **7.1.2 Sensor Measurements**

Data sets have been built up as a result of application of a range of sensor and detector to tests in reduced scale and full-scale environments. These have included measurements of smoke by obscuration and optical scatter, and gases by electrochemical sensors and NDIR measurement. Results from some of these measurements have merely confirmed expectations of relatively low or imperceptible effects by test fires at the locations in the test environments used for detector location. Generation of CO<sub>2</sub> and consumption of O<sub>2</sub> were observed but as is to be expected for early stages of fires where only a small fraction of the O<sub>2</sub> content of the enclosure is involved, only modest changes were observed. Similarly tests directed at sensing hydrogen using an electrochemical sensor showed no or only small and irreproducible generation of that gas.

Temperature measurements were carried out throughout the study but not presented in this document. Generally temperature rises at the detector locations were as for standard tests, small for all but rapidly growing flaming fires.

Commercial ionization based smoke detectors were deployed throughout the tests but results were not presented as it was found that the dynamic range of such units is too small to allow useful analysis. This did indicate a need to include detectors in any future tests with dynamic range modified to more nearly match that of the MIC devices on which some standards are based.

As expected substantial amounts of carbon monoxide were detected at sensor/ detector locations, but more significantly measurement with an electrochemical sensor having a broad range response to oxidisable gases showed that in addition to the CO, test fires produced substantial amounts of other oxidisable products. The broad range oxidisable gas detector cell (Honeywell 7EtO type) does not provide any indication of the identity of these oxidisable gases but signals expressed as equivalent ppm CO concentrations were much higher than the actual CO concentrations measured at the same time as indicated in the summary shown in Table 65 below:

Emulation at UCLan.	TF2	TF3	TF4	TF5	UL fire A	UL fire B	UL fire C
Total oxidisables as ppm CO / measured CO ppm	~5	~2.5	~3	~3	~2.5	~2.5	~2.5

**Table 65 Approximate response ratio of total oxidisable gas and CO sensors both calibrated with CO and with signals expressed as CO ppm or CO pp equivalent**

This result indicates at least that there is substantial production of oxidisable gases as fire products, which may provide a basis for fire detection.

An issue with the generation of reduced scale test fires is whether having achieved a match to the smoke obscuration behaviour of full-scale test fires, other parameters including production of gases are also matched. Measurement of carbon monoxide was carried out using the same sensors in the UCLan enclosure and in tests in the BS EN 54/7 standard room at BRE. Table 66 below shows ranges of CO concentrations observed towards the end of the BRE BS EN54/7 test fires and their emulations at UCLan.

Fire	TF2	TF2	TF3	TF3	TF4	TF4	TF5	TF5
	UCLan	BRE	UCLan	BRE	UCLan	BRE	UCLan	BRE
CO ppm range	20-90	70-100	10-70	45	20-60	40	15-25	27

Table 66 Ranges for CO concentration from measurements in UCLan reduced and BRE full scale EN54/7 test fires TF2,TF3, TF4, and TF5.

There is a reasonable match for in CO levels across the range of test fires. This suggests that matching the smoke obscuration characteristics has resulted in a match in fire gas generation and transport. If this is true for CO it seems probable that it should hold broadly true for other gases and vapours.

### 7.1.3 GC/MS study

The most substantial part of the study involved a series of GC/MS analyses on fire products collected on absorbent media from a large number of tests in the UCLan enclosure and much smaller set carried out at BRE. Although a variety of sample capture methods were considered, the convenience of capture onto absorbent materials and relative stability of such samples, meaning they could be transported and stored, resulted in the work concentrating on collection onto such media. Earlier work was predominantly with a Tenax absorbent but it became clear that this was not able to retain many of the smaller more volatile molecules, which might be present. The use of absorption tubes containing a Carboxen absorbent was introduced and work was continued using both materials. Protocols for GC/MS analysis of material desorbed from the Tenax and Carboxen sample tubes using different columns and conditions were developed. Handling of absorbent resins is complex with a number of potential pitfalls. Accumulation of moisture is one and this had to be addressed for samples generating substantial water vapour, particularly toasting bread. The absorbent resins are also not perfect in that they can produce either high background signals or artefacts. Tenax for example produces ghost peak artefacts, which are identified as Bis-phthalates.

GC retention time chromatograms were recorded for samples desorbed from Carboxen and Tenax for each of the test series carried out and these are presented in chapter 4 of this thesis as groups of ~6 traces for each test type/absorbent material combination. For

each test type the sets of chromatograms, there is generally a resemblance of form and major peak occurrence. However even for nominally identical tests, the GC traces can show significant variability. Calibration checks on the GC/MS equipment with standard test sample mixtures generally indicated good reproducibility for the equipment. The source of variability for GC/MS chromatograms for the experimental samples is not clear. It may reflect true variability in output from the test fire sources, or issues with sample collection, retention or desorption processes. However for each test type a reasonably representative GC/MS trace could be identified and such are presented in chapter 5.

Comparison of the GC/MS chromatograms for the EN54/7 test fire emulations carried out in the UCLan enclosure with chromatograms for the corresponding full-scale tests at BRE, does not show great similarity in the GC peak distributions or relative intensities. The BRE traces show background effects which may indicate sampling or instrumentation issues. Instrumentation issues may have arisen as a result of GC/MS equipment shut down in the period between analysis of the UCLan and BRE samples. Viewing the BRE sample chromatograms on an expanded scale does show more peaks, which may be correlated with those, observed for the UCLan tests.

In chapter 5 a set of selected representative GC chromatograms are presented on more expanded scale than used in chapter 4. These chromatograms are accompanied by table of MS fragmentation data for identified elution peaks, and where appropriate compound identification. The analysis of fragmentation data was not confined to the test runs identified in chapter 5. The product mixes in as far as they could be identified tended not to differ greatly from those indicated in chapter 5 and for reasons of space and convenience further results for duplicate tests are not presented here.

Inspection of the MS fragmentation data tabulated in chapter 5 and linked to GC/MS elution peaks indicates that a large and quite diverse set of compounds is identified. Given the complex mixtures present and evidence of incomplete peak resolution, some peaks show mass fragment mixes which do not allow compound identification, and for the same reason some of the identifications presented may be questionable, especially where the peaks in the retention time plots show overlap or significant baseline elevation. However certain species feature in the GC/MS analysis of Carboxen absorbed samples from many if not all fires, including propene, furan, acetone, and benzene.

Table 67 below reproduced from chapter 5 lists compounds commonly identified for the EN54/7 test emulations in the UCLan enclosure.

Peak identity	TF2		TF3		TF4		TF5	
	F	R	F	R	F	R	F	R
B : Propene	730	901	850	788			769	758
E : Acetaldehyde	809	893						
H : Furan	855	876	933	897	720	766	777	789
I : 2 – Propanal			867	803	830	733	959	942
J : Acetone	906	933	750	775	761	722		
R: 2 Methyl furan			910	899	717	906		
V : Benzene	877	923	902	899	891	901	801	855

Table 67 Common gases observed in the scaled standard fires in the UCLan enclosure with the library match values presented (F,R>750 considered good match)

Several of these species are also present in the Carboxen absorbed samples from non standard fires and nuisance sources such as cooking and toasting indicating they do not potentially provide means of discriminating against such sources. Benzene appears discernable for most tests other than overheated PCB.

The analysis for samples captured on Tenax yielded complex GC/MS chromatograms with many peaks for which identification is feasible but with some uncertainty due to peak and background overlap. The Tenax results for almost all samples do indicate the presence of benzene and larger aromatic compounds, anthracene and others.

It is clear from the GC/MS chromatograms that full separation was not achieved for many tests and this complicates the analysis. The Sorption tubes were sourced from two different suppliers (Analytix and Sigma) have different mesh and pore sizes which leads to variation in how samples are desorbed and transferred to the GC column. Utilizing the CDS 5000 pyrolyser as a mechanism for injecting samples onto column was not ideal. Although rapid desorption was employed to minimise the plug of analyte injected onto column there is some spread which contributes to the poor peak shape observed particularly for early eluting compounds. This possibly could be corrected to some extent by use of a cyro- injection system where the fire gases enter a cold trap capillary, rapidly condense, and are then flashed onto the column. This could reduce the injection slug size and should result in better peak shapes.

#### **7.1.4 Optical Scatter and Particle Size Measurements**

Optical scatter measurements were made for a large number of the fire tests carried out during this study being initially employed to aid development of the reduced scale test fires. A range of experimental devices operating at wavelengths other than the near standard ~850 nm were introduced to determine whether fire type could be distinguished by the relative response of their smokes to different wavelengths as has been suggested based on Mie scattering theory [147]. Tests used devices operating predominantly in the blue (465 nm) and near IR (~850 nm) regions. The results for the standard BS EN54/7 tests at BRE and emulations in the UCLan enclosure, and in the Sunbury smoke tunnel indicated that small differences in smoke transport to detectors could effectively obscure any useful wavelength based effect. Devices where dual wavelength scatter measurements were integrated into the same detector showed more promise and relative stability of signal ratio where substantial smoke was present. Where smoke and therefore signal levels were low, the response ratio was less stable indicating difficulties in employing this technique for early stage fire detection and discrimination. Results with a smoke detector provided with a near UV source were subject to the same issues but given the early development stage for such devices the results may indicate further work is warranted if UV LED prices continue to fall.

A series of smoke particle size measurements were completed using a cascade impactor unit. There was reasonable reproducibility fire to fire but the dynamic range for the system probably does not extend to small enough particle sizes for the information to be informative when considering optical scatter or ionization based smoke detector response characteristics.

#### **7.1.5 FAIMS measurements**

A short study was completed employing an Owlstone FAIMS instrument during standard EN54/7 tests at BRE and some attempts to emulate those tests in the smoke tunnel at TYCO Sunbury. The tests demonstrated that the technique could give real time response to fire product gases but the nature of the response did not indicate any very substantial discriminatory capability. This is not surprising given the complexity of such fire products indicated by the GC/MS study. However these results constitute an initial

study only without any attempt to optimise the technique and further measurements with false alarm sources may be warranted. The FAIMS devices may have a future as a fire detection tool but in its present instrumental is too dependant on ancillary equipment and the price and power requirement would have to be very substantially reduced.

## **7.2 Summary, Applications and Future Developments**

The impetus for this research was to determine whether there were any substantial gaseous fire products that could have potential for development of detector technologies with improved discrimination between real fires and against non fire nuisance sources. The work has demonstrated the existence of significant levels of oxidisable gases other than CO but that this certainly consists of a wide mixture of diverse species. The nature of this diversity does not indicate a route to discrimination against fume sources such as cooking, and may indicate that research effort should not be directed to progressing gas sensor development for detection of specific fire targets other than CO.

A somewhat disappointing aspect of the work was a failure to establish reliable connections between GC/MS peak areas and product quantities, and to obtain and analyse samples at time stages through the fires. GC/MS is perhaps not the best technique to approach real time sampling but previous work had indicated the inadequacy of direct methods such as FTIR at low concentrations.

The appearance of aromatic and polyaromatic species in some analyses prompted further examination of combustion related literature, which confirmed that polyaromatics have been widely identified in extracts from smoke and also within flames. Initial attempts in this study to carry out fluorescence measurements on smoke deposits were unsuccessful but have indicated requirements for future studies, which may enable discrimination of smokes rather than gases.

The work on development of test fires at a conveniently reduced scale has potential to aid further work in the area impeded by limited access to full-scale fire room facilities.



- 
- <sup>1</sup> BS EN 54-7 : 2001 BSI. *Fire detection and fire alarm systems. Smoke detectors. Point detectors using scattered light, transmitted light or ionization*. London: BSI.
- <sup>2</sup> UL 217 Underwriters Laboratory. (2006). *Standard for Single and Multiple Station Smoke Alarms*. Standard.
- <sup>3</sup> UL268 Underwriters Laboratory. (2006). *Standard for Single and Multiple Station Smoke Alarms*. Standard.
- <sup>4</sup> Finley Jr P (2001) *Residential FireAlarm Systems :The Verification and Response Dilemma*, Applied Research Project submitted to the National Fire Academy, 1-78
- <sup>5</sup> Perdell, N (2006) *Fire Deaths and Injuries in Scotland – a need for urgent action*, CT, 60-61.
- <sup>6</sup> Electrical World(1888) Volumes 11-12, *The Electrical World*, Prinston University, Digitalized in 2010 and retrieved from <http://books.google.com/books?id=zYVMAAAAYAAJ&pg=PA120&sig=791huvN7EweoyBkBmxZHiowz6g8&hl=en> (Checked 13-4-2011)
- <sup>7</sup> CP 327.404/402/501 (1951) *Fire Detection and fire alarms for buildings, Part 1: Code of practice for system design, installation, commissioning and maintenee* . replaced by BS 5829-2002 . British Standards Institute .
- <sup>8</sup> Merzhanov, A.G. (1997) *Fundamentals, achievements, and perspectives fro development of solid-flame combustion*, Russian Chemical Bulletin, 46 (1), 1-27.
- <sup>9</sup> Bradbury, A.G.W, Shafidzadeh, F.(1980) *Role of oxygen chemisorption in low temperature ignition of cellulose*, Combustion and flame, 37, 85-89.
- <sup>10</sup> Mealy, C. L. (2009). *Smoke Alarm Response: Estimation Guidelines and Tenability Issues*. National Fire Protection Agency.
- <sup>11</sup> Han D, Lee, B, (2009) *Flame and smoke detection for early real-time detection of a tunnel fire*, Fire Safety Journal, 44(7), 951-961.
- <sup>12</sup> Jackson, M., & Robins, I. (1994). *Gas sensing for fire detection: Measurements of CO, CO<sub>2</sub>, H<sub>2</sub>, O<sub>2</sub>, and smoke density in European standard fire tests*. Fire Safety Journal , 22 (2), 181-205.
- <sup>13</sup> Tewarson, A. (2008). SFPE Handbook . In N. F. Engineers, & C. C. Beyler (Ed.), *SFPE Handbook of Fire Protection Engineering* (4th Eddition ed.). Quincy, Mass, Bethesda: National Fire Protection Association .
- <sup>14</sup> Sokolik, A. K. (1967). *Turbulent combustion of gases*. Combustion, Explosion, and Shock Waves , 3 (1), 61-76.

- 
- <sup>15</sup> Lang, L, Zhou, F. (2010) *A Comprehensive hazard evaluation system for spontaneous combustion of coal in underground mining*, International Journal of Coal Geology, 82 (1-2), 27-36
- <sup>16</sup> Semenov, N. (1933) "Tsepnaia teoriia i okislitel'nye protsessy" (*Chain theory and oxidation processes*). Uspekhi khimii (Progress of chemistry) 2, (5), 590–621.
- <sup>17</sup> Frank-Kammenstskii, D. (1967). *Diffuzia i Teploperedacha v Khimicheskoi Kinetike (Diffusion and heat transfer in chemical kinetics)*. Izd. Nauka, Moscow – In Russian .
- <sup>18</sup> Watt, S., Staggs, J., McIntosh, A., & Brindley, J. (2001). *A theoretical explanation of char formation on the ignition of polymers*. Fire Safety Journal , 36 (5), 421-436.
- <sup>19</sup> Drysdale D (1998), *An Introduction to Fire Dynamics*, 2<sup>nd</sup> Edition (Revised) (1998), John Wiley and Sons Ltd, ISBN-10: 0471972916
- <sup>20</sup> Quintiere J.G. (2006), *Fundamentals of Fire Phenomena* Wiley Blackwell ISBN-10: 0470091135
- <sup>21</sup> Lilley D.G. (1996) *Fire causes and ignition*, Energy Conversion Engineering Conference, 1996. IECEC 96. Proceedings of the 31st Intersociety
- <sup>22</sup> Drysdale D, Bowman, M, (1999) *Introduction to fire dynamics : Methane Flame*, table 1.15, 2<sup>nd</sup> Edition, Wiley ISBN 0471972916
- <sup>23</sup> Calcote, H. (1981). *Mechanisms of soot nucleation in flames—A critical review*. Combustion and Flame , 42, 215-242.
- <sup>24</sup> Hasson, A. T. (2009). *Branching Ratios for the Reaction of Carbonyl-Containing Organic Peroxy Radicals with Hydroperoxy Radicals*. American Geophysical Union .
- <sup>25</sup> Thomas, P. M. (2010). *Cavity ringdown spectroscopy of the NIR View the MathML source electronic transition of allyl peroxy radical (H<sub>2</sub>C=CH-CH<sub>2</sub>OO·)* . Chemical Physics Letters , 491 (4-6), 123-131.
- <sup>26</sup> Drysdale D, (1999) *Introduction to fire dynamics : Section 11.1 – 11.1.1*. Wiley ISBN 0471972916
- <sup>27</sup> Pfister, G. (1983). *Detection of smoke gases by solid state sensors -- A focus on research activities*. Fire Safety Journal , 6 (3), 165-174.
- <sup>28</sup> Amamoto, T., Tanaka, K., Takahata, K., Matsuura, S., & Seiyama, T. (1990). *A fire detection experiment in a wooden house by SnO<sub>2</sub> semiconductor gas sensors*. Sensors and Actuators B: Chemical , 1 (1-6), 226-230.
- <sup>29</sup> Higgins, E., Fiorca, V., Thomas, A., & Harvey, V. (1972). *Acute toxicity of brief exposures to HF, HCl, NO<sub>2</sub> and HCN with and without CO*. Fire Technology , 8 (2), 120-130.

- 
- <sup>30</sup> Fabian, T. G. (2007). Smoke Characterization Project. *Underwriters Laboratories . The Fire Protection Research Foundation*.
- <sup>31</sup> Sakuma, H., Munakata, S., & Sugawara, S. (2010). *Volatile Products of Cellulose Pyrolysis*. Agriculture Biological Chemistry , 44 (2), 443-451.
- <sup>32</sup> .G Zizak,G., De Luliis, S, Cignoli,F. (Laboratorio di Combustione e Diagnostiche Laser, Milan, Italy), (N.D).*Combustion and Laser Diagnostics retrieved from <http://www.tempe.mi.cnr.it/zizak/cld-main-eng.htm#endlabel>* (Checked 10-01-2011)
- <sup>33</sup> Pinnick, R.G., Hill, S.C., Nachman,M.P.,Videen,G., Chen, G., Chang R.K.(1998) . *Aerosol Fluorescence Spectrum Analyzer for Rapid Measurement of Single Micrometer-Sized Airborne Biological Particles*. Aerosol Science and Technology, 1521-7388, Volume 28, (2), 95 – 104
- <sup>34</sup> Lambert, C., McCue, J., Portas, M., Ouyang, Y., Li, J., Rosano, T., et al. (2005). *Acrolein in cigarette smoke inhibits T-cell responses*. The Journal of allergy and clinical immunology , 116 (4), 916-22.
- <sup>35</sup> Ashley, K. (2003). *Developments in electrochemical sensors for occupational and environmental health applications*. Journal of Hazardous Materials , 102 (1), 1-12.
- <sup>36</sup> Hedberg, E. K. (2002). *Chemical and Physical Characterization of Emissions from Birch Wood Combustion in a Wood Stove*. Atmos. Environ , 36, 4823-4837.
- <sup>37</sup> Simoneit, B. S. (1999). *Levoglucosan, a tracer for cellulose in biomass burning and atmospheric particles*. Atmospheric Environment , 33, 173-182.
- <sup>38</sup> Drysdale D, (1999) *Introduction to fire dynamics (Second Edition) Chapter 4 section 4.3*. Wiley ISBN-10: 0471972916
- <sup>39</sup> Osgood, D. (1996). *The Detection of the Early Stages of Fire*. PhD Thesis, South Bank University.
- <sup>40</sup> Lingens, A., Windeisen, E., & Wegener, G. (2005). *Investigating the combustion behaviour of various wood species via their fire gases*. Wood Science and Technology , 39 (1), 49-60.
- <sup>41</sup> Olsson, M., Ramnas, O., & Petersson. (2004). *Specific volatile hydrocarbons in smoke from oxidative pyrolysis of softwood pellets* Journal analytical applied pyrolysis , 71, 847-854.
- <sup>42</sup> Gottuk, D., Roby, R., & Beyler, C. (1995). *The role of temperature on carbon monoxide production in compartment fires*. Fire Safety Journal , 24 (4), 315-331.
- <sup>43</sup> Milke, J. (1999). *Using multiple sensors for discriminating fire detection*. NIST technical report 140

- 
- <sup>44</sup> DiNunno, P.J. (2008) SFPE Handbook of Fire Protection Engineering (4<sup>th</sup> Edition) National Fire Protection Association ISBN-10: 0877658218
- <sup>45</sup> Nelson, G. (1998). *Carbon Monoxide and Fire Toxicity: A Review and Analysis of Recent Work*. Fire Technology , 34 (1), 39-58.
- <sup>46</sup> Lampe, U., Simon, E., Pohle, R., Fleischer, M., Meixner, H., Frerichs, H., et al. (2005). *GasFET for the detection of reducing gases* Sensors and Actuators B: Chemical , 111-112, 106-110.
- <sup>47</sup> Pitts, W. (1995). *The global equivalence ratio concept and the formation mechanisms of carbon monoxide in enclosure fires.* *Progress in Energy and Combustion Science* , 21 (3), 197-237.
- <sup>48</sup> Mulholland, G. (2002). *Smoke Production and Properties*. SFPE Handbook of Fire Protection Engineering (2nd edition) , Chapter 15 (Section 2), 217-222.
- <sup>49</sup> McGrath, T. W. (2007). *Formation of polycyclic aromatic hydrocarbons from tobacco: The link between low temperature residual solid (char) and PAH formation*. Food and Chemical Toxicology , 45 (6), 1039-1050.
- <sup>50</sup> Scorsone, E. P. (2006). *Development of an Electronic Nose for Fire Detection*. Sensors and Actuators B: Chemical , 116 (1-2), 55-61.
- <sup>51</sup> Smith D.A., C. G. (1992) *Major chemical species in buoyant Turbulent diffusion flames*. Combustion and flame , 91, 226-238.
- <sup>52</sup> Fleming, J. (2004). *Photoelectric and Ionization Detectors – A Review of The Literature Re – Visited* . Retrieved December 31, 2010, from The Official Website of the Commonwealth of Massachusetts:  
[http://www.mass.gov/Eeops/docs/dfs/osfm/boards/specific\\_meetings/j\\_flwming/photo\\_vs\\_ion\\_revisited\\_2004\\_j\\_fleming.pdf](http://www.mass.gov/Eeops/docs/dfs/osfm/boards/specific_meetings/j_flwming/photo_vs_ion_revisited_2004_j_fleming.pdf)
- <sup>53</sup> Ishii H., K. K. (1997). *A Fire Detection System Using Optical Fibers for Utility Tunnels*. Fire Safety Journal , 29, 87-98
- <sup>54</sup> Litton, C. (1977). *A mathematical model for ionization-type smoke detectors and the reduced source approximation*. Fire Technology , 13 (4), 266-281.
- <sup>55</sup> Qiyuan, X., Hongyong, Y., & Huiliang, G. (2004). *Experimental Analysis on False Alarms of Fire Detectors by Cooking Fumes*. Journal of Fire Sciences , 22 (4), 325-337.
- <sup>56</sup> Thuillard M(1996) *The development of algorithms for a smoke detector with neuro fuzzy logic*, Fuzzy Sets and Systems, 77(2):117-124, 1996
- <sup>57</sup> Segal B . "*Federal appeals court upholds \$2.8M award for faulty smoke alarm*". Bob Segal Investigates Indianapolis News Weather. WTHR.  
<http://www.wthr.com/global/story.asp?s=8109077>. Retrieved on 2008-10-28.  
<http://www.wthr.com/global/story.asp?s=8109077>. Retrieved on 2008-10-28.

- 
- <sup>58</sup>Loepfe, M., Ryser, P., Tompkin, C., & Wieser, D. (1997). *Optical properties of fire and non-fire aerosols*. *Fire Safety Journal* , 29 (2-3), 185-194.
- <sup>59</sup> Werkmeister, W., Hanse, T., Turner, J., Gruner, G., Bergmann, R., Haug, C., Hensel, A. (2009) *Simulation of light scattering for different Aerosols in a Fire Detector and Comparison with Experimental Data*, Proceedings From 14<sup>th</sup> Int. Conf. On Automatic Fire Detection, AUBE'09, Duisberg, Germany, (2), 65.
- <sup>60</sup> Miles, S. (2007). Smoke alarms go "Toast Proof" With fire Angel. *Pocket -Lint On line news and reviews resource* .08/08/2007 Retrieved April 2009
- <sup>61</sup> BS ISO 7240-8:2007, BSI. (2007). *Carbon monoxide fire detectors using an electro chemical cell in combination with a heat sensor*. ISO Standard, British Standards Institute .
- <sup>62</sup> Cleary, T. A. (1999). *The Fire Emulator/Detector Evaluator*. National Institute of Standards and Technology, U.S. Deptment of Commerce. Gaithersburg, MD: Internal Report.
- <sup>63</sup> Su, J., Crampton, G., Carpenter, D., McCartney, C., & Lerouz, P. (2003). Kemano Fire Studies – Part 1: Response of Residential Smoke Alarms. *Research Report 108* .
- <sup>64</sup> Cooper, L. (1986). *Why we need to test smoke detectors*. *Fire Journal* , 80, 43-95.
- <sup>65</sup> UK Statistics. (2007). *Fire statistics monitor covering period up to 31st December 2006*. Fire Reseach and Statistics Division. Department of the Deputy Prime Minister.
- <sup>66</sup> Greater Manchester Fire Authority. (2007, December 5th). *Fire Chief calls on businesses to take action*. *News and Events* , p. 1.
- <sup>67</sup> Edwards R. (2004) Concern over 'safety shortfall' uncovered at Scots nuclear sites; 14 fires and 486 false alarms spark accident fears. *The Sunday Herald*, 10 October . Retrieved from <http://www.highbeam.com/doc/1P2-10005784.html> (Checked 11-01-2011)
- <sup>68</sup> Tyne and Wear Fire and Rescue Service. (2007, November). *Check list to reduce false alarms* .
- <sup>69</sup> Qiyuan, X., Hongyong, Y., & Huiliang, G. (2004). *Experimental Analysis on False Alarms of Fire Detectors by Cooking Fumes*. *Journal of Fire Sciences* , 22 (4), 325-337.
- <sup>70</sup> Kliener, K. (2005) *Smart fire detector could slash false alarms*, *New Scientist*, 25 October 2005 retrieved from <http://www.newscientist.com/article/dn8205-smart-fire-detector-could-slash-false-alarms.html>
- <sup>71</sup> Johnson, E. (1998). *Study of Technology for Detecting Pre-ignition Conditions of Cooking Related Fires Associated with Electric and Gas Ranges and Cookertops*. National Standards Institute. NIST.
- <sup>72</sup> Cleary, T. G. (1999). *Smoke Detector Response to Nuisance Aerosols*. NIST, Building and Fire Research Laboratory. Duisburg: AUBE '99.

- 
- <sup>73</sup> Guofeng, S., Qiyuan, X., JinJun, W., Hongyong, Y., & Yongming, Z. (2005). *Experimental Study on False Alarms of Smoke Detectors caused by Steam*. Fire Safety Science , 14 (1).
- <sup>74</sup> Xie, Q., Yuan, H., Su,G., Yongmingm Z., (2002-2003) *Experimental Study On The Sensitivity And Nuisance Immunity Of Smoke Detectors*, Journal of Applied Fire Science Volume (4), 323-334
- <sup>75</sup> M Dennekamp, S Howarth, C.A.J Dick, J.W Cherrie, K Donaldson, A Seaton (2001) *Ultrafine Particles and Nitrogen Oxides Generated by Gas and Electric Cooking*. Occupational Environmental Medicine , 58, 511-516
- <sup>76</sup> "Cooking oil." *Wikipedia, The Free Encyclopaedia*. Wikimedia Foundation, Inc. 22 July 2004. Web. 10 Aug. 2000 retrieved from [http://en.wikipedia.org/wiki/Cooking\\_oil](http://en.wikipedia.org/wiki/Cooking_oil)
- <sup>77</sup> R. L. Cooper and A. J. Lindsey (1955) *3:4-Benzpyrene and Other Polycyclic Hydrocarbons in Cigarette Smoke*, Br J Cancer.(2): 304–309.
- <sup>78</sup> AS1603 (1997) *Automatic Fire Detection and Alarm Systems*, Fire Protection Association Australia
- <sup>79</sup> AS3786 (1993) *Smoke Alarms*, Fire Protection Association Australia
- <sup>80</sup> BS 5839 (2004) *Design, Installation and Maintenance of Fire Detection and Fire Alarm Systems in Dwellings*, BSI
- <sup>81</sup> Grosshandler, W. (1995). *Review of Measurements and Candidate Signatures for Early Fire Detection*. NISTIR 55555 , 1-36.
- <sup>82</sup> Personal communication Don Brighenti, Tyco Fire Protection Products, USA
- <sup>83</sup> Focus (2011) *Elevatng Smoke Detection*, {iblication of the FIA, Issue 18 , 2011 sourced on web [http://www.fia.uk.com/filemanager/root/site\\_assets/news/fia\\_focus/focus\\_18\\_published\\_38379.pdf](http://www.fia.uk.com/filemanager/root/site_assets/news/fia_focus/focus_18_published_38379.pdf) Checked 26/04/2011
- <sup>84</sup> Morikawa, T. (1988) *Evolution of toxic gases from burning polymeric materials in a small-scale box model*. Fire and Materials , 12(2),43-49
- <sup>85</sup>
- <sup>86</sup> Barbrauskas V. (1995). *The generation of CO in bench-scale fire tests and the prediction for real-scale fires*. Fire and Materials , 19, 203-213.
- <sup>87</sup> Grosshandler, W. (1997). *Towards the Development of a Universal Fire Emulator-Detector Evaluator*. Fire Safety Journal , 29, 113-128.
- <sup>88</sup> Cleary, T. A. (1999). *Evaluating Multi-Sensor Fire Detectors In the Fire Emulator/Detecto Evaluator*. NIST, Building and Fire Research Laboratory National Institute of Standards and Technology. NIST.
- <sup>89</sup> Babrauskas, V. (1997). *Temperatures inflames and fires*. Fire Science and Technology Inc. Issaquah, SE

- 
- <sup>90</sup> Olenick, S., & Carpenter, D. (2003). *An Updated International Survey of Computer Models for Fire and Smoke*. Journal of Fire Protection Engineering , 13 (2), 87-110.
- <sup>91</sup> Weinert, D. W., Cleary, T. G., Mulholland, G. W., *Size Distribution and Light Scattering Properties of Test Smokes.*, AUBE`01, 12<sup>th</sup> Int. Conf. on Automatic Fire Detection, March 2001, Maryland, USA
- <sup>92</sup> Center for Environmental Research Information (1997). *Compendium method to-17 determination of volatile organic compounds in ambient air using active sampling onto sorbent tubes*. EPA/625/R-96/010b,
- <sup>93</sup> Health and Safety Executive (1997). *MDSH 88 methods for the determination of hazardous substances* Health and safety Laboratory.
- <sup>94</sup> Cao, X.L., and Hewitt, C.N.(1999). *Reactive Hydrocarbons in the Atmosphere* Academic Press, Edited by C.N Hewitt, San Diego, pp. 119–157
- <sup>95</sup> Fastyn, P., Kornacki, W., Gierczak, T., Gawlaski, J., Niedzielski, L.(2005) *Adsorption of Water Vapour From Humid Air By Selected Carbon Adsorbents*, Journal of Chromatography A, 1078, (1-2), 7-12
- <sup>96</sup> Health and Safety Executive (1993) *MDHS 72 Volatile Organic Compounds In Air*, Occupational Medicine and Hygiene Laboratory.
- <sup>97</sup> Dass C,(2007) *Fundamentals of Contemporary Mass Spectrometry*, Wiley - Interscience Series on Mass Spectrometry, New York 1<sup>st</sup> edition . ISBN – 13 : 978-0471682295
- <sup>98</sup> Holcapek M (2008) *Chromedia Tutorials on spectroscopyNOW.com: Capillary GC Coupled with Mass Spectrometry (GC-MS)* retrieved from [www.themcshanefirm.com/file.../McShane\\_resume.pdf](http://www.themcshanefirm.com/file.../McShane_resume.pdf)
- <sup>99</sup> McLafferty F W, Turecek F.(1993) *Interpretation of Mass Spectra*, University Science Books, 4th Edition ISBN 0935702253
- <sup>100</sup> Kirleis, E (2008) *On-Site Trace Chemical Detection Part 2: IMS and DMS Working Together*. Sensors retrieved from <http://www.sensorsmag.com/sensors/article/articleDetail.jsp?id=49353>
- <sup>101</sup> Shvartsburg et al (2006) *High-Resolution Field Asymmetric Waveform Ion Mobility Spectrometry Using New Planar Geometry Analyzers*. Analytical Chemistry ,78, (11) 3706-3714
- <sup>102</sup> Eiceman G A, Karpas Z (2005) *Ion mobility spectrometry*, Volume 1, CRC Press, ISBN 0849322472
- <sup>103</sup> City Technology. (2006). *6th Sense Eco Sure - Product data Sheet*. Retrieved December 31, 2010 from City Technology: <http://www.citytech.com/>

- 
- <sup>104</sup> Savitzky, A., Golay, M.J.E. (1964). *Smoothing and Differentiation of Data by Simplified Least Squares Procedures*. Analytical Chemistry 36 (8): 1627–1639
- <sup>105</sup> Brown, J. B. (2002 ). *A Tool for Selecting an Adsorbent for Thermal Desorption Applications*. Supelco. Sigma Aldrich.
- <sup>106</sup> Hagen, CHR, B, Milke, J, A. (2000) *The use of gaseous fire signatures as a means to detect fires*, Fire Safety Journal, 34 (1), 55-67
- <sup>107</sup> Weber R.O (1991) *Modelling fire spread through fuel beds*, Progress in Energy and Combustion Science , 17(1), 67-82
- <sup>108</sup> Williams, F. (1969). *Scaling Mass fires*. Fire Research Abstracts and Reviews , 11 (1), 1-22.
- <sup>109</sup> Hottel, H. (1961). *The Use of Models in Fire Research* . Publication 786 , 32-47.
- <sup>110</sup> Quintiere, J. (1989). *Scaling in fire research*. *Fire Safety Journal* , 15, 3-29.
- <sup>111</sup> Alpert, R.L. (1972) *Calculation of Response Time of Ceiling-Mounted Fire Detectors*. *Fire Technology* 8 (1972): 181-195.
- <sup>112</sup> Drysdale, D. (1998). *An Introduction to Fire Dynamics*. An Introduction to Fire Dynamics, 2<sup>nd</sup> Edition (Revised) (1998), John Wiley and Sons Ltd, ISBN-10: 0471972916 1998
- <sup>113</sup> Grosshandler, W. (1995). *Review of Measurements and Candidate Signatures for Early Fire Detection*. NISTIR 55555 , 1-36.
- <sup>114</sup> Quintiere, J.G. (1989) Scaling in fire research. *Fire Safety Journal* 15, 3-29.
- <sup>115</sup> Karlsson, B. Q. (2000). *Enclosure Fire Dynamics - Illustrated edition*. London: CRC Press.
- <sup>116</sup> Croce, P., & Xin, Y. (2008). *Scale Modeling of Quasi-Steady Wood Crib Fires in Enclosures*. Progress in Scale Modeling, 121-132.
- <sup>117</sup> Block, J. (1971). *A Theoretical and Experimental Study of Nonpropagating Free-Burning Fires*. Proceedings of the Combustion Institute , 13, 971-978.
- <sup>118</sup> Gross, D. J. (1962). *Experiments on the burning of cross piles of wood*. J Res. National Bureau of Standards , 99-105.
- <sup>119</sup> Babrauskas, V. (2002). *Ignition of Wood: A Review of the State of the Art*. Journal of Fire Protection Engineering , 12 (3), 163-189.
- <sup>120</sup> Westbrook, C. (1998). *A Comprehensive Modeling Study of n-Heptane Oxidation*. Combustion and Flame , 114 (1-2), 149-177.

- 
- <sup>121</sup> Steinhaus, T. W. (2007). *Large sacle pool fires*. Thermal Science Journal (3), 1-19.
- <sup>122</sup> Joulain, P. (1998). *Behavior of Pool Fires : State of the Art and New Insights*. Proceedings of 27th Symposium on Combustion , 1-11.
- <sup>123</sup> Mudan, K. (1984). *Thermal radiation Hazards from Hydrocarbon Pool Fires*. Prog. Energy Combustion Science , 10, 59-90.
- <sup>124</sup> E18 Grey 500 X 500 X 20mm foam from Custom Foams, Deans Road, Old Wolverhampton, Milton Keynes, MK12 5NA
- <sup>125</sup> AG, T. (2005, Jan 1). *Testo AG*. Retrieved August 28, 2009 from Testo : [www.testo.XX/cooking-oil](http://www.testo.XX/cooking-oil)
- <sup>126</sup> Adam T., M. S. (2006). *Quantitative puff- by- puff resolved characterization of selected toxic compound in cigarette mainstream smoke*. Chemical Research in Toxicology , 19, 511-520.
- <sup>127</sup> Jackson M.A., Robins I.(1994) *Gas sensing for fire detection: Measurements of CO, CO2, H2, O2, and smoke density in European standard fire tests* . Fire Safety Journal, 2, 181-205.
- <sup>128</sup> Pfister. G .(1983) *Detection of smoke gases by solid state sensors – a focus on research activities*. Fire Safety Journal, 6(3):165–174.
- <sup>129</sup> Amamotoa T.,Tanakaa K., Takahataa K, Matsuuraa S and Seiyamaa T., (1990) *A fire detection experiment in a wooden house by SnO2 semiconductor gas sensors*, Sensors and Actuators B: Chemical Volume 1, Issues 1-6, Pages 226-230.
- <sup>130</sup> McLafferty, F.W (1980) *Interpretation of Mass Spectra*, 3rd Edition, University Science Books, Mill Vally, CA
- <sup>131</sup> McLafferty, F.W. , Turecek, F. (1993) *Interpretation of Mass Spectra*, 4th Edition, University Science Books, Mill Vally, CA
- <sup>132</sup> NIST/EPA/NIH Mass Spectral Library (Agilent NIST05a Libraries) (2005), NIST-Wiley Publishing, Hoboken, NJ
- <sup>133</sup> Stein, S (1999) *An Integrated Method for Spectrum Extraction and Compound Identification from GC/MS Data*, Journal of the American Society of Mass Spectrometry,10, pages 770-781
- <sup>134</sup> Scientific Instrument Services MS Tools , <http://www.sisweb.com/mstools.htm>, checked 2011 .
- <sup>135</sup> McLafferty, F.W (1995) *Mass Spectrometry and analytical chemistry*, Journal of the American Society for Mass Spectrometry, 6(11), 993-994
- <sup>136</sup> NIST Web book, <http://webbook.nist.gov/chemistry/>, data retrieved December 2010, last checked Jan 2011

- 
- <sup>137</sup> Weinert, D.W., Cleary, T.G., Mullholand, G.W.(2001) *Size distribution and light scattering properties of test smokes*. Proceedings of the 12 International conference on automatic fire detection, AUBE 2001, 58-70
- <sup>138</sup> Keller,A., Loepfe, P., Nebiker, P., Burtscher, H.(2006) *On-line determination of the optical properties of particles produced by test fires*. Fire Safety Journal , 41, (4) , 266-273
- <sup>139</sup> Van De Hulst, H.C. (1981) *Light Scatting by Small Particles (Structure of Matter Series)*, Dover Publications, 470 pages (ISBN-10: 04866342284)
- <sup>140</sup> Schuler, F (1997) *Dual Wavelength Fire Detectoion Method and Apparatus*, US Patent 5,850,182, filed 7 Jan 1997, Issued 15 December 1998
- <sup>141</sup> Werkmiester, W., Hanses, T., Turner, J., Gruner, G. , Bergmann, R., Haug,C., Hensel, A. (2009) *Simulation of Light Scattering for Different Aerosols in a Fire Detector and Comparison with Experimental Data*, Proceedings from AUBE 2009 .
- <sup>142</sup> Personal communication John Shaw, Tyco Fire Protection Products, Sunbury, UK
- <sup>143</sup> Rubow, K.L., Marple, V.A, Olin, J.G, McCawley, M.A.(1987) *A Personal Cascade Impactor : Design Evaluation and Calibration*, American Hygiene Association Journal, 48,6,532-538
- <sup>144</sup>Owlstone Nanotech Inc(2008) Lonestar User Manual, © 2008 Owlstone
- <sup>145</sup> Owlstone Nanotech Inc (2006) Owlstone Nanotech White Paper OWL-WP-1 v3.0 21-3-06
- <sup>147</sup> Bohren, C. F.; Huffman, D. R.(1983) *Absorption and scattering of light by small particles*, New York, Wiley-Interscience,2010 [ISBN 3527406646](https://doi.org/10.1002/9781118134463)